# Exploring the beneficial effects of cardiorespiratory fitness and exercise on cerebrovascular health in Huntington's Disease:

# A cross-species approach

*This dissertation is submitted for the degree of*

*Doctor of Philosophy*

*at*

*Cardiff University*

**Hannah Furby**

September 2016

“Tell me and I’ll forget; show me and I may remember; involve me and I’ll understand”

**Chinese proverb**

# Declaration

## DECLARATION

This work has not been submitted in substance for any other degree or award at this or any other university or place of learning, nor is being submitted concurrently in candidature for any degree or other award.

Signed ..... (candidate) Date 29/09/2016

## STATEMENT 1

This thesis is being submitted in partial fulfilment of the requirements for the degree of PhD.

Signed ..... (candidate) Date 29/09/2016

## STATEMENT 2

This thesis is the result of my own independent work/investigation, except where otherwise stated, and the thesis has not been edited by a third party beyond what is permitted by Cardiff University's Policy on the Use of Third Party Editors by Research Degree Students. Other sources are acknowledged by explicit references. The views expressed are my own.

Signed ..... (candidate) Date 29/09/2016

## STATEMENT 3

I hereby give consent for my thesis, if accepted, to be available online in the University's Open Access repository and for inter-library loan, and for the title and summary to be made available to outside organisations.

Signed ..... (candidate) Date 29/09/2016

**STATEMENT 4: PREVIOUSLY APPROVED BAR ON ACCESS**

I hereby give consent for my thesis, if accepted, to be available online in the University's Open Access repository and for inter-library loans **after expiry of a bar on access previously approved by the Academic Standards & Quality Committee.**

Signed …… (candidate) Date 29/09/2016

# Acknowledgment of Financial Support

The work presented in Chapter 2, Chapter 3 and Chapter 5 was funded by the Cardiff University Neuroscience and Mental Health Research Institute (NMHRI), while Chapter 4 was co-funded by the NMHRI and The Waterloo Foundation.

# Acknowledgments

Firstly, I would like to express my sincere gratitude to my supervisors Prof. Richard Wise and Prof. Stephen Dunnett for the continuous support throughout the past 3 years. Thank you, Richard, for your prompt feedback and support for my (often over-ambitious) ideas and to Steve for your patience and statistical prowess.

Thanks to the ASL crew in CUBRIC; particularly to Kevin, Molly, Esther, Mark, Alberto, Alan, Jo, Ian and Ilona for your expertise in times of crisis. Your genius will forever inspire me. A big thank you to Jess Steventon for being such a good mentor and friend.

Thanks to everyone in the Brain Repair Group; to Ngoc Na for your microscopy wisdom; to Susanne, Kyle, Emma and Yat for making me feel so welcome in the lab even though my visits were intense and sporadic; and particular thanks to Harri Davidson, for all your help. Your passion and dedication really encouraged me and you never failed to make me chuckle.

Thanks to Andrew Stewart for the long, long, long days that I made you spend scanning with me in EMRIC. Your light-hearted attitude and realist opinions were a breath of fresh air in some of my darkest moments!

Thanks to the 2012 Wellcome Trust PhD crew; Lucy, Nick, Tim, Jack, Laura and Alison for sharing this whole journey with me. I wish you all the very best, wherever life may take you next.

Thanks to everyone in the Cardiff Huntington's Disease Centre, for making me feel so welcome and for your help with recruitment. Candace Farman, your organization and calmness is an asset to the Centre.

Thank you to my housemates Laura and Alison for the midnight rants, chocolate binges and cups of tea over the last year. Who knew that sticking googley eyes on doorknobs and vegetables could turn the day around?!

A special thank you to all my friends and family for sticking by me over the past few years and providing me with refuge when I have needed to get away. I hope I will continue to make you proud. Thank you to Matt, for your patience and support over the last year, your easy nature and smiley face has meant so much. And of course, the on-tap IT support…

**Finally, a huge thank you to the members of the Huntington's Disease community. To the patients; your positivity and motivation has been incredible. Your time and dedication spent taking part in this research has taught me so much and I will endeavour to improve the scientific understanding of this terrible disease in my years to come.**

*In loving memory of*
*Gran and Pa*

# Glossary of Abbreviations

| | |
|---|---|
| AIx | Augmentation Index |
| aBV | Arterial Blood Volume |
| AC | Arterial Compliance |
| ANCOVA | Analysis of Covariance |
| ANOVA | Analysis of Variance |
| BBB | Blood Brain Barrier |
| BCa | Bias-corrected and accelerated |
| BOLD | Blood Oxygen Level Dependent |
| BP | Blood Pressure |
| BPS-O | Behavioural Pattern Separation – Object version |
| BrdU | 5-bromo-2'-deoxyuridine |
| CA1 | Cornu Ammonis region 1 |
| CBF | Cerebral Blood Flow |
| CBV | Cerebral Blood Volume |
| CIs | Confidence Intervals |
| $CMRO_2$ | Cerebral Metabolic Rate of Oxygen |
| CNS | Central Nervous System |
| $CO_2$ | Carbon Dioxide |
| CoW | Circle of Willis |
| CP | Caudate Putamen |
| CSF | Cerebrospinal Fluid |
| CVR | Cerebrovascular Reactivity |
| DG | Dentate Gyrus |
| Dias | Diastole |
| ECG | Electrocardiogram |
| FAIR | Flow-sensitive Alternating Inversion Recovery |
| FAS | Functional Assessment Score |
| FDR | False Discovery Rate |
| fMRI | Functional MRI |
| FOV | Field of View |
| GFAP | Glial Fibrillary Acidic Protein |
| GM | Grey Matter |
| HADS | Hospital Anxiety Depression Scale |
| HD | Huntington's Disease |
| HET | Heterozygous |
| HOM | Homozygous |
| i.p. | Intraperitoneal |
| IB | Inclusion Body |
| IPAQ | International Physical Activity Questionnaire |

| | |
|---|---|
| IS | Independence Score |
| KI | Knock -in |
| M1 | Primary Motor Cortex |
| MAP | Mean Arterial Pressure |
| MCA(v) | Middle Cerebral Artery (Velocity) |
| mHTT | Mutant Huntingtin |
| MRI | Magnetic Resonance Imaging |
| n.s | Not significant |
| NHS | Natural Horse Serum |
| NO | Nitrous Oxide |
| OEF | Oxygen Extraction Fraction |
| PAL | Paired Associates Learning |
| PASL | Pulsed Arterial Spin Labelling |
| pCASL | Pseudo-continuous ASL |
| PET | Partial Pressure of End Tidal |
| PFA | Paraformaldehyde |
| PICORE | Proximal Inversion with a Control for Off-Resonance Effects |
| PVC | Partial Volume Correction |
| QUIPPS | Quantitative Imaging of Perfusion using a Single Subtraction |
| RCT | Randomised Clinical Trial |
| RER | Respiratory Exchange Ratio |
| ROI | Region of Interest |
| ROI | Region of Interest |
| RPE | Rating of perceived exhaustion |
| SCOLP | Speed and Capacity of Language Processing |
| SDMT | Symbol Digit Modalities Test |
| SMC | Smooth Muscle Cells |
| SNR | Signal to Noise Ratio |
| SVD | Small Vessel Disease |
| SVZ | Sub-ventricular zone |
| Sys | Systole |
| TAT | Tissue Arrival Time |
| TBS | Tris buffered saline |
| TCD | Transcranial Doppler |
| TFC | Total Functional Capacity |
| TI | Inversion Time |
| TMS | Total Motor Score |
| TTC | Time to Climb |
| TTT | Time to Turn |
| UHDRS | Unified Huntington's Disease Rating Scale |
| VEGF | Vascular Endothelial Growth Factor |
| VO2max | Maximal Oxygen Volume |
| WHO-QL | World Health Organisation Quality of Life Questionnaire |
| WM | White Matter |
| WT | Wild Type |

# Table of Contents

# List of Figures and Tables

## Chapter 5

# Thesis Summary

This thesis explores the benefits of physical activity on cerebrovascular health in healthy subjects and in Huntington's Disease (HD), where cerebrovascular health is thought to be jeopardised. A cross-species approach was employed, to inform the relevance of MRI findings in humans, using histology and pre-clinical imaging.

In Chapter 2, measurement of cerebrovascular markers using arterial spin labelling (ASL) MRI showed that arterial compliance and resting cerebral blood flow was lower in subjects with higher cardiorespiratory fitness, whilst differences in cerebrovascular reactivity (CVR) to a breath-hold task were not statistically significant.

Measurements of vessel density in Chapter 3 showed that running mice had greater vessel density than non-running mice following a 6-week voluntary wheel running intervention, which may be attributed to a process of angiogenesis.

Methods developed in healthy subjects were subsequently applied to investigate the cerebrovascular benefits of exercise in HD. In Chapter 4, pre-/early-symptomatic patients with HD were assessed for subtle differences in cerebrovascular health and whether this varied with cardiorespiratory fitness. Disease-related differences were observed in cognition, and ASL measures including resting CBF and CVR, but no clear relationship with fitness was observed.

Preclinical imaging was used in Chapter 5 to measure longitudinal changes in resting CBF and CVR in a transgenic Q175 mouse model of HD, prior to behavioural deficits (preHD). Neither CBF or vessel density differed between preHD animals and controls, and did not appear altered by voluntary running.

It is concluded that physical activity may convey cerebrovascular benefits to healthy individuals early in life, including increased arterial compliance, blood flow efficiency and angiogenesis, however the pre-/early-stages of HD may be too early to detect the cerebrovascular benefits conveyed by physical activity.

# Aims of thesis

A growing body of evidence now demonstrates the link between maintaining a healthy, active lifestyle and cognitive health, and that this may be mediated by alterations in cerebrovasculature. Neuroimaging methods are being developed by which to non-invasively assess these changes in the human brain, however the challenge lies in the sensitivity of these methods for detecting these alterations before overt cognitive function is affected. The majority of exercise MRI research has been applied to the aged or diseased brain. However, it is important that we explore these changes in the young adult brain if we are to recommend exercise as a prophylactic for cognitive decline.

Complex interactions between neurons, glia and cerebral blood vessels play critical roles in maintaining cerebrovascular health which cannot be addressed using MRI. Consequently, the brain's ability to provide sufficient flow to active regions may lead to brain dysfunction. Alterations in these cellular interactions are known to occur in Huntington's Disease and also to be improved by exercise. Whether exercise can mediate these cellular interactions in the context of Huntington's Disease is not yet known, and will be the focus of this thesis.

This thesis will tackle this question using a translational approach by which use of non-human subjects, enables interpretation of macrostructural *function* in terms of microstructural changes, using *ex vivo* histology to complement *in vivo* MRI.

The studies described in this thesis, including planning, data collection and analysis were carried out by myself except where otherwise indicated,

## Human Subjects

### Chapter 2:

- To identify neuroimaging biomarkers of cerebrovascular health in a cohort of young healthy males with a broad range of $O_{2MAX.}$ using PASL in humans

### Chapter 4:

- To characterise cerebrovascular and cognitive function in pre/early symptomatic HD patients compared to matched controls using PASL measures developed in Chapter 2.
- To address whether CBF changes vary with fitness ( $O_{2peak}$) and can explain differences in cerebrovascular and cognitive function.

## Non-human Subjects

### Chapter 3:

- To investigate changes in blood vessel density following a 6-week voluntary wheel-running intervention in young healthy male C57/BL6 mice.

### Chapter 5:

- To measure cerebrovascular function in an asymptomatic male Q175 HD mouse model compared to WT controls using PASL MRI (resting CBF and CVR) and vascular histology (vessel density).
- To assess cerebrovascular changes following a 6-week voluntary wheel-running intervention in Q175 mice compared to WT controls.

# Chapter 1

# General Introduction

## 1.1 The cerebrovascular architecture

No organ in the body depends on a continuous supply of blood as much as the brain. Interruption of cerebral blood flow (CBF) causes brain function to cease within seconds, and leads to irreversible cellular damage within minutes (Hossmann, 1994). The brain's dependence on blood flow is attributable to both its lack of fuel reserves and high energy demands. The importance of the cerebrovasculature is frequently overlooked, and often thought of as a silent bystander to the healthy function of the neuron. The cerebrovasculature is in fact vastly complex and is constantly working to maintain blood flow through 1) prioritisation of systemic circulation to the brain when cerebral perfusion is threatened, 2) cerebral autoregulation to protect the brain where normal fluctuations in arterial pressure are observed and 3) through regulation of CBF distribution according to the functional activity of different brain regions.

### 1.1.1. The Cerebrovascular tree

The cerebrovascular system is complex and is made up of different vessel subtypes which serve different functions. Large cerebral arteries branch into smaller arteries and arterioles that run along the surface of the brain known as the pial arteries. Pial arteries consist of an endothelial cell layer, a smooth muscle cell layer and an outer layer of leptomeningeal cells, called the adventitia which is separated from the brain by the Virchow-Robin space (Peters et al, 1991). As the arterioles penetrate deeper into the brain (penetrating arteries), this space disappears and the vascular basement membrane comes into direct contact with the astrocytic end feet at the level of the intracerebral arterioles and capillaries (Figure 1.1).

### 1.1.2. Major cerebral arteries

The major arteries are vital for supplying blood to the brain. Major cerebral arteries include the internal carotid (ICA) and vertebral arteries (VA). The ICA's originate from the common carotid arteries, located in the neck, whereas VAs branch from the subclavian arteries within the thorax and continue throughout the cervical region of the spinal cord. Vertebral arteries anastomose at the level of the brainstem to form the basilar artery (BA), which bifurcate to form the left and right posterior cerebral arteries (PCAs) whilst the ICAs, bifurcate to form the middle and anterior cerebral arteries (MCA and ACA respectively). The Circle of Willis is formed by the communicating arteries between the posterior and middle cerebral arteries, and between the middle and anterior cerebral arteries (Figure 1.1).

### 1.1.3. The neurovascular unit

The neurovascular unit comprises neurons and non-neuronal cells including vascular cells (endothelial cells, vascular smooth muscle cells and pericytes) and glia (astrocytes, microglia and oligodendroglia). These non-neuronal cells form the anatomical, biochemical and immune blood-brain barriers (BBBs) of the central nervous system, maintaining the chemical cellular composition of the neuronal 'milieu', required for proper functioning of neuronal synapses and circuitry. Perivascular neurons, astrocytes and vascular cells constitute a functional unit, of which the main role is to protect the brain by maintaining the homeostasis of the cerebral microenvironment. The neurovascular unit also provides a first line of defence against the detrimental effects of brain injury such as cerebral ischemia (Iadecola, 2004).

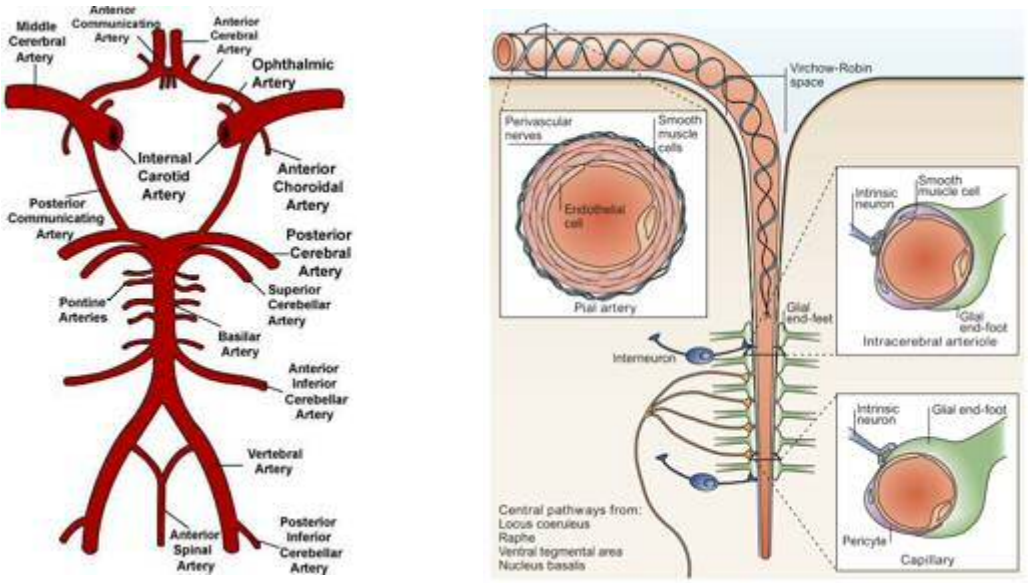


**Figure 1.1 Cerebrovascular Architecture.** Left) Schematic of the major cerebral arteries. The main supply of arterial blood comes from the internal carotid (ICA) and vertebral arteries (VA). The VA joins up at the level of the caudal pons to form the basilar artery (BA), which together with the ICA supplies the Circle of Willis. The major arteries branching from the Circle of Willis are the anterior (ACA), middle (MCA) and posterior (PCS) cerebral arteries. Right) Pial arteries have a dense structure of perivascular nerves (blue) originating from the peripheral nervous system in the outer layer (tunica adventitia) of the arteries. Arteries and arterioles have a thick middle layer (tunica media) which consists of smooth muscle cells (purple) as well as elastin and collagen fibres. The tunica adventitia and media, become thinner along the vascular tree such that intracerebral arterioles and capillaries are innervated by neurons and interneurons. Intracerebral arterioles but not capillaries have a single layer of smooth muscle cells, and both are surrounded by astrocyte end-feet and pericytes which aid blood flow regulation. Figure taken from (Iadecola, 2004. Nature Reviews, Neuroscience, 207, 2, 141-152).

## 1.2 Healthy cerebrovascular function

### 1.2.1. Cerebral pressure autoregulation

Cerebral pressure autoregulation is the process by which cerebral arteries and arterioles, maintain a constant blood flow (CBF) during changes in cerebral perfusion pressure, in order to protect the brain from oxygen and nutrient depletion (Peterson et al., 2011). Quantification of cerebral autoregulation is calculated by measuring the variation of CBF in response to changes in blood pressure. Arterial blood pressure can be most accurately measured using an invasive arterial line. However, non-invasive finger arterial pressure can also be measured using a volume clamp

technique, which is an inflatable finger cuff in combination with an infrared plethysmograph, or an infrared plethysmograph on its own.

Ever since a study in 1959 which measured total brain blood flow from 7 studies involving 11 different patient groups with a wide range of drug- and/or pathology-induced BP levels (Lassen, 1959; Figure 1.2.), it has been generally well accepted that CBF appears to be completely stable across blood pressures, ranging between 50-150mmHg. Although regularly cited, the view that CBF remains constant within this mean arterial pressure (MAP) has come into contention. For example, one study showed that blood flow velocity in the MCA tracked a drop in MAP following release of an inflated thigh occlusion cuff used to produce transient hypotension, following which CBF recovered quickly (Aaslid et al., 1989). This and other studies since have challenged the classical view that CBF is constant in this range, and that cerebral arteries may in fact play an active role in mechanically buffering relative flow in the brain (Willie et al., 2014)

Maintaining a continuous CBF profile in the face of changing BP, requires increased cerebrovascular resistance within the vessels, that is, a change in vascular tone of the smooth muscle cells, to withstand the high-pressure blood flow arising from the heart. Whether increased resistance occurs within the smaller pial arterioles alone, or whether the major cerebral arteries are also able to be compliant to BP fluctuations is under scrutiny (Peterson et al., 2011; Warnert et al., 2015a; Willie et al., 2014).

The majority of research into human cerebral autoregulation uses CBF velocity measurements by Transcranial Doppler (TCD) ultrasound assessments of the MCA or PCA. A study by Ainslie et al. (2005) observed increased cerebrovascular resistance but no change in peak MCA velocity following a hand grip task. The limitations of TCD will be discussed in more detail below, but it is important to mention that TCD measures assumes that cerebral arteries do not change in diameter, and may therefore overlook changes in the compliance of the cerebral arteries that contribute to altered cerebrovascular resistance (Willie et al., 2011).

A recent study using ASL MRI, observed increased cerebrovascular resistance with increased BP during post-exercise ischemia, caused by decreased compliance of the major cerebral arteries, such as the MCA, with no change in CBF (Warnert et al., 2015a). This promising evidence suggests that compliance of the major cerebral arteries may actually contribute to autoregulation by buffering BP fluctuations at the major vessels and thereby protecting downstream tissue from damage (Santisakultarm et al., 2012).

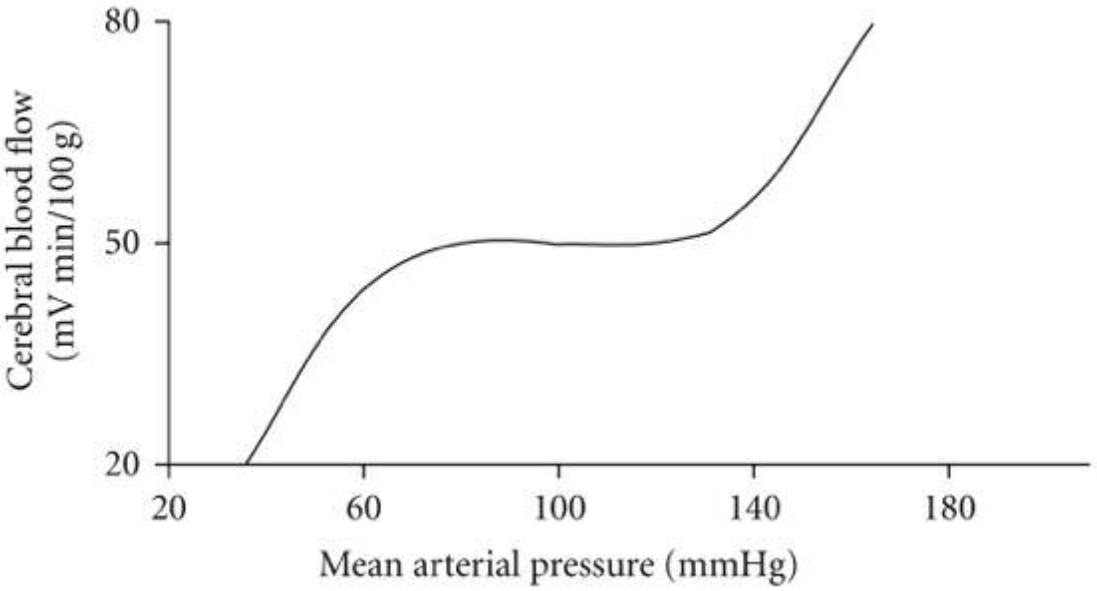


**Figure 1.2 Cerebral Blood Pressure Autoregulation.** Idealised curve demonstrating cerebral blood pressure autoregulation. (Lassen, 1959). Cerebral blood flow is thought to remain relatively stable within a wide arterial pressure range (50-150mmHg) via the process of cerebral autoregulation. More recent evidence suggests that this may not be the case and that cerebral arteries may play a role in buffering BP fluctuations (Willie et al., 2014) ; figure taken from (Peterson et al., 2011).

### 1.2.2. Arterial compliance

Low arterial compliance is associated with increased arterial stiffness. Arterial stiffening occurs with normal ageing and disease, whereby arteries are less able to regulate CBF fluctuations with changes in BP such that CBF becomes increasingly pulsatile (Figure 1.3). Increased pulsatile stress can lead to damage of small vessel walls and has been associated with cerebrovascular pathologies such as cerebral

small vessel disease (O'Rourke and Hashimoto, 2007), neurodegenerative diseases such as Alzheimer's Disease (Hughes et al., 2015) and cerebral aneurysms (Dusak et al., 2013).

Where arterial compliance is inversely related to cerebrovascular resistance (Thiele et al., 2011), arteries constrict in response to increases in BP, to resist pressure fluctuations. A decrease in compliance is thought to be caused by an increase in the tone of the active smooth muscle cells (SMC) in the arterial walls, since the elastin and collagen components are thought to be passive (Bank et al., 1996). Whilst SMC tone does not affect the mechanical properties of the arterial wall at low transmural pressures, relative contributions from all three components alters the stiffness of the arterial wall. At high transmural pressures, >100mmHg, an increase in SMC tone also causes increases in arterial stiffness (Bank et al., 1995).

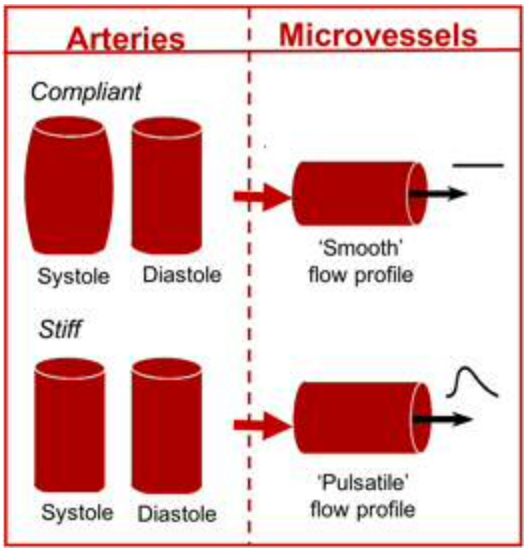


**Figure 1.3 Arterial Compliance.** Arterial compliance is inversely related to the stiffness of the artery wall and is thought to be mediated by the tone of the smooth muscle cells (SMCs). In the healthy brain, compliant arteries are able to buffer the pulsatile blood flow arriving to the brain from the heart, such that flow profile into the microvessels is smooth. In the case of ageing and disease, arteries become stiffer which may be detrimental to downstream microvessels where capillaries are prone to rupture with pulsatile flow (O'Rourke and Safar, 2005). This could consequently lead to small vessel disease and cognitive decline (Prins et al., 2005).

### 1.2.3. Cerebral flood flow regulation

Among the factors that influence CBF are the perivascular nerves which constrict or dilate arteries and arterioles (Drake and Iadecola, 2007), the astrocytes which envelope arterioles and influence arteriolar diameter (Carmignoto and Gómez-Gonzalo, 2010), the endothelial cells which release vasodilators (e.g. nitric oxide;

NO) and vasoconstrictors such as endothelin (Faraci and Heistad, 1998), and finally the pericytes which can cause capillary contraction and relaxation (Hall et al., 2014). Together these factors work together to ensure that the brain is properly perfused, and that brain tissue has the oxygen and nutrients it needs to function. If the function of one or more of these mechanisms is impaired, the brain is vulnerable to hypoperfusion and increasing risk of cerebrovascular disease.

Endothelial cells produce vasodilators such as nitric oxide (NO), prostacyclin, carbon monoxide and the endothelium-derived hyperpolarizing factor, and vasoconstrictors such as endothelin and the endothelium-derived constrictor factor (Busse and Fleming, 2003; Faraci and Heistad, 1998). Endothelial reactive oxygen species (ROS) also influence vascular tone, whereby they act as vasodilators at low concentrations, but can cause vascular dysregulation such as hypertension and hyperhomocysteinaemia at high concentrations (Iadecola and Gorelick, 2004). Endothelial vasoactive substances are released by receptor-dependent agonists or by changes in the viscous drag that is generated at the luminal surface of endothelial cells by the flowing blood, known as 'shear stress' and the strain upon the vessel wall that results from pulsatile changes in blood pressure (Busse and Fleming, 2003). Electrical signals between endothelial and/or smooth muscle cells through gap junctions mean that vasodilation or constriction can travel rapidly along the vessel wall (Segal, 2000).

Smooth muscle cells and pericytes finally convert the chemical signals that originate from endothelial cells, neurons and astrocytes into changes in vascular diameter by inducing changes in intracellular $Ca^{2+}$ concentration and altering the phosphorylation state of light chain myosin (Carmignoto and Gómez-Gonzalo, 2010) (Figure 1.4). Astrocytic end-feet almost completely surround intra-parenchymal blood vessels and also contribute to vasomotor activity through multiple pathways (Stobart and Anderson, 2013). Astrocytes are enriched in potassium ($K^+$) channels. Potassium is released from astrocyte end-feet and the amount of $K^+$ released is directly proportional to astrocyte $Ca^{2+}$ level. Potassium is subsequently taken up into smooth muscle through which causes dilation at low concentrations and constriction at high concentrations. Intracellular Ca2+ also activates NO to produce $CO_2$, which also triggers dilation via the smooth muscle.

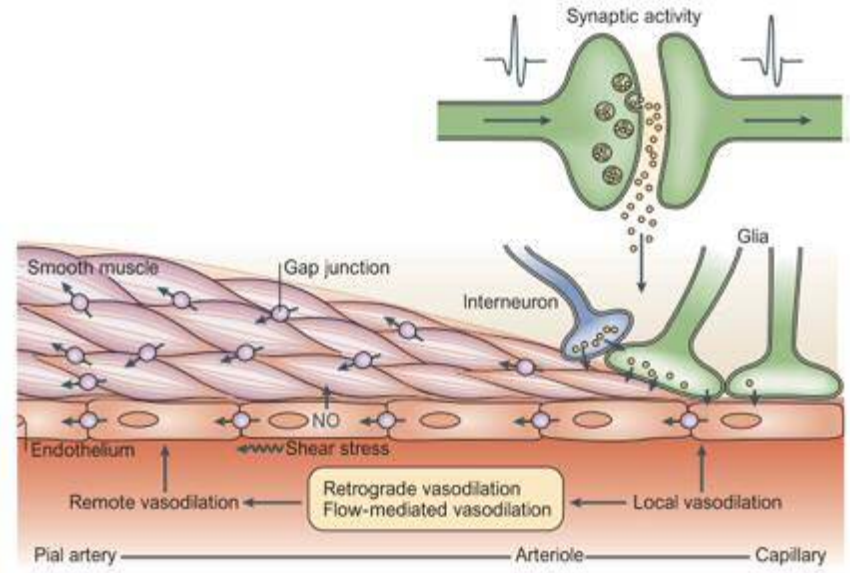


**Figure 1.4 Propagation of vasodilation within vessels.** Vasodilation from vessels in the activated site (arterioles and capillaries) propagates to resistance arteries upstream (pial arteries). Local release of vasoactive agents from neurons and glia (astrocytes, pericytes) causes relaxation of the smooth muscle which propagates upstream through gap junctions that link neighbouring endothelial and smooth muscle cells. An increase in blood flow upstream causes an increase in shear stress on endothelial cells which causes further vasodilation through the release of endothelium-dependent vasodilators (flow-mediated vasodilation). (Figure taken from Iadecola, 2004, Nature Reviews, Neuroscience, 102, 2, 141-152).

## 1.3 Cerebrovascular pathology and disease

Poor cerebrovascular function, including reduced blood flow, capillary loss, arterial stiffening and breakdown of the BBB, or both, are just some of the factors thought to precede many neurodegenerative diseases and or age related cognitive decline (Bell et al., 2011; Ruitenberg et al., 2005). Despite an emerging amount of evidence, there is still no consensus regarding the role of the vascular component in neurodegeneration (Zlokovic, 2011). This section will highlight some of these cerebrovascular deficits in more detail.

### 1.3.1. Arterial Stiffening

Aortic stiffness is known to increase with age and other vascular risk factors, and is associated with an increased risk for structural and functional brain abnormalities. In cases where cerebral autoregulation is jeopardised or MAP is outside normal limits, cerebral microcirculation is exposed to the harmful effects of excessive pressure and flow pulsatility. High flow organs such as the brain and kidneys are especially sensitive to excessive pressure and flow pulsatility (Mitchell et al., 2008). High CBF is associated with low microvascular impedance, which facilitates penetration of excessive pulsatile energy into the microvascular bed. Pulsatility in the distal arterial bed is thought to cause deterioration of vessel walls, which in the brain can manifest as cerebral small vessel disease (SVD)(Poels et al., 2012). Incidence of cerebral SVD increases with ageing and has been associated with cognitive decline, such as slowed processing speed and deficits in executive function (Prins et al., 2005) in healthy older people at risk for dementia and Alzheimer's Disease (AD).

### 1.3.2. Hypoxia and angiogenesis

Whilst interpretation of cerebral angiogenesis is as a beneficial mechanism by the brain to increase blood flow by forming new blood vessels from pre-existing vessels, increased vascularity is also known to occur in brain pathologies such as tumour (Yancopoulos et al., 2000), stroke (Beck and Plate, 2009), AD (Biron et al., 2011) and HD (Lin et al., 2013) as a compensatory response to combat deficits in blood flow circulation. In the healthy brain, angiogenesis is initiated by vascular endothelial growth factor (VEGF) (LaManna et al., 2004), and this can be triggered in response to hypoxia via the hypoxia-inducible factor-1 (HIF-1) transcription factor (Saint-Geniez and D'Amore, 2004).

It appears that with age, there is a decline in the capacity for cerebral angiogenesis where the responsiveness of HIF-1 to hypoxia decreases (Rivard et al., 1999), thereby reducing VEGF expression in ageing (Banderro and LaManna, 2011). Failure of the vasculature to recover from hypoxia-induced capillary loss with age and disease, is therefore thought to reflect a loss of cerebrovasculature which may underpin some of the functional deficits observed.

Angiopoietins such as Angiopoietin-1, are a group of proteins that contribute to blood vessel maturation and capillary stability. Pericytes signal the release of angiopoietin-1 which activates the Tie-2 receptors on endothelial cells. Activation of the Tie-2 receptors is thought to maintain vascular integrity and stability whereas under hypoxic conditions, activation of other angiopoietins such as angiopoietin-2, occupies these binding sites such that pericytes move away from the capillaries, consequently destabilizing them.

### 1.3.3. Blood-brain Barrier Leakage (BBB).

The BBB refers to the extensive network of capillary blood vessels, comprised of highly specialized endothelial cells, which compartmentalize the brain from the peripheral blood. The BBB controls the passage of metabolites and other substances from the blood to the neurons, via gap junctions between endothelial cells. Disruption of the blood-brain barrier has been strongly implicated in neurodegenerative diseases such as AD (Zlokovic, 2011), Parkinson's Disease (Guan et al., 2013) and Huntington's Disease (Drouin-Ouellet et al., 2015) (Figure 1.5.).

In AD, recent evidence has observed a deposition of β-amyloid within arteries which results in cerebral amyloid angiopathy, in more than 80% of AD cases (Jellinger, 2010). Disruption to the BBB leads to reduced vascular integrity and leakage such that peripheral cells are able to enter the CNS compartment, and in doing so, result in inflammatory cascades and release of neurotoxins (Zlokovic, 2010). BBB leakage, also leads to a loss of blood flow such that neurodegenerative substances, such as mHTT in the case of HD (Drouin-Ouellet et al., 2015) and β-amyloid in the case of AD, are not properly cleared (Sagare et al., 2012) thereby potentiating blood flow dysfunction and vascular-mediated neurodegeneration.

### 1.3.4. Hypoperfusion

Sufficient cerebral blood flow (CBF) is vital to neuronal function, thus, cerebral perfusion (millilitres of blood passing through a volume of tissue over a given duration (ml/100g/min)), has been used as a useful indicator of cerebral health. CBF is normally coupled to cerebral oxygen metabolism ($CMRO_2$) and glucose consumption in steady state (Hoge et al., 1999), such that disruption of this system hints towards compromised vascular function and/or metabolism.

It is not surprising that decreased resting cerebral blood flow (CBF) and cerebrovascular reactivity to neuronal activation are associated with an elevated risk of cerebrovascular diseases such as AD, stroke and hypertension (Jennings et al., 2013), and occur with healthy aging (Fisher et al., 2013). With healthy human aging, a progressive decline in CBF has been repeatedly observed in the order of 28–50% from the age of 30 to 70 years (Ogoh and Ainslie, 2009). In AD, perturbations in microvascular flow in association with an over-expression of amyloid precursor protein, appear to precede detectable neuronal dysfunction (Farkas and Luiten, 2001). This has led to the belief that CBF may play important roles in the progression and clinical expression of neurodegenerative disease. In AD, loss of cholinergic innervation of brain blood vessels (Roman and Kalaria, 2006) is thought to reduce cerebral perfusion. Hypoperfusion is also correlated with increased expression of the hypoxia-inducible factor HIF1α and number of white matter lesions (Fernando et al., 2006). Regional effects of age on CBF are thought to be independent of those seen in cortical atrophy, so that reduction in CBF cannot be explained by a decline in gross volume differences (J. J. Chen et al., 2011).

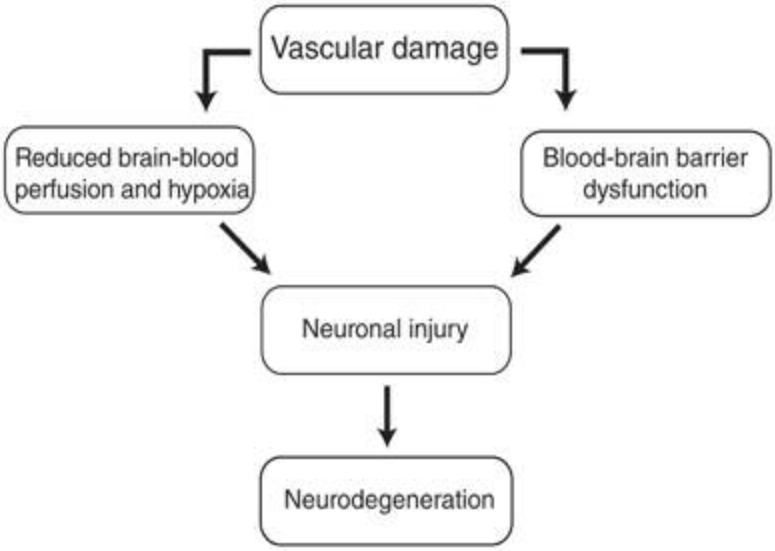


**Figure 1.5 The vascular hypothesis of neurodegeneration.** Vascular damage can result in reduced CBF and hypoxia from one end and BBB dysfunction from the other. The BBB breakdown might lead to accumulation of potentially toxic serum proteins inside the brain. Reduced CBF and BBB disruption might contribute to secondary neuronal injury and the development of neurodegenerative changes (figure taken from Zlokovic, 2010, Nature Medicine, 16, 12, 1370-71).

## 1.4 How can cerebrovascular health be measured in humans?

Evidence of decreased (CBF) over the lifespan and in cerebrovascular disease (Stoquart-ElSankari et al., 2007) has been described and is the most widely reported non-invasive marker of cerebrovascular health. CBF can be measured by a number of techniques whereby quantification and definition of blood 'flow' is variable, but used interchangeably. For example, studies utilising trans-cranial Doppler ultrasound frequently refer to changes in CBF but do not directly quantify cerebral blood flow, rather cerebral blood velocity of major cerebral arteries (e.g. Middle cerebral artery). Interpretation of different studies, therefore require an understanding of how CBF is quantified.

### 1.4.1. Non MRI methods for measuring CBF

#### *1.4.1.1. Single-photon emission computed tomography (SPECT)*

SPECT is a 3D nuclear medicine tomographic imaging technique using gamma rays. The technique requires delivery of a gamma-emitting radioisotope into the patient via intravenous injection. A marker radioisotope is attached to a specific ligand to create a radioligand which bind to specific tissue types which can then be viewed using a gamma camera. The most common gamma-emitting tracer used in functional brain imaging is 99mTc-HMPAO (hexamethylpropylene amine oxime). Combining HMPAO to 99mTc allows it to be taken up by brain tissue in a manner proportional to brain blood flow, such that CBF can be assessed. Tight coupling between CBF and local brain metabolism means that 99mTc-HMPAO tracer is used to assess regional brain metabolism regionally, in an attempt to diagnose and differentiate the different causal pathologies of neurodegenerative diseases such as dementia.

#### *1.4.1.2. Positron Emission Tomography (PET)*

Positron emission tomography (PET) is also capable of providing in vivo quantitative measures of CBF and $H_2{}^{15}O$ PET has evolved to be considered the gold standard for studying cerebral hemodynamics (Chen et al., 2008). Caveats of PET imaging involves the injection of radioactive tracers, which limit repeatability and application in healthy subjects. It also has low temporal and spatial resolution, low signal-to-noise ratio (SNR), and requires a cyclotron, often rendering it an inconvenient option. ASL MRI in contrast is widely available and has a relatively high spatial and temporal resolution.

#### *1.4.1.3. Transcranial Doppler (TCD)*

TCD is a type of Doppler ultrasonography that measures the *velocity* of blood flow through the cerebral arteries, by measuring the echoes of ultrasound waves moving transcranially. TCD can be used as an efficient tool to access blood velocities within the cerebral vessels, cerebral autoregulation, cerebrovascular reactivity to $CO_2$, and neurovascular coupling, in both physiological states and in pathological conditions such as stroke (Willie et al., 2011). Compared to MRI, these parameters are global measures and not regionally specific. Developments in TCD equipment mean that it is portable and therefore practical for clinical purposes and

benefit from being far cheaper than MRI for assessing cerebrovascular function. A drawback of TCD is that it cannot measure arterial geometry, such as volume or diameter such that changes in blood flow velocity can only be interpreted by if there is no change in arterial diameter. Accurate TCD sonography assessment also relies upon the examiner's technical skill and anatomical knowledge.

### 1.4.2. MRI methods for measuring CBF

#### *1.4.2.1. DSC-MRI*

Dynamic contrast enhanced (DCE)-MRI is performed by acquiring a dynamic image in which an intravenous bolus of standard small molecular weight gadolinium-based contrast agent is injected in to the subject. Signal intensity changes can be analysed to derive parametric maps of microvascular biomarkers. MR images can be acquired using either T2 * or T2 weighting (also known as dynamic susceptibility contrast MRI (DSC-MRI)) or T1 weighting (T1 weighted DCE-MRI).

DSC-MRI is currently the clinical method of choice for measurement of cerebral blood flow (CBF) and Cerebral Blood Volume (CBV) with MRI. DSC-MRI images result from changes in local field strength within the tissue induced by the paramagnetic contrast molecules. Water molecules at some distance from the contrast can be affected, so that the apparent contrast agent concentration measurement will be dependent upon the local vascular structure. For example, the same amount of contrast in a diffuse capillary bed will have a larger signal than it would if contrast were concentrated in a single large vessel, due to dispersion of the local changes in field strength (O'Connor et al., 2011). Imaging of signal changes resulting from T2* and matched T2 weighted sequences, where susceptibility effects are smaller, can be used to gain information regarding the size and distribution of blood vessels within the voxel, known as "vessel size imaging" (Batchelor et al., 2010).

A caveat of DSC-MRI is that increased blood-brain barrier permeability can cause extravasation of the contrast agent where susceptibility contrast is reduced, such that signal appears to be greater (Sourbron et al., 2009). This can be an issue in diseases where BBB is thought to be disrupted. Another major source of error in DSC-MRI is

the difference between blood and tissue relaxivity which needs to be accurately estimated as this enters into the quantification of CBV and CBF (Kiselev, 2005).

#### *1.4.2.2. Arterial Spin Labelling (ASL)*

ASL utilises blood as an endogenous tracer whereby arterial blood water is magnetically labelled and then imaged. Arterial blood water is first magnetically labelled below the region (slice) of interest by applying a 180° radiofrequency (RF) inversion pulse. This inversion pulse leads to a net magnetisation of blood water that flows into the tissue of interest after a period (inflow time) where it exchanges with tissue water. Inflowing inverted spins within the blood water subsequently reduce the tissue magnetization and attenuate the MR signal. During this time, an image is taken (known as the tag image). Acquisition of an image in which arterial blood has not been labelled, is known as the control image. A perfusion image is calculated by subtraction of the control image from the tag image to produce a perfusion image, also referred to as cerebral blood flow. This image will reflect the amount of arterial blood delivered to each voxel of tissue within the inflow time (Figure 1.6).

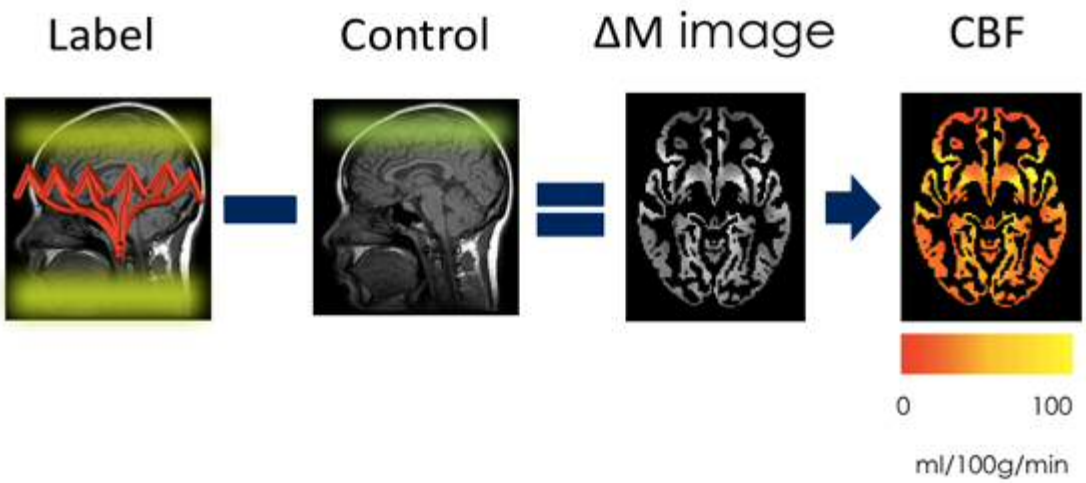


**Figure 1.6. Basic PASL principles**. Blood is magnetically labelled in the neck, and an image is acquired in the brain after an inflow time. A control image in which blood has not been magnetically labelled produces a change in signal intensity proportional to the exchange of water into the tissue (i.e. perfusion). Models can be used to quantify the amount of blood delivered per 100 g brain tissue per minute (ml/100 gr/min)(Buxton et al., 1998).

#### 1.4.2.2.1. ASL labelling schemes.

There are two main ASL labelling schemes, these are pulsed arterial spin labelling (PASL) and pseudo-continuous ASL (pCASL). Pseudo-continuous ASL evolved from the continuous ASL (CASL) labelling scheme whereby hydrogen molecules are continuously inverted as blood flows through the tagging plane, using a relatively long radiofrequency (RF) pulse (~ 1-2 seconds). The need for a long and continuous RF pulse meant that this method was not feasible for use in humans due to high specific absorption rates (SAR) and specialist system hardware, such that the development of pCASL came about. In pCASL a single, long, RF pulse is substituted for a train of short RF pulses. In comparison, pulsed ASL (PASL) magnetically labels the blood with a single short RF pulse covering a large slab of tissue (~10-20 cm). pCASL has benefits over PASL, since the longer labelling duration, yields potential for increasing the signal-to-noise ratio (SNR).

#### *1.4.2.2.1.1. Pulsed ASL (PASL)*

PASL sequences differ according to the zone of labelling with respect to the slices, known as symmetrical and asymmetrical (Ferré et al., 2013).

Symmetric Methods. The basic symmetrical method is flow alternating inversion recovery (FAIR), in which the control image is acquired using a non-selective global inversion pulse, and the tag image is acquired with a slice-selective gradient for labelling (Kim, 1995; Figure 1.7). During the slice-selective inversion time, intra-vascular spins are fully relaxed. During the non-selective global inversion time, inflowing spins were relaxing back to M0 according to T1. Static tissue should have relaxed to the same extent in both images, such that residual signal within the image is flow weighted. By measuring the T1 of grey matter, the effect of the inflowing spins on the apparent T1 relaxation constant (T1app) following the slice selective inversion can be used to quantify CBF. The symmetric nature of this sequence automatically thereby compensates for MT effects.

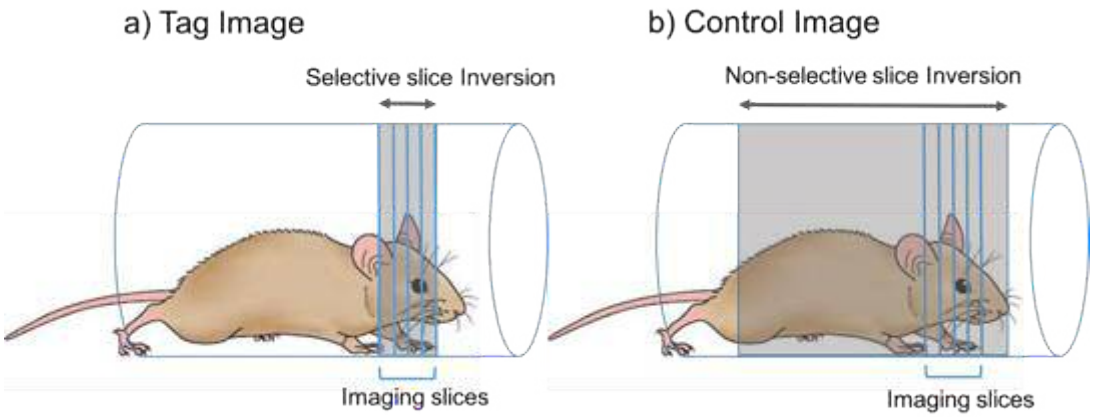


**Figure 1.7 FAIR Imaging Principles.** The flow-sensitive alternating inversion-recovery (FAIR) pulse sequence generates tagged and control images. The tagged images (a) are produced after applying a slice-selective 180 inversion pulse to the imaging slice; Since the spins outside the imaging plane are not inverted, their entry into the imaging slice as the result of blood flow will modulate the T1 relaxation of the imaging slice. The control images (b) are produced at the same plane as marked in (a) but after applying a non-slice-selective inversion pulse to the entire sensitive volume of the RF coil as shown by the gray area in (b).

Asymmetrical methods. Asymmetrical methods such as echo-planar MR imaging and signal targeting with alternative radio frequency (EPISTAR) have a thick labelling zone of ~10–15 mm, located upstream from the volume of interest. An inversion pulse labels the blood after saturation of the magnetization. During the control acquisition, the inversion volume is located downstream from the volume of interest to control for MT effects (Edelman et al., 2004). Several modifications of this sequence have been made since such that multiple slices could be properly acquired (Edelman and Chen, 1998), including limiting the MT effects (TILT sequence) (Golay et al., 1999), improving the profile of the labelling slice (PICORE) (Wong et al., 1998) and to reduce the sensitivity of the arterial transit time (QUIPPS, QUIPPS II, Q2TIPS sequences) (Luh et al., 1999; Wong et al., 1998) and these are the most common PASL sequences used in human imaging.

## 1.5 What is Cardiorespiratory Fitness and how can it be measured?

Cardiorespiratory fitness refers to the ability of the circulatory and respiratory systems to supply oxygen to the body during sustained physical activity. Fitness can be improved by regular exercise, where oxygen delivery becomes more efficient, through a number of mechanisms, including enlargement of the heart muscle to provide more blood to the body, and by increasing the number of small arteries that supply oxygen to the metabolising tissue.

Research methods for investigating the link between cardiorespiratory fitness and cerebral health are broad, and can be split into cross-sectional or interventional designs. Interventional studies attempt to address within-subject differences, by making measurements before and after a well-defined exercise programme. Whilst interventions are more beneficial for assessing causation, they have more methodological challenges since they are often time-consuming, expensive and require more participant investment. Cross-sectional studies tend to take a single measure of cardiorespiratory fitness as the independent variable, and correlate these scores with aspects of brain function and for identifying individual differences. These

will be the basis of the human methods used in this thesis. There are several means of measuring fitness, and these will be discussed in this section.

### 1.5.1. Self-report

Subjective physical activity is most commonly measured via self-report, making this an easy, low-cost measure and more efficient when large sample sizes are required. A big caveat, is that self-reported physical activity, especially where clear desirability biases are present, due to lack of understanding, differing perceptions of item content and cross-cultural reliability (Sallis and Saelens, 2000). It is recommended that internationally validated tests such as the International Physical Activity Questionnaire (IPAQ) should be used where possible (Craig et al., 2003).

### 1.5.2. Accelerometry

Accelerometry is often used as an objective measure of physical activity, as the device is light to carry and non-invasive. Data from accelerometers are not, however, entirely accurate since more common accelerometers are unable to detect increased energy cost from upper body movements, load carriage, or changes in terrain (Hendelman et al., 2000). More advanced measures such as acceleration signals recorded at different locations such as lower back, heels and wrists may improve accuracy and information about gait, especially in clinical populations (Micó-Amigo et al., 2016).

### 1.5.3. The $O_{2MAX}$ test

The $O_{2MAX}$ test is considered the gold standard test of maximal oxygen uptake and is a fundamental measure of cardiorespiratory fitness, where $O_{2MAX}$ refers to the maximal capacity for oxygen consumption at a maximal rate of exertion (Hill, Long and Lupton, 1924). $O_{2MAX}$ values can be reported as an absolute rate of litres of oxygen per minute (L/min), but are more commonly reported as a relative rate, standardized by body mass (mL/ min/Kg) such that values can be compared across individuals. Typical exercise tests take place on a treadmill or cycle ergometer,

whereby intensity is progressively increased while measuring the end-tidal gases for measures of ventilation $O_2$ and $CO_2$.

$O_2$ is defined as the amount of oxygen taken up, transported, and used at the cellular level by the body, and is the difference between the amount of O2 inspired and O2 expired (Plowman and Smith, 2003, p. 124). Working muscles increase oxygen uptake as a result of increased cardiac output (heart rate × stroke volume), which may increase to up to 6 times resting heart rate. Cardiac output is also redistributed away from non-active tissues to the skeletal muscles, to prioritise O2 delivery where it is most needed. Blood flow increases due to an increase in both the cardiac output and by vasodilation of the blood vessels. As O2 is extracted from the blood into the perfusing tissue, a widening of the arteriovenous oxygen (a− O2) difference is seen.

Accurate $O_{2MAX}$ tests require intense physical effort for a sufficient period, such that the aerobic energy system is fully exerted, and such that O2 plateaus. It is not uncommon for subjects to complete a graded exercise test without reaching this classical plateau. As such several secondary criteria have been established in guidelines by the American College of Sports Medicine (2010) to characterize whether a $O_{2MAX}$ has been reached. These include 1) high levels of blood lactate (8mmol-1) post exercise (Howley et al., 1995) 2) elevated respiratory exchange ratio (RER) >1.0 (Aspenes et al., 2011), >1.10 (Nelson et al., 2010), or > 1.15 (Howley et al., 1995) 3) Percentage of subject's age adjusted maximal heart rate. 85% of 220-age (Jackson et al., 2009) or 95% of 220-age (Edvardsen et al., 2014) 4) subject's rating of perceived exertion (RPE) using the Borg Scale rating or Visual Analog Scale (Church et al., 2008). Consensus of the best criteria to use are varied, with a great deal of subject exclusion in older cohorts where rigid criteria are used (Edvardsen et al., 2014).

Cardiac output, pulmonary diffusion capacity, oxygen carrying capacity, and peripheral limitations like muscle diffusion capacity, mitochondrial enzymes, and capillary density are all determinants of $O_{2MAX}$. If one of these factors is not functioning properly, as might be expected in ageing and disease, then this will affect

O2MAX. Since this test is the most widely used and most accurate measure of aerobic fitness, this test has been adopted as the method of choice in this thesis.

### 1.5.4. Predictive $O_{2MAX}$ tests

In many cases, it is not feasible to carry out a full O2MAX. test and thus predictive tests are used to estimate O2MAX. where ventilation information is not available. Validated tests include the Storer Maximal Bicycle Test (Storer et al., 1990) and the submaximal Rockport Walking Test (George et al., 1998), The 1-Mile Jog Test (George et al., 1998), Single Stage Submaximal Treadmill Test (Waddoups et al., 2008) and The YMCA Submaximal Bicycle Test (YMCA, 1989), which have been shown to correlate with O2MAX. at an R > 0.85. The most well validated however, is the Storer Maximal Bicycle Test which has R>0.93, by accounting for variance associated with age, gender, weight and maximal load (Storer et al., 1990). End-tidal measurements make O2MAX. a favourable measure of fitness, however calculation of predicted O2MAX is an interesting measure to complement O2MAX since it can account for gender differences in O.

## 1.6 Aerobic exercise for improving cerebrovascular health

The British Heart Foundation (Townsend et al., 2015) recommends that adults engage in physical activity for >10mins per day, totalling 150mins of moderate exercise or 75mins vigorous exercise per week, in order to maintain health and wellbeing. Whilst exercise-related benefits have been well documented in chronic systemic illnesses such as cardiovascular disease, cancer, diabetes, obesity, hypertension and osteoporosis (Warburton et al., 2006), the benefits to the brain have only been addressed in the past couple of decades. A great deal of research is now focussing on the long-term side effects of inactivity upon mental health and cognition, and whether exercise should be recommended as a preventative measure for cognitive decline and general cerebral health. In review of the neurological

changes that are taking place in the brain therefore, we need to look to research from both humans and animals.

### 1.6.1. Cognitive Function associated with Exercise

Maintaining a physically active lifestyle has been associated with benefits to cognitive function and differences in cognitive functioning can provide a useful metric by which to assess the beneficial outcomes of exercise (Dupuy et al., 2015; Wendell et al., 2013). Meta-analyses have demonstrated that the greatest benefits occur on measures of executive control such as task coordination, planning, goal maintenance, working memory, and task switching (Colcombe and Kramer, 2003; Dupuy et al., 2015). These declines, particularly when they escalate to dementia, can have a dramatic impact on the independence, safety, activities of daily living, and overall quality of life of older adults. A cross-sectional study in older highly fit and aerobically trained individuals, showed task relevant increases in prefrontal and parietal cortices, which are regions involved in spatial selection and inhibitory functioning (Colcombe et al., 2004). Interventional studies have also reported alterations in WM (Colcombe et al., 2006; Voss et al., 2013) and GM (Erickson et al., 2011) structure within task functionally relevant regions, as well as functional alterations in fMRI BOLD during a motor task in regions including the hippocampus and frontal lobe (Voelcker-Rehage et al., 2010).

Few studies have observed any cognitive benefits of physical activity in young people, due to ceiling effects in the tests used, or compensatory strategies that may mask impaired functioning in implicated brain regions (Hillman et al., 2006). Studies that have detected fitness related differences in young adults have measured performance on tasks sensitive to executive function, such as the stop signal reaction time task (SSRT) (Mujika and Padilla, 2001), Stroop (Dupuy et al., 2015) and task switching (Kamijo and Takeda, 2010), although the evidence is not unequivocal and it has been recommended that only strongly theoretically driven tasks be used (Etnier et al., 2009).

### 1.6.2. Cerebrovascular benefits of exercise: Ageing and Disease

The view that cerebrovascular health may mediate the positive association between physical exercise and a better cognitive reserve, is becoming increasingly widespread (Davenport et al., 2012). In a study of women aged 50-90 years old, it was found that physically fit women had a lower resting arterial pressure (MAP) and greater cerebrovascular tone (cerebrovascular conductance (CVC)) than sedentary women, and that these cerebrovascular measures were predicted by $O_{2MAX}$. Fitness in addition to measures of macrovascular health are also able to predict global cognitive function, particularly in domains of cognitive speed, verbal ability, perception, and executive function (Brown et al., 2010).

MRI studies have provided further evidence for the mediating link between fitness and cognitive function. Using ASL, Zimmerman et al., (2014) reported that age-related declines in CBF could be explained by declines in aerobic fitness and that CBF was related to alterations in MAP. In a short term interventional study, subjects aged 57-75 years carried out a 12-week aerobic exercise intervention, 3 times/week and PASL MRI was carried out at 3 time points at baseline, mid and post training. Higher resting CBF was observed within the anterior cingulate and hippocampus, following exercise and hippocampal CBF was correlated with improved memory performance after just 12 weeks of training (Chapman et al., 2013), indicating that CBF may be the mediating factor between ageing and cognitive function, and that this can be moderated by exercise, at least in later life.

### 1.6.3. Cerebrovascular benefits of exercise: Young adulthood

There is some evidence that has reported a positive association between chronic physical activity and cerebrovascular functioning in young healthy adults. In a cross-sectional TCD study involving sedentary and aerobically trained healthy young and older adults, Bailey et al. (2013) reported a positive relationship between fitness ( $O_{2MAX}$) and 1) resting blood flow velocity of the middle cerebral artery (MCAv) as well as 2) MCAv response to hypercapnia (cerebrovascular reactivity). In another

study of young and elderly adults, a 12-week aerobic intervention did not find a fitness related elevation in resting MCAv although an MCAv CVR did increase by 10-15% (Murrell et al., 2013). Barnes et al. (2013) however, observed a positive relationship between MCAv and $O_{2MAX}$, both at rest and in response to hypercapnia, but only in elderly adults and not in the younger cohort.

The scarcity of research reporting exercise related differences in cerebrovascular function suggests that we need to identify more sensitive markers of vascular health. It is fundamentally important to understand whether exercise is beneficial earlier in life, despite the absence of any apparent cognitive decline since exploring this question in late adulthood may mean missing a critical window for preventative interventions, whereby health, mobility and task processing become more difficult with age. It is also worth noting that naturally occurring variation in fitness levels within the general 'non-athletic' population is narrow, and it may be that the absence in the observed association between fitness ( $O_{2MAX}$) and outcome measures of cerebrovascular health cannot be teased apart where the sample is tightly clustered around the norm. Studying a broader range of fitness levels within an experimental sample may help resolve this issue.

### 1.6.4. Cerebrovascular benefits of exercise: Preclinical Studies

Despite its common usage as a marker of cerebrovascular health, what drives alterations in CBF between individuals is less clear since it can be due to a number of mechanical, neuronal and chemical factors which are difficult to quantify non-invasively in the human brain. The benefit of using animal models, is the ability to measure neuroprotective physiological and cognitive enhancing effects of physical activity since potential to manipulate exercise intensity (aerobic vs anaerobic), duration (chronic vs acute) and methods (voluntary wheel running vs forced treadmill running) is far more versatile than in humans. The use of non-human animals, is also better suited for determining the physiological and neurochemical mechanisms that underpin some of the macroscopic effects described above. Observing changes in the human brain non-invasively enables us to guide the questions we ask in non-human studies. Interpreting similar MRI differences in combination with the molecular

context, then allows us to translate our findings from rodents back into interpretation of human MRI research.

Evidence from preclinical research studies suggest that exercise may exert its mediatory effects by a range of mechanisms. Production and release of neurotrophins such as vascular endothelial growth factor (VEGF; Udo et al., 2008), brain derived neurotrophic factor (BDNF; van Praag et al., 1999) and nerve growth factor (NGF; Hall et al., 2013) are shown to be upregulated in the rodent brain following either voluntary wheel or forced treadmill running. Release of these neurotrophins can explain the growth of vessels (angiogenesis) (Bloor, 2005; Isaacs et al., 1992; Muramatsu et al., 2013; Rosenstein et al., 1998; Swain et al., 2003; Udo et al., 2008; Wälchli et al., 2014) and neurons (neurogenesis) (Brown et al., 2003; Creer et al., 2010a; Gould et al., 1999; Sahay et al., 2011) and neuronal plasticity (Allen and Messier, 2013; Ferris et al., 2007) that have also been associated with running activity. Elevation of glutamate transporters on epithelial cells of capillaries of running animals has been observed (Allen and Messier, 2013) which may relate to increases hippocampal metabolites such as glutamate and glutamine (Biedermann et al., 2012). Cytogenetic alterations have also been reported as result of exercise where cerebral mitochondrial respiratory capacity is increased within the striatum (Herbst and Holloway, 2015) whilst spine density (Stranahan et al., 2007) and progenitor cell survival in the hippocampus is increased (Herbst and Holloway, 2015).

Several these mechanisms are known to be altered in neurodegenerative diseases. In this thesis, we were interested in whether exercise and/or fitness might mediate some of these mechanisms, and their outcomes, in a clinical disease such as Huntington's Disease for which 1) there is a need for therapeutic targets, 2) diagnosis can be made prior to symptom onset such that physical exercise is a feasible recommendation, 3) both mouse models and patient cohorts are readily available for assessment and 4) there is a cognitive and motor symptom profile by which to assess the possible benefits of exercise and/or fitness.

## 1.7 What is Huntington's Disease?

Huntington's disease is an autosomal-dominant neurodegenerative disorder in which those affected present with a range of motor, cognitive, psychiatric, and metabolic abnormalities. Disease prevalence is 3-12 cases per 100, 000 (Evans et al., 2013). Patients with HD develop involuntary movements, known as chorea, although deficits in other domains are often present prior to this the onset of motor symptoms. Possibly the largest burden to both patient and carers are the cognitive impairments, behavioural abnormalities and psychiatric changes that worsen with disease progression (Paulsen, 2011). Results from a multinational prospective observational study of Huntington's disease (HD) (TRACK-HD) reports clinical and biological phenotypes of disease progression over three years as well as baseline predictors in people with pre-manifest HD (preHD) and early-stage HD (Tabrizi et al., 2013, 2009). The following sections will detail these genetic, cognitive, neuropsychiatric, motor and neurological impairments further.

### 1.7.1. Genetic profile

Clinical and pathological signs of HD result from an abnormal CAG repeat expansion in exon 1 of the *huntingtin* gene (*HTT*) leading to expression of the mutant huntingtin (mHTT) protein. It is this mutant protein which encodes and gives rise to oligomers and fibrillary structures that ultimately lead to the formation of insoluble protein aggregates within the cytoplasm and nucleus of neurons, which are thought to lead to either a gain of toxic function or a loss of function of the altered protein (Cisbani and Cicchetti, 2012). HD patients typically carry alleles containing more than 35 glutamine-encoding CAG repeat lengths. The mean age of clinical onset is understood to be strongly related to length of the CAG trinucleotide such that the greater the repeat length, the earlier the disease onset, and the worse the severity. A parametric survival model that predicts the age-specific probability of onset has been determined for CAG repeat-lengths between 36-56, with much narrower confidence intervals than described previously. For example, a 40-year-old individual with a repeat length of 42 has a 90-93% chance of symptom onset by age 65 (95% confidence interval) (Langbehn et al., 2011, 2004). Individuals with a

CAG repeat length greater than 55 typically have symptom onset before the age of 20 (juvenile HD) and this makes up an estimated ~5% of all HD cases (Quarrell et al, 2012).

### 1.7.2. Cognitive profile

Cognitive and behavioural symptoms (and signs) of HD are thought to be evident at least 15 years prior to motor diagnosis (Paulsen et al., 2008), where subtle emotion recognition deficits and poorer cognitive performance are observed compared to gene-negative controls (Stout et al., 2011).

Pre-symptomatic Stage. Pre-symptomatic gene-carriers show subtle impairments in recognising facial expressions, such as recognising disgust, which is thought to be an early symptom of decreased insula function (Hennenlotter et al., 2004). More proximal to disease onset are impairments that manifest in a similar pattern to mild cognitive impairment (MCI) , including impairments in visuo-motor performance, working memory and executive function (Kirkwood et al., 2000; Papp et al., 2013). Nearly 40% of participants were found to meet criteria for mild cognitive impairment at this pre-symptomatic stage (Duff et al., 2010). Slowed cognitive processing becomes progressively worse closer to disease onset, which can be detected in tasks of processing speed. These symptoms implicate the early dysfunction of the caudate nucleus and prefrontal cortex (Ho et al., 2003). Impoverished performance on cognitive tests including emotion recognition as well as the STROOP test and Symbol Digit Modalities Test, thought to tap into executive functioning, can be seen in patients with pre-manifest HD <10 years from disease onset, which continues to get worse with disease progression (Tabrizi et al., 2013). Decline in executive function with disease progression implicates striato-cortical dysfunction which is known to be downregulated in HD

Early- Stage. Memory deficits are observed at the more advanced stages of the disease, where deficits are greatest in memory retrieval rather than memory encoding (Rohrer et al., 1999). Compared to Alzheimer's Disease, where the profile of deficits is thought to be more cortical in nature, cognitive deficits in manifest HD

are thought to be more subcortical in origin whereas semantic memory and delayed recall memory are less affected (Ho et al., 2003; Kirkwood et al., 2000).

Late-stage. Towards the more advanced stages HD patients show deficits in tests of verbal fluency, i.e. the ability to retrieve vocabulary whilst suppressing inappropriate or repeated word retrieval. Decline in verbal fluency over time is less marked compared to other executive function tasks, such as the Stroop (Ho et al., 2003), and it has been supposed that fluency deficits are secondary to slowed processing speed and verbal ability (Henry et al., 2005). Slowed processing is a general feature of HD, which manifests also in the motor (bradykinesia) and psychiatric domains (apathy), suggestive of an overlapping neuronal basis (Zamboni et al., 2008). By the late stages of the disease cognitive symptoms are debilitating, although patients can usually still understand speech and recognize familiar faces.

### 1.7.3. Neuropsychiatric profile

According to the Europe-wide REGISTRY study, 20% of patients at all disease stages displayed severe psychiatric problems (Orth et al., 2011). Characteristic features include depression, apathy, anxiety, irritability perseveration and suicidal ideation (Duff et al., 2007; Epping et al., 2014; Tabrizi et al., 2013).

Depression symptoms in the pre-symptomatic stage do not increase with proximity to formal HD diagnosis (Epping et al., 2014) unlike the majority of cognitive symptoms. Prevalence is estimated at 33-69% depending on disease stage (van Duijn et al., 2007). Depression has been shown to decrease with disease progression as quantified using the Unified Huntington's Disease Rating Score (UHDRS) motor scale (Van Duijn et al., 2013) which may occur due to adaptation to illness and acceptance of their diagnosis. It has also been suggested that neurodegeneration of the CNS and communication of negative emotional states is impaired.

Apathy encompasses a loss of initiation, spontaneity, motivation, interest and concern about self-care. Compared to depression more generally, prevalence and severity of apathy is known to increase with disease progression (Tabrizi et al., 2013).

Prevalence rates vary between 34-76% for apathy depending on disease stage and measurement criteria (van Duijn et al., 2007). Apathy is negatively associated with worse global and executive functioning and use of medicines such as neuroleptics and benzodiazepines (Duijn et al., 2010)

Anxiety is also a prominent symptom, with prevalence estimated between 13% and 71% depending on the sample and rating scale used (Dale 2015)

Irritability is a prominent symptom of both pre- and symptomatic HD with an estimated prevalence of between 38-73% (Paulsen et al., 2008) and has been shown to be associated with impulsivity and aggression, presumed to be driven by an underlying disruption to emotional processing circuitry. Irritability has been found to increase with motor impairment (Van Duijn et al., 2013).

Psychosis and other symptoms. Less commonly experienced psychiatric symptoms include psychosis, delusions, hallucinations (van Duijn et al., 2007). Obsessive and compulsive symptoms, such as repetitive behaviours, inflexibility, perseveration, and preoccupation with idiosyncratic topics are common features of HD whereby obsessive symptoms are twice as prevalent as compulsive symptoms (Anderson et al., 2011).

Suicidal Ideation. Suicidal ideation co-occurs with depression, anxiety and irritability as well as by substance abuse. HD patients have a suicide rate which is 4-6 times higher than the normal population with 19% pre-symptomatic patients reporting current suicidal ideation (Wetzel, et al., 2011).

### 1.7.4. Motor profile

Subtle motor symptoms such as oculomotor deficits, slowed movement speed, weak tongue protrusion, slowed reaction time, and abnormalities in muscle stretch are observable even prior to clinical diagnosis (Kirkwood et al., 2000; Smith et al., 2000). Slow motor tapping speed can be detected more than 10 years prior to symptom onset, whilst other motor symptoms such as tongue and grip force is not affected until <10 years prior to symptom onset (Tabrizi et al., 2013). Accurate diagnosis of

clinical onset depends therefore, on the sensitivity of the measure used. Formal diagnosis of adult-onset HD is made after the onset of a motor symptom profile including chorea, coordination deficits, poor handwriting, oculomotor dysfunction and rigidity. With disease progression, involuntary movements become more pronounced, patients often present with dystonia and parkinsonism as well as difficulties with balance, speech, gait, swallowing, manual dexterity, and slowed voluntary movements. Towards the end of life, language and mobility is jeopardised because of deficits such as rigidity and bradykinesia. Loss of muscular control often leads to difficulty swallowing as well as bladder and bowel control (Girotti et al., 1988; Tabrizi et al., 2009).

### 1.7.5. Neurological Deficits

#### *1.7.5.1. Microscopic changes*

Toxic function of the mHTT manifests in a number of cellular changes that produce HD pathology. Although HTT protein expression is ubiquitous at the cellular level, selective neuronal loss occurs in the medium spiny neurons (MSNs) of the striatum with sparing of the cortical interneurons. Ninety-five percent of the striatum is made up of these (GABA)-ergic projection medium spiny neurons (MSN's), with just ~ 5% classified as interneurons. Neuronal loss extends to other brain regions including the cortex, thalamus and sub-thalamic nucleus as the disease progresses. Microscopic changes begin in the head of the dorsal caudate and progress to the ventrolateral striatum. Protein aggregates form specifically within the nucleus, cytoplasm and neuronal processes, known as neuronal inclusion bodies (IBs) (Vonsattel and DiFiglia, 1998). These IBs appear to occur in higher concentrations within the cortex than the striatum, although the role of the aggregates is still not fully understood (Arrasate and Finkbeiner, 2012) and it has been suggested that aggregation of mHTT may be a coping mechanism to clear toxic mHTT from the cell. A number of paths by which mHTT may cause cell death have been proposed. Studies in a number of HD mouse models find that mHTT alters histone acetyltransferase activity, and indicate that aberrant activity of this enzyme might underlie transcriptional dysregulation in Huntington's Disease.

Mitochondrial damage within striatal cells has also been linked to metabolic deficiency in HD patients. Mitochondrial dysfunction facilitates impaired Ca2+ homeostasis which has been linked to the glutamate receptor-mediated excitotoxicity. Interactions between mHTT and neuronal functioning is thought to lead to glutamate excitotoxity, thereby increasing cell vulnerability. Even in the absence of excessive levels of glutamine, the increased vulnerability of the cell means that even normal amounts glutamine can cause excitotoxins to be expressed (Damiano et al., 2010).

Furthermore, an abnormal increase in the number of astrocytes and microglia have been reported, possibly in response to immune activation as an early defence mechanism (Lobsiger and Cleveland, 2011).

#### *1.7.5.2. Macroscopic changes*

Post-mortem and MRI studies have shown gross atrophy throughout the brain of HD patients, which increases throughout the disease. The earliest effects occur in the striatum which is comprised of the caudate nucleus and the putamen (Domínguez et al., 2013) where volume decreases of ~56% have been reported (Lange et al., 1976). Further basal ganglia including the globus pallidus and cortical atrophy supports the vulnerability of striato-thalamo-cortical circuitry in HD (Rosas et al., 2003; Tabrizi et al., 2009). Of the cortex, premotor and sensorimotor cortices (Douaud et al., 2006) are particularly affected and longer disease duration has been associated with more widespread cortical changes, suggesting that cortico-striatal circuits are affected in HD.

Two projection pathways from the striatum are thought to define the symptoms observed in HD. A direct pathway projects axons to the globus pallidus or substantia nigra, whilst the indirect pathway projects axons to the external segment of the globus pallidus, and it is the MSN's of the latter pathway that are affected in the early stages of HD, leading to disinhibition of the subthalamic nucleus and thalamus. It is this disinhibition of the thalamus, that leads to overstimulation of the motor cortex and subsequently, the erratic and uncontrolled motor movements that are characteristic of HD (Deng et al., 2004).

The basal ganglia are also known to be involved in many of the cognitive symptoms that manifest in HD through altered cortico-striatal circuitry such as obsessive-compulsive behaviours (Anderson et al., 2011). Functionally distinct cortico-striatal loops have been proposed, that may explain the heterogeneous cognitive symptoms experienced by patients. Core circuits arise from different cortical areas and project to the globus pallidum and substantia nigra via the striatum, then projecting to the thalamic nuclei and back to the frontal cortex. Degeneration in the cerebral cortex however is more likely to underlie the cognitive disturbances in executive function and psychiatric symptoms experienced.

There is now an increasing body of research showing white matter abnormalities are another pathological feature of HD, independent of neuronal loss (Paulsen et al., 2008; Tabrizi et al., 2009). Changes in white matter are thought to occur due to a number of factors, including loss of axons, demyelination, and as a direct effect of grey matter atrophy known as Wallerian degeneration.

### 1.7.6. Cerebrovascular health in Huntington's disease

Alterations in cerebral blood flow (CBF) have been described in several neurodegenerative disorders, including Alzheimer's disease (AD) (Iadecola, 2004), Parkinson's disease (PD) (Borghammer, 2012) and Huntington's disease (Ma and Eidelberg, 2015) suggesting important and likely early commonalities in fairly distinct pathophysiological diseases. In AD, perturbations in microvascular flow have been linked to overexpression of amyloid precursor protein and to precede neuronal dysfunction. It is likely therefore, that alterations in CBF might play an important role in the expression and progression of HD symptoms.

Primarily HD mouse models have been used to probe differences in cerebrovascular health further at a molecular level, although post mortem patient tissue is also used. Visualisation of greater vascular density has been reported in both transgenic and post mortem patient studies (Cisbani et al., 2013; Drouin-Ouellet et al., 2015; Franciosi et al., 2012; Lin et al., 2013), in addition to other morphological changes in the vasculature including alterations in length, lumen size, branching and vessel type (Franciosi et al., 2012; Lin et al., 2013). Blood-brain-barrier permeability has also

been shown to increase with HD, whereby a decrease in the proteins that form the tight junctions of the BBB such as occluding and claudin-5 in the caudate and putamen has been observed in post mortem tissue from HD patients (Drouin-Ouellet et al., 2015).

A few studies conducted in the 1990's showed reduced CBF in the basal ganglia of HD patients secondary to cell loss. Harris et al. (1999) observed perfusion deficits using SPECT in the caudate and putamen in addition to volumetric differences in these regions in patients <6 years from predicted onset. Another study, observed extended perfusion deficits in the frontal and parietal cortices, and a positive linear relationship between executive function and rCBF in the caudate using SPECT (Hasselbalch et al., 1992). However, both SPECT and CT provide relatively low spatial resolution and/or tissue contrast compared to MRI measures. A more recent SPECT study observed a reduced elevation in blood flow during a maze learning compared to rest, than HD negative controls in the caudate and orbitofrontal cortex (Deckel et al., 2000). Whilst interesting, SPECT provide relatively low spatial resolution and tissue contrast compared to MRI imaging, where more regional CBF changes can be examined.

A study by Chen et al. (2012) used PASL MRI where they observed perfusion deficits in cortical regions in which atrophy was not observed, suggesting an important role of perfusion abnormalities in the pathophysiology and regional selectivity of HD. A CASL MRI found decreases in rCBF particularly within the lateral prefrontal cortex, which declined with proximity to motor symptom onset (Wolf et al., 2011). Alterations in CBF are not homogenous however, since in the striatum increases in CBF have been observed in the putamen (Chen et al., 2012) and the pallidum (Wolf et al., 2011). A recent study at 7T used an LL-EPI ASL sequence, and observed a significant increase in arterial CBV in cortical gray matter in the HD cohort but not in the putamen or caudate (Drouin-Ouellet et al., 2015).

## 1.8 Animal models of HD

Following the discovery of the *HTT* gene in 1993 (The Huntington's Disease Collaborative Research Group, 1993), several mouse models have been genetically engineered, and have contributed to our understanding of the pathogenesis of HD as well as for evaluating new therapeutics. These HD mouse models differ greatly in terms of the background strain, CAG repeat length, disease onset, presentation and severity.

Genetic mouse models can be grouped into 3 main categories according to how they are engineered, N-terminal transgenics, full-length transgenics and knock-in (KI) models. N-terminal transgenic animals carry the 5' proportion of the human *HTT* gene, which contains CAG repeats whereas full-length transgenic models carry the full length *HTT* sequence and express the full length HTT protein containing the expanded CAG repeats. In comparison, knock-in mouse models, have an HD mutation which is directly manipulated by varying the number of CAG repeats at the *huntingtin (Htt)* genomic locus. As a result, phenotypes of the disease vary greatly because of the species of origin, repeat length, background strain and promoters that drive expression.

### 1.8.1. Knock-In (KI) Mouse Models

In contrast to N-terminal and full-length HD transgenic models, KI HD models are generated by insertion of a CAG repeat mutation into the endogenous animal Huntingtin (Htt) gene via homologous recombination techniques or when the animal exon 1 is replaced with the pathologically expanded human exon 1 (Ishiguro et al., 2001; Wheeler et al., 2000). Over-expression of the gene does not occur as there is no change in the number of copies of the gene. The endogenous Hdh promoter means therefore that KI models should produce a similar expression profile to that seen in the human condition and therefore express the complete mutant gene. This makes knock-in models advantageous in that the variability in expression levels and tissue distribution is eliminated compared to microinjection based HD models. As a result, effective manipulation of the *Htt* gene dosage (i.e. one mutant and one normal

allele) has enabled the generation of an allelic series of knock-in mice that differ in CAG repeat length, and enable us to investigate the influence of CAG size on disease phenotypes. As a result, KI models more closely reflect the genetic context of human patients with HD. Knock-in models may contain either expanded CAG repeat length within an unmodified murine gene (e.g. Hdh (CAG (150)) or a chimeric human/mouse exon 1 carrying both the expanded CAG repeat region and the human polyproline region (e.g. CAG 71, CAG 94, CAG 140, and the zQ175 models.) The severity of motor and cognitive symptoms as well as age of symptom onset tend to correlate with the CAG repeat length and are thought to resemble the pre-symptomatic stages of HD.

### 1.8.2. Q175 Knock-in Mouse Line

Genetic Background. The HdhQ175 (zQ175) mouse line is one of the more recently characterised knock in lines (Menalled et al., 2012). This mouse-line was derived from a spontaneous expansion of the CAG repeat number identified in a litter from a CAG 140 KI colony (Menalled, 2005) derived by Scott Zeitlin. Founder mice from this litter were used to establish a novel colony carrying around 175 CAG repeats, leading to the name zQ175. The inverse relationship between age of HD onset and CAG repeat length means that the zQ175 mouse line is expected to produce a more robust and earlier abnormal phenotype in both heterozygotes (HETs) and homozygotes (HOMs).

Behavioural characterisation has shown more potent deficits in homozygous animals than in heterozygous animals when compared to wild-type littermates and have an overall decreased life span (Menalled et al., 2012). Where the human condition is characterised by a single allelic mutation, heterozygous zQ175 animals were chosen for investigation in this thesis as they may be more realistic in terms of the severity of symptoms seen in humans than the homozygous animals. Because these mice exhibit a more rapid disease progression compared to earlier mouse-lines carrying fewer repeats, progression of HD symptoms can be observed within a shorter period, making this a more robust model for long term assessment than transgenic HD models, or those carrying shorter repeat lengths.

Motor Impairments. HOMs display a reduction in grip strength from 4 weeks of age, hypoactivity in open field testing as young as 16 weeks of age (36 weeks in HETs), increased rearing at 8 weeks of age decreased latency to fall from the rotarod at 30 weeks (HOMS and HETS). HETs show increased rearing frequency at 2-4 months of age (Heikkinen et al., 2012; Menalled et al., 2012) and altered gait from as early as 1 month of age (G. A. Smith et al., 2014).

Cognitive Impairments. Deficits in HET mice in a more complex visual discrimination reversal task with a touchscreen have been found previously (Murphy et al, unpublished). Deficits in procedural response learning in zQ175 HOM mice was seen at 58 weeks but no impairment was detected in the HET mice. HOMs showed impaired performance on the procedural two choice swim test, a discrimination learning test of stimulus – response association, at 12months compared to WT mice, but HETs showed no difference (Heikkinen et al., 2012). Decreased alternation on the Y-maze and a decreased capacity to nest build has been reported at 16 months (G. A. Smith et al., 2014).

Neurological Impairments. Behavioural validation and longitudinal characterisation with MRI has been carried out. Whereas Heikkinen et al. (2012) reported whole brain, cortical and striatal volumetric decreases in HOM but not HET Q175 mice using MRI at 12months of age, a histological study by Smith et al. (2014) did observe significant cortical thinning and striatal volume decreases in HET Q175 at 12 months compared to WT controls. Metabolic deficits in glutamate transmission compared to WT controls in both HOM and HET has also been observed by 12 months using magnetic resonance spectroscopy MRI (MRS) (Heikkinen et al., 2012). Electrophysiological examination revealed early hyper excitability of MSNs of HET zQ175 animals at 4 months of age and evidence for striatal IB's within the striatum has been in HET Q175 mice from 6 months of age (G. A. Smith et al., 2014). Further still, decreased levels of the synaptic protein, dynein, in the striatum at 6 months of age as well as changes in cytoskeletal and axonal transport at 12 months of age (Smith et al. 2014).

## 1.9 Treatment options in HD

HD is a heterogeneous disease, whereby each patient displays a different symptom profile. Current treatment options are limited to symptomatic therapies as there are currently no available treatments that are known to slow the neurodegeneration or loss of function known to occur with disease progression. Over the last ten years however, there have been many more clinical trials for symptomatic and small molecular therapies that are being trialled.

### 1.9.1 Symptomatic treatments

*Motor Symptoms.* Drugs that act to reducing dopamine neurotransmission, via presynaptic depletion or via D2 receptor blockade, are thought to reduce excessive movement and is the basis of most pharmacological treatments for movement. Tetrabenazine (TBZ) is the only medication currently FDA-approved for treatment of chorea in Huntington's Disease and works by reversibly inhibiting the vesicular monoamine transporter 2 (VMAT-2) in the CNS (Hayden et al., 2009). Since VMAT-2 packages dopamine, serotonin and norepinephrine from the cytoplasm into presynaptic vesicles, inhibition leads to premature degradation of these monoamines. Although this drug is useful for reducing symptoms of chorea via dopamine depletion, a side-effect is depletion of serotonin and norepinephrine can worsen symptoms of depression and anxiety, symptoms which are already more likely in patients with HD (Huntington Study Group, 2006). Furthermore, depletion of dopamine itself can also give rise to extrapyramidal symptoms including parkinsonism and dysphagia. More recently, a randomized, double-blind, placebo-controlled trial found promising effects of deutetrabenazine (SD- 809) on chorea, in which deuterium-carbon bonds require more energy for cleavage such that that fewer and lower doses are needed to obtain the same benefit as TBZ (Huntington's Study Group, 2017). A comparator study between TBZ and SD-809 is needed to compare the efficacy of these drugs better.

Another common option are antipsychotics, as they may simultaneously act to improve psychiatric symptoms associated with HD. Antipsychotics such as haloperidol, olanzapine, rispiridol and fluphenazine are commonly used, however

they have varying affinity for the D2 receptor, and as such, vary in their ability to control chorea. They also lead to a range of extrapyramidal side effects and controlled research studies have shown only mixed effect on chorea. Atypical antipsychotics are also poorly supported by research evidence to support their use in patients with HD.

Amantadine, is an NMDA antagonist has anti-dyskinetic properties in Parkinson disease, and thus might be expected to treat chorea in HD. High doses of amantadine are thought to be required to reduce chorea, but also leads to side effects including sleepiness, hallucinations, confusion, insomnia, agitation, and anxiety (O'Suilleabhain and Dewey, Jr, 2003). Riluzole, is another anti-glutamatergic drug thought to alleviate excitotoxicity, but this drug failed to yield improvement in functional independence, chorea, behavioural symptoms or cognitive symptoms, compared to those of placebo in a large 3-year RCT (Landwehrmeyer et al., 2007).

*Cognitive Symptoms.* There is currently a lack of good evidence for any drugs that can be used to enhance cognition in HD. There have been a few small open-label studies which suggest improvement in cognitive testing after treatment with short- and long-term treatment with rivastigmine (Sešok et al., 2014), but these rely on sufficient cognitive tests to detect alterations following drug administration. Memantine is a non-competitive glutamate receptor antagonist that stabilizes glutamatergic tone and it has been suggested that this might benefit patients with HD by reducing excitotoxicity caused by large amounts of glutamate coming into the striatum from the cortex and thalamus. One small, open-label study observed a potential neuroprotective effect following long-term treatment in HD (Ondo et al., 2007) but this warrants replication. In the absence of efficacious drug therapies, supportive measures should be recommended, including strategy formation, such as providing cues, minimizing multitasking, and time allocation for cognitive training.

*Psychiatric Symptoms.* Depression is the most common psychiatric symptom of HD. Despite this, in a review of the European HD cohort (REGISTRY) of 1,993 patients, only half that reported moderate to severe depression were on medications for their symptoms (Duijn et al., 2014). A systematic review reported a lack of sufficient evidence to guide anti- depressant treatment in HD (Moulton and Mrcp, 2014),

although anecdotally, patients appear to respond well to selective serotonin reuptake inhibitors (SSRIs) (Wyant et al., 2017). For example, SSRIs, fluoxetine and citalopram appear to have the most notable effects on a self-reported measure of depression (Beglinger et al., 2015). VenlafaxineXR is an SNRI (selective noradrenergic reuptake inhibitors) that has been found to improve depressive symptoms after 4weeks of treatment (Wyant et al., 2017). Other behavioural disturbances include apathy, OCD, anger, irritability and psychotic episodes in a small number of individuals (van Duijn et al., 2007). For adjunctive therapy, anti-psychotics and mood-stabilizing antiepileptic drugs (AEDs) are favoured by clinicians, such as valproate, carbamazepine, lamotrigine, and topiramate (Wyant et al., 2017). However, with little research evidence to suggest the efficacy of these drugs, education of families and caregivers on trigger identification and behavioural strategies is favoured in combination with a supportive, structured environment with routines and cue identification.

### 1.9.2. Disease Modifying Therapies

Since the discovery of the Huntington's disease gene, there have been many attempts at disease modification based on likely functions of the huntingtin gene and on theories of neuronal injury. Despite this, we do not fully understand the important functions that huntingtin protein (HTT) plays in the brain, or exactly how mHTT causes the disease. Ideas have ranged from metabolic interventions to protect neurons, to cell transplantation and gene silencing therapies. There is also an ongoing work looking for genetic modifiers that determine symptom onset and non-pharmaceutical interventions that may delay the progression of the disease.

#### *1.9.1.1. Cell-based therapies*

Animal research has provided promising evidence for the use of foetal primary transplants. Transplantation of embryonic striatal tissue grafts following an excitotoxic lesion have been shown to not only survive and proliferate, but to also express a range of cellular markers characteristic of neuronal viability and behavioural phenotypes that are characteristic of normal striatal function (Mazzocchi-Jones et al., 2009; Dunnett, 2010). Clinical trials using foetal primary transplants

have produced mixed results, with evidence of a short-term but not long-term clinical improvement (Dunnett and Rosser, 2014). A multi-site study of 5 transplanted patients across the UK (NEST-UK) yielded non-significant long-term benefits 10 years post-surgery (Barker et al., 2013). A caveat of this line of research is the limited supply of donor tissue such that standardisation and quality control is a challenge. Alternative transplantation options using human cells lines include 1) embryonic stem cells (ESC's) derived from blastocysts 2) foetal stem cells, neural progenitor cells taken from an embryo, foetus, or neonate, 3) adult neural stem cells, with neural progenitor cells isolated from the adult sub-ventricular zone (Vazey and Connor, 2010) 4) embryonic germ cells that are isolated from the gonadal ridge of the embryo, 5) non-neural stem cells, such as adult bone marrow stem cells or umbilical cord cells, and 6) induced pluripotent stem cells (iPS cells) which can be generated from adult human fibroblasts (Mattis et al., 2013). Whilst promising, further work is needed to improve reliability of transplant survival, whilst simultaneously tackling the practical, ethical and regulatory difficulties in this field (Dunnett and Rosser, 2014).

#### *1.9.1.2. Gene-based Therapies*

*Reducing Huntingtin Expression.* Gene-based therapies offer a potential powerful treatment option for the future by targeting the expression of mHTT. Such strategies are known as "gene silencing" because they act by down-regulating transcription or preventing translation of mHTT, although no approach is expected to completely stop mHTT expression altogether. These approaches are considered among the most promising emerging therapeutics for prevention of HD and include 1) RNA interference (RNAi) using short interfering RNA (siRNA); 2) translational repression using single-stranded DNA-based antisense oligonucleotides (ASOs); and 3) transcriptional repression using zinc finger proteins (ZFPs). By reducing the levels of mHTT protein in this way, it is hoped that disease progression will be delayed or halted by mitigating it at the source. The IONIS-HTTRx is an antisense oligonucleotide drug (ASO) delivered via intrathecal injection that binds to huntingtin RNA and signals the cell to destroy it and is currently in phase 1 clinical trials. This technique has already been shown to reduce HTT expression in mice by approximately 75% following injection into the lateral ventricle (Kordasiewicz et al., 2012). Ongoing clinical trials are taking place with the hope that the benefits of

lowering the toxic mHTT protein will significantly outweigh the potential side effects of lowering wild-type HTT, since it is unknown what the effect of lowering wild-type HTT is in humans. Allele selective silencing methods circumvent this by targeting the mutant allele selectively to achieve allele-selective knock-down, or by identifying single nucleotide polymorphisms (SNPs) on the mutant allele so that allele- selective mHTT silencing for a certain percentage of HD mutation carriers, can lead to an individualised genomic medicine (Lombardi et al., 2009). However, targeting polymorphisms increasing the chance of off-target effects. Finally, Zinc-finger proteins (ZFPs) can repress protein production by reducing transcription (Papworth et al., 2006). Successful selective repression of mHTT and reduction of motor manifestations have been reported in the R6/2 HD mouse model (Zeitler et al., 2014) and therefore provides an exciting avenue for genome editing work in the future.

*Protein Homeostasis.* After expression has occurred, mHTT interacts with other proteins, undergoes post-translational modification, forms intra-nuclear and cytoplasmic aggregates, and may be cleared through autophagy. There are therefore, several potential therapeutic targets under investigation, but prioritization is limited by our understanding of the most toxic HTT species. The most prominent targets have been reviewed in a paper by Wild and Tabrizi, et al (2014) and include small-molecule kinase inhibitors which modulate N-terminal mHTT phosphorylation (Atwal et al., 2011), infusion of gangliosides (e.g. GM1) thought to improve membrane functioning and cell signalling (Pardo Di et al., 2012), upregulation of chaperone proteins to reduce harmful misfolding of mHTT (e.g. HSJ1a (Labbadia et al., 2012), TCP1-ring complex (Trice) (Kitamura et al., 2006) and ApiCCT1) and upregulating autophagy for mHTT clearance by therapies such as mammalian target of rapamycin (mTOR) inhibition (Ravikumar et al., 2004) and promoting acetylation with inhibitors such as Selisistat which inhibits deacetylase sirtuin 1 (M. R. Smith et al., 2014).

*Histone Deacetylase Inhibition.* Histone deacetylase (HDAC) inhibitors such as suberoylanilide hydroxamic acid have been under study for several years, with the aim of correcting transcriptional dysregulation. Suberoylanilide hydroxamic acid has been shown to regulate transcription through chromatin modification and have been shown to ameliorate the motor phenotype in R6/2 mice (Hockly et al., 2002). Systematic work has shown HDAC4 to be the only HDAC among 11, to ameliorate

the HD phenotype in mouse following genetic knockdown. Potent, selective small-molecule inhibitors of its enzymatic function have been developed and the noncatalytic functions of suberoylanilide hydroxamic acid are currently under study (Benn et al., 2009).

*Phosphodiesterase (PDE) Inhibition.* Detailed study of phosphodiesterases (e.g. PDE10A and its pharmacological inhibition) is underway to validate it as a therapeutic target in HD. PDE10A is almost exclusively expressed in the striatum (Coskran et al., 2006) and its function is linked to the synaptic biology of MSNs whose death is a prominent feature of HD. PDE10A regulates cyclic adenosine monophosphate (cAMP) and cyclic guanosine monophosphate signalling, synaptic plasticity and the response to cortical stimulation (Threlfell and West, 2014), which are known to be impaired in HD. In the R6/2 mouse, PDE10A inhibition with TP-10 has been found to ablate motor deficits, reduce striatal atrophy and increased (BDNF) levels in HD (Apostol et al., 2008).

*Mitogen-Activated Protein Kinase (MAPK) Cell Signalling.* Abnormal MAPK signalling is a feature of HD. Over-activation of the MAPKs JNK (c-Jun terminal kinases), ERK (extracellular signal-regulated kinases), and p38, and the upstream kinase mixed lineage kinase 2 (MLK2), is seen in HD (Gianfriddo et al., 2004). Small-molecule approaches to activate MKP-1 and ERK, or to inhibit MLK2, JNK, and p38 (Taylor et al., 2013), are being explored, but the pathways, roles, targets and means of modulating these pathways are incompletely understood.

*Neurotrophic Factors Depletion.* Depletion of BDNF is characteristic in Huntington's Disease. BDNF is produced by cortical interneurons and promotes neuronal growth, survival, and plasticity, especially within striatal neurons affected prominently in HD, and BDNF is thought to protect against excitotoxicity (Zuccato et al., 2010). Restoration of neurotrophins including BDNF and glial cell–derived neurotrophic factor (GDNF), is problematic since protein-based drug delivery to the CNS is difficult. Delivery using viral or stem-cell vehicles have shown some potential, for example intraparenchymal AAV-mediated delivery of the GDNF analogue neurturin to the putamen in PD has been shown to be safe and well-tolerated (Jr et al., 2010). Small-molecule agonists such as TrkB agonists, have been developed to mimic the effects

of BDNF with some success (Simmons et al., 2013). Another approach is to target the transcriptional dysregulation that partly underlies the BDNF deficiency in HD, for example a compound, C91, has been found to increase BDNF mRNA levels in Htt-knockdown and mHTT-expressing zebrafish models (Conforti et al., 2013).

### 1.9.2. Environmental enrichment

In the absence of successful pharmacological treatments, researchers have begun looking for more holistic approaches by which to either optimise general neuronal health or work in concert with other cellular or gene treatments to optimise outcomes. Physical, social and cognitive interventions, may bring us closer to a disease-modifying treatment in HD.

#### *1.9.2.1. Cognitive training*

Cognitive training, with a particular focus on tasks of executive function, have been conducted in patients with Parkinson's (Milman et al., 2014; París et al., 2011) and Alzheimer's disease (AD) (Bahar-Fuchs et al., 2013) and have shown promising evidence for improvements in both cognitive and motor outcomes. A recent study in the Q111 mouse model, observed that an operant attentional training task improved motor performance 8 months later, compared to those that had not received training (Yhnell et al., 2016). Future investigations of cognitive training programmes in HD patients is warranted to explore these effects further.

#### *1.9.2.2. Environment*

Environment has been suggested to play a role in the variability of HD age-of-onset, according to the U.S. –Venezuela Collaborative Research Project (Wexler, 2004). This research estimated that 60% of the variance in age of onset, unexplained by CAG repeat length, lies in the shared environmental factors between siblings and 40% is attributable to other genetic factors e.g. polymorphisms in genes that encode neurotransmitter receptors, energy metabolism, Htt-interacting proteins, stress response, synaptic processes and apoptosis (Arning and Epplen, 2013) . Shared and non-shared environmental factors have thus received an increasing amount of scientific attention and as such there has been an increasing number of preclinical and clinical support for physical and cognitive activity, stress and diet as potential

modulators of HD onset and progression. These are nicely summarised in a review by Mo et al. (2015). Typically, environmental enrichment is operationalised by providing objects, food and bedding in the home cage. In a study by Hockly et al. (2002), even minimal enrichment, including the addition of a cardboard tube and bedding yielded slower decline in Rotarod performance in R6/2 transgenic mice compared to non-enriched controls. Perhaps the most promising research has shown that environmental research may be more beneficial in altering the psychiatric symptoms associated with mood. A study in R6/1 transgenic mice, showed that home cage enrichment, including larger cages, and novel objects led to a reduction in anxiety and reduced stress response but non depressive-like symptoms (Renoir et al., 2013).

It is known that an enriched and healthy lifestyle is beneficial, and can improve brain health, such that it is not absurd to believe that such factors would benefit patients, however evidence in mice is not consistent (Skillings et al., 2014) and there remains an absence of well-controlled studies to address the effects of environmental enrichment in humans.

#### *1.9.2.3. Exercise*

To date, it is not known to what extent exercise is beneficial to patients with HD. There is growing belief that exercise delivered in home and community settings may be of functional benefit in other neurodegenerative disease such as MS (Rietberg et al., 2005) and PD (Goodwin et al., 2008), that cannot be explained by the impact of environmental enrichment.

Studies in HD mouse models have been mixed. Voluntary wheel running has been shown to delay onset of motor symptoms (Pang et al., 2006; van Dellen et al., 2008), preserve cognition (Harrison et al., 2013; Kim et al., 2015; Pang et al., 2006) and reduce neuropathology by improving mitochondrial function (Herbst and Holloway, 2015) and altering striatal mHTT expression (Harrison et al., 2013). Other findings have suggested that exercise may actually increase neuropathology including reduced BDNF production, sparser MSN spines (Döbrössy and Dunnett, 2006) impoverished motor and cognitive function and reduced striatal volume (Potter et al., 2010).

Only a few studies have employed exercise interventions in HD patients, ranging from balance training or a combination of muscle strengthening, stretching and cardiovascular exercise. Findings have ranged from patients showing preserved (Zinzi et al., 2007) or improved (Quinn and Rao, 2002) balance, cognitive and motor performance, whilst reported case studies have suggested that exercise cannot delay onset (Altschuler, 2006) or may in fact be detrimental. A recent randomised clinical trial (RCT) in Huntington's disease patients, observed improved performance in measures of gait speed, balance, function and level of physical and no related adverse events (Khalil et al., 2013a). A 12-week intervention involving a weekly supervised gym session of stationary cycling and resistance exercises in addition to a twice weekly independent home-based walking program, yielded improvements in cognition and walking (Busse et al., 2013). Results from the first multi-site longitudinal RCT, where a 12week intervention of progressive exercise three times per week including aerobic (stationary cycling) and strengthening exercise are the most promising so far for the feasibility, safety and motor improvements (UHDRS mMS) of exercise is HD patients.

Large scale RCT's are needed to investigate the clinical potential of exercise, using neuroimaging outcome measures such as macrostructure, microstructure and cerebrovascular changes in response to exercise that can be performed longitudinally. To date, the benefits of physical exercise or cardiorespiratory fitness have not been assessed using MRI methods. Piloting of feasible, reliable and informative MRI measures related to exercise in HD patients is warranted before these measures can be introduced into large scale RCTs and will be the goal of this thesis.

# Chapter 2

# Investigating the relationship between aerobic fitness and cerebrovascular health in young adult males using PASL MRI.

## Chapter Summary

The primary aim of this chapter is to examine whether MRI correlates of cerebrovascular health are associated with cardiorespiratory fitness in a cohort of healthy young adult subjects. The second aim was to explore the feasibility of these MRI measures before applying them in Chapter 4, to a patient population. As outlined in the General Introduction, there is a mounting array of research that has highlighted the importance of the cerebrovasculature for efficient brain metabolism. In this chapter, we address the challenge of identifying whether and, if so, how exercise may exert these beneficial effects on the brain by focusing on potential MRI biomarkers of cerebrovascular health. The present study uses pulsed arterial spin labelling (PASL) techniques to explore the relationship between cardiorespiratory fitness and markers of cerebrovascular health, including resting cerebral blood flow (CBF), cerebrovascular reactivity to $CO_2$ (CVR) during breath-holding. Arterial compliance of the middle cerebral arteries (MCAC) was also assessed using ASL methods, and is the first time this has been assessed in relation to cardiorespiratory fitness. Healthy males aged 20-24 years with varying levels of cardiorespiratory fitness (maximal oxygen uptake ( $O_{2MAX}$) range= 38-76 ml/min/kg) underwent MRI scanning at 3 Tesla followed by cognitive testing in domains previously shown to be influenced by cardiovascular health. Contrary to previous findings, subjects with higher cardiorespiratory fitness demonstrated *lower* GM CBF and *lower* CBF CVR, although the latter was not significant. In line with non-MRI evidence, arterial compliance of the MCA was associated with higher aerobic fitness. $O_{2MAX}$ was not associated with cognitive performance on tests of pattern separation, paired associate learning or the n-back tasks of memory and executive function. The results of the current experiment suggested that exercise-induced differences in

cerebrovascular health can be detected in early adulthood despite the absence of any cognitive differences.

## 2.1. Introduction

It is fundamentally important to understand whether exercise is beneficial earlier in life, despite the absence of any apparent cognitive decline. It is possible that ceiling effects, insensitive cognitive tests or a bias away from reporting null results, has contributed to the absence of reported effects. Exploring this question in late adulthood may be too late for the implementation of therapeutic exercise interventions where motor function may already be impaired, and as such the need for understanding these early physiological processes becomes more important. This warrants continued efforts into the search for sensitive non-invasive biomarkers of cerebrovascular health that precede changes in cognition.

Studies using ultrasound methods have reported improvements in parameters of cerebrovascular health such as resting cerebral blood flow velocity (Ainslie et al., 2008) and cerebrovascular reactivity (Bailey et al., 2013) associated with cardiorespiratory fitness, however these methods often lack spatial specificity, reliability and consistency across individuals (Willie et al., 2011). Evidence has demonstrated that MRI may be a better tool than TCD for assessing fitness-associated changes in cerebrovascular function, as it is a more sensitive and quantifiable measure of regional changes in blood flow (Ainslie and Hoiland, 2014). Nonetheless, TCD studies provide a useful platform from which to direct further investigation. Advances in arterial spin labelling (ASL) magnetic resonance imaging (MRI) have brought us closer to identifying non-invasive biomarkers of cerebrovascular health due to its enhanced spatial sensitivity for quantifying individual differences in whole brain cerebral dynamics (Wolk and Detre, 2013). Application of novel MRI methods, can bring us closer to understanding the relationship between cardiorespiratory fitness and cerebrovascular health.

One mechanism by which exercise may improve cerebrovascular health and prevent cognitive decline, is by preventing the typical vessel stiffening seen with ageing (O'Rourke and Safar, 2005). Non-MRI studies that have used ultrasound imaging and simultaneous arterial applanation tonometry of the arterial waveform have demonstrated that central arterial stiffness is reduced in those who exercise regularly. In a cross-sectional study, Tanaka et al. (2000) found that central arterial compliance

was 20-35% higher in endurance-trained men than in less active controls. Complementary findings have been shown in the radial artery, following a 6-month aerobic exercise intervention, whereby stiffness, as quantified using the radial augmentation index (AIx), declined by 3% as a result of exercise (Tabara et al., 2007). Whilst these findings are insightful, the beneficial effects of cardiorespiratory fitness on cerebral arteries are yet to be adequately addressed.

Due to the inability to assess diameters of intracranial arteries, changes in arterial compliance using methods such as Doppler sonography are only able to inform us about compliance of the vascular bed of the extracranial arteries and not the local stiffness profile of the cerebral vessels themselves (Carrera et al., 2011). Promising advances in ASL methods allow for more precise quantification of the *local* arterial wall properties rather than those distal to the site of measurement (Warnert et al., 2014; Warnert et al., 2015). This method relies on ASL to measure changes in arterial blood volume (aBV) within the major cerebral arteries throughout the cardiac cycle. Given the novelty of this method, the present experiment is the first to probe MCA differences in compliance in relation to cardiorespiratory fitness using PASL.

More established MRI measures of cerebrovascular health include resting cerebral blood flow (CBF) and cerebrovascular reactivity (CVR), although reported changes in these MRI parameters in relation to fitness or exercise is lacking. Cerebral blood flow (CBF) is possibly the most commonly reported parameter of cerebrovascular health in studies that investigate the effects of exercise or fitness, however quantification and definition of blood 'flow' depends upon the method used. Most of the studies to date that have reported fitness mediated alterations in cerebrovascular health (Ainslie et al., 2008; Bailey et al., 2013; Guiney et al., 2014) tend to rely upon TCD measures; reporting resting MCAv (middle cerebral artery velocity) and regulation of MCAv to hypercapnia, as CBF or CVR respectively. As described previously, these methods have their caveats (Ainslie and Hoiland, 2014) such that MRI studies in younger cohorts are still needed to validate these findings.

Data reporting a relationship between cardiorespiratory fitness and resting CBF using ASL MRI in *elderly* cohorts suggest a positive association between cardiorespiratory fitness and grey matter/regional CBF (Thomas et al., 2013b;

Zimmerman et al., 2014) but contrary to TCD findings (Bailey et al., 2013; Chapman et al., 2013) MRI data observed a *reduction* in regional CVR with increased levels of fitness (Gauthier et al., 2014; Thomas et al., 2013). Since CVR is generally considered to be a marker of cerebrovascular health, these results are counter-intuitive, and may in part be attributable to the use of BOLD MRI to measure CVR which is a complex hemodynamic response and may not directly relate to alterations in blood flow or cerebrovascular health (Buxton et al., 1998). Further investigation using ASL MRI methods to measure changes in CBF in younger cohorts is needed in order elucidate and extend our understanding of the association between cardiorespiratory fitness and cerebrovascular health.

The present study examined the potential association between cardiorespiratory fitness $O_{2MAX}$), cognition and a number of cerebrovascular parameters in a cohort of healthy young males. Computer based cognitive tasks known to tap into aspects of hippocampal and executive function were chosen since performance on these are thought to be influenced by exercise (Colcombe and Kramer, 2003). Indirect evidence of the systemic vasculature suggests a relationship between $O_{2MAX}$ and vascular compliance (Vaitkevicius et al., 1993) leading us to hypothesise that the same would be true of the cerebrovasculature, as measured using ASL by assessing the compliance of the MCA. In the absence of sufficient ASL research in highly fit young adults, it was also hypothesised that those with higher aerobic fitness $O_{2MAX}$) would show elevated resting CBF such as that seen in highly-fit elderly cohorts (e.g. Zimmerman et al., 2014). Furthermore, this study hypothesised that CBF CVR to $CO_2$ during breath-holding, would show a similar relationship to that reported in previous fMRI studies (Gauthier et al., 2014; Thomas et al., 2013), whereby an inverse relationship has been demonstrated between $O_{2MAX}$ and BOLD CVR. To maximise the variance within our sample, we recruited participants across a range of fitness levels. Exploring fitness related differences in measures of cerebrovascular health in young adulthood will help to shed light on the possible mechanisms underlying the benefits of exercise on the brain.

## 2.2. Methods

### 2.1.1. Participants

Eleven healthy males, aged 20-24 years old, provided informed consent under ethical approval from the University of South Wales (USW) and Cardiff University School of Psychology Ethics Committee, and all experiments were performed in accordance with the guidelines stated in the Cardiff University Research Framework (version 4.0, 2010).

Initial recruitment took place at USW. Recruitment was carried out to maximise the range of cardiorespiratory fitness within the sample. Participants who regularly engaged in aerobic exercise were recruited from running and cycling clubs whereas other subjects were recruited through University-wide advertisement and word of mouth. During session 1 at USW, subjects underwent a detailed clinical examination that included 12-lead functional diagnostic exercise electrocardiography and were excluded if they showed signs of any cardiovascular, cerebrovascular or respiratory disease. Participants were also screened by self-report for any neurological or psychiatric illnesses, regular smoking or prescribed medication. Testing at Cardiff University (session 2) was carried out within 6 months of $VO_{2MAX}$ assessment and subjects who reported any change in their physical activity patterns between experimental sessions were excluded from the study.

### 2.1.2. Fitness testing ( $O_{2MAX}$) (Session 1)

Online respiratory gas analysis (Medgraphics, MA, USA) was performed during an incremental cycling exercise test to volitional exhaustion on an electronically braked, semi-recumbent cycle ergometer (Lode Corival, Cranlea & Company, UK) for the specific determination of ventilation, $O_2$ and $CO_2$. The test began with 2 minutes of rest, followed by 5 minutes of unloaded pedalling (0W) and increased by 5W every 10s thereafter. Participants were required to maintain a cadence of ~70 revolutions per minute (RPM). Maximum exertion and corresponding $O_{2MAX}$ was confirmed when at least two of the following established criteria were met: 1) Failure to increase $O_2$ with increasing exercise load 2) a respiratory exchange ratio (RER; the ratio

between PET $CO_2$ and PET $O_2$ during cycling) of >1.15, or 3) a heart rate within 10 beats of an age-predicted maximum (*i.e.* 220 – age in years) (Barnes et al., 2013).

### 2.1.3. MRI data acquisition (Session 2)

All scanning was carried out using a 3T GE HDx scanner (GE Healthcare, Milwaukee, WI, USA) equipped with an 8-channel receive-only head coil. All participants underwent whole brain $T_1$-weighted structural scans (3D FSPGR, 1x1x1 $mm^3$ voxels, TI= 450ms, TR =7.8ms, TE = 3ms) for registration purposes.

#### *2.1.3.1. Arterial compliance and Resting CBF*

Tissue perfusion (or CBF) can be measured with ASL by magnetically labelling blood before it reaches the volume of interest. This method is typically used to measure tissue perfusion which represents delivery of blood to the capillary bed, usually at an inversion time (TI) of >1sec after the label has been applied. Before reaching the capillary bed, blood must first flow through the *macrovasculature* of the brain, namely the arteries and arterioles, which have arrival times of <1sec. Imaging at shorter TI's therefore results in images of arterial blood flowing through major arteries such as the middle cerebral artery. Using the multi-TI sequence described below, acquisition over a range of inversion times from short (250ms) to long (2000ms) enables examination of the signal arising in both arterial and tissue compartments for measuring arterial compliance or resting CBF respectively.

A multi-inversion time (MTI) PASL acquisition was performed (PICORE with a QUIPSS II cut-off at 700ms (Wong et al., 1998)). Ten inversion times (TI's) were acquired, whereby short (TI's = 250, 350, 450, 550, 650ms) medium (TI's = 750, 850) and long TI's (TI's = 1,000, 1,500, 2000ms) were acquired as separate scans in which the label (width 200mm) was applied 10mm below the most proximal slice. Images were acquired with similar parameters to those described elsewhere (Warnert et al., 2015b) using a spiral gradient echo sequence (TE=2.7ms) with the following acquisition parameters: a variable repetition time (1,000ms to 3,400ms), eight control–tag pairs per TI, 12 slices, slice gap=1mm, voxel size=3x3x7$mm^3$. Total acquisition time was ~18 minutes. For quantification of perfusion, a ($M_0$) calibration scan was acquired without labelling in which the same acquisition parameters were applied as above except for the TR=4s. Brachial artery blood pressure (BP) was

measured at 3 time-points across the scan session using an MRI-compatible BP cuff (OMRON, Tokyo, Japan).

#### *2.1.3.2. Cerebrovascular Reactivity (CVR)*

A breath-hold paradigm was carried out as described elsewhere (Bright and Murphy, 2013). Breath-holding as a form of gas-challenge was chosen for a number of reasons. It is more time efficient and easier to administer than other gas modulation paradigms and importantly, we wanted to assess the feasibility of the paradigm for use in patient cohorts (Chapter 4). Breath-holding removes the uncomfortable presence of a face mask within the head coil, and is self-directed such that it allows the patient to abort the task at any point, thereby improving safety and providing reassurance for the patient where recruitment is troublesome.

Participants were instructed to complete 5 end-expiration breath-holds (15s each) interleaved with 30s periods of paced breathing at rate of 12 breaths per minute (Murphy et al., 2011b). After each breath-hold the subject was cued to exhale first to obtain a measure of peak end-tidal $CO_2$ (fig. 2.1) Total scan duration was ~4 minutes during which quantitative arterial spin labelling (PASL) and BOLD-weighted images were acquired with a single-shot PICORE QUIPSS II (Wong et al., 1998) pulse sequence (TR=2.2 s, TI1=700ms, TI2=1500ms, 20-cm tag width, and a 1-cm gap between the distal end of the tag and the most proximal imaging slice) with a dual-echo gradient echo (GRE) readout (Liu et al., 2002) and spiral acquisition of k-space (TE1=2.7ms, TE2= 29ms, flip angle=90°, field of view (FOV)=22 cm, 64×64 matrix). Twelve slices of 7mm thickness were imaged, with an inter-slice gap of 1mm.

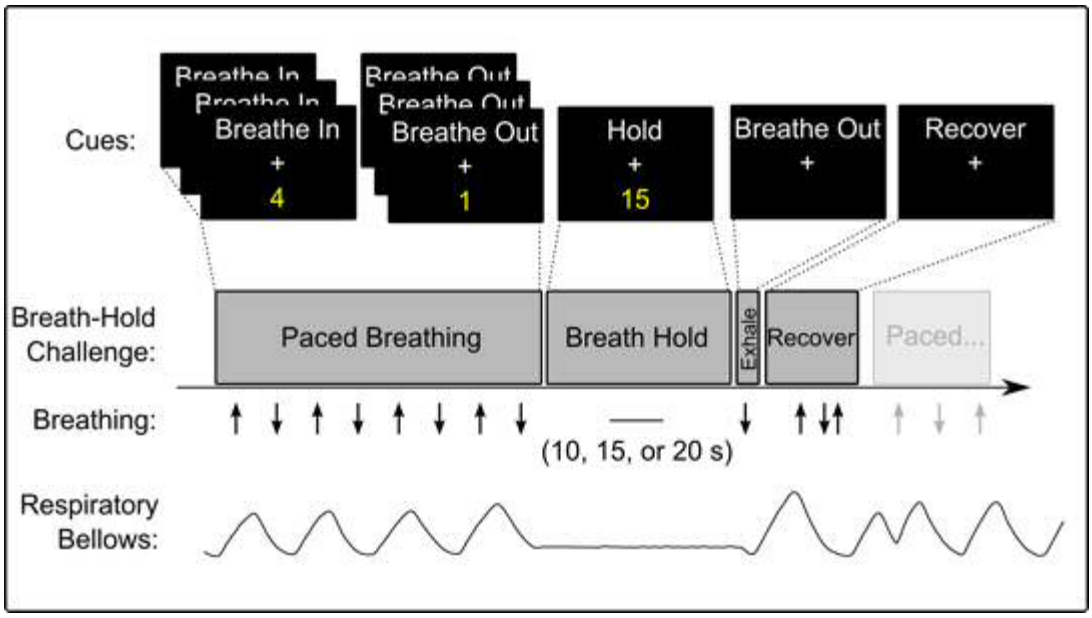


**Figure 2.1 Breath-hold paradigm.** Each breath-hold challenge (N=5, duration=15s) was preceded by paced breathing and ended on an exhalation. Participants were instructed to produce a small exhalation following the hold to provide accurate end-tidal measurements. An example trace from the respiratory bellows is provided (figure adapted from Bright & Murphy, 2013).

#### *2.1.3.3. Physiological Monitoring*

Throughout scanning, the cardiac pulse was recorded using a finger plethysmograph and a pneumatic belt just below the ribcage was used to measure the respiratory cycle. Expired gas content was monitored continuously via a nasal cannula whereby end-tidal O2 and CO2 data were recorded using a rapidly responding gas analyser (AEI Technologies, PA, USA) to provide representative measures of arterial partial pressures of both gases at the prevailing barometric pressure.

### 2.1.4. MRI Data analysis

#### *2.1.4.1. Physiological Noise Correction*

Physiological noise correction was carried out on the raw data using a modified RETROICOR pipeline (Glover et al., 2000). For the raw CBF data, the 1st and 2nd harmonics of the cardiac and respiratory cycles (and the interaction term) were calculated, as well as variance related to end-tidal $CO_2$, end-tidal $O_2$, heart rate, and respiration volume per time (RVT; Birn et al., 2009) using a general linear model framework and subsequently regressed from the raw CBF signal. For the MCAC

data, only respiratory noise correction was performed since the cardiac trace was necessary for retrospective synchronisation of aBV maps across the cardiac phase.

#### *2.1.4.2. ROI masking*

MCAC masking. Masking was carried out as described previously (Warnert et al., 2015b). For each participant, an average ΔM image was obtained for the full-time series of TI=750ms. Regions of interest were determined based on data from TI=750ms because on average this has been shown previously to be the TI with the maximum intensity in the raw difference images (Warnert et al., 2015b). An ΔM image mask was created such that each slice only contained the 5% of voxels with the highest intensities. Broad ROIs were manually drawn around the bilateral MCAC territories within each slice. Each of the broad masks was multiplied by the thresholded ΔM image to produce the ROI maps (~6 slices).

Resting CBF and CVR masking. Individual whole brain tissue segmentation was performed on the $T_1$-weighted images using the FMRIB automated segmentation tool (FAST; Zhang et al., 2001). Individual temporal, occipital, frontal and parietal lobe masks were defined by registration of MNI lobular masks to subject's individual grey matter mask's derived from FAST using FMRIB's Linear Image Registration Tool (FLIRT; Jenkinson and Smith, 2001).

#### *2.1.4.3. Arterial Compliance Quantification*

Arterial compliance measurements were carried out using the methods described by (Warnert et al., 2015b). Arterial blood volume (aBV) within the bilateral middle cerebral arteries (MCA) was assessed in systole and diastole (fig. 2.2). Brachial artery blood pressure cuff recordings were averaged over three time points to calculate average systolic and diastolic BP for each subject. Only data from short TI's (250-850ms) were necessary for deriving aBV to ensure that signal being measured was originating from the arteries rather than the tissue.

To determine systole and diastole, the cardiac cycle was divided into 5 phases using the finger plethysmography trace. The short TI images were retrospectively organized into the 5 cardiac phases and an arterial input function was fitted voxel-wise for each of the 5 phases. Fitting of the acquired images were retrospectively

synchronised to account for a 225ms delay between the cerebral and finger pulse (fig. 2.2a). This time period was deduced from delay times found in the literature between the R-peak in the electrocardiogram and the left finger (Myllylä et al., 2012) and the time delay between R-peak in the ECG and the onset of the carotid pulse wave (Holdsworth et al., 1999). The cardiac phases with the maximum and minimum blood volumes, averaged over both MCA, were used as systole and diastole, respectively.

Voxel-wise differences between $aBV_{Sys}$ and $aBV_{Dia}$ were calculated to reflect arterial distensibility, normalised for the aBV in diastole to produce arterial compliance values of percentage change in aBV/mmHg (%/mm Hg) (fig.2.2.c, d) within the bilateral MCAC mask.

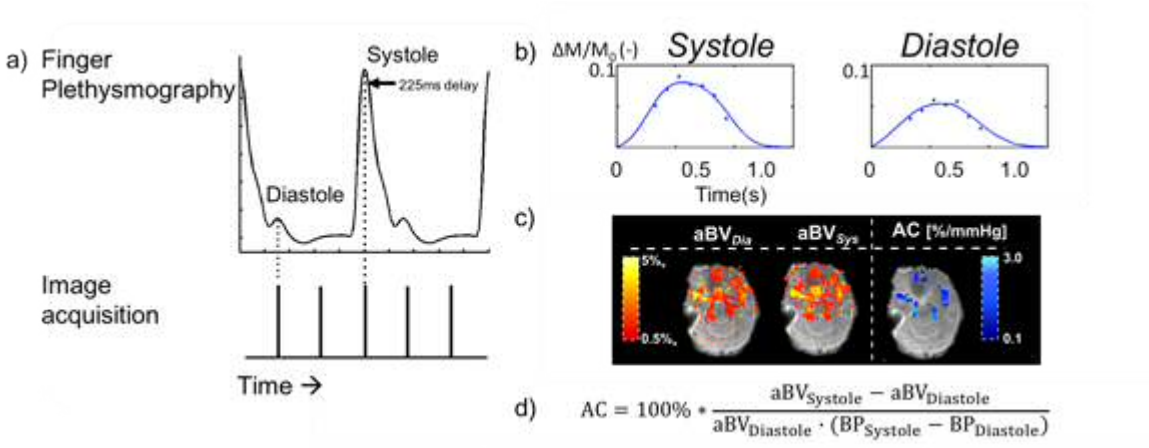


**Figure 2.2 Measuring Arterial Compliance.** (a) Images acquired during scanning are retrospectively synchronised to the cardiac cycle according to finger plethysmography. (b) Signal from images acquired within the systolic pressure phase have greater signal than images acquired within the diastolic pressure phase. (c) Arterial compliance (AC) is quantified by determining the voxel-wise percentage

### *2.1.4.4. Resting CBF Quantification*

The full MTI time series was used for quantification of resting CBF. Signal within the ventricles ($M_{0\ CSF}$) was used to estimate $M_{0\ blood}$ (Lu et al., 2004) and subsequently modelled to calculate whole brain perfusion maps based on the entire MTI dataset using FSL BASIL toolbox (FMRIB Software Library, Oxford, UK). Whole-brain and

lobular grey matter masks were applied to CBF maps to produce average GM CBF estimates within each region.

#### *2.1.4.5. Cerebrovascular Reactivity Quantification*

Simultaneously acquired CBF and BOLD time-series images were corrected for head motion with MCFLIRT (Jenkinson et al., 2002), brain-extracted (Smith, 2002) and spatially smoothed with a Gaussian kernel of 6 mm using SUSAN (Smith and Brady, 1997). BOLD images were calculated from the second echo data using interpolated surround averaging of the tag and control images to yield a BOLD weighted time-series, as described previously (Liu and Wong, 2005). The first echo data were used to calculate a subtraction time-series (Murphy et al., 2011a) from which CBF was quantified to the standard single-compartment CBF model (Wong et al., 1998).

BOLD and CBF time-series data were converted to percentage change in the signal relative to the baseline (mean) of the time-series to produce a %ΔBOLD and %ΔCBF time-series respectively. Signal was averaged across whole-brain GM and lobular GM ROIs. A regression analysis was performed to measure %ΔBOLD/ %ΔCBF per mmHg change in absolute end-tidal $CO_2$ with a 3rd order polynomial included to remove slow signal drift. Temporal lag-fitting (time-shift steps of 0.1s) was also carried out, to account for the delay between end-tidal $CO_2$ increase in response to breath-holding and the subsequent blood flow response (Bright and Murphy, 2013). CVR was thus defined as the beta-weight from the regression model, where BOLD and CBF were measured in units of %BOLD/mmHg or %CBF/mmHg respectively. Whole-brain and lobular grey matter masks were applied to the CVR time-series to produce average CBF and BOLD CVR estimates within each region.

### 2.1.5. Cognitive Testing

The cognitive testing session was conducted prior to the MRI scan session and lasted approximately 30 minutes. Testing was conducted in a quiet testing room at Cardiff University Brain Research Imaging Centre (CUBRIC). Participants carried out each test in isolation to prevent distraction and were informed to instruct the experimenter between tests.

#### 2.1.5.1. N-back (2-back)

To test working memory, a version of the N-back task was used. This task requires on-line monitoring, updating, and manipulation of remembered information and is thought to place great demands on a number of key processes within working memory (Owen et al., 2005). The *n*-back task has been shown previously to vary with aerobic exercise training in subjects of different ages (Hansen et al., 2004; Voelcker-Rehage et al., 2010).

The task was developed and validated at Cardiff University using MATLAB 2012b software (MathWorks, Natick, Mam USA)), using the Psychophysics Toolbox extensions (Brainard, 1997; Pelli, 1997; Kleiner et al, 2007). During this task, the volunteer was required to monitor a series of numbers as they appeared on an LCD screen positioned in front of them, and to respond whenever a stimulus was presented that was the same as the one presented *n* trials previously, where *n* is a pre- specified integer, 0, 1, or 2, such that working memory load increased with *n*. Six blocks were presented for each *n*-back and each block consisted of ten trials, such that there were 60 trials for each load. Scores were calculated as the total number of correct responses within each block, out of 60.

#### 2.1.5.2. Paired Associates Learning (PAL)

To test spatial recognition memory, a paired associates learning task was adopted. Performance on this task has been shown previously to improve with exercise training (Fabre et al., 2002) and is thought to implicate the hippocampus (Yoon et al., 2011), a target region known to be functionally and structurally effected by exercise (e.g. Creer et al., 2010). It is commonly used to assess memory impairments in aging clinical populations (Gould et al., 2005).

The PAL was adopted from a battery of publicly available cognitive assessment tools that were designed and validated at the Medical Research Council Cognition and Brain Sciences Unit (Owen et al., 2010) and made freely available at http://www.cambridgebrainsciences.com.

During this test, subjects were required to remember pattern-location associations (fig. 2.3a). Each box was uncovered for a total of 3 s and then closed again before

the next box opened in a randomized sequence. Participants were required to remember the object located inside each box. Subjects then viewed each object on the centre of the screen after which participants were required to respond by clicking the box in the location in which that object had appeared. Task difficulty increased (+1 box) on consecutive trials, beginning with two boxes being uncovered. Feedback was not provided after each response, although if the choice was correct then the task automatically continued to increase in difficulty, by the addition of another open box. Participants could make three errors in total before the test was terminated. Following an error, task difficulty decreased, and continued to increase on successful trials. Performance was assessed according to the average number of correct object-place associations ('paired associates') in the trials that were successfully completed. The maximum number of possible correct associations was 25.

#### *2.1.5.3. Behavioural Pattern Separation Task – Object Version (BPS-O)*

The BPS-O task was chosen to assess Pattern Separation, a type of recognition memory, known to implicate the hippocampus (Yassa et al., 2011). The BPS-O task has been shown to be a sensitive measure for observing changes in memory performance across the lifespan and may be useful for the early detection of memory impairments (Stark et al., 2013). Better performance and has also been associated with wheel running in mice (Creer et al., 2010b).

Renamed to the Mnemonic Similarity Task (MST) in 2015, this task was designed and validated at the University of California and made freely available at online at http://faculty.sites.uci.edu/starklab/mnemonic-similarity-task-mst.

In the first part of the experiment (implicit encoding), participants were presented 128 pictures (duration=2s) of everyday items and participants were asked to make an arbitrary judgement, by deciding whether the item was an OUTDOOR or an INDOOR item (fig. 2.3b). In the second part of the experiment, participants were presented with 64 of the previously seen pictures (targets), 64 of very similar items (lures), and 64 new items (foils). Participants were instructed to categorize the items as old ('O'), new ('N'), or similar ('S') within 2s. The outcome measure was a score of recognition

memory, quantified as the percent of targets endorsed as ‘‘Old’’ minus the percent of foils endorsed as ‘‘Old’’ (Hits - false alarms).

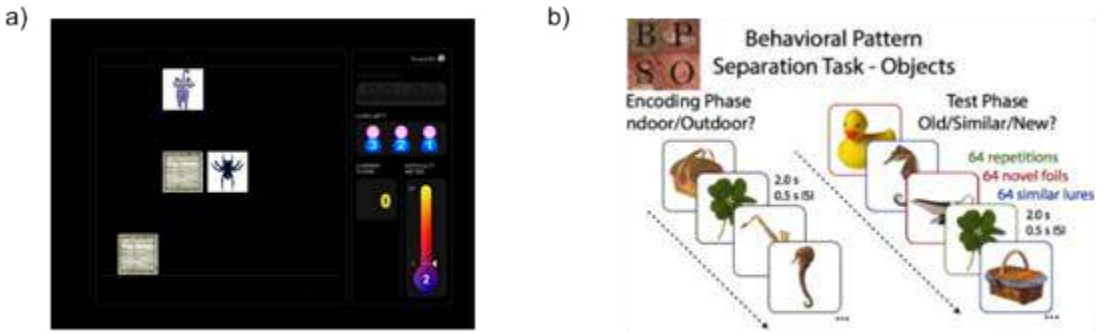


**Figure 2.3 Computerised cognitive paradigms.** (a) Example screen view of the Paired Associate Learning (PAL) task. Participants viewed the contents of each box sequentially after which participants were shown a cue image (e.g. cat) and required to retrieve the location (box) where that image had been seen previously. This task increased in difficulty until a total of 3 errors were made. (b) Behavioural Pattern Separation – Object (BPS-O) task. During the encoding phase participants were required to make an arbitrary indoor/outdoor judgement. During the test phase, participants were required to decide whether a series of images were old, new or similar.

## 2.1.6. Statistical Analysis

To assess whether fitness could predict individual measures of cerebrovascular function and neurocognitive performance linear regression was carried with $O_{2MAX}$ as the predictor variable. Pearson correlation coefficients were used to assess the relationships between MCAC, CVR and CBF where a predictor variable was not predetermined. Repeated-measures analysis of variance (ANOVA) was used to assess differences between ROIs and for cognitive data where there were multiple levels and to assess differences in arterial parameters between systole and diastole. The significance threshold was set at 0.05.

### *2.1.6.1. Data Quality*

Data quality was visually inspected and assessed for outliers using Cook’s distance. Outliers were removed where stated in the Results. Statistical assumptions of parametric testing were assessed (SPSS, version 20) using the Shapiro-Wilks test

to confirm distribution normality and visual inspection of residual values was performed to ensure homogeneity of variance.

#### *2.1.6.2. Bootstrapping*

Unless stated otherwise, bootstrapped confidence intervals (95%) were computed, whereby all linear regressions and Pearson's correlations were bootstrapped to 1000 samples.

Bootstrapping was used as it enables more accurate inferences when the sample size is small and where such that data is not normally distributed. This method depends upon resampling of the sample data such that it is possible to make inference about the population even when the sample data is skewed. For a given sample of data, a bootstrap sample is taken from the original sample and replaced multiple times, with a new mean being calculated for each sample. When this is done repeatedly, i.e.1000 times, a population distribution can be calculated such that the reliance upon assuming normality is removed. Computation of the bootstrap distribution of a parameter-estimator enables calculation confidence intervals for its population-parameter. Samples can subsequently be corrected for bias and skewness between the bootstrap distribution and the sample distribution using statistical software packages i.e. SPSS, such that bias-corrected and accelerated (BCa) confidence intervals (CIs) and adjusted p-values can be calculated.

## 2.3. Results

### 2.3.1. $O_{2MAX}$, Heart rate, Blood Pressure and Body Mass

$O_{2MAX}$ ranged from 38-76 ml/min/kg (57.3 ± 12.7 ml/kg/min) with body mass (76.6± 8.3), systolic BP (122 ±4), diastolic BP (72 ±9), heart rate (63.9 ± 9.5). Participants with higher $O_{2MAX}$ had a lower heart rate, but this was not significant ($r(11) = -0.44$, $p > 0.05$). There was no relationship between fitness and systolic/diastolic blood pressure, body mass or age in this sample (p-values < 0.05).

### 2.3.2. $O_{2MAX}$ and Middle cerebral arterial compliance (MCAC)

Nine participants contributed to the MCAC analysis as two were removed due to severe head movement.

Averaged over all participants, we calculated bilateral MCAC to be 0.41 ± 0.16 %/mmHg. Linear regression revealed a significant relationship between $O_{2MAX}$ and MCAC, whereby fitter individuals showed the hypothesised increase in compliance of the middle cerebral arteries (fig. 2.4a) and this relationship was significant ($r^2$ = 0.64, β=0.01, $F$ (1, 8) =12.6, $p$=0.03, 95% CI [0.003, 0.018]). These values indicate that arterial compliance in the MCA increased by 0.01%/mmHg for each ml/min/kg increase in $O_{2MAX}$.

A second linear regression was performed to rule out the possibility that the relationship between MCAC and $O_{2MAX}$ could be explained solely by differences in resting heart rate. MCAC was not inversely correlated with heart rate ($r^2$ = 0.31, β=-0.01, $F$ (1, 8) =0.75, $p$=0.31, 95% CI [-0.02, 0.03]) as would be hypothesised if a higher stroke volume through the MCAs was mediating this effect.

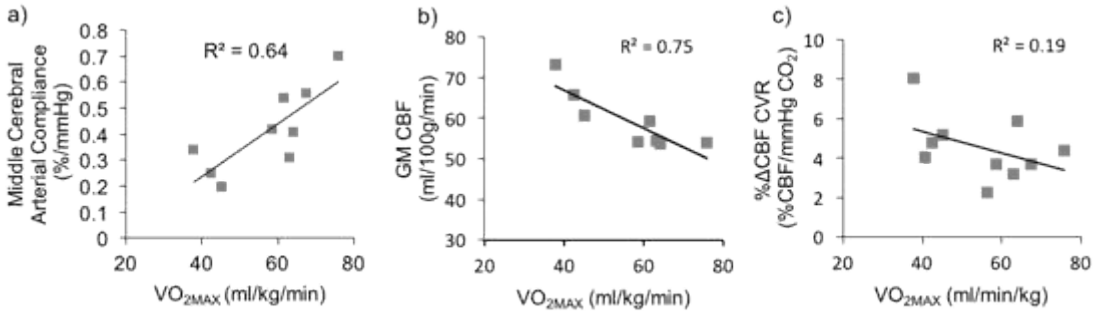


**Figure 2.4. Relationship between $VO_{2MAX}$ and cerebrovascular MRI measures.** Increased $VO_{2MAX}$ is associated with (a) increased arterial compliance within the bilateral middle cerebral arteries (MCA) (b) decreased GM CBF at rest (c) decreased GM CVR.

Retrospective synchronisation of images across the cardiac cycle was inspected to ensure that there was not a bias between the number of tag and control images for a particular TI or phase. A repeated-measures ANOVA revealed that the number of tag and control images did not differ significantly between TI (F (6,48) =1.3, p=0.30,

n.s.) or phase (F (1,8) =0.7, p=0.43, n.s.), nor was there an interaction between the number of images within each phase at each TI (F (6,48) =0.54, p=0.78, n.s.). On average, for a single TI there were 6 tag and 7 control images in diastole, and 6 tag and 6 control images in systole.

Individual parameter maps for aBV (%v) as well as arterial arrival time (Δt), and dispersion (σ) calculated for five different cardiac phases were acquired by fitting the model on a voxel-by-voxel basis. Median values were calculated within the bilateral middle cerebral arteries just above the Circle of Willis in systole and diastole (figure 2.5.) To investigate differences in aBV, Δt, and σ between systolic and diastolic phases, repeated-measures ANOVA was carried out on aBV, Δt, and σ in a single slice above the Circle of Willis. On average aBVSys (3.8±2.9) was 60% higher than aBVDia (2.3±1.5) (range 48-89%) although this was not significant when collapsed across participants (F (1,8) =0.33, p=0.58, n.s.).

On average ΔtSys (501±64) was 41ms longer than ΔtDia (460±96), however this was also not significant (F (1,8) =1.5, p=0.26, n.s.). In addition, σDia (117±37) was on average 1.4ms larger than, σSys (188±35) although this was also not significant (F (1,8) =0.1, p=0.91, n.s.). To address whether variance within the parameter estimates for aBV, Δt, and σ could be attributable to individual differences related to cardiorespiratory fitness, a repeated-measures ANOVA was repeated with $O_{2MAX}$ as a covariate. The interaction term showed that fitness was unable explain the variance in Sys and Dias in aBV (F (1,7) =1.6, p=0.25, n.s.), Δt (F (1,7) =2.5, p=0.16, n.s.) or σ (F (1,7) =1.4, p=0.27, n.s.).

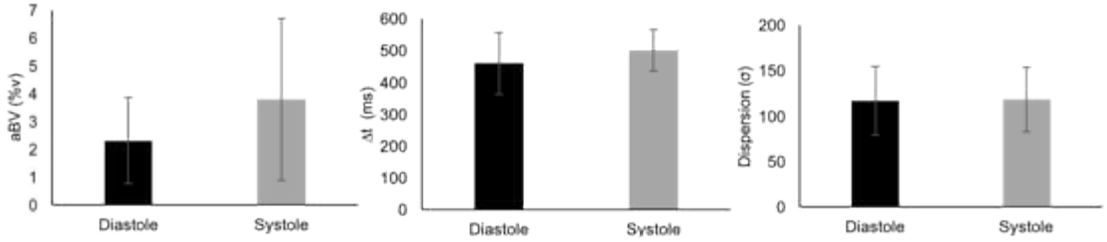


**Figure 2.5 Arterial Flow Metrics.** Regional median results for aBV, Δt, σ for the slice just above the circle of Willis (averaged across subjects). Arterial blood volume, Δt and σ are given for systole (pattern) and diastole (black). Mean ± S.E.M.

### 2.3.3. $O_{2MAX}$ and resting grey matter perfusion (CBF)

Whole-brain GM averaged CBF values ranged from 53.8 - 73.1 ml/100g/min (59.4 ± 6.7). Eight participants contributed to baseline CBF analysis (3 were excluded due to severe head motion). Linear regression revealed a significant inverse relationship between $O_{2MAX}$ and resting whole-brain GM CBF ($r^2$ = 0.75, β=-0.47, $F$ (1,7) =18.3, $p$= 0.03, 95% CI [-0.68, -0.24]; fig 2.3.1b). Whole-brain grey matter CBF decreased 0.47 ml/100g/min for each ml/min/kg increase in $O_{2MAX}$. An inverse relationship was observed within each cortical ROI, however none of these were significant ($p$>0.05; fig. 2.6).

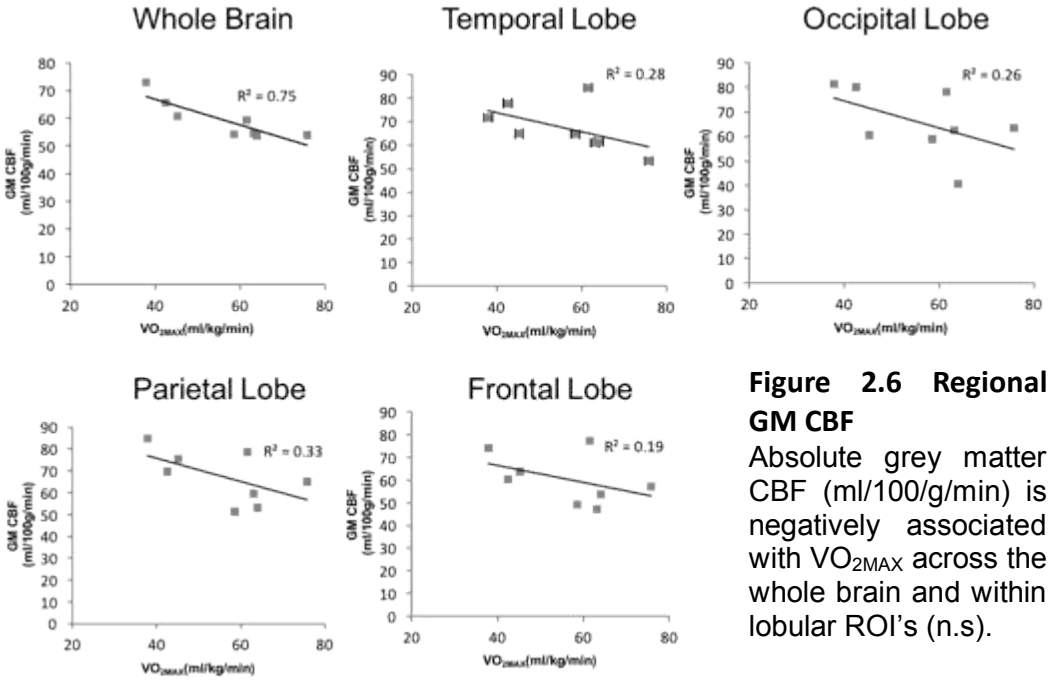


**Figure 2.6 Regional GM CBF**
Absolute grey matter CBF (ml/100/g/min) is negatively associated with $VO_{2MAX}$ across the whole brain and within lobular ROI's (n.s).

### 2.3.4. $O_{2MAX}$ and Cerebrovascular Reactivity (CVR)

Cerebrovascular reactivity data was excluded for one participant because the subject was unable to breathe through his nose, so that 10 subjects contributed to the CVR analysis. BOLD data (fig. 2.7a) demonstrated better signal-to-noise (SNR) than CBF measurements (fig. 2.7b) in response to breath-holding, however, CBF CVR was positively correlated with the BOLD CVR measurements across whole brain GM ($r^2$= 0.52, β=12, $F$ (1,9) =8.8, $p$=0.01, 95% CI [0.034, 0.078]; fig. 2.7c). CBF CVR, like

BOLD CVR showed a decline in CVR with increased $O_{2MAX}$ within whole-brain grey matter (fig. 2.4c) and cortical ROIs (fig. 2.8). Linear regression did not find this to be significant for either the BOLD or CBF response (p-values>0.05). Neither BOLD CVR ($F$ (3,24) =0.69, $p$=0.57, n.s.) or CBF CVR ($F$ (3,24) =0.56, $p$=0.65, n.s.) was found to vary between cortical ROIs in relation to fitness (p-values>0.05).

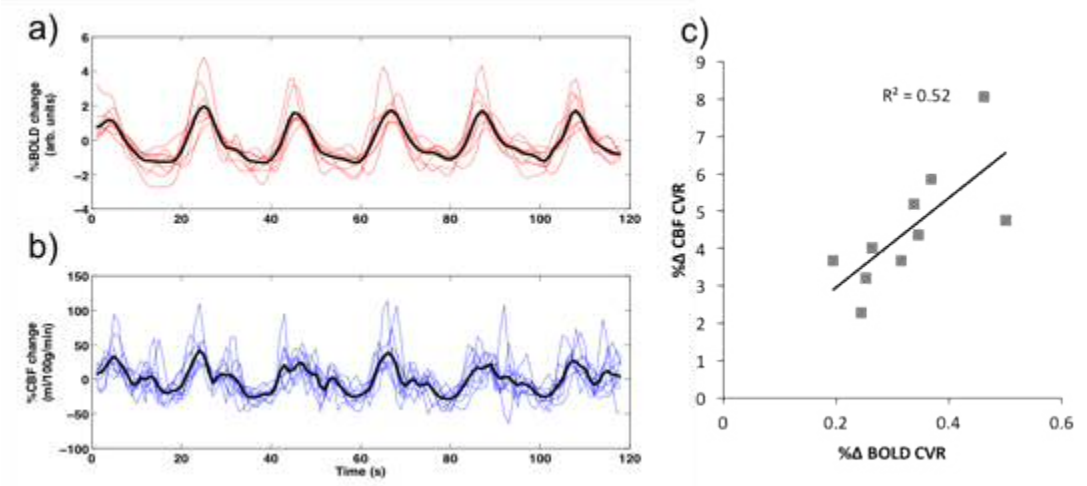


**Figure 2.7 Grey matter BOLD CVR and CBF CVR are correlated.** Individual subject's BOLD (a) and CBF (b) responses to the breath-hold task. Black lines reflect the average response across participants. BOLD time-series showed better signal-to-noise than CBF, but were significantly correlated (c).

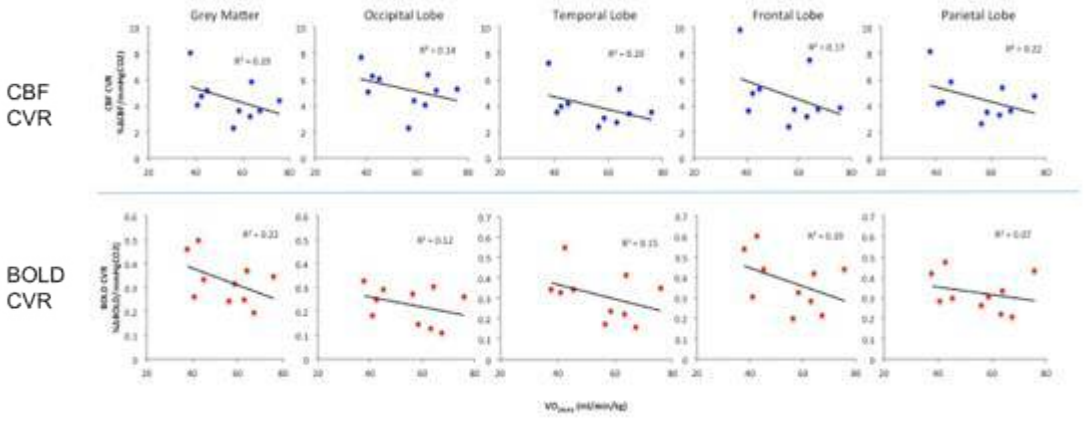


**Figure 2.8 Relationship between $VO_{2MAX}$ and regional CVR.** Percent CBF (top row) and % BOLD (bottom row) CVR was negatively associated with $VO_{2MAX}$ within a grey matter whole brain and lobular regions of interest, however these relationships were not significant.

### 2.3.5. Relationship between measures of cerebrovascular health

Arterial compliance was not correlated with either BOLD CVR ($r$ (7) =-0.20, p=0.68, n.s, 95% CI [-0.89, 0.44]), CBF CVR ($r$ (7) =-0.14, p=0.78, n.s, 95% CI [-0.54, 0.39]), nor with resting grey matter perfusion ($r$ (7) =-0.45, p=0.30, n.s, 95% CI [-0.73, -0.33]). There was, however, a significant correlation between resting grey matter perfusion with both CBF CVR ($r$ (7) =0.76, p<0.05, 95% CI [0.04, 0.95]; fig. 2.9) and BOLD CVR ($r$ (7) =0.78, p=0.04, 95% CI [-0.35, 0.97]) after bootstrapping.

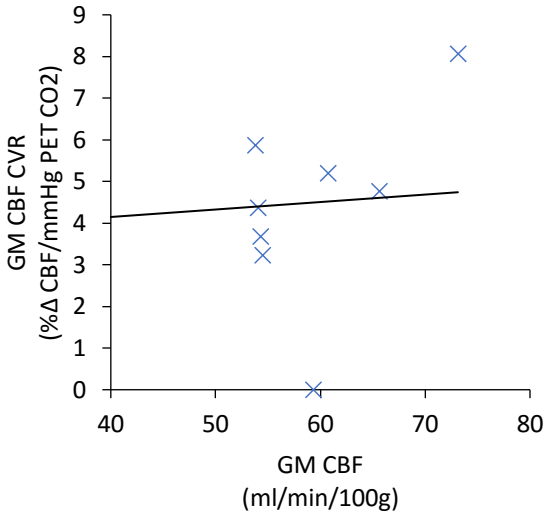


**Figure 2.9 Whole-brain GM CBF and CVR are related.** Grey matter resting CBF and %CBF CVR were significantly correlated (N=7).

### 2.3.6. $O_{2MAX}$ and Cognition

#### *N-Back*

A repeated-measures ANOVA revealed that accuracy decreased as working memory load increased across the group (F (2,20) = 63, p<0.001). Post-hoc t-tests indicated that accuracy for each load significantly differed from accuracy for each of the other loads (means: 0-back 97.3 ± 2, 1-back 81.9 ± 8, 2-back 66.7 ± 9). However, performance did not differ with $O_{2MAX}$ on either the 0 –back ($r^2$ (9) = 0.03, β=-0.05, $F$ (1,9) = 0.25, p= 0.51, n.s, 95% CI [-.47, 0.34]), 1-back ($r^2$ (9)= 0.01, β=-0.002, $F$

(1,9) = 0.001, *p*= 0.99, n.s, 95% CI [-0.45, 0.45]), or 2-back ($r^2$ (9) = 0.08, β=0.21, *F* (1,9) = 0.79, *p*= 0.41, n.s, 95% CI [-2.5, 0.56] fig. 2.10a).

### *Paired Associates*

Participants remembered an average of 5.3 (± 1) object locations. $O2_{MAX}$ was not associated with performance on the PAL task ($r^2$ (9) = 0.06, β=0.007, *F* (1,9) = 0.61, *p*= 0.36, n.s., 95% CI [-0.06, 0.11] fig. 2.10b).

### *Pattern Separation*

Recognition memory across participants averaged 138 (± 16) objects out of a maximum 192 objects, however, was not associated with $O_{2MAX}$ ($r^2$ = 0.06, β=0.30, *F* (1,9) = 0.53, n.s, *p*= 0.5, 95% CI [-0.42, 1.31]). Behavioural pattern separation accuracy, after correcting for response bias, averaged 76(± 7) %, but this was also not associated with $O2_{MAX}$ ($r^2$(9) = 0.33, β=0.37, *F* (1,9) = 1.07, *p*= 0.4, n.s, 95% CI [-0.20, 0.70], fig. 2.10).

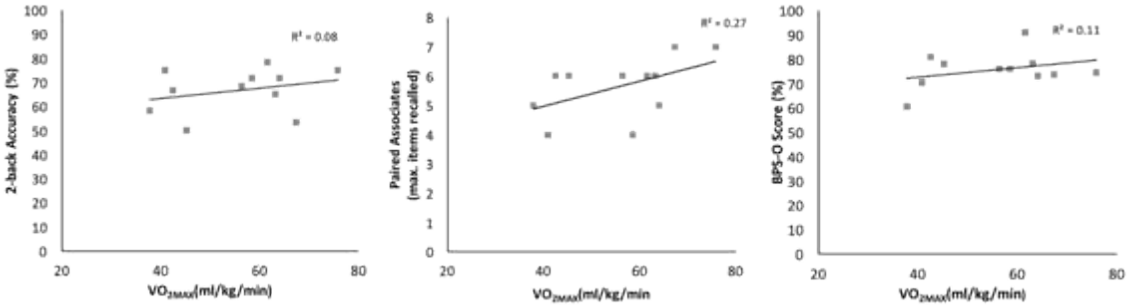


**Figure 2.10 Neurocognitive differences did not differ significantly with $VO_{2MAX}$.** Working memory performance on the **a)** N-back task (2-back block), **b)** spatial object memory on the Paired Associate Learning task (PAL) nor **c)** object recognition memory on the Behavioural Pattern Separation – Object (BPS-O) task were associated with cardiorespiratory fitness ($VO_{2MAX}$).

## 2.3.7. Cognition and cerebrovascular function

To assess whether cognition was related to cerebrovascular function, Pearson's correlations were run to assess whether individual scores on the 2-back, PAL task and BPS-O task were related to MCAC, resting CBF and CBF CVR. There was no

relationship between performance on either the paired associate learning and 2-back tests and any of the cerebrovascular measures. However, a two-tailed test revealed an inverse relationship between CBF CVR and pattern separation performance ($r(10) = -0.66$, $p=0.04$, n.s., 95% CI [-0.95, 0.60]; fig. 2.11) such that reduced CBF CVR predicted better performance on the BPS-O task, however this was no longer significant after FDR correcting for multiple comparisons ($p=0.11$, n.s).

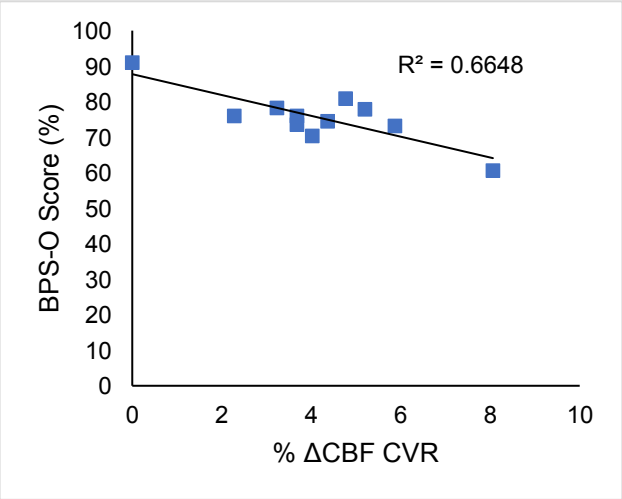


**Figure 2.11 Relationship between CBF CVR and pattern separation performance.** CBF Cerebrovascular reactivity (CBF CVR) showed an inverse relationship with pattern separation performance on the BPS-O task, but this was not significant after correction for multiple comparisons ($p>0.05$).

## 2.4. Discussion

### Key Findings:

- MCA compliance is positively and significantly associated with $O2_{MAX.}$
- Absolute resting perfusion is inversely and significantly related to $O2_{MAX.}$
- CBF CVR is positively and significantly associated with BOLD CVR
- CBF CVR does not vary significantly with $O2_{MAX}$ although a negative trend was evident,
- Cognitive performance does not vary significantly with $O2_{MAX.}$
- Cognitive performance does not vary significantly with cerebrovascular health.

Whilst the benefits of physical activity on cognition and mental health are well established, the physiological mechanisms by which exercise exerts its beneficial effects on the young adult brain remain poorly understood. In this study, we demonstrate that arterial spin labelling MRI is a useful tool for understanding local and absolute changes in blood flow that may shed new light on the exercise-related changes reported previously using alternative methods. We also demonstrate that fitness-related cerebrovascular differences are detectable in the absence of any measured differences in cognitive performance.

### 2.3.8. Compliance of the Middle Cerebral Artery

One proposed mechanism by which exercise is thought to improve cerebral health is by increasing compliance of the cerebral arteries to changes in blood pressure. To date, measures of compliance in relation to exercise have relied upon ultrasound imaging of cerebral arteries, where compliance within the brain can only be inferred. The present study utilised a novel, non-invasive, measure of middle cerebral arterial compliance using PASL MRI to demonstrate the link between cardiorespiratory fitness and MCA compliance in a sample of young males across the spectrum of cardiorespiratory fitness. It was observed that arterial compliance within the middle cerebral arteries is higher in individuals with higher $O_{2MAX}$, consistent with other non-MRI methods in other major arteries throughout the body (Tabara et al., 2007; Tanaka et al., 2000). The present study is the first to use MRI to measure fitness related changes in MCAC and provides promising evidence towards the cerebrovascular benefits of physical activity, as well as insight into the mechanisms at play.

The ability of cerebral arteries to dampen changes in pulse pressure in order to maintain a continuous flow prevents downstream tissue damage where vessels are vulnerable to deterioration (Poels et al., 2012). Arterial compliance, as measured here, can be thought to reflect healthy, more 'elastic' vessel walls, providing efficient blood supply and delivery of nutrients to metabolising tissue (Prins et al., 2005). Improving arterial compliance or preventing age-related arterial stiffening through physical exercise is thought to contribute to the cognitive benefits that have been reported as a result of exercise (Davenport et al., 2012; Mitchell et al., 2011). More compliant cerebral arteries could act to buffer pressure pulses, preventing rupture of

the small vessels and thereby continuing to perfuse neural tissue, such that cognitive function is preserved. Whilst a relationship between MCAC and cognitive function was not observed in the present study, it is possible that preserving cerebral compliance throughout the lifespan by engaging in regular exercise is necessary before these differences in cognitive performance can be detected.

The present findings corroborate indirect evidence from TCD literature that suggests an increase in extracranial compliance with cardiorespiratory fitness (Tanaka et al., 1998). Validation of this link, lends support for future interventional exercise studies, where the mechanisms underpinning this link can be explored further. Such studies should take care to control for how MCAC varies in subjects who perform different *types* of exercise. For example, resistance training has been found previously to reduce AC of the carotid artery where aerobic training leads to increased AC (Miyachi et al., 2003). The present study utilised $O_{2MAX}$ as an index of aerobic fitness, however it would have been interesting to investigate, in the same sample, whether an index of strength, such as a maximum isometric strength test, had an inverse relationship with MCAC, reflecting a decrease in MCAC. Further research into the effects of different types of exercise on AC using this novel MRI method to elucidate this dichotomy is warranted. Current guidelines recommend a combination or resistance and aerobic exercises in order to reduce sarcopenia (age-related loss of muscle mass and strength) and preserve functional capacity however a full understanding of the clinical trade-off between these exercise types is still unclear.

Moderate or higher load of training may be required to influence endothelial function in healthy asymptomatic subjects (Green et al., 2004) where repeated shear stress stimulation is required to drive adaptation (Green et al., 2005). Average compliance across participants in the present study was 0.41%/mmHg (± 0.16) which is consistent with the literature although the range is wider in our sample (0.2-0.7%/mmHg) than reported previously (Warnert et al., 2015b) possibly due to the wide range of fitness levels in our sample. Aerobic exercise is associated with systemic changes in pulse pressure and heart rate, which generate recurrent changes in hemodynamic and shear stress patterns. These differing patterns may differentially affect arterial remodelling (Newcomer et al., 2011) of endothelial and vascular smooth muscle cells that are located within the medial layer of the artery

walls, which regulate the physiological function and the pathological changes that take place within the arterial wall (Peterson et al., 2011). Whilst resting heart rate was lower in fitter subjects, this was not significant in this modest cohort. MCAC was also not related to resting heart rate, suggesting that resting MCAC in fitter subjects is not explained simply by a reduction in heart rate and higher stroke volume through the arteries. It would be interesting to explore the association between MCAC and maximal heart rate when shear stress is thought to occur, however, this data was not available for this thesis. A caveat of the present study was that a full history of the type, duration and intensity of physical activity was not taken. As such it is not possible to determine whether activity type was driving the changes in MCAC observed. Future research may wish to investigate MCAC differences in individuals who perform different activity types e.g. resistance exercise or high intensity training (HIT).

The present study did not find any differences between aBV, arterial arrival times or dispersion between systole and diastole, evidence that has been shown previously as evidence of cardiac pulsatility (Warnert et al., 2015b). Reasons for this difference in findings is likely due to the noise within the present dataset. In the paper by Warnert et al. (2015b) image acquisition was longer such that the number of images acquired was sufficient for retrospective division across 8 cardiac phases, each with sufficient SNR to characterise aBV. In the present study, acquisition was shorter such that images were binned into just 5 phases to maximise signal within each phase, at the expense of accuracy in characterising aBV across the entire cardiac cycle. Whilst the calculated range of aBV, $\Delta t$ and $\sigma$ are within the ranges reported elsewhere (Warnert et al., 2014a; Warnert et al., 2015b), the variance across subjects and across the cardiac phase are greater, and is likely to be attributed to noise in the signal.

The current findings demonstrate improvements in cerebral arterial compliance only in the MCA. Using MRI it is also possible to investigate changes within the posterior and anterior cerebral arteries that branch from the Circle of Willis (CoW) (Warnert et al., 2014a, 2014b; Warnert et al., 2015a). In the present study, a compromise was made between acquisition time and the number of scans run in the session. As such, SNR was too low in these smaller arteries and therefore the data has not been

investigated here. Increasing the number of images acquired during the short TIs, would improve the signal quality and allow more accurate investigation of compliance in these smaller cerebral arteries. Furthermore, the present method is not appropriate for measurement of arteriole compliance, distal from the CoW, where 850ms may be too short to measure labelled blood travelling from the neck into these more distal arterioles. Development of this method in this respect could yield insight into the additional role that arterioles play in maintaining cerebral perfusion (Warnert et al., 2015b).

The present study used peripheral blood pressure (brachial BP) as a surrogate for intracranial blood pressure. The assumption that BP is consistent between the arm and the head is not optimal since pulse pressure in young adults is lower in the carotid than in the brachial artery because the latter is located closer to reflection sites of the pressure wave through the vascular tree (Laurent et al., 2012). It is possible that using brachial BP could result in an underestimation of AC, where pulse pressure within cerebral arteries positioned between the carotid and the capillary bed is likely to be decreased. Invasive measurement would therefore be necessary to obtain local pulse pressures.

### 2.3.9. Grey Matter Perfusion

Contrary to our hypothesis, we report a reduction in resting CBF with increased fitness levels, an effect which is in conflict with much of the existing literature, whereby fitness has been positively associated with blood velocity or flow (Ainslie et al., 2008; Bailey et al., 2013; Zimmerman et al., 2014).

There is a shortage of reported studies that examine cerebral perfusion with ASL in healthy young adults, especially with such a high $O_{2MAX}$ range. Whole-brain GM averaged CBF values ranged from 53.8 - 73.1 ml/100g/min (59.4 ± 6.7 ml/100g/min), which are physiologically consistent, although slightly higher, than the range reported elsewhere in other healthy male cohorts. We attribute this finding to the broader range of fitness levels recruited into our sample. Our study measured CBF throughout the grey matter of the brain, where the signal is derived from the perfusion occurring within the capillaries of the local tissue. This regional sensitivity within the

tissue itself is informative above and beyond TCD measures of arterial velocity in which exercise research has been primarily focussed.

With so few studies measuring baseline grey matter CBF with MRI in young healthy adults with exercise, it is open to speculation as to what may be driving the negative relationship seen in the present study. Possible differences in resting CBF could arise for many reasons such as constriction of the arterioles, changes in capillary density, or an alteration of tissue oxygen utilization. Since exercise has been shown to decrease the intima media thickness (IMT) of the artery wall, thereby increasing lumen diameter and allowing for an *increase* in blood flow through the artery (Sandrock et al., 2008), our observation is unlikely to be due to constriction of arterioles. However, the increase in lumen diameter is not a consistent observation in young subjects (Popovic et al., 2011) and has not been explored in the cerebral arteries, making it worthy of further investigation. It is also unlikely that lower CBF with $O_{2MAX}$ is due to capillary reduction, since a number of preclinical studies have provided evidence for an increase in angiogenesis in the rodent brain with exercise (Swain et al., 2003; van Praag et al., 2005). Conversely, it is possible that angiogenesis could in fact *reduce* the demand for CBF, in a situation where shorter diffusion distances mean nutrient extraction is preserved, thereby requiring less blood flow to the metabolising tissue bed. To investigate this further *ex vivo* preclinical work is needed to validate this link. This raises a useful question as to whether healthy individuals have more efficient mechanisms for oxygen utilization, whereby efficient gas exchange from the capillary bed necessitates a reduction in the amount of flow needed to supply the metabolizing tissue with adequate oxygen.

It has been shown previously, that a reduction in CBF seen *during* exercise was accompanied by an increase in oxygen extraction, resulting in a maintained cerebral metabolic rate of oxygen consumption ($CMRO_2$; Trangmar et al., 2014). The equation $CMRO_2 = CA \times CBF \times OEF$ (where CA is the arterial concentration of oxygen and OEF is the oxygen extraction fraction in tissue) states that if OEF is fixed, then increases in metabolic demands can be met by a proportionate increase in CBF or arterial oxygen concentration. Should OEF and/or arterial oxygen content be increased in athletes, then CBF increase may not be necessary for a given increase in oxygen metabolism.

Future research could use calibrated fMRI measures of oxygen extraction and $CMRO_2$ (Germuska et al., 2016; Merola et al., 2016; Wise et al., 2013) in highly fit individuals, to assess whether metabolic efficiency can explain the inverse relationship between $O_{2MAX}$ and CBF. To assess this hypothesis, datasets from common subjects in which $VO_{2MAX}$ and OEF had been independently measured, were analysed (data permissions from Catherine Foster and Dr Alberto Merola respectively). In this dataset, it was found that OEF was positively associated with $VO_{2MAX,}$ although this only approached significance in this sample of 7 subjects ($R^2$= 0.33, $F$ (1,95) =2.5, $p$=0.17, n.s., 95% CI [-0.001, 0.015]; fig. 2.12). The software package G*Power (v3.1.9.2) estimated that a sample size of 15 subjects is needed to achieve satisfactory power based on the effect size observed in this pilot study. This can be deemed as a promising explanation and useful avenue for future research.

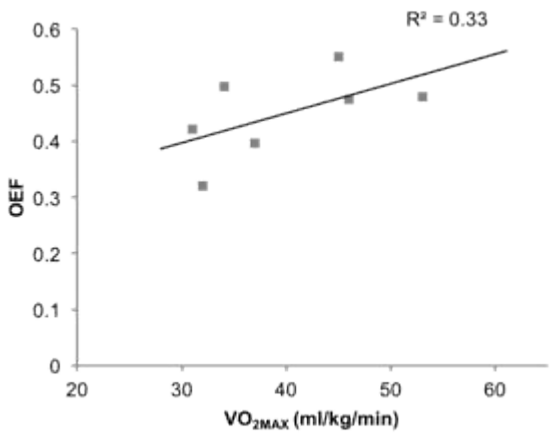


**Figure 2.12 Preliminary evidence linking $VO_{2MAX}$ with increased OEF.** Preliminary data suggesting a potential link between cardiorespiratory fitness ($VO_{2MAX}$) and oxygen extraction fraction (OEF) within the same participants, measured on different days (N=7). Data permissions received from Alberto Merola and Catherine Foster.

Further to this, where arterial concentration of oxygen is known to influence rate of oxygen consumption, future research should consider measuring haematocrit in the blood to compliment these measures, where haematocrit is reported to be less in athletes (Sharpe, 2002), known as 'sports anaemia', compared to sedentary controls due to elevated plasma volume and increased total mass of red blood cells (Mairbäurl, 2013) although, haematocrit may be increased in over-trained and/or iron deficient athletes (Brun et al., 2000).

### 2.3.10. Cerebrovascular Reactivity

Another aim of the current study was to explore whether physical fitness predicted the reactive capacity of the cerebrovasculature to transient increases in blood flow with hypercapnia (Murphy et al., 2011b), otherwise known as CVR. To date, studies that have investigated the relationship between CVR and fitness have relied upon either ultrasound methods (Ainslie et al., 2008; Bailey et al., 2013) or BOLD measurements (Gauthier et al., 2014b; Thomas et al., 2013b). Since the BOLD response is a complex haemodynamic measurement, BOLD CVR alone is not sufficient for understanding the mechanisms at play (Buxton et al., 2004). The current study used pulsed ASL methods that allowed simultaneous measurement of BOLD and CBF, to assess whether differences in BOLD previously reported are likely due to a change in blood *flow*, a solely hemodynamic measurement. As hypothesised, both whole brain and regional CVR was lower in fitter subjects in the present cohort, although this was not statistically significant for either BOLD or CBF measures.

Within the healthy brain, an increase in arterial carbon dioxide is expected to produce a rapid vasodilatory response, yielding an elevation in blood flow. Where a decline in CVR with age and disease is deemed to mark a decline in vascular health, studies showing a similar trend to that observed in the present study warrant it worthy of further investigation. For example BOLD CVR was found to decrease in a study of elderly masters athletes with increased $O_{2MAX}$ in response to a 5% $CO_2$ hypercapnic challenge (Thomas et al., 2013b). Similarly, a separate study found reductions in frontal BOLD CVR with increased $O_{2MAX}$, after co-varying for the effects of age (Gauthier et al., 2014b). A possible explanation for their findings, is that chronic elevations in venous carbon dioxide during prolonged periods of exercise over years of training lead to desensitisation of the vasodilatory signalling pathways such as NO, that mediate the reactivity of the blood vessels and regulate blood flow (Green et al., 2004).

There are several methodological considerations that may explain these non-significant results. It is possible that the breath-hold paradigm used here was not sensitive enough to detect a significant difference in CVR, where forced gas

challenges has been shown previously to yield more robust results (Tancredi and Hoge, 2013). Targeted gas challenges, in which subjects breath a predetermined level of $CO_2$ over a stable period of time, tend to provide a more robust measure of CVR (Tancredi and Hoge, 2013). Confidence that subjects are experiencing a comparable level of hypercapnia means that data is more reliable and less noisy. Nonetheless, these designs are problematic when it comes to testing patient groups who may experience discomfort both physically, due to the presence of a face mask, or psychologically, where the hypercapnic periods cannot be controlled by the participants themselves.

A breath-hold task was used such that we could assess the feasibility for use in patients. It has been previously shown that breath-holds are a reliable measure of BOLD CVR, even when breath-holding is poor (Bright and Murphy, 2013), however, SNR is inherently low in CBF data. To our knowledge, this experiment is the first time that the breath-hold paradigm has been used to measure CBF CVR in relation to fitness. We observed that whilst the relationship between CBF (or BOLD) CVR and fitness was not significant, there was a significant relationship between BOLD and CBF CVR measures. We interpret this evidence to suggest that using a breath-hold task, albeit noisy, can be used as a feasible, more direct, measure of cerebrovascular health.

### 2.3.11. Neurocognitive Function

Whereas exercise is thought to prevent typical age-related decline throughout the lifespan, particularly in tasks of executive function and spatial memory (Colcombe and Kramer, 2003), there is little evidence to demonstrate an association between fitness and cognition in young adults. In this study, we did not find an association between $O_{2MAX}$ and performance on tests of working memory, pattern recognition or spatial memory despite alterations in cerebrovascular health. It is possible that the cognitive benefits of exercise are less apparent due to 'ceiling effects', where performance is clustered around the maximum and more sensitive tests should be adopted. Increasing sample size would increase our confidence in accepting the null hypothesis, since our sample size is too small to detect true differences in cognition within healthy functioning adults. Nonetheless, the absence of a cognitive effect considering differences in cerebrovascular health is interesting as it supports the

hypothesis that physiological effects of exercise may take place earlier in the lifespan, before functional outcomes are observed.

We observed a correlation between pattern separation performance and CBF CVR across whole-brain grey matter. However, this did not reach significance after correcting for multiple comparisons. Nonetheless, this can be interpreted as a promising link between cerebrovascular health and cognition as shown previously (Chapman et al., 2013). Where fitness did not appear to mediate this effect in our cohort, expanding the sample size and repeating these tests later in life would be interesting. Future research should also consider looking at sub-regional changes in CBF, such as in the hippocampus, which is known to be primarily affected by ageing and to underpin performance on pattern separation (Creer et al., 2010a; Erickson et al., 2011).

### 2.3.12. Limitations

Care should be taken when generalizing these findings since the cohort used here was small. These results are preliminary and should be expanded upon in a sample of equally well-trained subjects. It is also important to consider that this study is limited by its cross-sectional design where cause and effect cannot easily be determined. Whilst randomized trials involving a specified mode, intensity, frequency and duration of exercise would be ideal, such studies are expensive and time-consuming and have their own limitations (Smith et al., 2011).

An implicit challenge of non-invasive imaging methods of assessing cerebrovascular function is the inability to tap into the biological mechanisms driving these changes. It is important to use complementary measures to support this MRI evidence, focusing on markers of endothelial function, including growth factors and signalling pathways known to influence vascular physiology. Exploring these changes in preclinical studies can bring us closer to achieving this goal and Chapter 3 will probe this in more detail, by addressing some of the possible mechanisms driving changes seen here.

### 2.3.13. Conclusions

In conclusion, $O_{2MAX}$ was found to be associated with several cerebrovascular parameters, including an elevation in arterial compliance, a decline in resting perfusion and an apparent but non-significant trend in grey matter CVR. This is the first time an association has been reported between $O_{2MAX}$ and arterial compliance *within* the brain using this novel MRI technique (Warnert et al., 2014). The relationship between fitness and MCA compliance in this, albeit modest, group of healthy young males, suggests that exercise may exert its beneficial effects early in life by protecting vessel compliance, even before cognitive decline becomes evident. An inverse relationship between CBF and $O_{2MAX}$ points towards adaptation effects such as differences in the efficiency of oxygen metabolism and is worthy of further investigation using MR techniques (Wise et al., 2013) and replication using preclinical MRI where mechanisms can be probed *ex vivo*. Whilst CVR did not vary in this cohort, use of breath-hold MRI for measuring CBF CVR is sufficient where gas challenges may not be appropriate.

# Chapter 3

# Investigating the cerebrovascular effects of voluntary wheel running in young male mice.

## Chapter Summary

In Chapter 2, the early cerebrovascular benefits of cardiorespiratory fitness were explored in healthy male adults. The present study was interested in whether these benefits would translate to young healthy male C57/BL6 mice following 6 weeks of voluntary wheel running. Histological changes were explored in mice following 6 weeks of running wheel exposure, of which 8 mice had unlimited access to a running wheel, and 8 mice to a stationary wheel inside the home cage. Histological analysis included measurements of vascular density and astrocyte number, two factors previously thought to be affected by exercise and to mediate the cerebral blood flow response measured by MRI. As hypothesised, running animals had an increased vessel density within the hippocampus, motor cortex and striatum after 6-weeks of exercise, which can be interpreted as exercise induced angiogenesis. Astrocyte number was not significantly different in running animals. These findings corroborate the general pattern of results seen following exercise, although these findings extend previous work as it was found that angiogenesis was observed even after 5 days following exercise cessation.

## 3.1. Introduction

As highlighted in Chapter 2 the relevance of exercise in young adults, where cognitive function appears unchanged, means that the early physiological changes that take place within the brain have not been thoroughly assessed. Understanding the physiological mechanisms, with focus on the cerebrovascular changes, that underlie macroscopic differences in blood flow and blood volume detected by MRI is a challenge that has motivated a few studies in non-human animals, particularly rodents, to explain these changes.

Several animal studies, predominantly in rats and mice, have demonstrated that running activity significantly increases the number of hippocampal cells born within the granule cell layer of the dentate gyrus. This region is known to be critical for memory formation and is one of the few regions of the brain, alongside the sub-ventricular zone of the striatum, that can generate new neurons throughout the lifespan. This process, known as neurogenesis (Kempermann et al., 1997) can be detected by injecting live animals using BrdU (5-bromo-2'-deoxyuridine) to label DNA in proliferating cells at the time of running compared to non-running controls (van Praag et al., 1999b).

Numerous studies have replicated and developed these findings, whereby both voluntary and forced running paradigms (Van Praag, 2008) have been shown to affect learning on a range of hippocampal tasks such as spatial memory (Clark et al., 2009) and pattern separation (Creer et al., 2010b). The latter study made a number of interesting observations. As expected, visualisation of BrdU delivered daily over 5 days during voluntary wheel running, revealed an increase in neurogenesis within the dentate gyrus and, interestingly, this was highly correlated with pattern separation performance on a touch screen task, analogous to the task described in Chapter 2 (Stark et al., 2013). More interesting still, was the finding that adult running mice had significantly greater blood vessel density within the hippocampus than non-running controls. This increase in blood vessel density can be thought to reflect a process known as *angiogenesis,* as a result of exercise, in which new blood vessels form from pre-existing vessels and will be the focus of this chapter.

Staining blood vessels with dyes such as *Lycopersicon esculentum* (tomato) lectin (Creer et al., 2010b; van Praag et al., 2005) or vascular endothelial antibodies such as collagen-IV (Clark et al., 2009), Glut-1 (Allen and Messier, 2013; Van der Borght et al., 2009) and RECA-1 (Ekstrand et al., 2008) have repeatedly demonstrated that an increase in blood vessel density and vascular morphology can co-occur alongside elevations in neurogenesis in running rodents compared to non-running controls, within the dentate gyrus. Angiogenesis is not however *limited* to areas in which neurogenesis occurs, although these regions have received more scientific attention. Rather, it seems to be linked to where neuronal activation is elevated. In a seminal study, a specific increase in capillary density was observed in the molecular layer of the cerebellum in running animals that could not be generalised to animals performing motor skills ('acrobatics') only (Black et al., 1990). This was replicated and extended in a study by Isaacs et al. (1992) who reported that an expansion of the vascular compartment within the cerebellum of exercising animals meant a shorter diffusion distance from the blood vessel to the neuropil. Whilst animals undergoing a control motor learning task showed an expansion of cells within the molecular layer, the density of the vasculature remained constant. They found therefore that *the ratio* of blood vessel volume to other components of the layer had increased as a result of exercise but not due to motor learning alone.

The lateral ventricle walls, or '*sub-ventricular zone'* (SVZ) of the striatum, is another neurogenic region which may depend on angiogenesis for improved cell survival and integration (Al-Jarrah et al., 2010; Ernst et al., 2014). Exercise in rodents has been linked to increased production and secretion of striatal BDNF (Aguiar et al., 2008; Marais et al., 2009) as well as neural activity (Shi et al., 2004) in the striatum. Furthermore, like the hippocampus, this coincides with an exercise-induced increase in angiogenesis (Ding et al., 2006). Vascular alterations within the striatum, may have functional cognitive significance (Chaddock et al., 2010). The dorsal striatum is implicated in a number of cognitive functions including stimulus-response challenges that require response selection demands, response resolution, motor integration, cognitive flexibility and the execution of learned behaviours. Whilst the striatum is historically more associated with motor dysfunction it has strong connectivity with cortical regions including the frontal lobe, temporal lobe and insula, as well as subcortical regions such as the amygdala and hippocampus (Haber, 2003). It is

therefore unsurprising that an increasing body of evidence is pointing towards the importance of striatal regions in influencing behaviour and cognition. These functions are jeopardised in a number of neurodegenerative diseases including Alzheimer's, Parkinson's and Huntington's disease (O'Callaghan et al., 2014) where cerebrovascular health is thought to be at risk (Al-Jarrah et al., 2010; Hsiao et al., 2015; Wells et al., 2014). Further still, evidence shows that function in these areas improves with exercise (Yau et al., 2014).

Vessel density increases have been reported anywhere between 20 (Black et al., 1990) -1000% (Thomas et al., 2012), depending upon the brain region being investigated and the duration of exercise. Increases in the vascular compartment could account for structural changes in grey matter volume that have been reported. For example, volumetric increases in anterior hippocampal volume following a 1-year aerobic exercise intervention in elderly adults, compared to matched subjects in a stretching-only control group (Erickson et al., 2011) have been shown, whilst clusters within the prefrontal cortex, a region implicated in task of executive function, also showed volumetric increases after 6 months of exercise in elderly subjects (Colcombe et al., 2006). MRI is currently unable to tease apart the contribution of different tissue components, yet differences in functionally relevant regions of the brain known to be implicated in cognitive enhancement following exercise may still be useful for localising regions of interest, where cerebrovascular function may be particularly affected.

Neuronal health is known to be tightly coupled to vascular health for efficient delivery of oxygen and nutrients to the metabolising cells; a process known as 'neurovascular coupling' (Palmer et al., 2000). While neurogenesis has received a great deal of scientific attention, the importance of flow metabolism coupling i.e. the process by which the brain regulated blood flow to meet functional metabolic demand, means that cerebrovascular health is essential for supporting neuronal health. It has been shown that angiogenesis may even *precede* neurogenesis. A study by Van der Borght et al. (2009) demonstrated that an increase in capillary density within the dentate gyrus occurred within 3 days from the onset of voluntary running and returned to baseline after just 24 hours following wheel removal. Neurogenesis on the other hand, took up to 10 days before a significant increase was observed in

running animals, however unlike vascular changes, neuronal survival persisted for up to 6 days after running cessation.

Astrocytic volume is also thought to respond to exercise (Kleim et al., 2002). Direct contact between endothelial cells and astrocytes, via the astrocytic end feet that envelope capillaries, are necessary to generate an optimal blood brain barrier (BBB) and through numerous signalling processes are thought to influence blood flow and other neuro-metabolic processes in the brain (Figley and Stroman, 2011). Astrocytosis after exercise, coupled with angiogenesis is thought to provide strength to the neurovascular unit (including the microvascular endothelium, astroglia, neurons and the extracellular matrix), thereby protecting the blood-brain-barrier (BBB). Evidence explaining exactly how exercise alters astrocytosis however is unclear. Brain tissues of exercised and non-exercised rats processed for expression of glial fibrillary acidic protein (GFAP), an astrocyte specific marker, have been shown to increase in the number following 6 weeks of exercise (Li et al., 2005). Other evidence, however, has described a decrease in astrocyte (GFAP) density following treadmill exercise and interestingly, a reduction in the production of nitrous oxide (Bernardi et al., 2013), an important vasodilator that drives cerebrovascular reactivity in the brain. High levels of NO released due to the high expression of inducible NO synthase (iNOS) has been shown to mediate a number of inflammatory neurodegenerative disease (Brown, 2007) and might be one mechanism by which exercise mediates the beneficial effects of exercise. Astrocytosis differs from neurogenic growth however, in that they are thought to return to baseline volume as soon as the animal is removed from the stimulating environment (Kleim et al., 2002) and evidence in the cerebellum has suggested that astroglial density varied with synaptogenesis, but not angiogenesis.

Nonetheless, the functional involvement of astrocytes in angiogenesis is well recognised, in part through production of a growth hormone called vascular endothelial growth factor (VEGF), which is also upregulated as a result of both acute and chronic physical activity (Bloor, 2005; Fabel et al., 2003). The interaction between astrocytes and cerebral blood vessels has a strong influence on the measurements we detect with MRI. Through active participation in capillary formation via VEGF signalling, angiogenesis increases the surface area by which cerebral

perfusion can take place. Astrocytes, which vastly outnumber neurons, also serve a number of functions throughout the CNS. They are critically involved in uptake and recycling of neurotransmitters such as GABA and glutamate, as well as the metabolic (both oxidative and glycolytic (Prichard et al., 1991) and hemodynamic processes that are detected by MRI (Kullmann and Asztely, 1998). Astrocytes circumscribe nearly all neuronal synapses and more than 99% of the total cerebrovascular surface area (Agulhon et al., 2008). They are responsible for regulating vasodilation in response to neuronal metabolic demand, a process known as *functional hyperaemia*, by a process of $Ca^{2+}$ signalling between 1-2s following stimulus onset (Winship et al., 2007). Astrocytes signal to vascular smooth muscle (VSM) in intraparenchymal arterioles, whereby a change in VSM tone following widespread neuronal activation, leads to dilation or constriction of pial arteries and intraparenchymal arterioles which alter CBF. It has been suggested that since astrocytes directly control vascular tone, and therefore cerebral microcirculation, the basis for fMRI neuroimaging techniques may be more closely related to astrocytic than to neuronal activity (Figley and Stroman, 2011). Exercise as a modulator of astrocytic function, likely yields some of its cerebrovascular effects through this pathway, such that astrocytes are essential for understanding mechanisms underlying the beneficial effects of exercise on the brain.

The focus of the present study was to investigate whether increases in vascular density (angiogenesis) are detectable following 6 weeks of voluntary exercise in young adult mice. It was hypothesised that elevations in vessel density would be seen in the hippocampus, striatum and motor cortex, as reported previously. As an extension to previous research, we wanted to assess whether 6 weeks of running, would lead to more long-lasting changes in vascular density than those reported previously after just 10 days of running (Van der Borght et al., 2009) by assessing vascular density 5 days after wheel removal. Where astrocytes are thought to mediate a number of the cerebrovascular changes induced by exercise and influence the hemodynamic response measured by MRI, we investigated whether differences in astrocyte number could also be detected after 5 days of running cessation. Whilst BrdU was injected for detection of cell proliferation during wheel exposure, data has not been presented here due to time-restraints, where BrdU antibody optimisation and image analysis pipelines have not been previously established in this lab.

Immunohistological differences in vessel density and astrocytic number because of voluntary exercise, may help to interpret differences in CBF seen in physically active human subjects.

## 3.2. Methods

### 3.2.1. Animals

Sixteen male 8-week-old C57Bl/6 mice (Charles River, UK), individually housed in temperature-controlled rooms under a 12-h light/12-h dark cycle (lights on at 6:00 am). A C57BL/6J mouse strain was chosen because they are well known to display enhanced behavioural performance from wheel running exercise, and thereby serve as a useful model to explore any neurobiological correlates (Clark et al., 2009). Mice had free access to water and food throughout the experiment and were weighed weekly to control for changes in body weight. All procedures were run in accordance with the United Kingdom Animals (Scientific Procedures Act of 1986), and subject to local ethical review.

### 3.2.2. Voluntary wheel running

Mice were housed in large standard mouse cages (25 x 12 x 42cm) equipped with a free-standing running wheel (ENV-044 Mouse Low-Profile Wireless Running Wheel, Med Associates Inc.; 37.82cm circumference, 25° from horizontal plane).

Wheel running activity was recorded via a wireless transmitter system that signalled to a hub located in the same animal holding room. Wireless Running Wheel Manager Data Acquisition Software (SOF-860; Med Associates Inc.) recorded and time-stamped each wheel rotation for subsequent analysis. Although revolutions were monitored continuously, activity occurred primarily during the dark phase. Mice were singularly housed such that wheel running could be recorded independently for each animal and to avoid fighting between littermates.

All mice had unlimited access to a running wheel 7 days a week for 6 weeks. Whilst exercising mice (N=8) could run freely on the wheels, mice in the control condition (N=8) had wheels that were fixed in position with a pin so that the environmental

conditions were identical except that the wheel was stationary. Wheel access was uninterrupted during the following weeks except for removal for BrdU injection on the second week as well as weekly health checks and animal maintenance.

### 3.2.3. BrdU

After one week of habituation to the wheel, *i.p.* BrdU injections (50µg/g; Sigma) were carried out at the same time daily (11:30-12:30) for 5 days (as described previously by Creer et al. (2010)) during the second week of wheel exposure. BrdU was freshly prepared daily over the 5-day injection period. Preparation was carried out according to manufacturer's instructions, whereby BrdU was dissolved in saline at a temperature of 50°C inside a water-bath.

### 3.2.4. Histology and Immunohistochemistry

Animals were deeply anaesthetised with 0.02ml sodium pentobarbital (Euthatal) and perfused trans-cardially with PBS, followed by ~110ml 4% paraformaldehyde (PFA), in 0.01M PBS at pH 7.4 at a flow rate of ~23ml/min for 5mins. Brains were post-fixed for 5h followed by equilibrium in 30% sucrose. Tissue was sectioned coronally at a thickness of 40 µm on a freezing microtome (Leica). A thickness of 40 µm has been recommended previously in order to obtain reliable 3D information about the vascular tree for quantification (Wälchli et al., 2014). Free-floating sections were stored as a 1:12 series in cryoprotectant solution and stored at −20°C until staining.

Assessment of striatal and motor cortex were taken from coronal sections located between +1.18mm and -0.26mm from bregma. Assessment of hippocampal tissue was taken from coronal sections in which dorsal dentate gyrus was most apparent, namely sections between -1.34mm and -2.8mm from bregma. Immunofluorescence was performed on a 1:12 series of sections, whereby sections were first washed in pH = 7.4 Tris buffered saline (TBS) three times (5mins x 3). After washing, a 3% normal horse serum (NHS) solution (Invitrogen, Paisley, UK) in TBS + 0.2% Triton X100 (TXTBS; pH=7.4) was applied to the sections for 1 hour to block non-specific binding sites. Primary antibody was applied immediately after blocking, in a solution of 1% NHS and TXTBS according to individual antibody concentrations (specified elsewhere) and left at room temperature overnight or at 4°C for 72hours. Tomato

Lectin was added at the same stage as the primary antibody. Sections were then washed in TBS (3 x 5mins) and incubated with either a species-specific Alexa Fluor-conjugated secondary antibodies (488, 555, 594) (Invitrogen) or Streptavidin Cy3 (Jackson) at 1:200 concentrations with 1% horse serum and TBS for 3 hours at room temperature or overnight at 4°C. All immunofluorescence experiments were co-stained with the nuclear marker Hoetsche (1:10,000) in TBS with 1% NHS for 10mins. Slides were washed again in TBS (3 x 5mins) and transferred to Tris non-saline (TNS) prior to mounting. Free-floating sections were mounted onto gelatinised slides. Finally, slides were dehydrated in a graded alcohol series (70, 95, 100% IMS for 5mins respectively) and cleared in xylene (~20mins) and cover-slipped using DPX mounting medium (RA Lamb, Eastbourne, UK).

## 3.2.5. Microscopy Parameters

### 3.2.5.1. Vascular Density (Tomato Lectin)

Tomato lectin is thought to provide the best labelling of CNS vasculature (Robertson et al., 2014) for labelling of the endothelial cells on capillaries and other small vascular elements (Mazzetti et al., 2004). This is supported by its correspondence to other markers of endothelial cells e.g. immunoreactivity to CD31 (Gee et al., 2003) with the added benefit of its non-specificity to blood vessel type and its' reliability. It is a member of the Lectin family, which are carbohydrate-binding proteins, distinct from antibodies, enzymes, and transport proteins (Barondes, 1988). Lectins label vascular elements in fixed tissue sections, by binding to carbohydrate components of endothelial plasmalemma (Jilani et al., 2003). Tomato lectin binds to complex-type N-glycans glycoproteins, particularly the poly-N-acetyllactosamine residues of complex carbohydrates including oligosaccharide sequences that contain the i and I— antigenic structures (Kawashima et al., 1990).

### 3.2.5.2. Blood Vessel Quantification

Lectin staining (*Lycopersicon esculentum*; Vector) was used to visualize blood vessels as described previously (Creer et al., 2010b) where group differences in blood vessel density was used as a surrogate measure of angiogenesis.

All images were acquired at ×20 magnification with identical parameters for each image using inverted microscopy (Axio Imager Z2, Carl Zeiss) for fluorescence, using

Zeiss AxioVision software (v4.8.2, Carl Zeiss). Specifically, 3 equidistant sections (480 μm apart) per brain. Images were acquired from sub-regions within our gross regions of interest including 1) dorsal striatum (dorsal SVZ/ ventral SVZ/ Caudate Putamen) 2) dorsal hippocampus (Dentate Gyrus / CA1) and 3) motor cortex (no sub-regions) (figure 3.1a). Images were acquired (450 x 340mm) and quantification was performed using Image J software (1.48v). Assessment of striatal and motor cortex were taken from coronal sections located between +1.18mm and -0.26mm from bregma. Assessment of hippocampal tissue was taken from coronal sections in which dorsal dentate gyrus was most apparent, namely sections between -1.34mm and -2.8mm from bregma (figure 3.1b).

Whole images were divided into quadrants in which vessel density was quantified. Vessel area within each image was measured since vessel counting within tissue is affected by vessel trajectory through the tissue. Images were initially binarised using Image J's Auto Thresholding tool (figure 3.1c), such that imaged pixels containing vessels were coded as 1 and all background noise as 0. Vessel area within each sub-region therefore reflects the percentage area within each quadrant that contained blood vessels (figure 3.1). Results were averaged within each sub-region and across hemispheres, such that vessel density within each section reflected the average of 8 measurements, which was then averaged across all sections to yield one sub-regional value of 'Area (%)' per region for each subject.

Linear regression was carried out to assess whether a dose response relationship exists between running distance over the 6 weeks and blood vessel density. Average daily running distance carried out by mice exposed to the free-turning wheel were entered into a linear regression with running as the predictor and vessel density as the dependent variable. All values were accelerated bootstrap corrected.

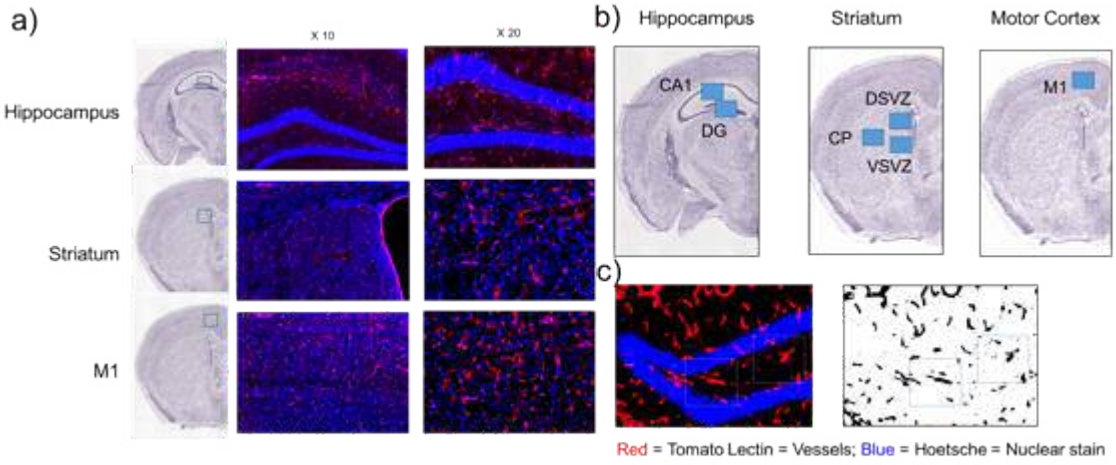


**Figure 3.1 Vessel density quantification a)** Regions of interest included the hippocampus, striatum and motor cortex. Three whole-brain equidistant sections were imaged at x2 0 magnification. b) Regions were subdivided into sub-regions for further analysis. c) Binarised vessel masks were created using Image J's Threshold tool and vessel density was quantified as % vessel area. Regions of interest included the hippocampus (top), striatum (middle row), primary motor cortex (bottom row) imaged at x10 and x20 magnification.

#### 3.2.5.3. Astrocytosis (GFAP)

GFAP (Glial fibrillary acidic protein) is a protein that is encoded by the GFAP gene in humans. Glial fibrillary acidic protein is an intermediate filament (IF) protein that is expressed by astrocytes within the CNS and widely used as an astrocytic marker.

##### *3.2.5.3.1. Astrocytic Quantification*

Images were acquired at x 10 magnification within (FOV = 450 x 340 mm) within the 3 striatal ROIs (DSVZ, VSVZ and CP). Image J was used to count cells that were co-labelled as positive for expression of the astrocytic marker GFAP and the nuclear marker Hoetsche (figure 3.2). Due to the difficulty of counting overlapping astrocytes in tissue sections, counts were performed on the entire image, where nuclei of the astrocytes were co-labelled and the absolute number of astrocytes counted per region (450 x 340 mm). One image per ROI, per section was acquired bilaterally.

Counts were averaged across hemispheres and sections and expressed in arbitrary units.

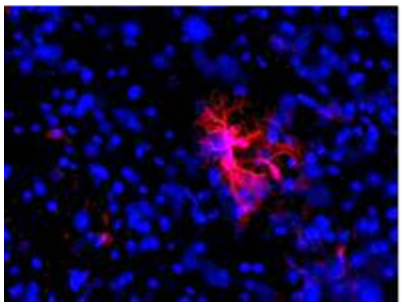

**Figure 3.2 Representative morphology of an astrocyte within the striatum.** Blue = Hoetsche, Red = GFAP = (x40 magnification).

## 3.3. Results

### 3.3.1. Running wheel activity

Following habituation to the presence of wheel in the home cage, running activity increased to approximately 25,000 (±6700) rotations/day equivalent to 8.7(±2.6) km/day. During BrdU administration, running activity dipped but returned to baseline level throughout the remaining 30-day running period (25,500 ± 4000 rotations/day) equivalent to 9.6 (± 1.5) km/day (fig. 3.3).

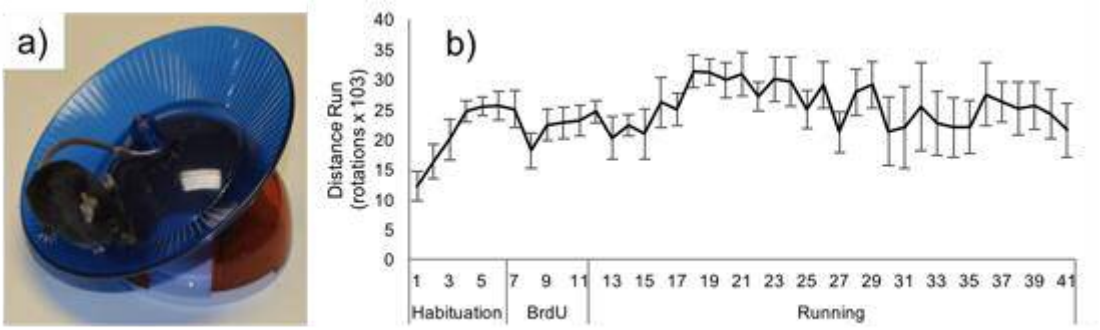


**Figure 3.3 Voluntary wheel running.** a) Wheel running activity in running mice (N=8) b) Average daily running activity during BrdU administration (22,203 ± 2,540 rotations/day) was similar to the average running activity across the remaining 30days after injection (25,489 ± 1,112 rotations/day). Error bars = S.E.M.

## 3.3.2. Vascular density

### 3.3.2.1. Sub-regional Analysis

To investigate whether exercise enhances angiogenesis, blood vessel density was calculated within the dorsal striatum, dorsal hippocampus and M1. Repeated measures ANOVA within sub-regions of the striatum (Dorsal SVZ, Ventral SVZ and Caudate Putamen) and hippocampus (Dentate Gyrus and CA1) were performed with GROUP (running vs. non-running) as the between-subject variable. The M1 was not divided into sub regions. One-tailed tests are used as running is known to increase vessel density in healthy animals.

*Striatum.* An example image from a running and non-running animal from the striatum can be seen in figure 3.4. Clear visual differences were evident in the tissue of running animals, where vessels were appeared denser and larger than that of non-running animals. Indeed, the mean vessel density was higher in running animals (fig 3.5), and this was supported by a significant main effect of Group ($F(1,14) = 21.9$, $p<0.001$, partial $\eta^2 = 0.61$). However, no main effect ($F(1.3,19) = 3.1$, $p=0.09$, n.s., partial $\eta^2 = 0.18$) or interaction ($F(1.3, 19) = 0.89$, $p=0.84$, n.s.., partial $\eta^2 = 0.01$)

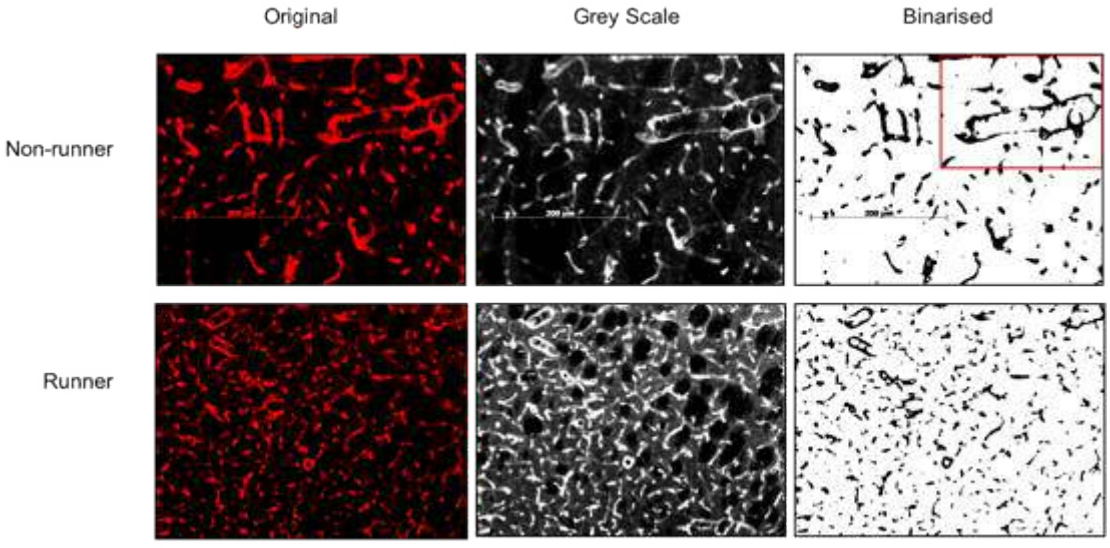


**Figure 3.4 Vessel quantification in running and non-running mice.** Example images from a dorsal striatal section in a non-running (top) and running (bottom) mouse (x20 magnification). Running animals visually demonstrated a greater number vessel density than non-running animals. Image quantification was performed by binarising original images using ImageJ using the Auto Threshold tool and %Area was quantified within each quadrant of the final binarised image (red square).

was seen between sub-regions within the striatum (Greenhouse-Geisser corrected for violation of the sphericity assumption).

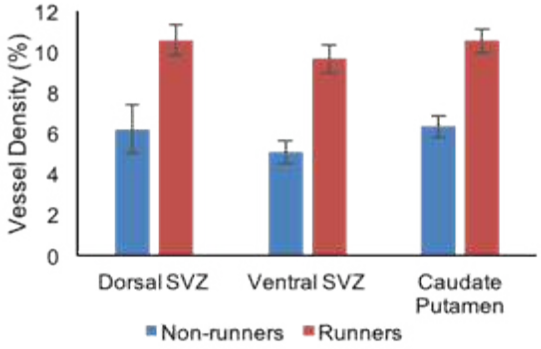


**Figure 3.5 Vessel density in the striatum after 6-weeks wheel exposure.** Wheel running mice (N=8) had a significantly higher vascular density of *tomato lectin* stained vessels than non-running mice (N=8) in the striatum and a similar difference was present in all striatal sub-regions. Mean ± S.E.M.

*Hippocampus.* Within the hippocampus, a similar trend was seen whereby the runners had an increased vessel density compared to non-runners ($F(1,14) = 4.1$, $p=0.03$, partial $\eta^2 = 0.23$; figure 3.6). There was no overall difference between vessel density in the DG and CA1 ($F(1,14) = 1.9$, $p=0.19$, n.s.).

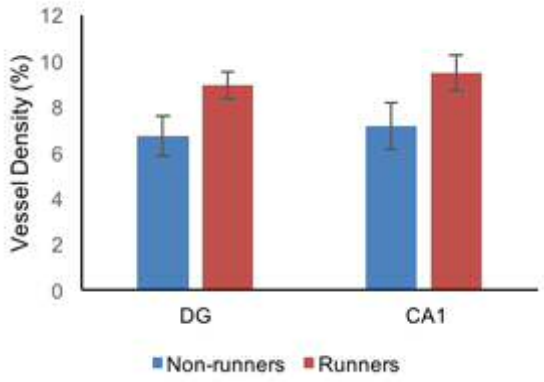


**Figure 3.6 Vessel density in the hippocampus after 6-weeks wheel exposure.** Wheel running mice (N=8) had higher vessel density of *tomato lectin* stained vessels than non-running mice (N=8). Both sub-regions showed this trend, such that a similar difference was present both the DG and CA1. Mean ± S.E.M.

*Motor cortex*. Only one ROI was imaged within the motor cortex, and so a between-subject ANOVA was performed. Again, a trend was observed whereby by runners showed greater vascular density within the M1, but this was not significant ($F(1,14) = 3$, $p=0.06$, n.s., partial $\eta^2$ effect size = 0.17; figure 3.7).

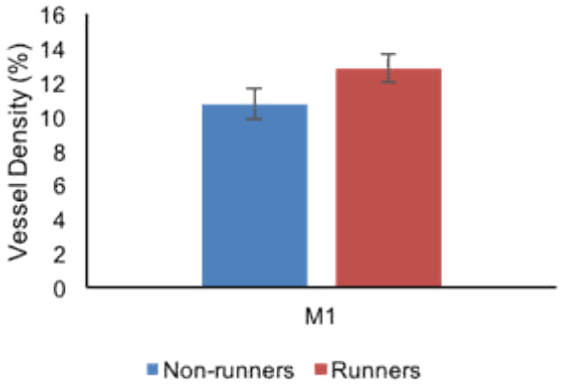


**Figure 3.7 Vessel density in M1 after 6-weeks wheel exposure.** Wheel running mice (N=8) had higher vascular density of *tomato lectin* stained vessels than non-running mice (N=8) in the motor cortex but this was not significant. Mean ± S.E.M.

### *3.3.2.2. Between-region Analysis*

Because there were no significant sub-regional differences within the striatum and the hippocampus, data were collapsed across regions. Vessel density was compared across gross bilateral ROI's (striatum x hippocampus x motor cortex) with Group (running x non-running) as the between-subject variable was performed, to address whether exercise has more of an effect in one region in particular.

Running animals had greater blood vessel density across all regions than non-running controls (Group; $F(1,14) = 7.45$, $p = 0.02$, partial $\eta^2 = 0.35$; figure 3.8). The greatest vascular density was observed in M1 and this was significant (ROI; $F(1,14) = 285.06$, $p < 0.001$, partial $\eta^2 = 0.95$) although ROI did not interact with Group, such that the density was greater in all running animals, across all regions (Group x ROI; $F(1,14) = 0.17$, $p = 0.69$, partial $\eta^2 = 0.01$).

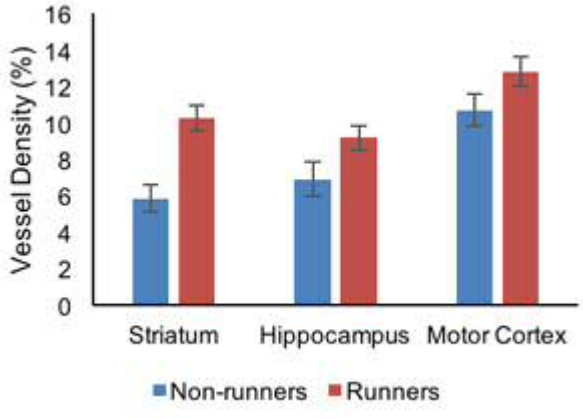


**Figure 3.8 Regional vessel density differences after 6-weeks wheel exposure.** Running mice showed increased vessel density in all three regions. Vessel density was higher in the motor cortex than the hippocampus or striatum, ROI differences did not interact with GROUP. Mean ± S.E.M.

### 3.3.3. Dose-response relationship

A dose relationship was not observed between individual subject's daily running activity and vessel density and was not found in the striatum ($R^2$ =0.03, F (1,6) =0.17, β=-4.21 x$10^5$, p=0.73, CI [0.00-0.001 x$10^5$]), hippocampus ($R^2$ =0.08, F (1,6)=0.51, β=<0.001, p=0.62, CI [-0.001-0.001]) or motor cortex ($R^2$ =0.02, F(1,6)=0.11, β=-726 x$10^5$ p=0.61) (figure 3.9).

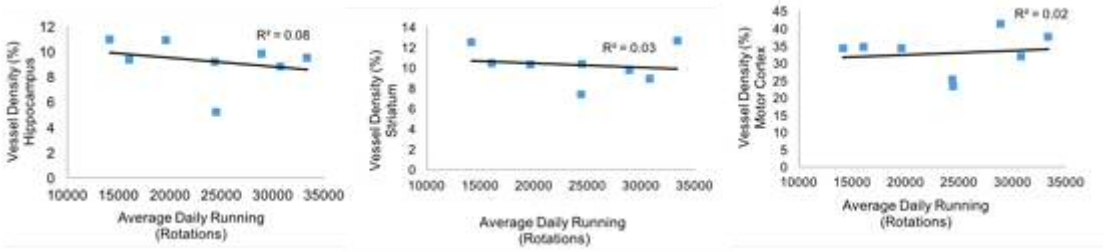


**Figure 3.9 Dose relationship between running distance and vessel density.** A dose response relationship was not observed between average daily running (N=8) and vessel density within the striatum, hippocampus or motor cortex.

### 3.3.4. Astrocyte Counts

Visual trends suggested an increase in astrocytes in runners compared to non-runners but this was non-significant between groups (F (1,14) = 0.59, *p*=0.46, partial $\eta^2$= 0.04). A repeated-measures ANOVA was performed to assess whether the number of GFAP+ cells within the striatum differed between runners and non-runners. No interaction was observed between groups within different sub-regions (F (2,28) = 0.3, *p*=0.75, partial $\eta^2$ = 0.02, figure 3.3.6.) although a significant effect of sub-region (F (2,28) = 8.1, *p*= 0.002, partial $\eta^2$ = 0.37) showed that in general there were significantly fewer astrocytes away from the lateral ventricle wall, within the caudate putamen.

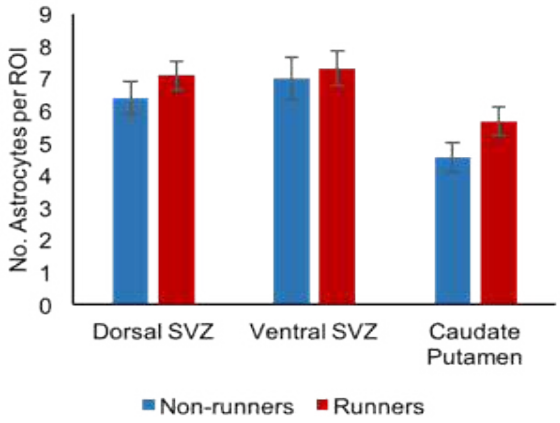


**Figure 3.10 Group differences in regional astrocyte count.** Wheel running mice (N=8) revealed showed had more astrocytes (GFAP+) than non-running mice, particularly within the Caudate Putamen. but this

## 3.4. Discussion

### Key Findings:

- Increased vessel density is significantly greater in the striatum and hippocampus of voluntary wheel-running mice compared to non-running mice, thought to reflect angiogenesis.
- Vessel density was increased in the motor cortex but this was not significant.
- Elevations in vascular density are significantly higher in runners even 5 days after running cessation, suggesting a longer-term effect of exercise upon cerebrovasculature than previously reported in mice.
- An effect of exercise on astrocyte number was not evident in this study.

This study aimed to establish whether 6 weeks of voluntary wheel running led to alterations in blood vessel density in the young adult mouse brain, specifically in regions of the brain that have previously shown changes in angiogenesis as a result of exercise, namely the hippocampus (Van der Borght et al., 2009) and striatum (Rhyu et al., 2010). It was found that running animals showed an overall increase in vascular density across all regions compared to non-runners, with the largest increase being seen within the striatum. Whilst running-induced increases in vascular density and angiogenesis have been reported previously within the motor cortex (Swain et al., 2003), this was not significant in the present study. An increase

in vascular density 5 days after exercise cessation adds to the literature, suggesting that cerebrovascular effects of exercise are more chronic than previously thought (Van der Borght et al., 2009). The present study did not observe a difference in the number of GFAP+ cells between runners and non-runners, which suggests that exercise does not have a stable impact on astrocyte proliferation within the striatum.

### 3.4.1. Exercise and angiogenesis

In the present study we applied tomato lectin which is known to reliably stain the endothelial cells in the vessel wall, for analysis of micro-vessel density (Robertson et al., 2014). Our findings support those found previously by studies whereby running-induced increases in vascular density, measured using tomato lectin, were attributed to the process of angiogenesis in the hippocampus (Creer et al., 2010a). Whilst a group difference in M1 vessel density did not reach statistical significance ($p=0.06$), there was a strong effect in the striatum and hippocampus.

The hippocampus is known to be critical for spatial working memory (Smith et al., 2013) and pattern separation (Sahay et al., 2011), whilst the striatum is increasingly being acknowledged a critical hub for tasks of executive function due to its broad connectivity that makes up the cortico-striatal circuitry (O'Callaghan et al., 2014). In, a meta-analysis of interventional studies that have reported cognitive benefits as result of exercise, performance on tasks of executive control and spatial memory had the largest effect sizes. Our findings contribute to a widening field in which the neurobiological basis of cognitive health is beginning to unfold, with a recent emphasis on the importance of cerebrovascular health. Animal behaviour was not measured in the current study, however it would have been interesting to explore the relationship between running, vessel density and behavioural function as others have done (Creer et al., 2010a; van Praag et al., 2005).

The present study extends previous findings in which the effects of exercise on vessel density have been described as transient. A previous study by Van der Borght et al. (2009) observed a significant increase in vessel density after just 10 days of voluntary wheel running, but that this returned to baseline after just 3 days of exercise cessation. It is possible that the much longer exercise duration applied in this study, can explain the prolonged period after exercise cessation in which these group

differences were observed. Since this experiment was not designed to assess duration or dose of exercise or 'detraining' we can only speculate, however this may explain why a significant difference was not observed in the M1, as cerebral morphology may have returned towards baseline.

Well-designed dose response studies are needed to unpick the cerebral dynamics of exercise duration and duration of 'detraining' in mice, and how this relates to humans is even less clear. In humans, 14days of physical deconditioning in highly trained subjects has been found to yield a reduction in $VO_{2MAX}$ of ~4% (Houmard et al., 1992), plasma volume, and endothelial function (Watts et al., 2004). Longitudinal studies in which cerebrovasculature is measured before and after a fixed exercise period is needed to unpick these differences. This is impossible using histology in the mouse, and prompts the use of MRI imaging as a non-invasive biomarker from which to assess longitudinal change. In combination with human MRI, questions regarding the exact time course of training and detraining on the brain can begin to be answered.

In this study, tomato lectin was used to visualise blood vessels since it indiscriminately stains endothelial cells regardless of vessel subtype. Furthermore, staining with lectins does not come with many of the caveats of immunohistochemistry, such as the specificity of the site to which it binds. Only one other study has used tomato lectin to visualise blood vessel ex vivo following a running intervention, where other studies have used antibodies such as CD31 (Rhyu et al., 2010) and collagen-IV (Clark et al., 2009). A further caveat of these antibodies, is that they may be affected by the intervention itself, for example, Co-IV relies upon the presence of collagen in the vessel wall, which is known to be influenced by age (Kang et al., 2015) and may itself be influenced by exercise (Fleenor et al., 2010).

### 3.4.2. Neurobiology of angiogenesis

There are several mechanisms which may explain the observed exercise-induced angiogenesis, particularly elevations in the levels of growth factors. Elevations in insulin-like growth factor 1 (IGF-1) appear to be a pre-requisite for the effects of exercise on the remodelling of vessels, as exercise promotes uptake of IGF-1 from the blood into the brain (Trejo et al., 2001). Indeed, the benefits of physical activity

on the cerebro-vasculature are absent in mice expressing low levels of IGF-1 (Lopez-Lopez et al., 2004). Other increasingly acknowledged angiogenic factors such as VEGF and angiopoietin 1 and 2, for example are known to be upregulated in the brain following physical activity (Bloor, 2005; Ding et al., 2006) and regulated by IGF-1 (Lopez-Lopez et al., 2004) . Expression of these growth factors requires un-fixed brain tissue to measure protein expression, which was unavailable in the present study. Nonetheless, the relationship between exercise and VEGF upregulation has been observed before in mice and humans (Vital et al., 2014).

### 3.4.3. Angiogenesis, astrocytosis and CBF regulation

One key aim of this study was to address some of the possible mechanisms that underpin the gross changes seen using MRI in humans. The present findings support previous research whereby angiogenesis is a marker of cerebrovascular health. Exactly how differences in vessel density maps onto the perfusion signals detected by MRI however is unclear. Two possible mechanisms were addressed in this study, angiogenesis and astrocyte function.

Angiogenesis in rodent studies has been used to explain observed increases in cerebral blood volume (CBV) MRI, and these findings have been interpreted as a sign of increased M1 (Swain et al., 2003) and hippocampal (Pereira et al., 2007) perfusion. Where hemodynamic processes are extremely complex, an increase in CBV masks multiple underlying processes. Increases in CBF as a result of exercise have been documented in rats using laser-speckle flowmetry and this has been shown to map onto increases in vessel density following MCA occlusion (Zheng et al., 2011). Where CBF measurements with MRI are thought to measure perfusion changes within the capillary bed, investigating differences in CBF with ASL methods could be a more translational approach from which to compare and assess exercise related differences between mice and humans. The relationship between CBF and angiogenesis has been established in preclinical studies, where CBF was able to predict the location of increased vessel density (angiogenesis) in post-ischemic rats using PASL MRI (Jiang et al., 2005) and laser speckle flowmetry (Zhang et al., 2013).

Astrocyte function is thought to contribute to differences in CBF detected by MRI (Figley and Stroman, 2011) since astrocytes express receptors or neuromodulators

known to regulate vascular tone (Bekar et al., 2012). They have also been shown to possess their own calcium dynamics which do not correspond to neuronal activity in response to visual stimuli (Schummers et al., 2008), which could in turn generate their own functional signals. In the present study, we did not detect a difference in in the number of astrocytes in running animals. A caveat of *ex vivo* studies is that detection of the real-time functional contribution of astrocytes in the living brain is challenging, and indeed have been shown return to normal rapidly after exercise (Kleim et al., 2002).

### 3.4.4. Limitations

In this pilot study, sample size was low and may have jeopardised the statistical power, particularly within the M1 where there was a clear visual increase in vascular density. Nonetheless, our results corroborate those found previously such that it is possible to be confident in the effects seen.

A caveat of the present study, is the inability of tomato lectin to differentiate between vessel *type.* In Chapter 2, the role of compliant arterioles in mediating cerebrovascular control was discussed (Peterson et al., 2011). An interesting question is whether there is a dichotomy in the type of vessel that drives the alterations in vessel density that has been so widely reported. It is thought that grey matter tissue is primarily made up of capillaries and small arterioles, of which only the latter are thought to control regional cerebral blood flow (Hill et al., 2015). Understanding the type of vessel that contributes to these exercise-induced effects, may shed light on the global benefits expected. Future research will extend the present findings to visualise vessels that possess smooth muscle actin ($\alpha$SMA), which is located in the walls of compliant arterioles. In addition, this may lead us closer to understanding the mechanism by which fitness or exercise leads to the increased compliance of major arteries reported in Chapter 2.

It is acknowledged that where the term angiogenesis is used, we have not addressed this directly, rather we have used an indirect surrogate marker, vessel density, as others have done. It was intended that this question would be more accurately acknowledged by designing the experiment such that mice underwent injection with the proliferative DNA marker BrdU during the first week of wheel running. Future

analysis will use immunofluorescence to co-stain for BrdU+ endothelial cells, such that proliferating vascular cells at the time of running can be directly quantified.

No behavioural measures were carried out in the present study, such that the functional outcome in young adult mice was not assessed. Unlike human studies where cognitive improvements are rarely seen with exercise in young adults, rodent studies tend to report a cognitive enhancing effect in subjects of an analogous age (Creer et al., 2010a). Training on behavioural tasks, particularly operant tasks, is time-consuming, requires high levels of handling and water deprivation to motivate subject learning. Since our major question was related to the cerebro-physiological differences between animals rather than cognition *per se,* we did not want to confound our results by introducing further environmental enrichment and handling stress that may influence our results, beyond that attributable to wheel running. Quick behavioural tasks such as the balance beam test of motor coordination, initiation and balance may be a feasible candidate for future experiments.

Finally, it has been noted that immunofluorescent imaging of GFAP+ cells may not be optimal for counting astrocytes in thick tissue sections (40$\mu$m). Whereas cultured astrocytes reveal a defined morphology with fluorescence, thick overlapping sections make the nuclei of astrocytes difficult to detect. Quantifying density of astrocytes using DAB stereology may be a better way of imaging sections in future (Li et al., 2005). Future work would also consider quantifying morphological changes in situ using high-resolution microscopy or live imaging (Escartin and Murai, 2014).

### 3.4.5. Conclusion

In this chapter, we show a significant difference in vessel density in the striatum and hippocampus, 5 days following exposure to a running wheel for 6 weeks. These changes were not accompanied by differences in astrocyte number within the striatum. M1 vessel density showed a non-significant elevation in running animals, and we hypothesise that a 5-day period of detraining may have masked an exercise related increase that has been reported elsewhere. Future work will utilise ASL MRI to assess whether the morphological differences in cerebrovasculature observed here, are related to *in vivo* differences in cerebral blood flow. Given the striking increases in striatal vasculature observed in this study with exercise, this led to the

question of whether exercise would be beneficial in Huntington's Disease, a neurodegenerative disease driven by striatal dysfunction.

# Chapter 4

# Investigating the relationship between aerobic fitness and cerebrovascular health in pre-/early-symptomatic HD patients using PASL MRI.

## Chapter Summary

Alterations in patterns of resting CBF have previously been observed in pre-/early-symptomatic HD patients compared to healthy controls using ASL methods including hypoperfusion of basal ganglia regions known to be involved in HD progression. In the absence of any pharmacological treatments, exercise is being explored as a possible therapeutic intervention by which to alleviate symptoms and improve quality of life. In this cross-sectional study, the relationship between cardiorespiratory fitness and cerebrovascular health was addressed. Fifteen pre-/early-symptomatic patients and 15 matched controls underwent a $O_{2MAX}$ test to assess aerobic fitness. On a separate session, participants underwent MRI scanning and cognitive testing. Resting CBF and cerebrovascular reactivity was measured using pulsed arterial spin labelling (PASL). Disease severity in HD patients was associated with decreased grey matter CBF, reflecting significant progressive global hypoperfusion in HD, although hyperperfusion in the left putamen was associated with significantly poorer functional capacity. Between-group differences were less clear, whereby CBF in the basal ganglia, particularly the left caudate, was lower in patients than controls, which was in line with previous studies, although this was not significant. Tissue arrival times across the whole-brain were also associated with a significantly higher disease burden. Executive function was significantly poorer in HD patients compared to controls and CBF in the thalamus was negatively related to performance on tasks of executive function, supporting its important role in the early pathology if HD. $O_{2PEAK}$

across groups was not found to be related to regional CBF in any of the brain regions assessed, however a group difference in the relationship between $O_{2PEAK}$ and CBF was observed in the left caudate, in which lower CBF was seen in patients with higher $O_{2PEAK}$. CBF CVR was lower in HD patients than controls and appeared to interact with $O_{2PEAK}$ although this was also not significant, possibly due to the small number of subjects who completed the breath-hold challenge effectively. From the present data, it is not clear that cardiorespiratory fitness is beneficial in HD. An interaction in the left caudate nucleus between $O_{2PEAK}$ and resting CBF does suggest that CBF may in fact be reduced in fitter patients but increased in fitter controls. Future work is required to investigate the implications of this relationship, and explore cerebrovascular health using preclinical MRI which may shed light on the mechanism at play in pre-/early-stage HD.

## 4.1. Introduction

Huntington's disease (HD) is an autosomal dominant inherited neurodegenerative disorder caused by a CAG repeat expansion mutation in the *HTT* gene on chromosome 4 (Vonsattel and DiFiglia, 1998). HD is characterized by progressive motor dysfunction, psychiatric disturbances, and cognitive decline, and there is currently no cure. Present efforts are focussed upon identifying therapeutic targets and developing treatments that may delay onset or slow the progression of the disease once clinical signs are manifest. Furthermore, there are currently very few objective measures of disease progression during the pre-manifest phase of the disease where patients are apparently asymptomatic.

People with Huntington's disease (HD) are known to be weaker (Busse et al., 2008), walk less and fall more (Busse et al., 2009) than age-matched healthy controls. Given the increased levels of apathy and anhedonia with disease progression (Tabrizi et al., 2013), HD sufferers will often reduce their activity patterns substantially as symptoms manifest. This passive lifestyle has been suggested to influence symptom onset in patients with Huntington's disease (Trembath et al., 2010). Moreover, as described in previous chapters, the evidence from exercise studies in animals (van Praag et al., 1999b), in healthy people (Ainslie et al., 2008) and people with other neurological conditions (Goodwin et al., 2008) suggest that exercise can be highly beneficial; improving mobility, cognition, general health and wellbeing such that administration of exercise programmes in HD may act to slow disease progression (Khalil et al., 2013b; Quinn et al., 2016b).

Prescribing aerobic and anaerobic exercises using principles based on healthy individuals has been shown to be safe and feasible in HD patients (Khalil et al., 2013b). Should exercise begin to exert its beneficial effects on the brain early in life, as described in Chapter 2, it is possible that this may delay the onset of neurodegeneration and cognitive decline. Exercise recommendations are a cost-effective and globally beneficial recommendation that could be encouraged by healthcare professionals, to those at genetic risk for HD prior to HD diagnosis, as

well as those post-diagnosis, prior to symptom onset, where mobility is less compromised.

To date, there have been no studies to investigate the benefits of physical activity on the brain in HD patients. Assessment using reliable non-invasive measures such as MRI, could be invaluable in determining the therapeutic potential of interventions (Aylward, 2007). Where it may be possible to detect changes early in the lifespan using sensitive imaging biomarkers, the ability to track early signs of degeneration prior to symptom onset would be invaluable for monitoring individual responses to a wide range of treatments, including exercise interventions. Before integrating neuroimaging into such complex interventions, however, it is necessary to review what is already known regarding the differences between the early-diseased brain and healthy controls, and whether a cross-sectional measure of fitness can predict these differences.

A number of neuroimaging studies have detected disease related differences between preclinical HD cases and gene-negative controls, including alterations in brain structure (Aylward, 2007; Tabrizi et al., 2009) , metabolism (Feigin et al., 2014) and perfusion (Harris et al., 1999; Tabrizi et al., 2009; Wolf et al., 2011). Interestingly, brain activation and perfusion differences in preHD have been demonstrated even in the absence of structural changes (Chen et al., 2012). It is possible that changes in cerebral blood flow and metabolism may be a more sensitive marker of cerebral health in subjects with early or pre-symptomatic HD (preHD) than volumetric measures alone. Studies using SPECT and PET, have demonstrated striatal and cortical changes in baseline rCBF (Harris et al, 1999) in both manifest HD and pre-manifest HD subjects. In their study, they observed that altered rCBF was associated with cognitive changes including changes in memory and executive function, even in preHD patients. An ASL study by Wolf and colleagues (2011) reported that preHD participants had lower rCBF than controls in the lateral and medial prefrontal cortex and left putamen, whilst in addition showing increased CBF in the left precuneus and right hippocampus. Hypoperfusion in the striatum was absent in those far from onset, but became significant in the precuneus as they approached motor onset. From this evidence, it is clear that the pattern of CBF changes may be region specific and could pinpoint regions which are more sensitive to therapeutic interventions.

Cerebrovascular reactivity is an informative measure of cerebral health, as it shows the ability of the brain to mount a flow response to areas in the brain that need it. Where cerebrovascular reactivity is jeopardized, there is a potential for chronic undersupply and that can threaten the neuronal tissue. To date, there have not been any studies to investigate whether vascular reactivity is jeopardized in HD patients. Human studies have observed hyporeactivity in AD (Cantin et al., 2011) whilst a preclinical MRI investigation has reported a similar decline in reactivity to a carbogen gas challenge in an HD mouse model (Hsiao et al., 2015). The absence of CVR research in HD patients may be due to the methodological challenges involved in delivering combined hypercapnic challenges with MRI. Dynamic end-tidal forcing (Wise et al., 2007) or prospective $CO_2$ targeting (Slessarev et al., 2007) gas challenges, require participants to breathe $CO_2$ enriched gas through a mask inside the scanner. This is not only uncomfortable for patients, but also requires thorough screening and exclusion criteria often apply to smokers and those with respiratory difficulties. Where patient recruitment is already challenging, additional exclusion criteria is not ideal. The present study used a breath-hold challenge, like that used in Chapter 2, to get around this issue since breathing is self-paced and participants can stop if they feel any discomfort. A caveat, is that for accurate end-tidal $CO_2$ measurement, participants are required to follow a series of instructions. Given the cognitive difficulties present in HD, it is unknown whether this paradigm is feasible in HD patients. However, this question is worthy of exploration since the development of new and feasible imaging biomarkers in HD is important for assessing disease progression and treatment efficacy.

HD is an exceptional disease, whereby diagnosis is possible years prior to symptom onset. This provides us with a unique window in which to recommend lifestyle changes that may improve prognosis, delay manifestation and slow decline. In previous chapters, the relationship between physical activity and cerebrovascular markers were observed, even early in the lifespan. Whether physical activity can mediate group differences in cerebral blood flow that have been previously reported in HD remains unexplored. The purpose of the present study is to assess whether differences in resting CBF and CBF CVR can be predicted by cardiorespiratory fitness in the same way for pre-/early-symptomatic HD patients as controls.

Participants took part in a $O_{2MAX}$ protocol on a cycle ergometer, like that performed in Chapter 2 but tailored to accommodate safety and feasibility in patients. $O_{2PEAK}$ was measured as a surrogate of $O_{2MAX}$ where patients were unable to reach the strict physiological boundaries associated with a true $O_{2MAX}$. On a second session, participants were scanned with PASL MRI at 3T. The relationship between fitness and CBF in pre-/early-symptomatic patients and healthy matched controls was investigated by acquiring measures of cerebrovascular function including baseline CBF, tissue arrival time (TAT) and CBF-CVR to a breath hold challenge. It was hypothesised that pre-/early-symptomatic HD patients would demonstrate locally distributed differences in CBF in frontal striatal regions, reflective of an early pathological process and that performance on a cardiorespiratory fitness test ( $O_{2PEAK}$) would be predictive of cerebrovascular and neurocognitive outcome measures.

## 4.2. Methods

### 4.2.1 Participants

21 patients (8 pre-symptomatic, 9 early-stage, 5 mid-stage) and 19 controls were initially recruited from the Cardiff Huntington's Disease Centre based at Cardiff University. All patients recruited were currently registered on the ongoing global longitudinal study of Huntington's Disease patients (ENROLL-HD) in which baseline motor, cognitive, psychiatric, demographic and CAG repeat data is collected annually and made centrally available to scientists working within participating sites. Recruitment was targeted towards HD patients with impaired cognition, operationalised as a score below 200 (indicative of mild impairment) on the Unified Huntington's Disease Rating Scale (UHDRS) whilst a control group was recruited based upon age, gender and education matching. All participants were deemed by their neurologist to have full capacity to consent and were informed of their right to withdraw at any time without giving reason, and that data would be held confidentially.

*Inclusion criteria:*

- Genetically-confirmed Huntington's disease (for patient group only)
- Aged 18-65 years
- Able to understand and communicate in spoken English (for consent purposes and cognitive testing)
- If regular medication is taken, the medication regime must have been stable for four weeks prior to initiation of the study and between sessions.

*Exclusion criteria*:

- Any physical or psychiatric condition that would prohibit the participant from completing the intervention or the full battery of assessments (including sports injuries where moderate exercise is not recommended, rest angina, hypotension or hypertension, ankle oedema, shortness of breath at rest, dizziness, epilepsy and/or any psychiatric condition that affects the ability to comprehend verbal or written instructions).
- A (self-reported) blood-borne disease and/or haemophilia.
- Inability to independently use the cycle ergometer.
- Currently actively involved in any interventional trial (i.e. have begun the intervention) or within four weeks of completing an interventional trial.
- MRI contraindications (e.g. a pacemaker) as established using CUBRIC's standard screening procedures.
- Any known neurological condition or abnormality (other than HD).
- Pregnancy or childbirth in the last 6 weeks.
- Current and/or history of cardiac (heart), vascular (blood vessel) or respiratory/pulmonary (breathing/lung) conditions, including high blood pressure.
- Currently experiencing dizziness or fainting on a regular basis.

### 4.2.2 Demographic Information

#### Education

The International Standard Classification of Education (ISCED) scale was used to determine years of education and education level, since educated people are thought to maintain a greater cognitive reserve than those with lower education status (Stern, 2009).

#### Disease Burden

The Disease Burden index is a measure of disease severity that estimates the cumulative toxicity of mutant Huntingtin based upon the number of polyglutamine (CAG) repeats and age, using the formula (age × [CAG-35.5]) (Penney et al., 1997), where higher scores indicate a greater level of impairment. This measure of disease severity was derived from a post-mortem study, in which a correlation between CAG repeat length and striatal atrophy was observed (Penney et al., 1997). Where older patients with the same repeat length will have had greater exposure to the effects of the CAG expansion, disease severity typically worsens over the lifespan in those who have a CAG repeat length greater than 35.5. Disease burden has been adopted by a number of studies, including the large-scale multi-centre TRACK-HD study (Tabrizi et al., 2009) which revealed strong associations between disease burden scores and several phenotypical features, including neurophysiological, oculomotor, cognitive, neuropsychiatric and brain atrophy in pre-manifest HD gene carriers. As a result, it was decided that this measure would be adopted in this thesis.

#### UHDRS Score

The Unified Huntington's Disease Rating Scale '99 (UHDRS) had been conducted by a research nurse at the Cardiff Huntington's Disease Centre as part of the ENROLL-HD within the year leading up to assessment in this study. The UHDRS was developed to assess the clinical features of HD and includes motor, cognitive, behavioural, and functional subscales ("Unified Huntington's Disease Rating Scale: reliability and consistency. Huntington Study Group," 1996). The UHDRS has been well validated with high inter-rater reliability and internal consistency. The availability of these assessment results is useful in terms of characterising the HD group in terms

of heterogeneity of symptoms and their severity, and for comparison with other study cohorts. (See Table 4.1. for participant UHDRS and Demographic scores).

Motor. The motor assessment examines 15 motor behaviours with a maximum score of 60 indicating maximum motor disability.

Functional Assessment Scale. The functional assessment contains 25 questions relating to daily functioning with a maximum score of 20 indicating functional capacity.

Independence. The independence scale is measured in percentage, with 100% representing no special care needed, and 10% representing tube fed / total bed care.

Total Functional Capacity scale. The Total Functional Capacity scale (Shoulson and Fahn, 1979) is the main assessment tool of functional status in HD clinical care and research, designed to assess progression of HD in symptomatic patients with emphasis on self-care, mobility, and independence. A maximum score of 13 indicates full capacity in all domains assessed. However, this scale may be less sensitive to functional changes in patients far from symptom onset.

Cognitive assessment score. Summed performance on the verbal fluency test (letters and categories), symbol digit modality test, and Stroop interference test, with a score > 200 indicating cognition in the normal range. This score was independent from the cognitive testing that took place during this study.

### 4.2.3 Participant preparation

Participants were asked to refrain from the consumption of alcohol and/or caffeine, and to refrain from moderate to high intensity exercise for 24 hours prior to the scan session since it is known that these factors affect cerebral perfusion. Participants were also asked to refrain from the consumption of cigarettes, caffeine and to avoid moderate intensity exercise for a period of three hours prior to the testing session.

All participants were screened for contraindications to:

- Exercise. High blood pressure, completion of the Physical Activity Readiness Questionnaire the American College of Sports Medicine (ACSM) checklist to identify cardiovascular risk for exercise and a 12-lead ECG electrocardiogram (ECG) assessment to ensure safety to initiate exercise.

- MRI. Comprehensive screening for MRI contraindications carried out during recruitment and on the day of scanning and immediately before each MRI scan.

### 4.2.4 Fitness test ( $O_{2MAX}$)

The $O_{2MAX}$ aerobic exercise assessment was conducted on a Lode Corival cycle ergometer (1000 watts, Cranlea Human Performance Ltd, Birmingham). Saddle heights were adjusted to accommodate knee flexion (170° to 175°) and feet were supported in the pedals by Velcro straps and taping where necessary to ensure feet were secure (Dawes et al., 2014). For the graded exercise test, the equipment used was the same as that used in the EXERT-HD study (South East Wales Research Ethics Committee, 06/11/2014, ref.:13/WA/0315) at Cardiff University.

#### *4.2.4.1. Physiological Measurements*

The following measurement were taken at rest and then every 2 minutes throughout exercise and 10mins following cessation of exercise to track recovery.

1. Heart rate was monitored using a heart rate monitor worn as a strap around the chest with transmission to a watch on the patient's wrist Polar Equine InZone Heart Rate Monitor (Polar, UK).

2. End-tidal $O_2$ and $CO_2$ was measured on a breath-by breath basis using a face mask connected to a gas analyser system (Metamax, Cortex Biophysik, Leipzig, Germany) from which physiological measurements including the respiratory exchange ratio (RER), ventilation volume (VE) and oxygen consumption ( $O_2$). The gas analysis system was calibrated according to manufacturer's instructions on the day of testing.

3. Borg's rating of perceived exertion (RPE) CR10 Scale (0-10) (Borg and Kaijser, 2006) was used to measure perceived fatigue of both the legs and breathing to self-monitor work rate.

4. Blood lactate concentration was used as an additional measure of exercise intensity, as it has been used previously as a reliable measure of aerobic exercise. Real time lactate measurements were taken every 2 minutes at the end of each work-load using a sterile lancet to take a pinprick of blood from the earlobe and gain an immediate reading using a Lactate Plus portable lactate analyser (Laktate, Donostia).

#### *4.2.4.2. $O_{2MAX}$ Criteria*

Baseline measurements were acquired prior to cycling, after which participants began a warm-up including 3 minutes of unloaded pedalling. Following this warm-up, load was increased to 50 watts and increased by 25 watts every 2 minutes (max 15mins) until subject met at least 3 of the following established criteria:

1. A plateau in $O_2$ with increasing load
2. Volitional exhaustion (Borg CR10 score ≥8)
3. Unable to maintain work rate above 40 rpm.
4. Heart rate above 95% of predicted maximum
5. RER above 1.1
6. Lactate above 8mM

### 4.2.5 Storer Maximal Bicycle Test for Predicted O2MAX

Where it is not feasible to carry out a full $O_{2MAX}$ and to account for gender differences, the Storer Maximal Bicycle Test (Storer et al., 1990) has been used to predict $O_{2MAX}$. This test has been used previously in exercise tests of HD patients

(Dawes et al., 2014; Quinn et al., 2013) and was calculated in addition to the more robust $O_{2MAX}$ measure using Equation 1.

Equation 1

Males:

$$VO2MAX\ ml.min\text{-}1 = 10.51\ W + 6.35\ Kg - 10.49\ years + 519.3$$

Females:

$$VO2MAX\ ml.min\text{-}1 = 9.39\ W + 7.7\ Kg - 5.88\ years + 136$$

### 4.2.6 Cognitive, Mood and Disease severity assessments

Participants completed a number of cognitive tasks and questionnaires relating to mood and daily activity levels.

#### *4.2.6.1. Cognitive tests*

Speed and Capacity of Language Processing (SCOLP): This short test of information processing speed required participants to verify as many sentences as possible in two minutes. Outcome measures included the number or correct answers within a time limit and error rate.

Forward digit span: This task of working memory required participants to read a sequence of numbers and recall the numbers in the order they heard them, from 2-9 digits in length.

Symbol Digit Modalities Test (SDMT): This substitution task of executive functioning required participants to use a reference key to pair specific numbers with given geometric figures in a 90 second period.

Letter Fluency task: Participants were required to generate words beginning with a given letter (e.g. words beginning with the letter F). Participants were given one minute to retrieve as many words as possible, avoiding repetitions and proper nouns (e.g. Friday or Fred). Outcome measures included the number of correct words, number of intrusions (i.e. inappropriate word) and number of perseverations (i.e. repeated word). The task was conducted three times, for the letters F, A and S.

Stroop task (colour and word reading, interference components): The full test included baseline measures for speed of colour naming and word reading as well as the interference task in which subjects were shown the names of colours, written in an incongruent colour (e.g. RED) and instructed to recall the colour that the word was written in. Outcome measures included number of accurate responses, errors and self-corrected errors made in 45 secs.

Trail Making Test Parts A & B: This pencil and paper task uses randomly placed letters (and numbers for part B) as stimuli which participants were required to connect in sequence by drawing a continuous line with a pencil (e.g. A-1-B-2-C-3 for part B). Outcomes included speed of completion and number of errors.

#### *4.2.6.2. Questionnaires*

Hospital Anxiety Depression Scale (HADS): This short scale was used to screen for depression and anxiety symptoms.

World Health Organisation Quality of Life Questionnaire (WHO-QL; Short version): A 26-item instrument to measure the following broad domains: physical health, psychological health, social relationships and environment.

International Physical Activity Questionnaire (IPAQ) 7-days SHORT: This short-form instrument assessed subjective physical activity undertaken during a representative week such that an average MET score can be computed by summation of the duration (in minutes) and frequency (days) of walking, moderate-intensity and vigorous-intensity (Craig et al., 2003).

Sociodemographic questionnaire**:** Participants were asked to report their gender, age, height, weight, ethnicity, handedness, alcohol and caffeine use, years in education, and occupation to determine confounding variables and to determine sample heterogeneity.

### 4.2.7 MRI Acquisition

All scanning was carried out using a 3T GE HDx scanner (GE Healthcare, Milwaukee, WI, USA) equipped with an 8-channel receive-only head coil.

#### 4.2.7.1. Structural Imaging

All participants underwent whole brain $T_1$-weighted structural scans (3D FSPGR, in-plane resolution = 1x1mm, slice thickness = 1mm, TI= 450ms, TR =7.8ms, TE = 3ms, matrix size= 256 x 192) for registration and structural segmentation purposes. An array spatial sensitivity encoding (ASSET) factor was applied to assess the sensitivity of the 8 coils so that fewer phase encoding directions could be sampled. This enables the use of a shorter TE with fewer distortions, which is advantageous as it speeds up acquisition time which is beneficial in HD patients. It was considered that faster acquisition was worth the trade-off in signal to noise ratio (SNR).

#### 4.2.7.2. Baseline CBF

Baseline CBF at rest was quantified as described in Chapter 2, using a multi-inversion time PASL sequence (PICORE with a QUIPSS II cut-off at 700ms (Wong et al., 1998)). Different inversion times were adopted for the present study whereby short (TI's = 400, 500, 600, 700) and long TI's (TIs = 900, 1000, 1500, 2,000ms) were acquired as separate scans in which the label (width 200mm) was applied 10mm below the most proximal slice. Images were acquired with the same parameters to those described previously in Chapter 2 but with, eight control–tag pairs per TI, 15 slices, slice gap=1.5mm, FOV=198mm, voxel size=3x3x7mm$^3$. Total acquisition for both short and long TI scans was ~7 minutes. As before, an $M_0$ CSF scan was acquired for calibration without labelling in which the same acquisition parameters were applied as above except for the TR=4s.

#### 4.2.7.3. Cerebrovascular reactivity

A breath-hold paradigm was carried out as described in Chapter 2 according to the methods of (Bright and Murphy, 2013). Imaging parameters were identical, except participants were required to complete 10 end-expiration breath-holds (15s each) interleaved with 30s periods of paced breathing at rate of 12 breaths per minute (Murphy et al., 2011b).

Total scan duration was ~8 minutes during which quantitative arterial spin labelling (PASL) and BOLD-weighted images were acquired with a single-shot PICORE QUIPSS II (Wong et al., 1998) pulse sequence (TR=2.4 s, TI1=700ms, TI2=1500ms, 20-cm tag width, and a 1-cm gap between the distal end of the tag and the most proximal imaging slice) with a dual-echo gradient echo (GRE) readout (Liu et al., 2002) and spiral acquisition of k-space (TE1=2.7ms, TE2= 29ms, flip angle=90°, field of view (FOV)=20 cm, 64×64 matrix, ). Fifteen slices of 7mm thickness were imaged, with an inter-slice gap of 1mm.

### 4.2.8 MRI Image Analysis

#### 4.2.8.1. Baseline CBF

Quality control was performed on the raw data, by visual inspection for gross movement prior to group matching. Subjects were excluded where gross movement was observed during either the short or long TI scans that could not be satisfactorily removed after motion correction.

Resting CBF was acquired using identical methods to those described in Chapter 2, with the addition of a partial volume correction step described in detail below. Briefly, tag-control difference images over full MTI time-series were calculated and used for quantification of resting CBF. Signal within the ventricles ($M_0$ CSF) was used to estimate $M_0$ blood (Lu et al., 2004) and modelled to calculate whole brain perfusion maps using FSL BASIL toolbox (FMRIB Software Library, Oxford, UK).

Partial volume correction was carried out as described previously (Chappell et al., 2011). Different tissue types within the same voxel influence the estimation of grey matter CBF in this type multi-TI ASL data where SNR is low. This method exploits differences in the kinetics between grey and white matter signals, and performs partial volume estimates of tissue type and spatially regularises the data such that the appropriate degree of smoothing is estimated from the data itself. In the case of ageing or atrophy, as would be expected in HD patients, the effects of PV (PVEs) are particularly problematic. Estimating the appropriate degree of smoothing is important since rapid spatial variations in the GM CBF means that smoothing is more

likely to result in contaminated voxels. In order to correct for partial volume of tissue, an additional step (Chappell et al., 2011) was added into the MTI CBF quantification performed in Chapter 2, using the oxford_asl tool within the FSL BASIL toolbox for quantification of CBF from ASL data (Chappell et al., 2009). For each subject, GM and WM masks were first segmented from individual T1 structural images using FSL FAST (Zhang et al., 2001) and transformed into low-resolution space of the ASL data using FSL FLIRT (Jenkinson et al., 2002; Jenkinson and Smith, 2001). Low resolution GM and WM masks were subsequently applied to the data, whereby the signal arising from GM and WM were modelled using the general kinetic model (Buxton et al., 1998).

#### *4.2.8.1.1 Baseline CBF in Regions of Interest*

##### *4.2.8.1.1.1 Cortical Masks*

Whole-brain and Frontal lobe grey matter masks were applied to voxel-wise CBF maps to produce average GM CBF estimates within each region as described previously, by performing individual T1 tissue segmentation to calculate a subject specific GM mask and deriving a Frontal Lobe mask based upon an MNI standard template. Raw data was screened for outliers, and values >3 S.D from the mean were removed. Assumptions were tested for normality, homogeneity of variance using Levene's Test, and collinearity in the case of multiple regression. FDR-corrected p-values (q values) are reported where applicable.

##### *4.2.8.1.1.2 Sub-cortical Masks*

To investigate CBF differences in subcortical regions, subcortical segmentation was performed on a subject by subject basis, using FSL FIRST (Patenaude et al., 2012) in which a surface mesh is created for each subcortical structure using a deformable mesh model. Subcortical masks were applied to individual Grey Matter CBF images, and the median CBF signal was derived for each ROI, for each hemisphere independently. ROIs of interest included the basal ganglia (caudate, pallidum, putamen, thalamus and accumbens) as well as the hippocampus (Fig 4.1). Raw data was screened for outliers, and values >3 S.D from the mean were removed. Assumptions were tested as described above and FDR-corrected p-values (q values)

are reported where applicable ($p<0.05$). Volumetric data will not be presented since it is not the focus of this thesis.

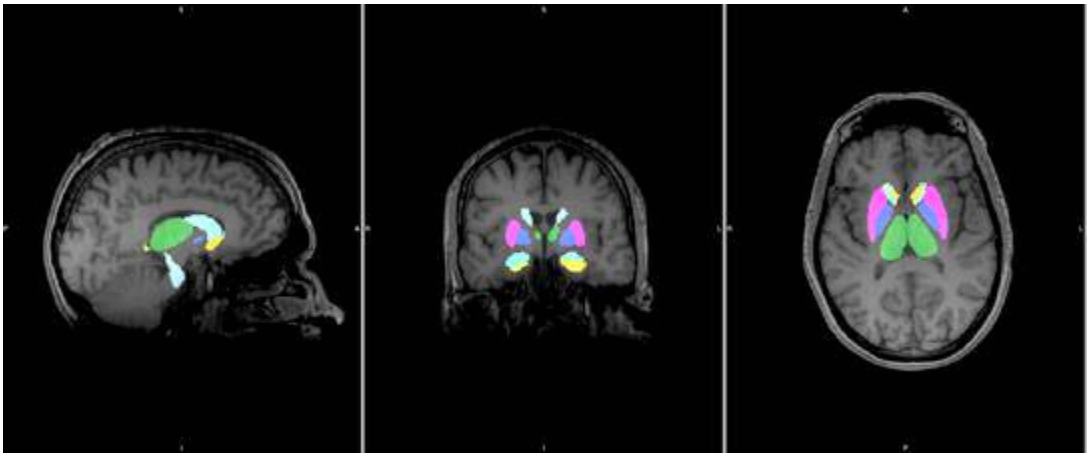

**Figure 4.1 Subcortical masks created by FSL FIRST.** Bilateral subcortical masks were created using FSL FIRST for masking ASL images to extract region specific CBF values. Green = thalamus, Pink = putamen, Light blue = Caudate, Yellow = hippocampus, Blue = pallidum, Orange = Accumbens.

#### 4.2.8.2. Cerebrovascular Reactivity

##### *4.2.8.2.1. Breath-hold paradigm and quantifying feasibility in HD patients*

Cerebrovascular reactivity was measured by quantifying absolute ΔCBF in response to a hypercapnic stimulus, which in this experiment utilised the breath-hold task as described in Chapter 2, since it is easier to administer in patients, where a face-mask may be restrictive and exclusion criteria, such as smoking, would limit the number of eligible patients for this experiment. Despite an increase in comfort, this task requires the ability to remember and follow instructions. Since cognitive impairment is common in patients at this stage, it was unknown how well subjects would perform on this challenge.

Since this is the first time such this breath-hold paradigm has been carried out in Huntington's Disease, a secondary interest was to assess feasibility for informing future studies. This was done by measuring the number of breath-holds that demonstrated a clear end-tidal peak immediately before resuming paced breathing. It is important that the peak end-tidal $CO_2$ measurement is recorded immediately

following the breath-hold to get the best CVR measurements, as this is used as a surrogate measure of arterial $CO_2$. Instructions were given on the screen inside the scanner, but due to the cognitive impairment experienced by HD patients, a video (~4mins) was shown immediately prior to entering the scanner, in which they observed the instructions of the task and were instructed to practice outside the scanner, with emphasis on holding breath with empty lungs. The video can be viewed by following this link https://youtu.be/k6RF4bFN0vU. The paradigm was conducted identically to that in Chapter 2, except 10 breath-holds instead of 4, were used to achieve greater SNR.

#### *4.2.8.2.2. CVR Quantification*

Cerebrovascular reactivity was quantified in a similar way to that described in Chapter 2. Briefly, dual-echo data was separated into the CBF and BOLD echoes respectively. Because CBF reactivity was the primary interest in this study and because BOLD and CBF CVR were highly correlated in Chapter 2, only absolute second-echo CBF data was analysed. However, due to the better SNR of the BOLD data compared to CBF, BOLD time-series data were motion corrected in MCFLIRT (Jenkinson et al., 2002) and these parameters were applied to the CBF time-series. The first echo data were used to calculate a subtraction time-series (Murphy et al., 2011a) from which CBF was quantified to the standard single-compartment CBF model (Wong et al., 1998). Two-dimensional time-series were extracted by averaging across a whole-brain GM and frontal cortical mask.

$CO_2$ data was pre-processed by manually validating end-tidal $CO_2$ values. $CO_2$ data was removed where the trace was too noisy to observe the breathing trace, due to chorea (figure 4.2.), and where the task was obviously not being performed, possibly due to cognitive difficulties following the task. The number of accurate end-tidal expirations prior to paced breathing were recorded out of a maximum of 10 possible breath-holds. Data was included in cases where the subject was holding their breath in-time with the on-screen instructions and at least 3 end-tidal expirations were performed accurately. Example $CO_2$ traces can be seen in figure 4.2 including one subject who carried out the end-tidal expirations perfectly (10/10) or poorly (1/10). Where <10 and >3 end-tidal expirations were performed accurately, end-tidal $CO_2$

peaks were manually added to the time-series by extrapolation based on the accurate end-tidal expirations during the task.

Finally, a regression analysis was performed to measure absΔCBF per mmHg change in absolute end-tidal $CO_2$ with a 3rd order polynomial included to remove slow signal drift. Temporal lag-fitting (time-shift steps of 0.1s) was also carried out, to account for the delay between end-tidal $CO_2$ increase in response to breath-holding and the subsequent blood flow response (Bright and Murphy, 2013).

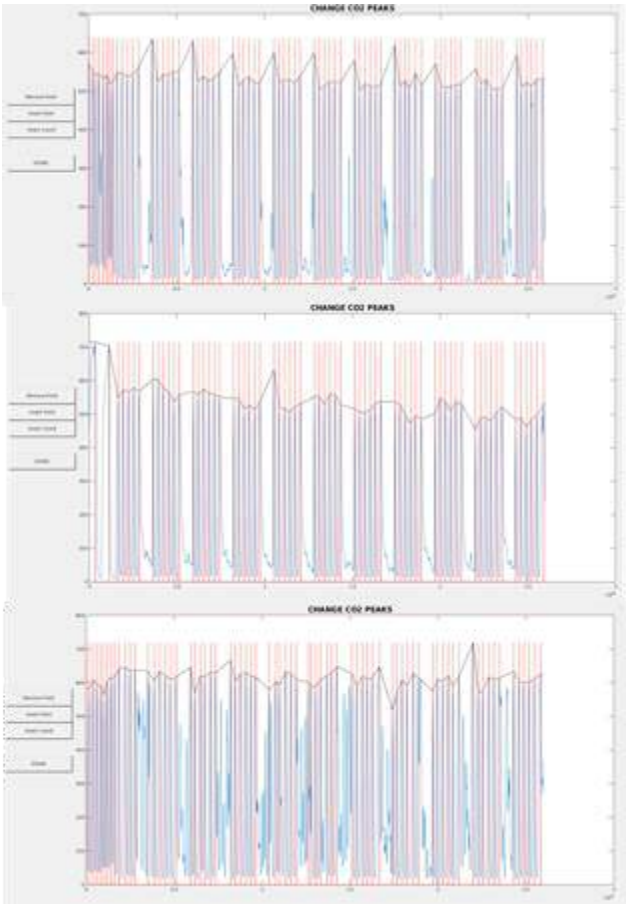

**Figure 4.2 Example end-tidal $CO_2$ recordings.** End-tidal $CO_2$ trace for three subjects. Top) A good $CO_2$ trace in which end-tidal $CO_2$ peaks can be observed at the end of each hold; Middle) A poor trace with only one accurate end-tidal breath, such that end-tidal $CO_2$ could not be reliably quantified; Bottom) A poor end-tidal trace from a subject who exhibited mild chorea, such that the end-tidal trace appeared extremely noisy. X-axis = scanner volumes, Y-axis = End-tidal $CO_2$ trace (mmHg x 15.2).

## 4.3. Results

Out of a total of 21 patients and 19 controls, a matched sample of 15 patients (6 pre-symptomatic, 9 early-stage) and 15 controls was selected based upon meeting inclusion criteria, for age matching and for data quality (Table 4.1). Data from these will be presented for the remainder of this thesis.

**Table 4.1. Demographic data and disease specific measures for the experimental cohort, before and after matching.**

| | Before Matching | | | After Matching | | |
|---|---|---|---|---|---|---|
| Measure | HD Group (N=21) | Healthy Group (N=19) | P-value | HD Group (N=15) | Healthy Group (N=15) | P-value |
| Age (years) | 46 ± 9 (32-65) | 43 ± 10 (29-63) | 0.47 | 44 ± 9 (32-64) | 44 ± 9 (30-63) | 0.83 |
| Gender: male, n (%) | 62 | 58 | 0.79 | 67 | 67 | 1.00 |
| Mass (Kg) | 77 ± 20 (48-118) | 80 ± 14 (60-121) | 0.63 | 77 ± 19 (48-118) | 80 ± 9 (71-98) | 0.50 |
| Diastolic BP | 79 ± 9 (63-95) | 82 ± 13 (66-118) | 0.43 | 79 ± 8 (64-92) | 85 ± 14 (66-118) | 0.12 |
| Systolic BP | 132 ± 12 (114-162) | 131 ±13 (108-155) | 0.79 | 130 ± 12 (114-162) | 132 ± 12 (108-149) | 0.75 |
| Resting Heart Rate (bpm) | 76 ± 15 (52-108) | 68 ± 12 (49-94) | 0.09 | 75 ± 16 (52-108) | 66 ± 11 (49-90) | 0.10 |
| Education (years) | 16 ±4 (11-23) | 19 ± 3 (13-28) | 0.02* | 16 ± 4 (11-23) | 19 ± 4 (13-28) | 0.05 |
| Disease Burden Score | 1975 ± 399 (1344-2730) | N/A | N/A | 1928 ± 387 (1344-2688) | N/A | N/A |
| UHDRS TMS | 24 ± 19 (0-68) | N/A | N/A | 21 ± 17 (0-46) | N/A | N/A |
| UHDRS Total Functional Capacity | 10 ± 3 (3-13) | N/A | N/A | 11 ± 3 (3-13) | N/A | N/A |
| UHDRS Independence Score (%) | 88 ± 14 (60-100) | N/A | N/A | 91 ± 13 (60-100) | N/A | N/A |
| UHDRS Functional Assessment Score | 22 ± 4 (12-25) | N/A | N/A | 23 ± 4 (12-25) | N/A | N/A |
| UHDRS Total Cognitive Score | 215 ± 77 (79-371) | N/A | N/A | 235 ± 73 (115-371) | N/A | N/A |
| CAG repeat length | 43 ± 2.6 (39-50) | N/A | N/A | 44 ± 2 (41-50) | N/A | N/A |

Mean ± SD (range). P value (independent t-test (independent variances assumed ) or chi-squared test). UHDRS TMS= Unified Huntington's Disease Rater Scale Total Motor Score.

### 4.3.1 Fitness Test ( $O_{2PEAK}$)

It was predicted that many patients would be unable to reach their true $O_{2MAX}$, such that their peak activity level ( $O_{2PEAK}$) would be considered for the following experiment. Nonetheless, established $O_{2MAX}$ criteria were applied to each individual's exercise test individually and the results can be seen in Table 4.2. Of the cohort 8/15 (53%) patients and 12/15 (80%) healthy controls met at least 3 of the defined criteria, whilst 11/15 (73%) patients and 15/15 (100%) healthy controls met 2 of the defined criteria.

**Table 4.2.** $\dot{V}O_{2MAX}$ criteria and proportion of patient and controls (%) who achieved them.

| Test Criteria | HD (% cohort) | Controls (% cohort) |
|---|---|---|
| Max Heart Rate Achieved (220 bpm -Age) | 67 | 80 |
| RER >1.1 | 40 | 73 |
| Lactate > 8 mMol/L | 53 | 100 |
| Borg RPE > 8/10 (Legs or Breathing) | 60 | 73 |

A trend between $O_{2PEAK}$ and disease burden was observed (figure 4.3) however this did not meet statistical significance ($r(15) = -0.41$, $p=0.06$). Whether fitness improves disease burden, or whether greater disease burden impacts fitness cannot be disentangled from this analysis.

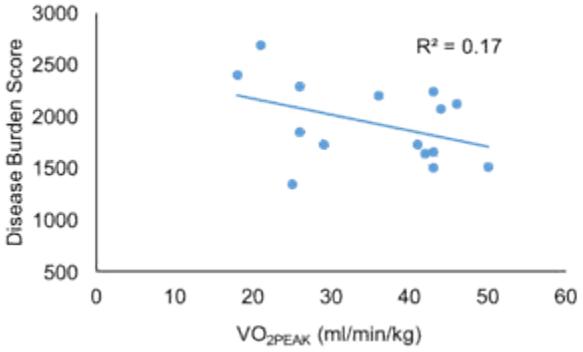


**Figure 4.3 Relationship between disease burden score and $VO_{2PEAK}$.** Disease Burden Score was inversely related to cardiorespiratory fitness ($VO_{2PEAK}$) in Huntington's Disease, although this was significant. Disease burden = (age × [CAG-35.5]) (Penney et al., 1997)

The HD group had a mean $O_{2PEAK}$ of 36 (±10) ml/min/kg compared to healthy matched controls who had a mean $O_{2PEAK}$ of 37 (± 11) ml/min/kg, such that the groups did not significantly differ in terms of fitness (t (28) =0.38, *p*= 0.70, n.s.). Groups also did not differ on the Storer measure of predicted $O_{2MAX}$ (t (28) =0.76, *p*= 0.45, n.s.) nor on the IPAQ measure of self-reported measure of physical activity levels (t (27) =-0.03, *p*=0.98, n.s.). Bivariate one-tailed Pearson correlation revealed that both the Storer (r (30) =0.60, *p*<0.001) and Self-reported IPAQ measures (r (29) = 0.46, *p*<0.01) were both highly correlated with the true $O_{2PEAK}$ values assessed in this study (Figure 4.4).

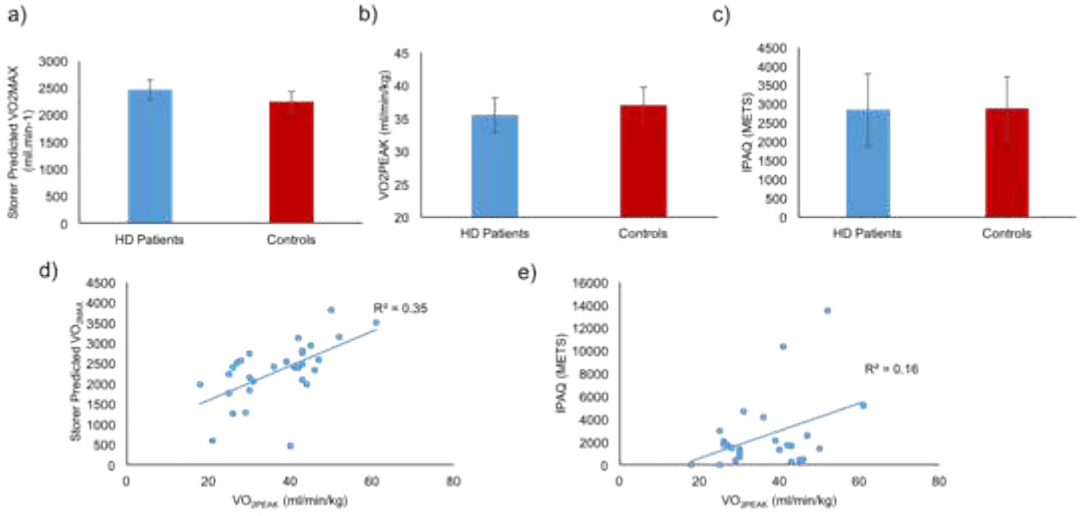


**Figure 4.4 Genotype differences assessed by subjective, predictive and quantitative fitness measures.** HD patients did not differ from matched controls in fitness as determined by a) $O_{2PEAK}$ b) Predicted $O_{2MAX}$ (Storer) or 3) Self-report (IPAQ) (Error bars = S.E.M d) Predicted and e) Self-reported fitness was significantly associated with the $O_{2PEAK}$ assessment.

## 4.3.2 Mood and Neurocognitive Function

### 4.3.1.1. Quality of Life

In a linear regression model, HD subjects scored significantly poorer than controls on several domains on the WHOQOL-BREF Quality of Life scale, including domains of physical health, psychology and social relationships but not environment (Table 4.3). In HD patients, these scores appeared to get worse with disease burden, however these associations were not significant (*p-values* >0.05, n.s.).

In a multiple regression with $O_{2PEAK}$ included as a covariate, no interactions were observed (p-values>0.05, n.s.), suggesting that the relationship between $O_{2PEAK}$ and Quality of life was the same in HD patients and controls.

### 4.3.1.2. Mood

HD patients scored more highly on reported depressive symptoms than controls, (Table 4.3) and disease burden appeared to be associated with more symptoms of depression and anxiety but these relationships were not significant (*p*>0.05, n.s.). $O_{2PEAK}$ was associated with *reduced* anxiety and depressive symptoms, although this was not statistically significant and this relationship appeared to be similar for both HD patients and controls (*p*>0.05, n.s; Table 4.3).

### 4.3.1.3. Cognition

#### *4.3.1.3.1. Group differences in Cognition*

Linear regression was carried out to address group differences on cognitive function. HD subjects performed worse than controls on all tasks including Verbal Fluency, Symbol Digits Modalities, Speed of Comprehension, Forward Digit Span, STROOP interference, and Trailmaking A and B tasks (*p*-values<0.05) and these were significant after FDR correction for multiple comparisons (Table 4.3).

#### *4.3.1.3.2. Disease Burden and Cognition*

One tailed Pearson's correlations were carried out to assess the relationship between disease burden and cognitive task performance, where cognition was

expected to decline with disease burden. Disease burden was associated with worse performance on most tasks, including STROOP (r (13) =-0.6, *p*=0.01), SCOLP (r (12) = -0.79, *p* <0.001), Trailmaking A (r (13) = 0.59, *p*= 0.02) and B (r (13) =0.70, *p*<0.01), and SDMT (r (13) =-0.62, *p*=0.01) but not Verbal Fluency (r (13) =-0.38, *p*=0.09, n.s.) or Forward Digit Span (r (13) =-0.20, *p*=0.18, n.s.). Reported p-values are FDR corrected for multiple comparisons.

#### 4.3.1.3.3. *$O_{2PEAK}$ and cognition*

Across subjects, the strongest relationship was observed between $O_{2PEAK}$ and performance on the Trailmaking B task but this was not significant ($r^2$ = F (1,28) = 2.22, p=0.15, n.s.). In HD subjects, a trend towards faster performance on the Trailmaking B task was associated with higher fitness (p=0.15, n.s.; Table 4.3.), whereas this association was not present in controls. Nonetheless, this interaction was not significant. In a multiple regression with fitness as a covariate, $O_{2PEAK}$ did not explain any additional variance between groups, such that the relationship between $O_{2PEAK}$ and performance on all cognitive tasks did not differ for HD patients and controls (p-values >0.05, n.s.; Table 4.3).

**Table 4.3. Relationship between $VO_{2PEAK}$ and Mood, Quality of life, UHDRS and Cognitive Scores for Patients compared to Healthy Controls.**

| | $VO_{2PEAK}$ | | | | | | Group | Group x $VO_2$ |
|---|---|---|---|---|---|---|---|---|
| | HD Group (N=15) | | | Healthy Controls (N=15) | | | | |
| Measure | Mean ± SD (range) | r | p-value | Mean ± SD (range) | r | p-value | F | F-change |
| HADS: Anxiety | 6 ± 5 (0-16) | -0.42 | 0.12 | 4 ± 2 (1-7) | -0.09 | 0.76 | 3.23 | 2.48 |
| HADS: Depression | 4 ± 4 (0-11) | -0.40 | 0.14 | 2 ± 2 (0-7) | -0.30 | 0.28 | 3.97 | 3.60 |
| WHOQOL-BREF: Physical Health | 22 ± 3 (17-26) | 0.46 | 0.08 | 25 ± 3 (19-29) | -0.04 | 0.28 | 6.26* | 1.04 |
| WHOQOL-BREF: Psychological | 20 ± 3 (14-23) | 0.52 | <0.05* | 22 ± 2 (20-25) | -0.06 | 0.89 | 4.96* | 2.31 |
| WHOQOL-BREF: Social Relationships | 11 ± 2 (7-15) | 0.62 | 0.01* | 13 ± 2 (9-15) | -0.12 | 0.84 | 4.48* | 2.11 |
| WHOQOL-BREF: Environment | 32 ± 4 (27-38) | 0.43 | 0.11 | 34 ± 3 (26-39) | -0.24 | 0.66 | 1.53 | 0.39 |
| STROOP Interference | 40 ± 18 (15-77) | 0.10 | 0.74 | 52 ± 11 (38-73) | 0.16 | 0.56 | 4.84* | 0.38 |
| Verbal Fluency (3-letters) | 32 ± 11 (12-52) | -0.04 | 0.88 | 51 ± 12 (31-74) | -0.15 | 0.59 | 21.20*** | 0.23 |
| Trailmaking A | 46 ± 37 (20-143) | -0.21 | 0.47 | 22 ± 6 (14-36) | -0.02 | 0.94 | 5.67* | 0.54 |
| Trailmaking B | 88 ± 76 (28-243) | -0.39 | 0.15 | 37 ± 9 (20-52) | 0.01 | 0.97 | 6.51* | 2.07 |
| Forward Digit Span (Raw) | 10 ± 2 (6-14) | 0.13 | 0.64 | 12 ± 2 (8-16) | <0.01 | 0.99 | 9.96** | 0.08 |
| SCOLP | 44 ± 18 (18-71) | 0.28 | 0.34 | 64 ± 10 (53-83) | -0.34 | 0.21 | 14.95** | 0.06 |
| SDMT | 55 ± 25 (22-97) | 0.04 | 0.88 | 85 ± 14 (53-100) | 0.09 | 0.77 | 14.45** | 0.08 |
| UHDRS FAS | 23 ± 4 (12-25) | 0.52 | <0.05* | N/A | N/A | N/A | N/A | N/A |
| UHDRS TFC | 11 ± 3 (3-13) | 0.45 | 0.09 | N/A | N/A | N/A | N/A | N/A |
| UHDRS IS | 91 ± 13 (60-100) | 0.43 | 0.11 | N/A | N/A | N/A | N/A | N/A |
| UHDRS TMS | 21 ± 17 (0-46) | -0.69 | 0.81 | N/A | N/A | N/A | N/A | N/A |
| UHDRS Cog | 236 ± 73 (115-371) | 0.26 | 0.36 | N/A | N/A | N/A | N/A | N/A |
| Disease Burden Score | 1928 ± 387 (1344-2688) | -0.41 | 0.13 | N/A | N/A | N/A | N/A | N/A |

HADS (Hospital Anxiety and Depression Scale); WHOQOL-BREF (World Health Organisation Quality of Life (BREF); SCOLP (Speed of Comprehension Test-Version C); SDMT (Symbol Digit Modalities Test). Unified Huntington's Disease Rater Scale (UHDRS); Total Motor Score (TMS); Functional Assessment Score (FAS); Independence Score (IS); Total Functional Capacity (TFC);.Pearson's correlations *p<0.05, **p<0.01, p<0.001. Multiple regression was used to assess group differences and interactions between Group and $VO_{2PEAK}$ (F-change).

## 4.3.3 Baseline CBF

### 4.3.3.1. PVC versus non-PVC CBF estimation in whole-brain GM

Cerebral blood flow measurements can be seen in Figure 4.5, both before and after partial volume correction. Partial volume corrected images yielded significantly higher estimates of whole-brain grey matter CBF (Method; F (1,28) = 299.00, $p$<0.001 partial $\eta^2$= 0.90) than images that had not been partial volume corrected. PVC CBF estimates were significantly higher in patients (70%) than controls (59%) (F (1,28) =4.60, $p$=0.04, partial $\eta^2$= 0.14). This would be expected where partial volume effects typically seen in atrophied brains are reduced due to the improved spatial accuracy gained using this method.

This relationship was similar for aBV and TAT estimates (p-values <0.001). Non-PVC data yielded outliers >2 S.D, in the control group such that data did not meet the assumption of normality (Shapiro Wilks; p<0.05). Since the relationship between groups appeared preserved and yielded fewer outliers when partial volume correcting the data, PVC data will be reported for the remainder of this thesis.

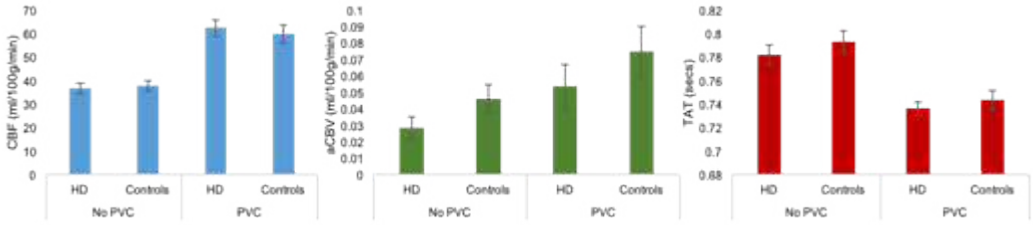


**Figure 4.5 Genotype differences in cerebral blood flow, volume and arrival time.** Bar graphs showing group differences between a) CBF b) aBV c) TAT (tissue arrival time), with and without PVC (partial volume correction). Error bars = S.E.M.

### 4.3.3.2. GM CBF estimates in HD patients compared to matched controls

Initial analysis aimed to rule out the impact of age on CBF, as CBF is known to decline with age. In an ANCOVA model, with age as a covariate and genotype as a between subjects factor, age was not associated with CBF in any of the regions studied ($p$-values > 0.05) and was not found to moderate group differences in CBF.

This was expected since groups were matched for age, and therefore age was not considered as a covariate in further analysis.

Independent t-tests were performed to assess differences in cortical and sub-cortical CBF (Figure 4.6) between HD patients and controls. There were no significant differences in resting CBF in any of the cortical or subcortical regions alone ($p$>0.05; Table 4.4), however a trend was evident, whereby HD patients appeared to have higher CBF in the cortex (Figure 4.7) and lower CBF in most subcortical regions within the basal ganglia, in particular, the left caudate which approached significance ($p$=0.06, n.s.). Both hemispheres showed a similar pattern of effects such that a repeated measures ANOVA revealed no difference between CBF in either hemisphere overall (Hemisphere; F (1,25) = 0.68, $p$=0.42, n.s.) and although this discrepancy appeared greater in the caudate of control subjects, there was no interaction between hemisphere and group (Hemisphere x Genotype; F (1,25) =0.42, $p$=0.52, n.s.).

**Table 4.4. Cortical and Subcortical grey matter CBF in HD patients compared to matched control subjects (Mean ± S.E.M ml/100g/min)**

| | | Controls | HD Patients | p-value (uncorrected) |
|---|---|---|---|---|
| **Whole Brain** | | 59.8 ± 4.0 | 62.4 ± 3.4 | 0.61 |
| **Frontal cortex** | | 63.9 ± 4.2 | 66.7 ± 3.9 | 0.62 |
| **Caudate** | Left | 46.2 ± 5.3 | 33.5 ± 3.9 | 0.06 |
| | Right | 32.8 ± 3.3 | 28.9 ± 3.2 | 0.41 |
| **Accumbens** | Left | 39.0 ± 3.7 | 35.1 ± 2.4 | 0.39 |
| | Right | 39.0 ± 4.5 | 41.8 ± 4.1 | 0.65 |
| **Putamen** | Left | 89.3 ± 8.6 | 84.5 ± 6.8 | 0.66 |
| | Right | 106.0 ± 10.4 | 94.6 ± 6.1 | 0.35 |
| **Thalamus** | Left | 65.8 ± 4.7 | 55.2 ± 4.7 | 0.28 |
| | Right | 60.9 ± 8.0 | 52.9 ± 5.2 | 0.41 |
| **Hippocampus** | Left | 58.2 ± 4.7 | 61.3 ± 5.1 | 0.66 |
| | Right | 66.9 ± 7.1 | 68.0 ± 6.9 | 0.91 |

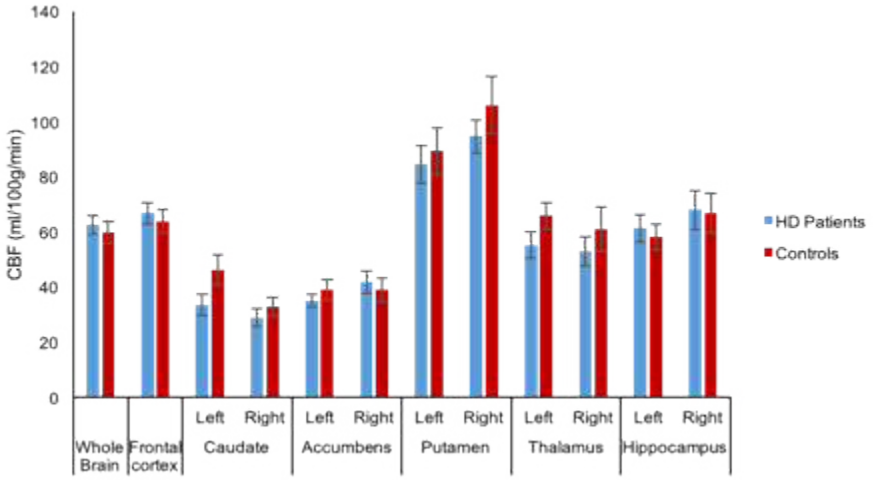


**Figure 4.6 Partial volume corrected grey matter CBF in cortical and subcortical ROIs.** Bars represent mean CBF in patients and controls. Groups did not differ significantly in any of the ROIs assessed, although a trend towards hypoperfusion in basal ganglia regions was observed. Error bars = SEM.

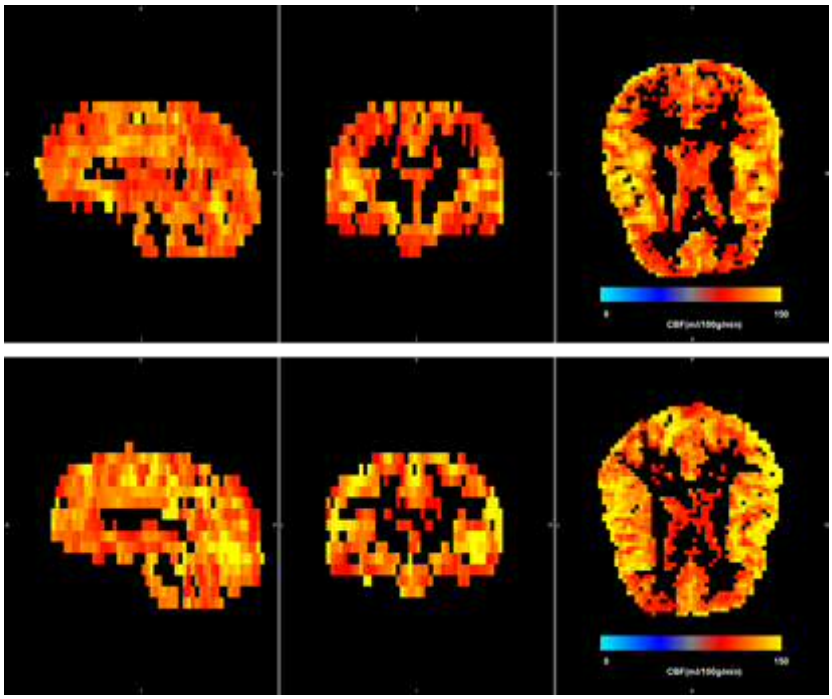

**Figure 4.7 Voxel-wise CBF maps in two representative subjects.** Grey matter CBF map in an example HD patient (bottom) and matched control (top) aged Age=~45 years, $O_{2PEAK}$ = ~45, Education ~ 20 years. Cortical hyperperfusion can be observed in HD patients compared to controls but this was not significant.

Further analysis was performed to address whether groups differed in tissue arrival times (TAT) in the cortical or subcortical regions studied. HD patients had similar TAT to controls (p-values <0.05), although visual trends revealed a slight increase in tissue arrival time in the HD group.

#### 4.3.3.3. GM CBF Relationship with Disease Burden

In HD patients, the relationship between Disease burden, CBF and tissue arrival time was assessed using Pearson's correlation. UHDRS total motor score (TMS), functional capacity (TFS), independence score (IS) and cognition (TCS) were also assessed for their relationship with regional rCBF.

##### *4.3.3.3.1. CBF*

In participants with HD, disease burden was negatively correlated with whole-brain grey matter CBF (r (13) =-0.68, $p$<0.01), however no correlations were observed between CBF in the subcortical regions or frontal cortex ($p$-values>0.05).

###### *4.3.3.3.1.1. Cortical ROIs*

Whole-brain GM CBF was also positively associated with UHDRS scores including TFS (r (13) =0.64, $p$=0.01, $q$=0.03) indicating better functional capacity, IS (r (13) =0.54, $p$=0.04, q=0.07, n.s.) indicating greater independence, CS (r (13) =0.59, p=0.02, q<0.04) indicating better cognitive functioning, and FAS (r (13) =0.65, $p$<0.01, $q$<0.01) indicating a wider degree of function, but not TMS (r (13) =-0.48, $p$=0.07, q=0.09, n.s.) in those with higher global CBF.

Frontal cortex CBF was *positively* associated with TMS (r (13) =0.64, $p$=0.02) such that those with higher motor dysfunction had elevated CBF in the frontal cortex. Frontal cortex CBF was also associated with lower functional capacity (TFC; r (13) =-0.63, $p$=0.01, $q$=0.02), lower independence (IS; (r (13) =-0.62, $p$=0.01, q=0.02) and a lower functional score (FAS; r (13) =-0.58, $p$=0.02, $q$=0.03).

###### *4.3.3.3.1.2. Subcortical ROIs*

Higher CBF the left (r (15) =0.61, $p$=0.08, q=0.10, n.s.) and right (r (13) =0.59, $p$=0.02, $q$=0.11, n.s) thalamus was associated with motor function (TMS), and the left

thalamus was also associated with lower levels of independence (IS; r (13) =-0.55, *p*=0.03, *q*=0.11, n.s.). CBF in left putamen was associated with lower functional capacity (TFC; r (13) =-0.53, *p*=0.04, *q*=0.01) and lower functional assessment scores (FAS; r (13) =-0.55, *p*=0.04, *q*=0.09, n.s).

#### *4.3.3.3.2. TAT*

There was a strong negative association between disease burden and tissue arrival time within whole-brain GM TAT (r (13) =-0.68, p<0.01). A similar association was seen within the left hippocampus (r (13) =-0.56, p=0.03, q=0.16) and right caudate (r (12) =-0.59, p=0.03, q=0.16), such that greater disease burden in HD was associated with shorter arrival times, however *p*-values (q) were no longer significant after FDR correction for multiple comparisons.

### 4.3.3.4. Group differences between CBF parameters and cognition

To explore these changes further, group differences were investigated to assess whether these relationships were the same for HD patients and controls.

#### *4.3.3.4.1. CBF*

##### *4.3.3.4.1.1. Cortical ROIs*

In controls, cognitive performance was positively associated with elevated CBF in several regions. Higher global GM was associated with performance on the SCOLP (r (12) =0.54, p=0.04) and forward digit span (r (12) =0.54, p=0.04). In controls, negative associations were observed between CBF in the frontal cortex and performance on the Trailmaking task (r (13) =-0.53, p=0.04, q=0.10, n.s.), SCOLP (r (13) =0.55, p=0.04, q=0.10, n.s.), and SDMT (r (13) =0.53, p=0.04, q=0.10, n.s.), but relationships were not significant after FDR correction.

In patients, neither whole-brain nor frontal GM CBF was associated with cognitive performance on any of the tasks assessed (p-values>0.05).

##### *4.3.3.4.1.2. Subcortical ROIs*

CBF in controls was positively associated with cognitive performance on a number of tasks. CBF in the left accumbens was associated with better performance on the

verbal fluency task (r (15) =0.73, $p$<0.01, $q$=0.01), forward digit span (r (13) =0.63, $p$=0.01, $q$=0.03), and SDMT (r (12) =0.68, $p$=0.008, $q$=0.02). CBF in the right putamen was positively associated with performance on the forward digit span r (13) =0.65, $p$=0.009, $q$=0.03), SCOLP (r (15) =0.60, $p$=0.02, $q$=0.03) and SDMT (r (12) =0.72, $p$=0.004, $q$=0.02). CBF in the left caudate was associated with better performance on the SDMT (r (12) =0.71, p=0.004, q=0.02).

In comparison, HD patients did not show the same widespread correlation between task performance and CBF in these regions. The only implicated subcortical region appeared to be in the left putamen, in which elevated CBF was associated with slower performance on the Trailmaking B task (r (13) =0.54, $p$=0.04, $q$=0.23, n.s), and the left thalamus which was associated with poorer performance on the SCOLP (r (13) =-0.54, $p$<0.05, $q$=0.11, n.s.) and the SDMT (r (13) =-0.55, $p$=0.03, $q$=0.11, n.s.) (Figure 4.8.). In contrast to the control group, our results suggest that elevated CBF in these regions was actually associated with poorer cognitive performance, although these results were no longer significant after FDR correction.

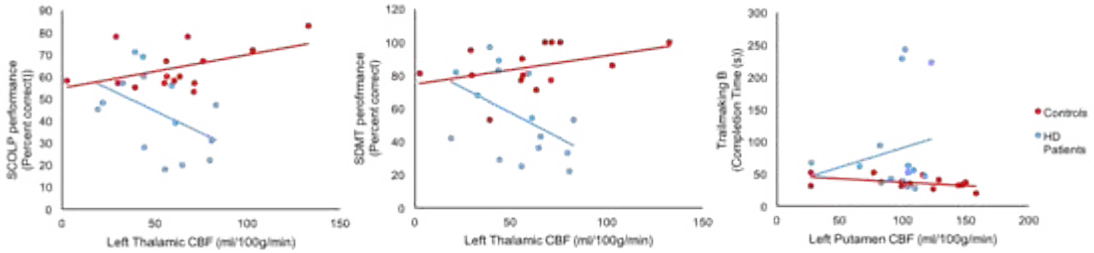


**Figure 4.8 Relationship between subcortical CBF and cognitive function in HD patients compared to controls.** Left thalamic CBF was negatively associated with cognitive performance on the Speed of Comprehension and Language Processing (SCOLP) test and Symbol Digit Modalities Test (SDMT). Left putamen CBF was associated with speed to complete the Trailmaking test, where longer times reflect poorer performance.

#### *4.3.3.4.2. TAT*

In controls, cognitive function correlated with TAT in a number of basal ganglia regions. Stroop task performance was positively associated with TAT in the left caudate (r (12) =0.64, $p$=0.01, $q$=0.08, n.s.) whilst SDMT (r (13) =-0.55, $p$=0.04, $q$=0.13, n.s) and SCOLP (r (13) =-0.67, $p$<0.01, $q$=0.04) was negatively associated with TAT in the left putamen. Only the relationship between TAT in the left putamen

and SCOLP performance was significant after FDR correction. Interestingly, this relationship between basal ganglia regions and cognitive function was entirely absent in HD patients (p values >0.05).

#### 4.3.3.5. Relationship between cardiorespiratory fitness and CBF

##### *4.3.3.5.1. CBF*

Pearson's correlation revealed that $O_{2PEAK}$ was not associated with CBF in any of the regions studied ($p$>0.05) when collapsed across groups (Table 4.5).

Next, we were interested to assess whether $O_{2PEAK}$ would predict CBF differently between HD patients and controls. A linear regression with $O_{2PEAK}$ as a continuous predictor, subject group as a categorical and regional CBF as the dependent variable was carried out, to assess whether HD status moderated the relationship between $O_{2PEAK}$ and CBF. Regression analysis was performed with bootstrapping at 1000 samples with 95% bias-corrected and accelerated confidence intervals.

**Table 4.5. Moderating effects of HD on the relationship between CBF and $VO_{2PEAK}$**

| | $VO_{2PEAK}$ | | | Genotype x VO2 | | |
|---|---|---|---|---|---|---|
| | $R^2$ | $\beta$ | p-value (uncorrected) | $R^2$ | $\beta$ | p-value (uncorrected) |
| Whole-brain GM | <0.01 | 0.07 | 0.80 | 0.01 | 0.08 | 0.61 |
| Frontal Cortex | 0.01 | -0.12 | 0.69 | 0.01 | -0.11 | 0.65 |
| R_accumbens | 0.03 | -0.26 | 0.37 | 0.04 | -0.25 | 0.73 |
| R_caudate | <0.01 | -0.03 | 0.89 | 0.03 | -0.06 | 0.41 |
| R_putamen | <0.01 | -0.02 | 0.97 | 0.03 | -0.06 | 0.36 |
| R_thalamus | <0.01 | -0.19 | 0.69 | 0.03 | -0.22 | 0.40 |
| R_hippocampus | <0.01 | 0.24 | 0.63 | <0.01 | 0.24 | 0.89 |
| L_accumbens | <0.01 | -0.08 | 0.73 | 0.03 | -0.91 | 0.38 |
| L_caudate | 0.05 | -0.45 | 0.24 | 0.18 | -0.40 | 0.05* |
| L_putamen | 0.05 | -0.68 | 0.22 | 0.06 | -0.66 | 0.60 |
| L_thalamus | 0.01 | -0.03 | 0.57 | 0.06 | -0.32 | 0.27 |
| L_hippocampus | <0.01 | 0.05 | 0.88 | 0.01 | 0.06 | 0.67 |

Reported Beta and p-values are based on 1000 bootstrap samples.

Overall, beta values consistently demonstrated a reduction in CBF with $O_{2PEAK}$. Genotype did not interact with the relationship between CBF in most regions studied ($p>0.05$, Table 4.5), except the left caudate in which HD patients showed a negative relationship with fitness and CBF, whilst controls showed an increase in CBF with increased fitness ($R^2$ (27) = 0.18, p=0.05, q=0.36; figure 4.9) however, this was no longer significant after FDR correction for multiple comparisons.

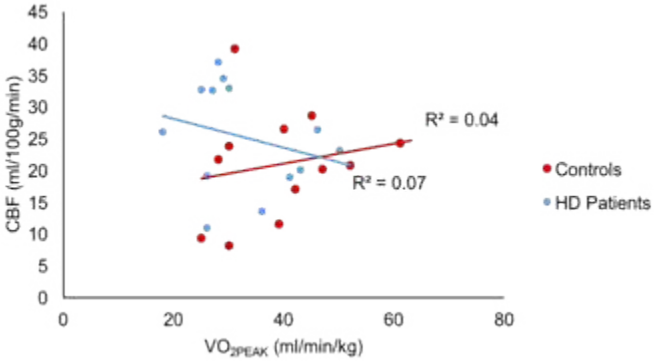


**Figure 4.9 $VO_{2PEAK}$ predicts CBF differently in HD patients in the caudate nucleus.**
Group differences in the relationship between fitness ( $O_{2PEAK}$) and CBF in the left caudate nucleus. Fitter HD subjects had lower CBF than less fit subject, in contrast to the positive relationship seen in matched controls (N=15 per group).

#### *4.3.3.5.2. TAT*

Pearson's correlation revealed that $O_{2PEAK}$ was not associated with TAT in any of the regions studied ($p>0.05$) when collapsed across groups. No interactions were found to suggest that TAT was affected differently by fitness between groups ($p>0.05$, n.s.)

### 4.3.4 Cerebrovascular Reactivity

#### *4.3.4.1. Feasibility of Breath-hold Paradigm for CVR quantification*

Out of 15 HD patients and 15 controls, breath-hold data was missing for 1 person within each group. Out of the 14 remaining subjects for each group, 9/14 controls and 10/14 patients successfully completed the breath-hold task with at least 3 correct breath-holds. Of those that did complete a valid task, HD patients and controls both performed the same number of end-exhalations correctly (Controls: 6 ± 1.6 holds, Patients: 6 ± 1.8 holds).

### 4.3.4.2. *Group differences in CBF CVR*

Partial volume corrected CBF CVR across the entire brain and within the frontal cortex can be seen in figure 4.10. A trend can be seen in which patients had lower CVR than controls. Independent samples t-test was performed corrected for inequality of variance and bootstrapped to 1000 samples. Grey matter CVR did not differ significantly between HD patients (0.15 ± 0.4) and controls (0.39 ± 0.11) within whole-brain (t (16) =1.22, p=0.25) or frontal grey matter (t (16) =1.84, p=0.08).

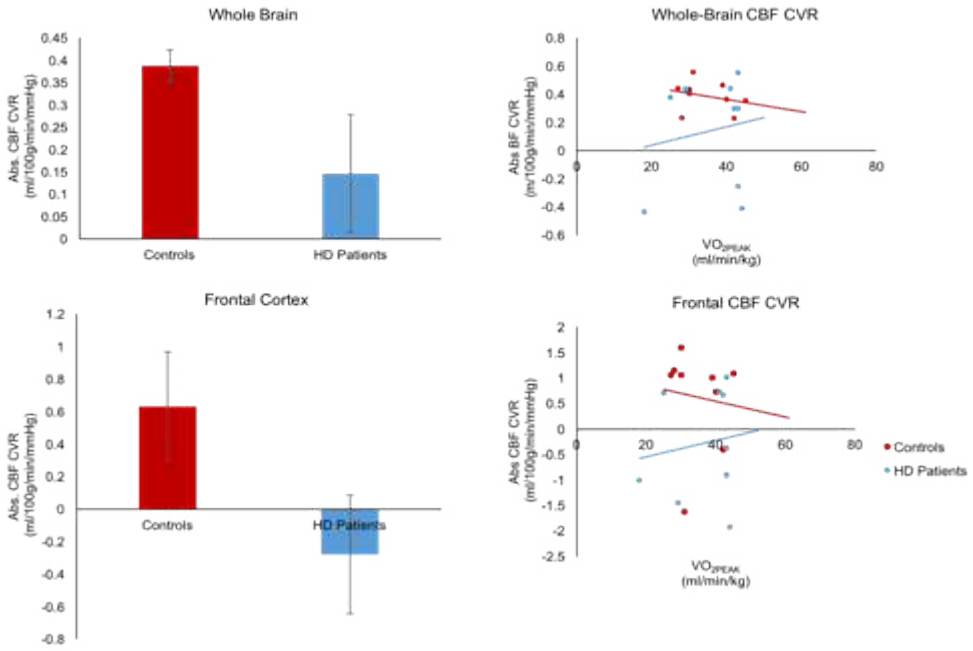


**Figure 4.10 Genotype differences in CVR and relationship with $VO_{2PEAK}$.** Left) CBF CVR was lower in HD patients than controls across the whole-brain and Frontal Cortex, although results were not statistically significant (N=9 per group; Error bars = SEM). Right) The relationship between CBF CVR and $O_{2PEAK}$ also did not differ between groups.

### 4.3.4.3. *Relationship between CVR and fitness*

A negative relationship between whole-brain CVR and $O_{2PEAK}$ was visible such that higher $O_{2PEAK}$ was associated with lower CVR, but this was not significant ($R^2$ = 0.15, F (1,16) =2.9; β =-0.01, *p*=0.11, n.s). Including GROUP as a moderator, explained an additional 6% of the variance between subjects but this was not significant (*p*=0.29). Nonetheless, simple relationships were explored using individual linear regression for each group independently. $O_{2PEAK}$ was unable to

predict Frontal CVR across subjects ($R^2$ = 0.18, F (1,7) =1.5; β =-0.01, *p*=0.99, n.s.), however genotype could account for an additional 18% of the variance, although this interaction with fitness was not significant (*p*=0.09). Frontal CVR in either HD patients, ($R^2$ = 0.02, F (1,7) =0.15; β =0.02, *p*=0.71, n.s.) or controls ($R^2$ = 0.01, F (1,7) =0.09; β =-0.016, p=0.79, n.s.) was not associated with cardiorespiratory fitness (Figure 4.9).

#### *4.3.4.4. Relationship between CVR and Disease Burden*

Frontal CVR was negatively associated with UHDRS TMS score (r (9) =-0.69, *p*=0.04), such that higher CVR was observed in those with greater motor disability, although this did not survive FDR correction. CVR was not associated with any other UHDRS scores or overall disease burden (p-values> 0.05).

#### *4.3.4.5. Relationship between CVR and Cognitive Function*

Whole-brain CVR was associated with better SCOLP (r (18) = 0.49, p=0.04, q=0.01) and verbal fluency (r (18) = 0.57, p=0.01, q=0.08, n.s.) performance, whilst Frontal CVR was associated with better performance on verbal fluency (r (18) = 0.67, p=0.003, q=0.02) and Trailmaking test B (r (18) = -0.54, p=0.02, q=0.07,. n.s). Together these results suggest that CVR is beneficial for a number of tasks that require executive functioning, but only the relationship between verbal fluency and Frontal CVR was significant after FDR correction.

## 4.4. Discussion

### Key Findings

- HD subjects with higher disease burden had significantly lower whole brain GM CBF.
- Symptom severity according to a UHDRS scores was associated with significantly lower whole-brain grey matter CBF.
- CBF within basal ganglia regions was lower in HD patients compared to controls, particularly within the left caudate but this was not significant after FDR correction.
- Tissue arrival times within a whole-brain mask, were significantly shorter in those with a higher disease burden.
- $O_{2PEAK}$ appeared to be negatively correlated with CBF in most basal ganglia regions when collapsed across all subjects, but this was not significant.
- HD subjects differed from controls in the relationship between $O_{2PEAK}$ and CBF in the left caudate, whereby fitter HD subjects had lower CBF in the left caudate, whilst CBF was elevated in controls. This interaction was no longer significant after correction for multiple comparisons between subcortical regions.
- HD subjects had lower whole-brain and frontal grey matter CVR than controls, in those subjects that completed the breath-hold task with reasonable efficacy, but was not significant.
- HD patients showed significantly poorer performance on a number of tasks that require executive functioning.
- Unlike controls, HD patients did not demonstrate a positive association between CBF and cognitive performance. Contrarily, they showed a negative relationship between CBF and executive function in the left

thalamus and left putamen, however these interactions were not significant after multiple comparisons.

- Pre-/early-HD patients reported having significantly poorer quality of life than controls in domains of physical health, psychology and Social Relationships.
- Partial volume correction yields significantly higher CBF estimates than without correction, and this discrepancy was greater for HD patients where atrophy is expected suggesting that PVC is a useful step when using ASL in neurodegenerative disease.

The present study looked to investigate previously reported alterations in CBF in the HD brain using PASL MRI and is the first time that the relationship between cardiorespiratory fitness and CBF has been assessed in HD. Compared to a well-matched group of healthy controls, HD subjects displayed hypoperfusion, shorter blood arrival times into grey-matter tissue, reduced CBF CVR to a breath-hold challenge and poorer performance on a range of tasks used to assess executive functioning that were associated hyperperfusion in the left thalamus and left putamen. The largest perfusion difference was seen in the left caudate, a region known to be heavily implicated in the progression of HD symptoms. Cardiorespiratory fitness appeared to be negatively associated with CBF across regions, although this was not significant in any region across groups. However, when considering HD status, this relationship differed between HD subjects and controls in the left caudate, where lower CBF in fitter HD patients differed from controls who had elevated CBF with higher $O_{2PEAK}$. This is the first study to explore this question in HD.

### 4.4.1. CBF in Huntington's Disease

Perturbations in microvascular flow, have been shown to precede the development of neuronal dysfunction, leading to speculations that alterations in CBF may play important roles in both progression and clinical expression of neurodegenerative disease. In the present study, lower CBF was observed in all basal ganglia regions, but not the cortex or hippocampus, where CBF appeared elevated. Group differences

were not found to be statistically significant, although group differences were evident in the left caudate and right putamen. Further analysis also revealed that disease severity, according to increased disease burden and UHDRS scores, was related to global CBF, where greater disease severity was associated with hypoperfusion throughout the brain.

Hypoperfusion of the *left* putamen has been found previously, in pre-symptomatic patients near to predicted disease onset (Harris et al., 1999 and Wolf et al., 2011), alongside hypoperfusion in the prefrontal cortex. However, unlike the present study, they did not observe group differences in the caudate. Whilst we observed a widespread pattern of hypoperfusion across regions, these results were not statistically significant and interpretation should be treated carefully. It is possible that the study by (Wolf et al., 2011) was more sensitive to these effects as their sample size was slightly larger (N=18) and variance reduced by tight recruitment regarding predicted time from onset. Their study also utilized PCASL which has greater SNR than PASL methods (Y. F. Chen et al., 2011) such that their measures may have been more sensitive to detect changes. Nonetheless, both the putamen and caudate are known to play key roles in the progression of HD, such that the results are likely to be reflective of real underlying physiological processes. It is within the caudate nucleus and putamen that the largest degree of medium spiny neuronal loss occurs during HD. Although it is not known why it is so highly affected, it is thought that mitochondrial dysfunction in the caudate may jeopardise metabolism, thereby leading to neuronal death. Blood flow in the caudate has been described as the single largest predictor of executive performance deficits in HD (Hasselbalch et al., 1992). Despite the clearest differences in baseline CBF being observed in left caudate, we did not observe a relationship between left caudate CBF and performance on any of the cognitive tasks in this study.

Although CBF differences in this study were not significant, it is possible, that the findings in the present study may be *more* sensitive to alterations in CBF than those reported previously. Unlike any other studies that have explored CBF in HD, the present study included a partial volume correction step during CBF estimation, to reduce distortions caused by spatial inaccuracies introduced by other tissue types within each voxel. Where atrophy is known to occur, correction for partial volume

becomes more necessary, especially within smaller grey matter structures where apparent changes in signal can, at least partially, be attributed to PVEs (Dukart and Bertolino, 2014). These PVEs could potentially obscure patterns of disease that may be of interest when investigating biomarkers and underestimate the confounding effect of atrophy. Studies that have shown more hypoperfusion than that observed in this study, may be attributable to the fact that less grey matter is present and thus the reported GM CBF signal is underestimated. Partial volume correction has been shown to inflate CBF estimates by up to 80% (Chappell et al., 2011) and in our study we observed a substantial difference between partial volume corrected and non-partial volume corrected images within a whole-brain grey matter mask. Where HD subjects showed an CBF estimation increase of 70% compared to 59% in controls, it is likely that this is due to the improved spatial accuracy after accounting for PVEs induced by atrophy. We did not assess these differences within smaller subcortical structures, although this would be worthy of further investigation to inform other ASL studies when attempting to draw conclusions about CBF differences in HD.

The present study also investigated the relationship between CBF and symptom severity based on clinical UHDRS scores. Reduced whole-brain grey matter perfusion was observed in those who had higher disease burden, and greater symptom severity in terms of independence, functional capacity, cognition and range of functions. Interestingly, this relationship was inverted in the frontal cortex where motor symptoms, functional capacity and independence was l*ower* in those with higher frontal perfusion. Previous studies have also observed elevated in CBF in prefrontal regions, in pre-symptomatic HD, and this has been suggested to reflect increased metabolism and activation attributable to 'compensatory' neural processes paralleling striatal degeneration and a subsequent impairment of cortico-striatal circuits (Paulsen et al., 2004). Future analysis will concentrate on subdividing the cortex into more specific ROI's such that the pattern of cerebral perfusion can be assessed, with particular focus on the prefrontal and sensorimotor regions which are thought to be vulnerable in HD (Wolf et al., 2011). Of all the subcortical regions assessed, the only sub-region to survive multiple comparison was the left putamen, in which higher CBF was associated with lower functional capacity. Where CBF in the putamen is commonly thought to be reduced in HD (Harris et al., 1999; Wolf et al., 2011) and right putamen CBF appeared higher in patients than controls in the

current study, it is counterintuitive that higher CBF in the left putamen is related to worse diagnosis. This is not the first time that elevated basal ganglia perfusion has been noted in pre-symptomatic HD patients (Chen et al., 2012) and has been thought to reflect interesting compensatory processes where striatal hypo-perfusion is observed elsewhere. Alternatively, this could be a methodological artefact as it has been recognised that this scale may be less sensitive to functional changes in patients far from symptom onset (Paulsen et al., 2010).

The importance of adequate perfusion of the basal ganglia to maintain executive function is supported in this study, whereby widespread regional CBF was positively correlated with performance on a range of cognitive tests which are known to be affect by HD. Interestingly, this relationship was only true of controls. HD patients showed a negative relationship between CBF and executive function. Elevated CBF in the left thalamus was associated with worse performance on the Speed of Comprehension and Language Processing Test and the Symbol Digit Modalities Test. The human thalamus has been shown to be crucially involved in executive functions (Marzinzik et al., 2008) due to its critical position and extensive reciprocal connections with almost all cortical regions (Behrens et al., 2003). Whereas a positive relationship between thalamic perfusion and performance on executive function was observed in the current study, the opposite relationship in HD provides support for a pathological relationship between thalamic CBF and cognitive function in HD. Despite its fundamental role in mediating the cognitive dysfunction known to occur in HD, this is the first time thalamic CBF differences have been observed in the ASL literature. Elevated baseline CBF in those that perform poorly on executive tasks, may be explained by pathological angiogenesis, that has been reported in HD patients and HD rodent models (Drouin-Ouellet et al., 2015) in patients who are cognitively symptomatic. Since these results are cross-sectional it is not possible to infer causation. However, further research would benefit from investigating the real-time functional changes in thalamic CBF during a similar executive task using ASL fMRI, such that causation may be inferred.

The precise physiological underpinnings of cerebral perfusion changes in HD have not been addressed by this study. Disturbance of nitric oxide and nitric oxide synthase systems have been seen in the R6/2 transgenic HD mouse model (Deckel

et al, 2002), where initial elevations were seen in neuronal nitrous oxide synthase (nNOS) expression in 'pre-symptomatic' mice aged 3 weeks, but a decline in expression as the disease progressed (at age 6 and 11 weeks). The most significant and early reductions in CBF are thought to occur in regions which have high metabolic activity relative to the global average (Leenders et al., 1990). Perturbations to microvascular flow regulation have been reported in AD models (Iadecola, 2004), where amyloid deposition is thought to actively exchange signalling mediators and trophic factors such as VEGF which may affect perfusion of the grey matter. Whilst the impact of mutant huntingtin protein on the endothelium has not been clarified, mHTT was found to directly affect expression and activity of NOS and reduction in vascular velocity, and possibly, flow (Deckel, 2002). The general pattern of hypoperfusion and the inverse relationship observed with disease burden may reflect a progressive reduction in nNOS expression observed with disease progression, such that CBF decreases with disease progression. Another explanation for the spatial variations observed in this study, could be due to the growth and loss of blood vessels at different stages throughout the disease. Increased vessel density has been reported in HD R6/2 mice from 7 weeks of age, and is thought to underpin an increase in cerebral blood volume in both the cortex and striatum which increases with disease progression (Lin et al., 2013).

The present study is the first to investigate whether any differences in tissue arrival times exist in HD patients compared to controls. Tissue arrival time is the time it takes for a tagged bolus of blood to reach the imaging voxel. Estimation of the TAT is necessary as it reflects tissue dispersion, which in turn is known to influence estimation of cerebral blood flow. Tissue dispersion can be influenced by a range of factors including the non-uniform cross-sectional flow profile of blood vessel, flow pulsatility and potential for multiple arterial supply routes and as such, differs throughout the brain where the caudate and putamen have been found to have the shortest arrival times (Gallichan and Jezzard, 2009). In this experiment arrival times observed in the basal ganglia were comparable to those reported previously (~0.7s) (Gallichan and Jezzard, 2009). No group differences were observed between resting TAT, such that it is unlikely that CBF estimates would have been affected by group differences in perfusion speed, however individual differences in disease burden was negatively associated with TAT across the whole brain as well as the hippocampus

and caudate. Whether tissue dispersion is reduced with disease progression is intriguing since arrival times are thought to increase in the normal ageing brain (Liu et al., 2011), however it may be attributable to extreme atrophy in these regions. Interestingly, basal ganglia TAT was related to cognitive scores in the control group, where shorter arrival times in the putamen were related to improved digit span and SCOLP performance, a result which was absent in HD subjects. It is unclear whether TAT is a useful parameter of cerebrovascular health as it is rarely reported, and whether one would expect striatal TAT to be altered in HD is unknown, and may be related to angiogenesis known to occur in HD. Evidence that TAT was inversely correlated with cognition is further evidence for the link between disease neuropathology in HD. Since this experiment had not initially planned to investigate TAT, future work should expand upon this work, by modelling TAT in HD.

### 4.4.2. Cardiorespiratory fitness in Huntington's Disease

The present study is the first to address the relationship between cardiorespiratory fitness and cerebrovascular health in people with Huntington's Disease. In Chapter 2, it was observed that fitness was negatively correlated with whole brain grey matter CBF in highly fit individuals. In the present study, whole group CBF appeared to be negatively related to $O_{2PEAK}$ but this was not significant for any of the sub-regions assessed. Group differences however, yielded an interesting interaction within the left caudate alone which, as described above, is highly implicated in HD pathology and cortical function. Specifically, $O_{2PEAK}$ was associated with elevated caudate CBF in controls, which is in line with the pattern of results reported previously in studies of CBF in the general population (Bailey et al., 2013; Chapman et al., 2013). Assuming that this is a beneficial effect of fitness on the brain, then the inverse relationship between fitness and CBF in HD patients is alarming. In the present study, the left caudate was the region in which the greatest hypoperfusion was observed relative to controls. Should fitness indeed decrease CBF in this critical region even further, this may in fact reflect a negative effect of exercise on the brain. This would not be the first study to report potentially negative effects of exercise on cerebral health. In their mouse study, Potter et al. (2010) observed that N171-82Q transgenic HD running mice had an earlier onset of disease symptoms (shaking, hunched back and poor grooming), reduced striatal volume and impaired motor behaviour,

hyperglycaemia, Morris water maze learning deficits, diminished neurogenesis, deficits in immature neuronal morphology, and more intranuclear mHTT inclusions from 11 weeks of age.

Care should be taken when over-interpreting the effects of fitness on the brain, since this is a cross-sectional study and therefore amount and type of exercise could not be directly manipulated. Exercise interventions are thought to be a better way by which to infer causality, and such interventions have been shown to be feasible and without negative side effects (Khalil et al., 2013b). Combining similar interventions with MRI would enable us to directly address the effects of exercise on the brain, although the timescale over which these changes are expected to occur is not known. Studies in rodent models of HD, where it is possible to directly manipulate and control for the amount of exercise are warranted to rule out the suggestion of negative effects of exercise on the brain.

It was important for the sake of this study, that the fitness range was similar between patients and controls such that MRI results could be compared. In both groups, average $O_{2PEAK}$ reached 36-37 ml/min/kg. However, a proportion of participants was unable to reach its true $O_{2MAX}$ for several reasons, which may be useful considerations for future studies in which a fitness test is explored. Of note, was that apathy may have affected patients' willingness to continue to exhaustion. Indeed, patients in this study did show elevated depressive symptoms relative to controls. Whilst this was not measured directly, this appeared to be the case in approximately 3 patients. In general, however, all participants were extremely motivated to push themselves to their limit. More apparent, was the observation that a number of participants were unable to maintain a repetition rate above 45rpm because their legs were tired. It appeared that muscle fatigue was reached before $O_{2MAX}$ was reached, such that it became more a test of muscle strength than aerobic capacity. The protocol was initially designed to include 25W step increases every two minutes since we were interested in taking regular measurements at each load. Future experiments should consider incorporating more regular, gradual step changes, to avoid termination due to leg fatigue and so that it is possible to observe the typical $O_2$ plateau used to qualify a $O_2$, where $O_2$ fails to increase with increasing load.

In the absence of a true $O_{2MAX}$ measurement in some subjects, it is possible that these methodological caveats could explain the absence of any clear relationship between fitness and CBF. Predicted and self-reported fitness were found to correlate strongly with $O_{2PEAK}$ although these measures remain less robust than the $O_{2PEAK}$ in the absence of physiological information.

### 4.4.3. CVR in Huntington's Disease

CBF change in response to increased $CO_2$ during a breath-hold challenge was reduced in HD patients compared to controls in those that completed the task satisfactorily, although this was not significant across the whole brain, or more locally within the frontal cortex. Averaged across whole-brain, an increase of 0.39 ml/100g/min per mmHg increase in $CO_2$ was observed in controls which is slightly higher than the result recorded in Chapter 2 in young healthy subjects (0.24 ± 1.2), compared to just 0.15 ml/100g/min/mmHg in HD patients.

To the best of my knowledge, this is the first study to measure cerebrovascular reactivity in patients with Huntington's Disease, although this has been investigated in a couple of HD mouse models. CBF CVR in the R6/2 mouse model, revealed decreased reactivity to a carbogen gas challenge at 7-weeks old, compared to wild-type mice, which sits in line with the trending results observed in this study (Hsiao et al., 2015). Impaired CVR may explain the hindered cerebral hemodynamics observed in this study and others, and may even precede the increase in brain atrophy during HD progression. It is not known how CVR is jeopardized in the HD brain, although in their paper Hsiao et al., (2015) propose a mechanism by which increased endothelial cell proliferation via a VEGF-A–dependent pathway may compromise the survival of pericytes which envelope the blood vessel and alter vascular tone in response to demands for increased blood flow. Impaired CVR has been reported in Alzheimer's disease, whereby diffuse yet predominant impairment of CVR is observed in the posterior areas (Cantin et al., 2011) that is also associated with cognitive deterioration (Silvestrini et al., 2006).

Studies of CVR in other diseases tend to focus on BOLD reactivity. As discussed in Chapter 2, CBF is a much more direct measure of vascular function, where the BOLD

signal is complex in its origin. Although we observed a strong correlation between BOLD and CBF CVR in Chapter 2, this relationship has not been assessed in the present study. Nonetheless, BOLD data was acquired and future work will take this investigation further by measuring BOLD reactivity in HD.

In the present study, we observed many subjects, particularly patients, and within the frontal cortex, who had a negative CVR response to the breath-hold task. Physiologically, this translates as a decrease in CBF with increased $CO_2$. It has been shown previously that rats with progressive hypertension exhibit reduced lumen diameter, increased arterial stenosis and a corresponding negative CBF CVR (Li et al., 2015). The same study also found enlargement of downstream vessels and formation of collateral vessels as compensatory responses to stenosis of the upstream vessels. In the context of HD this may in part explain the typical angiogenic response seen in the microvasculature in parallel with a reduction in artery number (Lin et al., 2013). Where this is the case, it reflects compromised cerebrovascular reserves, and is clinically relevant in HD as similar mechanisms have also been also associated with increased risk of stroke (Kuroda et al., 2001) and dementia (Marshall and Lazar, 2011). Future work will look more closely at the arterial blood volume, using the compliance measures (Warnert et al., 2015b) described in Chapter 2, to assess whether arterial stiffening can be detected in HD patients using ASL. An alternative explanation for the reduction in CVR, is that this is a vascular artefact around the ventricles in HD patients. It has been proposed previously that a reduction in the CSF volume fraction during hypercapnia, leading to blood vessel dilation, may cause a reduction in signal where the less intense blood signal replaces the more intense CSF signal (Thomas et al., 2013a). This would yield a net decrease in the signal measured, which is likely to be greater in HD where registration around the atrophied ventricles can be poor.

A peripheral research question in this study, was the feasibility of a breath-hold challenge for assessing CVR. In total, 10/14 patients and 9/14 controls were considered valid for inclusion, whereby they completed a minimum of 3 breath-holds effectively. This arbitrary number was used because 3 end-tidal $CO_2$ measurements was considered sufficient for extrapolation to the other breath-holds in which inhalation rather than exhalation followed the hold. Of those that did complete a

valid task, HD patients and controls both performed the same number of end-exhalations correctly (6 ± 2). The primary reason for excluding control data was due to consistent inhalations rather than exhalations following the hold, such that end-tidal peaks in $CO_2$ were not recorded. In addition, patient data were also excluded due to failure to do the task (possibly due to cognitive impairment) or due to obvious movement issues (chorea) whereby $CO_2$ data were too noisy. The fact that patients did not differ significantly from controls, suggests that real emphasis needs to be put into explaining the breath-hold task thoroughly to all participants, since even cognitively unimpaired controls did not follow the instructions perfectly. In the current study, we went to great lengths to explain the task and showed them a video immediately prior to scanning, such that the instructions would be as clear as possible. According to the present results, future research should consider including enough breath-hold challenges since this would increase the number of end-tidal measurements from which to extrapolate and consider increasing subject power to allow for subject removal where necessary.

With thorough briefing and cognitive screening, CVR using the breath-hold paradigm appears feasible for use in pre-early symptomatic stage HD patients, however it is not recommended for more advanced HD where cognitive and motor symptoms may pose a challenge. It should also be noted that extrapolating the end-tidal $CO_2$ values is not ideal, and future work will develop this analysis pipeline further, to ensure the most robust measurements are acquired.

### 4.4.4. Determining disease severity

In this Chapter, disease burden score was calculated in addition to clinical UHDRS scores as a measure if HD progression. First proposed by (Penney et al., 1997), the disease burden score used here is well established within the field of HD research, and is more suited for determining the discrete progression of the disease than the UHDRS scales, which require subjective assessment of ambiguous probabilities and can suggest a false dichotomy between sick and well (Ross et al., 2014). In a sample of pre-/early-manifest HD patients, including age and genetic burden better reflects

the progression of disease over the lifespan, and is thought to be more sensitive to the effects of therapeutic interventions, such as exercise.

Variations in the way 'disease burden' or 'genetic burden' is estimated have been more thoroughly explored in recent years, including slightly different modelling procedures (Paulsen et al., 2014; CAP = age × (CAG – 33.66)). In a cohort of 1,078 HD gene carriers from the multi-site PREDICT-HD study, it was found that a variety of outcome measures including cognitive performance on the STROOP test, putamen volume using MRI and total motor score (TMS) were strong predictors of disease diagnosis beyond that of CAG repeat length and age alone (Paulsen et al., 2014). Incorporation of these outcome measures is recommended, to glean the most accurate estimate of disease severity in a patient sample. Whereas STROOP scores, total motor scores and volumetric data was acquired within this thesis, due to time limitations it was not possible to statistically probe these predictive contributions in greater depth. Future work will further explore the use of composite scores to probe the relationship between physical activity and disease progression and will also consider the importance of MRI biomarkers of cerebrovascular health for improving predictive accuracy.

### 4.4.5. Conclusion

In this study, we could replicate a pattern of hypoperfusion that has previously been observed in pre-symptomatic HD patients using PASL as well as impoverished performance in a wide range of cognitive tasks of executive function. It is likely that our results were more robust than those reported previously, where CBF has not been corrected for partial volume effects and would be a recommendation to future studies. Our main question was to address the impact of fitness on cerebrovascular health in HD to assess whether it may moderate the effects seen in controls. Implication of the most severely affected region, the left caudate, was observed, suggesting that fitness may moderate CBF differently in HD patients to controls. This study is cross-sectional such as the effects of exercise should be treated with care. Since this is not the first time controversial effects of exercise have been observed, further research in preclinical HD mouse models is warranted, to assess the impact of exercise more directly upon caudate function and to rule out any detrimental effects. In this study, perfusion within the putamen, caudate

and thalamus appeared to be the most associated with disease severity and cognitive function which is in line with the atrophy and functional connectivity known to occur within these regions. This is the first study to assess CVR in human HD patients, where hypo-reactivity was observed in patients. Future work will aim to improve the robustness of this pipeline, to account for non-compliance to the breath-hold challenge itself. Assessing cerebrovascular reactivity using the breath-hold task is a challenge due to the cognitive demand of following task instructions. Nonetheless, we observed similar performance between patients and controls. Thorough briefing and screening for chorea and cognitive function would likely overcome these issues.

# Chapter 5

# Investigating the cerebrovascular effects of voluntary wheel running in pre-symptomatic Q175 HD mice: combining PASL MRI and immunohistochemistry.

## Chapter Summary

Evidence from human (Wolf et al., 2011) and rodent (Cepeda-Prado et al., 2012) studies have shown differences in cerebral blood flow (CBF) and cerebral blood volume (CBV), respectively, using MRI prior to onset of any behavioural or cognitive impairments. In Chapter 3 we observed clear running related increases in vessel density in the striatum, the primary region known to be affected in Huntington's Disease. In this study, we hypothesised that exercise may interact with cerebrovascular health in a knock-in mouse model of HD. The present study sought to investigate early cerebrovascular differences in the Q175 HD mouse model prior to symptom onset, compared to wild-type littermates. Thirteen male heterozygous Q175 mice and 18 WT controls (age 11 weeks) were scanned, using a flow-alternating inversion recovery (FAIR) EPI MRI pulsed ASL sequence (TR = 5 secs, TI's = 100, 200, 400, 600, 800, 1000, 1200, 1400, 1600, 1800, 2000, 2500, 3000ms, shots = 2, slice thickness = 1mm, matrix size= 128 x 96 mm, segments =2, slices = 5, bandwidth = 300,000Hz) before (Time 1) and after (Time 2) a 6-week voluntary wheel running intervention. Mice were singularly housed with (Q175; N=7) or without (Q175; N=6) a free-turning running wheel. All mice were assessed on a balance-beam at both time points to test for any clear motor or behavioural impairments. Q175 mice displayed a hyperactive behavioural profile at 11 weeks of age, according to running wheel activity and the time to climb (TTC) parameter, but no other behavioural or motor symptoms were observed on the balance beam as would be expected at this early stage in the disease lifespan of the Q175 model. CBF was slightly higher in HD mice but this was not significant, and there was no clear effect of the running intervention on CBF measured in the striatum, motor cortex or

hippocampus. Animals were culled after Time 2, and histology was performed to assess vessel density as described in Chapter 3 (*Lycopersicon esculentum*) and expression of the toxic mutant huntingtin protein (mHTT) using an S830 antibody. Vessel density did not appear higher in Q175 mice at this early disease stage (Drouin-Ouellet et al., 2015), nor did exercise appear to increase vascular density in WT mice. We conclude that it may be too early to detect vascular changes in this mouse model and that vascular differences may have returned to baseline levels following a prolonged period of exercise cessation. Although cerebrovascular deficits were not clear, a decrease in diffuse S830 staining for mHTT in running mice was observed, which is suggestive of an early benefit of exercise upon HD pathology (Harrison et al., 2013).

## 5.1. Introduction

Evidence is accumulating that vascular dysfunction plays a pivotal role in the degeneration of the nervous system (Zacchigna et al., 2008) such that any abnormality occurring in the cerebrovasculature is likely to compromise neuronal integrity. Even small changes in the cerebrovasculature are thought to be associated with various brain pathologies (Farkas and Luiten, 2001; Pantoni, 2010), from structural modifications, such as changes in vascular size, density, and morphology, to functional changes, such as altered perfusion and blood–brain barrier (BBB) dysfunction (Backman et al., 1997; Meyer et al., 2008). In Chapter 3, we discuss the potential benefits of physical exercise on cerebrovascular health in healthy young mice, by increasing vascular density within regions known to be affected by neurodegenerative diseases, including the hippocampus, motor cortex and striatum. Whether exercise can preserve vascular health and ameliorate disease progression in a mouse model of Huntington's Disease remains unclear, and will be the focus of the current study.

It has been shown in healthy rodents and humans, that exercise benefits general health and brain function (Hillman et al., 2008). In rodents, running increases hippocampal neurogenesis, spine density, vascularization, neurotrophin levels, learning and long-term potentiation (Cotman et al., 2007; Neeper et al., 1996; van Praag et al., 1999a). However, it remains unclear whether exercise is able to delay or prevent symptom progression in neurodegenerative diseases, such as Huntington's Disease, where neurovascular health is jeopardized (Drouin-Ouellet et al., 2015). To address this question, the use of rodent HD models has allowed researchers to look inside the brain in a way that is not possible in the living patient brain.

Physical exercise is a form of environmental enrichment, which is proven to have a number of beneficial effects upon neuronal health (van Praag et al., 1999b). Environmental enrichment has been shown in the R6/1 transgenic HD mouse model, to delay symptom onset and reduce striatal atrophy (van Dellen et al., 2000). In addition however, R6/1 mice who engage specifically in running wheel activity, show

normalization in some aspects of motor function such as rearing behaviour and delaying deficits in rear-paw clasping (Pang et al., 2006) with major benefits occurring in clinically relevant measures of cognitive function including spatial working memory in the Morris water maze and procedural and reversal learning on a T-maze (Harrison et al., 2013; Pang et al., 2006; van Dellen et al., 2008). Neuronal inclusion size has also been shown to differ in the R6/1 mouse model, where intracellular neuronal inclusions were larger in exercising mice than non-exercising mice (Harrison et al., 2013). It has been hypothesized previously, that larger inclusion size represents a compensatory mechanism where intracellular inclusions are neuroprotective. It seems therefore, that exercise can improve both underlying pathological and behavioural phenotypes of HD, but how this ties in with alterations in cerebrovascular health is unclear.

In Chapter 3 we addressed the question of whether fitness, as a surrogate measure of exercise, might mediate any differences seen in baseline cerebrovascular function using PASL MRI. MRI is an advantageous technique since it is non-invasive and can be repeatedly carried out *in vivo*, such that it is possible to scan the same subject multiple times to address the impact of an intervention. In human patients, we are limited to the use of imaging techniques such as MRI and PET, where post mortem tissue is scarce and may not accurately reflect the state of the living tissue. A caveat of MRI is that it is not possible to visualise directly the small-scale changes such as molecular signalling and morphological cellular changes that are taking place. Pre-clinical MRI imaging of rodents, where subsequent post-mortem evaluation can be carried out, allows us the benefit or translating what we see with MRI to humans whilst unpicking the mechanisms taking place on a more microscopic level *ex vivo*. To understand the changes observed in Chapter 3 therefore, we decided to address the influence of voluntary running on cerebrovascular health in a mouse model of HD using both MRI and histology.

Higher blood vessel density has been observed in a number of HD rodent studies compared to control mice (Cisbani et al., 2013; Cisbani and Cicchetti, 2012; Franciosi et al., 2012; Lin et al., 2013). Other morphological changes have been reported include an increase in wall thickness and decrease in lumen diameter (Franciosi et al., 2012) and a dichotomy in the type of blood vessel itself. For example, it has been

shown that while the number of microvessels increases in the R6/2 mouse model, the number of arteries is fewer than in WT controls (Lin et al., 2013). Where oxygen diffusion differs between arterioles, venules, and capillaries most oxygen diffusion occurs within the capillary bed and it is the perfusion signal from within the capillaries and pre-capillary arterioles within the metabolizing tissue which is thought to drive the CBF signal measured by ASL MRI (Hall et al., 2014). Whether an increase in the density of capillaries is a compensatory mechanism by which to maintain sufficient oxygenation of the surrounding tissues in HD is unknown, since a pathological decrease in the number of large blood vessels would presumably reduce macrovascular flow to downstream capillaries. How disease related differences in vascular morphology map onto cerebrovascular function, therefore requires the use of *in vivo* techniques such as MRI to complement those observed with histology.

Use of structural MRI has increased in recent years to study animal models of HD and has proven capable of detecting subtle variations in brain volume (Bohanna et al., 2008; Cepeda-Prado et al., 2012; Lin et al., 2013; Rattray et al., 2013). However, functional MRI for detection of cerebrovascular function has not been widely implemented to study mouse models, owing partly to its limited spatial resolution. Studies, that have measured cerebral blood volume (CBV) using contrast agents in HD mouse models, tend to show an increase in blood volume compared to WT controls, even at an early disease stage prior to demonstrating signs of disease (Cepeda-Prado et al., 2012). CBV increases within regions, including the neocortex, striatum, thalamus and hippocampus over time in the R6/2 transgenic mouse line suggest metabolic changes (Cepeda-Prado et al., 2012) which could not be attributed to a focal loss of tissue, since rCBV was not related to tissue loss in the same regions. Lin et al. (2013), compared early regional increases of rCBV to differences in microvascular morphology, and showed that both microvascular density (using immunohistochemistry) and small vessel volume fraction (extracted from 3DΔR2-μMRA images) were also increased from 7 weeks in an R6/2 mice compared to WT controls that continued to increase with age (Lin et al., 2013). The small vessel abnormalities detected in this study suggest that this could be an authentic feature of HD. Furthermore, the early onset of such abnormality in the brains of these HD mice suggest that imaging cerebrovasculature with MRI, independent from brain structure, could serve as a biomarker for detecting, as well

as providing a surrogate marker for detecting the benefits of therapies, including drugs and/or other interventions such as voluntary wheel running.

Despite a mounting appreciation of the importance of the cerebrovascular changes in HD, there has only been one study to explore differences in cerebral blood *flow* non-invasively in the brains of HD mice using PASL. In that study (Hsiao et al., 2015) flow alternating inversion recovery (FAIR) PASL was used to assess blood flow in response to a 5% $CO_2$ (carbogen) challenge and revealed impaired CVR in HD R6/2 suggestive of impaired cerebrovascular regulation and vasodilatory capacity, despite increases in angiogenesis. Cerebral blood flow studies offer a more informative measure of physiological and metabolic function than changes in relative CBV, which require administration of an exogenous contrast agent, such that measurements can also be influenced by impaired blood brain barrier function and require complex assumptions in modelling.

In the present study, we aimed to measure resting CBF in anaesthetised animals, before (MRI 1) and after (MRI 2) a 6-week running intervention in a sample of young adult mice (aged ~11 weeks), comparable to those used in Chapter 3. In addition to resting state measurements of CBF, we also subjected mice to a $CO_2$ challenge in which inhalation gas was switched from medical air to 95% medical air and 5% $CO_2$ at Time 2 to assess whether vascular reactivity was diminished in HD mice, as reported previously (Hsiao et al., 2015). In contrast to the transgenic R6/2 model used in their study, the present study used the Q175 mouse model (zQ175). This knock-in line has been shown to exhibit both motor and cognitive signs earlier in the lifespan than other KI lines such as the Q150 or Q111 strain, the repeat length of which are much shorter. It is thought that this animal model is more representative of HD in humans from genetic, neural, and behavioural aspects since both homozygous (Q175+/Q175+) and heterozygous (Q175+/Q175-) mice exhibit first signs of motor symptoms from 3-4 months and behavioural deficits by 8 months of age, with a slow disease progression such that the symptom onset is thought to reflect the human condition more closely (Menalled et al., 2012). The gradual symptom development also means that this strain is ideal for longitudinal investigations of pre-symptomatic therapies.

Like studies reported previously, we aimed to relate any genotype differences in CBF to differences in histological measures including vessel density and number of mHTT inclusions. We were interested in whether voluntary wheel running prior to the onset of cognitive or motor deficits would moderate these previously reported differences in HD mice. In the present study, we attempted to address functional differences in microvasculature in the Q175 knock-in mouse model of HD by measuring CBF and CVR, non-invasively, using MRI and combining this with histological differences in vessel density, balance beam performance and expression of the mutant huntingtin (mHTT) protein following a six-week exercise intervention.

## 5.2. Methods

### 5.2.1 Animals

Thirteen male heterozygous Q175 mice congenic to a C57BL/6J background and 18 wild-type littermates, aged 11.5 (±0.3) weeks at the start of testing were chosen for the present study (Menalled et al., 2012). Generation of the Q175 knock-in mouse line has been reported previously (Menalled et al., 2012) and was chosen for the present study due to the temporal profile of behavioural and pathological changes, in which we wished to 1) closely match the age of mice to the young adult cohort used in Chapter 3 and 2) are thought to analogously match the asymptomatic/pre-symptomatic patient cohort used in Chapter 4. Neurodegeneration, according to histological measures of striatal / cortical volume, ventricle size and MSN counts, is not typically evident in this mouse model until 12 months of age (G. A. Smith et al., 2014). A homogenous male sample was chosen in order to reduce gender differences in activity patterns, thought to vary with oestrous (Basterfield et al., 2009). The Q175 mice in this study carried between 188 and 210 (mean = 199) CAG repeats and were bred, tail-tipped and genotyped. All genotyping was performed by Laragen Inc. using probe based qPCR to generate the length of the CAG repeat on both chromosomes.

Mice were individually housed to minimise the risks of fighting because of prolonged separation after scanning, and to gain individual recordings of running activity within the cage. Mice were housed in temperature-controlled climate rooms under a 12-h light/12-h dark cycle (lights on at 8:00 am) and given free access to water and food

throughout the experiment. Mice were weighed weekly to control for changes in body weight. All procedures were run in accordance with the United Kingdom Animals (Scientific Procedures Act of 1986), and subject to local ethical review. All mice survived until the end of the study.

## 5.2.2 Behaviour

### *5.2.2.1. Voluntary wheel running*

Identical procedures to that reported in Chapter 3, were used in the present study. To investigate the effects of exercise, mice were housed in large standard mouse cages equipped with a free-standing running wheel (ENV-044 Mouse Low-Profile Wireless Running Wheel, Med Associates Inc.; 37.82cm circumference, 25° from horizontal plane). Wheel running activity was recorded via a wireless transmitter system that signalled to a hub located in the same animal holding room. Wireless Running Wheel Manager Data Acquisition Software (SOF-860; Med Associates Inc.) recorded and time-stamped each wheel rotation for subsequent analysis.

All mice had unlimited access to a running wheel for 7 days a week over 6 weeks. Whilst exercising mice (Het = 7; WT = 9) could run freely on the wheels, mice in the control condition (Het = 6; WT = 9) had wheels that were fixed in position to avoid any confounding influence of environmental enrichment provided by the wheel. Wheel access was uninterrupted during the following weeks except for removal during the administration of BrdU injections on the second week as well as weekly health checks and animal maintenance to limit enrichment introduced by excessive handling.

### *5.2.2.2. Balance beam*

The balance beam apparatus was set up as described previously (Harrison et al., 2013). A tapered balance beam was used (1.5 cm to 0.5 cm) with a ledge 2cm below the running surface along the length of the beam to prevent the animals from falling, and to aid in the identification of foot-slips (Schallert, 2006). The beam was 1m in length and angled at 17°with the start point 15cm from the lower end and a goal box at the high end, where the end was marked 10 cm from the top (figure 5.1).

Methods were adapted from those described by Harrison et al., (2013) whereby animals were trained for two days followed by testing on two trials, on the two subsequent days. On training Day 1, animals were initially acclimatised to a box at the top of an inclining beam for 30s before being removed and placed in position 1. Distance away from the house box was gradually increased (positions 2-4) until the animal was at the start area of the beam (position 5), whereby the animal was encouraged to traverse the beam until it could enter the box. Where animals stayed still for a prolonged period, they were encouraged to keep moving by touching their flank. Finally, animals were positioned at the bottom of the incline, facing away from the box. To reach the box, animals were required to turn around before climbing up towards the box. After 10 seconds respite inside the box, animals were encouraged to traverse from 3 positions, incrementally further down the beam until the subject was comfortable traversing the entire length of the beam. Training Day 2 consisted of 2 trials where the animal was placed facing away from the 'house' box and needed to turn around and traverse the beam to enter the 'house' box at the top.

Training took place at the beginning of the experiment, followed by 2 days of testing at the pre- and post-exercise time-points. Training was not repeated prior to the second (post-exercise) time-point. On each test day, animals were given one practice run, followed by two experimental trials, separated by ~5 minute intervals. Ability (counting any foot slips) and speed to traverse the beam were recorded as measures of motor function, balance and coordination and time to turn 180° on the beam were used as a measure of motor initiation. Time-to-turn (TTT), time to climb (TTC), as well as front and back paw foot slips were recorded as described previously (Brooks et al., 2012). One side was scored live and the other video recorded for subsequent bilateral scoring. Experimenters were blinded to subject condition.

Animals were assigned to experimental condition according to performance on the first balance beam session, by ranking animals and assigning alternate animals to the running or non-running condition, to remove bias towards one condition in terms of behavioural performance.

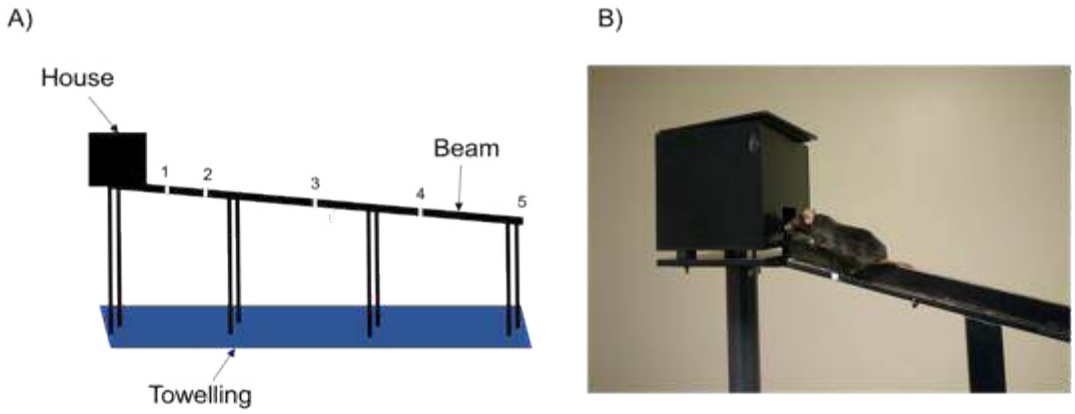


**Figure 5.1 Balance beam apparatus used for testing and training schedule**.
A) The balance beam apparatus was constructed from wood painted black, with a goal 'house' located at the top of the beam. During training animals were initially placed at position 1 and encouraged to traverse the beam and enter the house located at the top. Mice were subsequently placed further down the beam (positions 2, 3, 4 and 5) and similarly encouraged to run along the beam to enter the house at the top. (B) Time to climb was recorded as the time in which the back feet crossed the white line before entering the house.

### 5.2.3 BrdU Administration

Identical procedures were used to those described in Chapter 3. After one week of habituation to the wheel, *i.p.* BrdU injections (50µg/g; Sigma) were carried out at the same time daily (11:30-12:30) for 5 days as described previously (Creer et al., 2010b) during the second week of wheel exposure. BrdU data is not presented here due to time constraints.

### 5.2.4 Magnetic Resonance Imaging

#### *5.2.4.1. Experimental Procedure*

All animals were scanned twice, once at baseline and once following 6 weeks of wheel exposure. At 11 weeks old, all 31 animals underwent a single baseline scan session (~45mins), followed by a second scan after 6 weeks of wheel exposure.

Scanning took place three days after exercise cessation to avoid measuring acute exercise-related effects (figure 5.2).

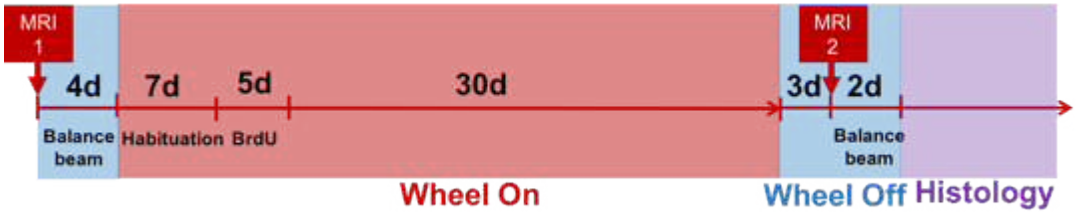


**Figure 5.2 Experimental design.** Baseline MRI measurement and balance beam was assessed prior to wheel exposure for 6 weeks. Follow up MRI and Balance beam performance was measured after 3 and 5 days of wheel deprivation respectively.

### *5.2.4.2. MRI setup*

Magnetic resonance imaging was performed with a 9.4 Tesla small bore (20 cm) Bruker Biospin system (Ettlingen, Germany) at EMRIC, Cardiff University. A transmit 1H 500W echo-planar imaging (EPI) volume coil was used along with a 4-channel array receive-only surface coil (Rapid Biomedical). ParaVision software (version 5.0, Bruker Biospin) was used for data acquisition. Mice were anesthetized under 4% isofluorane in medical air (flow rate at 1L/min) and maintained at 1.8% throughout perfusion imaging. Animals were free breathing for the duration of scanning. Core temperature and respiration rate were monitored using a rectal probe and pressure pad (SA Instruments, Stony Brook, NY, USA) respectively. Core temperature was maintained at ~36° C to 37°C using heated water tubing through the bed and a warm air blower with feedback system fed into the scanner bore (SA Instruments). Image analysis was performed using FSL (FMRIB Software Library, Oxford, UK) and AFNI (Cox, 1996) software packages.

### *5.2.4.3. Resting Cerebral Blood Flow (CBF)*

To quantify cerebral blood flow, a flow-alternating inversion recovery (FAIR) EPI PASL scan was carried out (TR = 5 secs, TI's = 100, 200, 400, 600, 800, 1000, 1200, 1400, 1600, 1800, 2000, 2500, 3000ms, shots = 2, slice thickness = 1mm, matrix size= 128 x 96 mm, segments =2, slices = 5, bandwidth = 300,000Hz) such that 13 images with increasing TI were obtained per slice, allowing determination of $T_1$. Images with slice selective inversion were acquired, followed by those with a non-

selective inversion, from which their respective $T_1$ was calculated, using a non-linear least square fit (Leithner et al., 2008). The total time for CBF measurement was ~10 mins.

CBF was quantified as described elsewhere (Leithner et al., 2008) on the basis of equation 2.1, with modification of the Bloch equation to include blood flow effects (Detre et al., 1992).

Equation 2.1 ——— — —

Where $T_1$ is tissue $T_1$, $T_{1app}$ is $T_1$ in the presence of flow and λ is the brain blood partition coefficient of water. In a pulsed ASL experiment with nonselective inversion, it is considered that measured $T_1$ reflects "true" tissue $T_1$ and with slice selective, inversion measured $T_1$ becomes $T_{1app}$ (Kwong et al., 1995). Assuming a λ value of 0.9 (Herscovitch and Raichle, 1985), CBF can therefore be quantified using equation 2.2.

Equation 2.2 ———— ————

Voxel-wise CBF was then averaged over ROI masks using FSL software, and median CBF values recorded per ROI to reduce the impact of outliers. CBF estimates were calculated across two masks per ROI, created by each of the two experimenters. CBF estimates within each ROI were averaged across experimenters and these values were used as the measure of interest.

#### *5.2.4.4. Cerebrovascular reactivity (CVR)*

To measure cerebrovascular reactivity, the FAIR ASL sequence was modified to include a single inversion time, such that image acquisition duration was shorter and thus changes in CBF in response to hypercapnia could be detected with greater temporal resolution. Baseline acquisition was carried out for 5 minutes before the inhaled gas mixture was switched from 100% medical air to 95% medical air and 5% $CO_2$ for 5 minutes. Hypercapnic blocks were repeated twice, separated by 15

minutes of breathing medical air such that animals had time to recover from the previous challenge (TR = 3500ms, TI = 1500ms, shots =2, segments = 2, slice thickness = 1mm, matrix size = 128 x 96, voxel size = 0.17 x 0.17 x 1mm, slices = 5, bandwidth = 300kHz).

The entire time-series were separated into selective and non-selective images and a simple subtraction performed, such that the difference in signal was related to the relative change in CBF on a voxel-wise basis. Average rCBF values were recorded during the two hypercapnic (10 volumes x 2) and three normocapnic (10 volumes x 3) periods, ignoring the first and last volumes to avoid noise introduced by gas-switching. Relative CBF values for each block were computed on a voxel-wise basis and ROI masks of the striatum, hippocampus and M1 were applied as described above, to create an average rCBF for each ROI per block. Median values were used to since mean values may be skewed by outliers where SNR is low. The normocapnic and hypercapnic blocks were then averaged together respectively, such that percentage change values could be calculated for estimating CVR in response to the $CO_2$ challenge (Equation 2.3).

Equation 2.3 $$CVR = \frac{\quad}{\quad}$$

#### *5.2.4.5. Regions of Interest*

ROI's were defined by two independent, blinded assessors (myself and an undergraduate research student). All masks were drawn using FSL upon the raw non-selective images, where contrast was good enough to identify anatomical landmarks. Bilateral hippocampi were drawn on the 2$^{nd}$ slice (located between -1.34mm and -2.8mm from bregma), whilst masks of the motor cortex (M1) and striatum were drawn on the 4$^{th}$ slice acquired for each animal (+1.18mm and -0.26mm from bregma) (figure 5.3). Hippocampal masks were drawn ventral to the corpus callosum and constrained between the third and lateral ventricles to avoid contamination of the signal by CSF. Striatal masks were drawn ventral to the corpus callosum, whereby the mask did not exceed the length of the lateral ventricle. Square

shaped M1 masks were positioned above the corpus callosum, above the cingulum bundle.

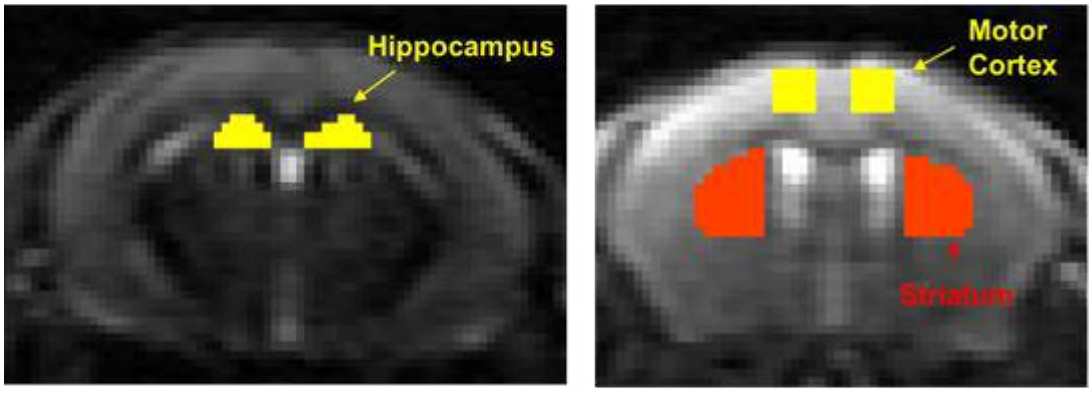


**Figure 5.3 ROI mask placement overlayed on an example non-selective image from one mouse.** Manually drawn ROI's were carried out by two independent experimenters. Representative slice location can be seen for the hippocampus positioned ~-1.34mm of bregma (left) and the motor cortex and striatum positioned ~+0.86mm of bregma (right). Masks were drawn on example raw non-selective images prior to CBF quantification from a single subject due to the higher image contrast.

## 5.2.5 Histology and Immunohistochemistry

### *5.2.5.1.*

### *5.2.5.2. Tissue Preparation*

Animals were deeply anaesthetised with 0.02ml sodium pentobarbital (Euthatal) and perfused trans-cardially with PBS, followed by heparin ~110ml 4% paraformaldehyde (PFA), in 0.01M PBS at pH 7.4 at a flow rate of ~23ml/min for 5mins. Brains were post-fixed for 5h followed by equilibrium in 30% sucrose. Tissue was sectioned coronally at a thickness of 40 µm on a freezing microtome (Leica). A thickness of 40 µm has been recommended previously in order to obtain reliable 3D information about the vascular tree for quantification (Wälchli et al., 2014). Free-floating sections were stored as a 1:12 series in cryoprotectant solution and stored at −20°C until staining.

### *5.2.5.3. Blood Vessel Visualisation and Quantification*

Identical immunofluorescence parameters were used to those described in Chapter 3. Lectin staining (*Lycopersicon esculentum*; Vector) was used to visualize blood

vessels as described previously (Creer et al., 2010b) where group differences in blood vessel density was used as a surrogate measure of angiogenesis (See Chapter 3 for methods).

Quantification procedures were identical to that described in Chapter 3. To investigate whether exercise alters angiogenesis in the HD brain, blood vessel density was calculated within the dorsal striatum, dorsal hippocampus and M1. Repeated measures ANOVA within sub-regions of the striatum (Dorsal SVZ x Ventral SVZ x Caudate Putamen) and hippocampus (Dentate Gyrus x CA1) were performed with Running and Genotype as the between-subject variables. The M1 was not divided into sub regions.

#### *5.2.5.4. Mutant Huntingtin (mHTT) Visualisation and Quantification*

Prior to immunohistochemistry, tissue sections were placed in TBS (pH 7.4) and washed three times, for 5 min. Pre-treatment with an antigen retrieval method was performed as described previously (Bayram-Weston et al., 2016) by incubation in citrate buffer (pH 6) for 20 min at 95°C for 5minutes at room temperature.

Endogenous peroxidase activity was inhibited by incubation in methanol containing 3% $H_2O_2$ (VWR International, UK) for 5 min and non-specific binding sites were blocked with 3% horse serum in TBS for 1 h. Sections were incubated with S830 (Prof.G Bates, King's College, London University; 1: 20,000 concentration) in TXTBS containing 1% horse serum) overnight at room temperature (21°± 2°C), after which they were washed three times in TBS (3 x 5mins). Sections were incubated in secondary antibody (raised in horse, anti-goat; Vector Laboratories) at a 1:200 concentration for 2h at room temperature. Following several washes in TBS, the sections were incubated with a biotin-streptavidin kit according to the manufacturer's instructions (Vector Laboratories) and rinsed three times in TBS. Peroxidase activity was visualized with 3,3'-diaminobenzidine (DAB; Sigma-Aldrich), and sections mounted on gelatin-coated slides, prior to dehydration and cover-slipping as described above.

Two-dimensional stereological quantification was conducted using Visiopharm Integrator System (VIS, version 4.4.6.9) software on an Olympus BX50 microscope

(Olympus Optical Co. Tokyo, Japan) with PC-based image analysis software (Olympus C.A.S. T. grid system v1.6.). Quantification was carried out as described previously (Bayram-Weston et al., 2016).

For each mouse, counts were formed on a 1:12 series, such that between 3 striatal (bilateral) sections per mouse were imaged at 1.25 X magnification upon which outlines were manually drawn around the striatum of each hemisphere. Defined striatal sections were then sampled systematically, such that ~150 cells were counted per brain, which equated to ~14 samples per hemisphere. Cells were counted at a 100 X magnification (oil), within a 2D optical dissector 285$\mu m^2$ counting frame. Cell diameter was established by measuring the longest and shortest diameter and computing the average. For consistency and to reduce bias, this was performed on the first cell counted within the first counting frame of each section. A representative image of the counting can be seen in figure 5.4. Cells located within the frame and all those touching the green lines were included in the count, whereas cells that touched either of the red lines were excluded.

Affected cells were identified and the total numbers estimated in terms of positive immuno-reactive-labelling. Due to the young age of the subjects, we expected more diffuse staining. Affected cells were further categorized in terms of whether they expressed 1) Diffuse nuclear staining alone 2) Frank nuclear inclusion bodies (IB's) with additional diffuse nuclear staining 3) Frank IB's without diffuse staining. For each section, one diffuse cell and one extracellular aggregate was systematically measured in size (length x width).

The total number of cells (C) in each striatal section was calculated using the equation 2.4.

Equation 2.4 $$C = \Sigma c \times (\Sigma A \times (\Sigma n \times a)) \times f$$

*C = estimated total number of cells, Σc = total number of cells counted, ΣA = sum of all striatal areas, Σn = total number of frames allocated to the included striatal area, a = area of sampling user grid (285$\mu m^2$), f = frequency of sectioning*

An Abercrombie correction factor was then applied to the total number of calculated cells using equation 2.5:

Equation 2.5 $aC = C \times (ST / (ST+D))$ (Abercrombie, 1946)

*aC = Abercrombie corrected cell count, C = estimated total number of cells, ST = section thickness, D = cell diameter.*

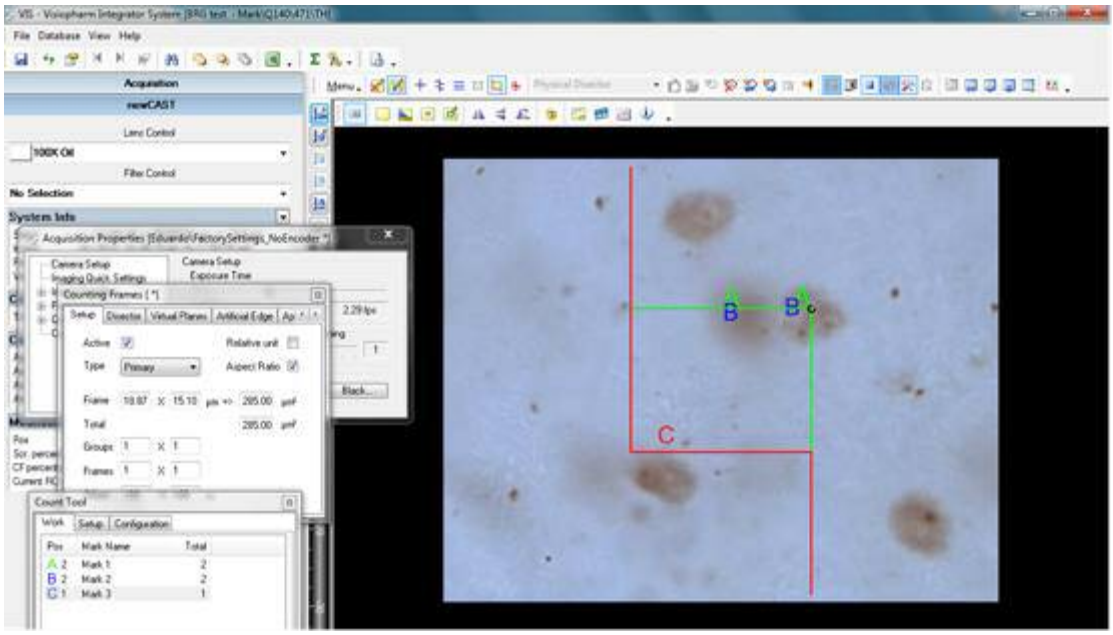


**Figure 5.4 S830 counting methods for mHTT quantification.** Representative image of stereological analysis conducted in Visiopharm Integrator System (VIS) software. The 285μm$^2$ counting frame can be seen in the centre of the image. Cells located within the counting frame and not touching the red lines were counted as diffusely stained cells (letter 'A') and those that also possessed nuclear inclusion bodies (IB's) were counted separately (letter 'B'). Extracellular aggregates were also counted (letter 'C').

## 5.3. Results

### 5.3.1. CAG repeat length

CAG repeat length is known to be positively related to disease burden and rate of progression. Average number of CAG repeats did not differ between the running group 198.4 (±6.7) compared to the non-running group 198.8 (±6.5) such that CAG repeat length is unlikely to influence the interpretation of the group differences reported here.

### 5.3.2. Body Weight

All animals showed an increase in body weight over the duration of the experiment (TIME = F (1,27) = 5.06, p<0.001, partial $\eta^2$= 0.37, figure 5.5). Non-running mice gained weight to a greater degree than running mice (Running x Time; (F (1,27) = 2.63, p=0.16, n.s., partial $\eta^2$= 0.09) regardless of genotype. A significant interaction between genotype and running was observed (Genotype x Running; (F (1,27) =6, p=0.02, partial $\eta^2$= 0.18), whereby WT mice differed more because of wheel exposure than HD mice. Nonetheless, an interaction including a repeated measure of time was not significant (Running x Genotype x Time; F (1,27) =0.24, p=0.63, n.s., partial $\eta^2$= 0.01), suggesting that this relationship was an inherent group related difference and could not be attributable to the exercise intervention itself.

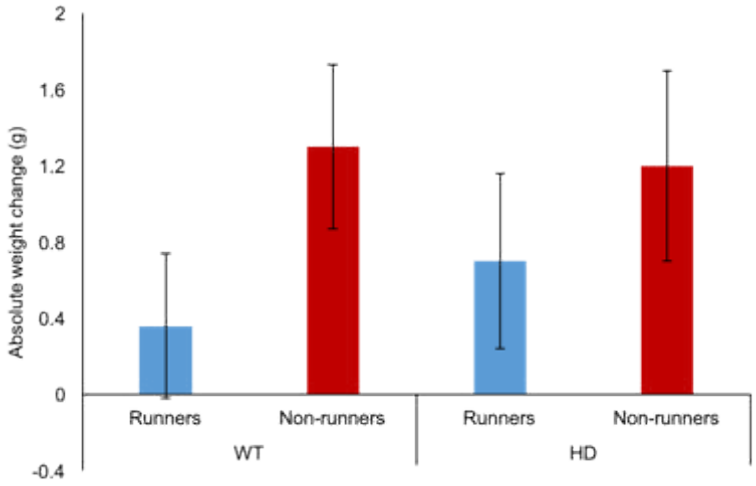


**Figure 5.5 Body weight change following intervention.** Non-runners increased in body weight more than running animals but this was not significant. There was no difference between weight change in HD mice compared to WT mice over time. Mean ± S.E.M.

## 5.3.3. Behavioural Data

### *5.3.3.1. Weekly running wheel activity*

On average, Q175 HD mice ran approximately 30% more (Mean = 533,125, SD = 156,238.73) than WT mice (Mean = 382,981.30, SD = 286,326.034; figure 3.2), but a one-way ANOVA revealed that this group difference was not significant ($F(1,15) = 1.58$, $p=0.23$, n.s, partial $\eta^2 = 0.1$).

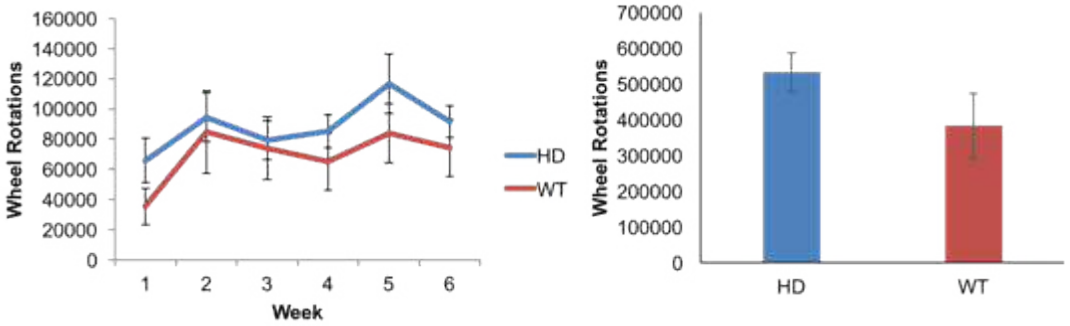


**Figure 5.6 Running wheel activity over 6 weeks in Q175 mice and wild-type controls.** HD mice (N=7) ran more overall (right) than WT mice (N=10; left), but this was not significant ($p>0.05$). Mean ± S.E.M.

### *5.3.3.2. Balance Beam*

HD mice did not appear to be obviously impaired on any aspects of balance beam performance compared to wild type animals (figure 5.7).

Time to climb the balance beam revealed a borderline significant interaction effect (Time x Genotype; $F(1,27) = 4.30$, $p<0.05$, partial $\eta^2 = 0.14$). Simple comparisons revealed that HD subjects climbed faster than WT mice at baseline, an effect that was no longer significant after 6 weeks. There was no influence of running on this effect (Time x Running X Genotype; $F(1,27) = 0.15$, $p=0.70$, n.s., partial $\eta^2 = 0.01$) such that this difference was not attributable to the running intervention, and is likely to be due to a disease phenotype progression over the 6 weeks.

No effect of Time, Running or Genotype was found to significantly influence time to turn on the beam ($p$ values $>0.05$), although in general time to turn around appeared to be faster at the 6-week time-point (Time; $F(1,27) = 1.6$, $p=0.21$, partial $\eta^2 = 0.06$) but this was not significant.

No clear trend was observed in the number of front foot-slips made by the animals, where number of foot slips made was minimal across trials at this age (p values>0.05). More apparent trends could be observed in the back-foot slips made, where all animals seemed to slip more at 0 weeks than at 6weeks, which is likely due to a practice effect (Time; F (1,27) =6.00, p=0.02, partial $\eta^2$= 0.18). HD animals appeared to produce fewer foot-slips than WT controls, although this did not meet significance (Genotype; F (1,27) = 2.40, p=0.13, partial $\eta^2$= 0.08).

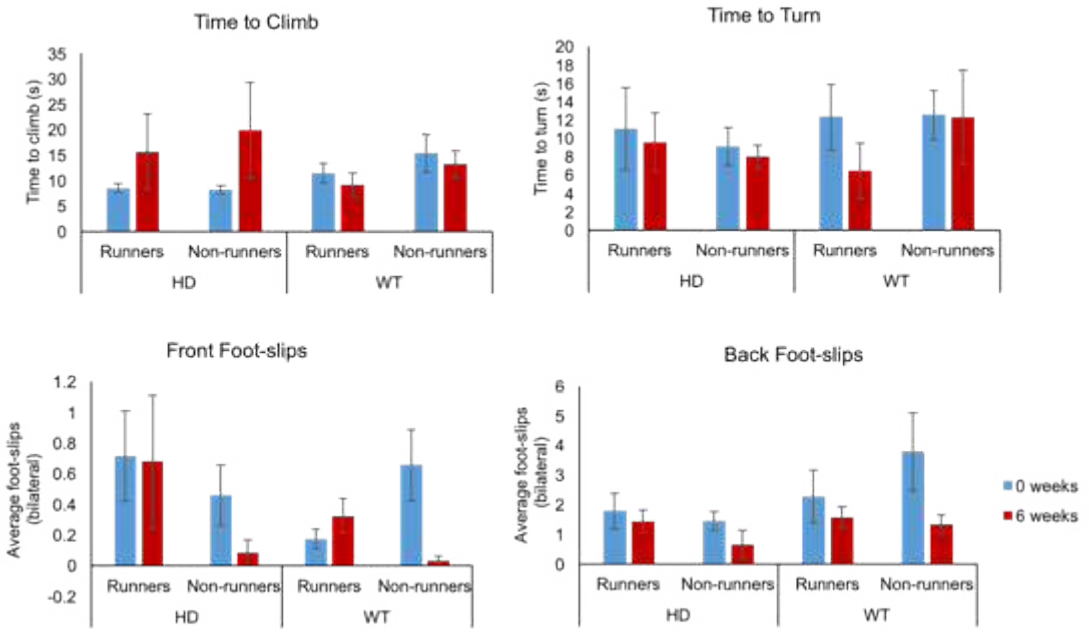


**Figure 5.7 Group differences in balance beam performance.** Balance beam performance before (blue bars) and after (red bars) 6-weeks of wheel exposure in HD (Q175) mice compared to wild type (WT) controls. Bars indicate mean values over 4 experimental trials. Mean ± S.E.M.

## 5.3.4. Baseline CBF Data

### *5.3.4.1. Data Quality*

Prior to averaging across experimenters, data quality was assessed by removing outliers that exceeded rCBF estimates >2 SD's from the group mean. Following outlier removal, CBF data was averaged across experimenters such that there was just one rCBF value per scan, per ROI, per subject. Where noise was consistent across experimenters, this meant that there was missing pre-exercise data in the

hippocampus for two subjects and motor cortex for one subject. Two subjects had to be removed from the within-subject analysis because data for their pre-exercise scan was acquired with incorrect parameters.

#### *5.3.4.2. Genotype differences in CBF at baseline*

We initially wanted to assess whether a baseline difference in rCBF existed between HD and WT mice prior to any exercise intervention at 11 weeks of age. In all regions of interest Q175 had very slightly higher baseline CBF than the WT mice and this was most prominent in the striatum (figure 5.8). Statistical differences between group were not found however, in the striatum ($F(1,26) = 0.16$, $p=0.69$, n.s., partial $\eta^2= 0.06$), hippocampus ($F(1,24) = 0.01$, $p=0.92$, n.s., partial $\eta^2< 0.001$) or M1 ($F(1,25) = 0.02$, $p=0.88$, n.s., partial $\eta^2= 0.001$).

#### 5.3.4.3. *Regional differences in CBF at baseline*

CBF differed significantly across regions (figure 5.8) with highest rCBF values detected in the motor cortex (Mean= 230ml/100g/min; SEM=4.3) and lowest in the hippocampus (Mean= 175.7ml/100g/min, S.E.M = 3.3ml/100g/min; ROI; $F(2,42) = 56.6$, $P<0.001$, partial $\eta^2= 0.73$). Post hoc tests revealed significant FDR-corrected CBF differences between each region ($q<0.017$). No interactions were found between CBF and Genotype across these regions (ROI x Genotype; $F(2,42) = 0.57$, $p=0.57$, n.s., partial $\eta^2= 0.03$).

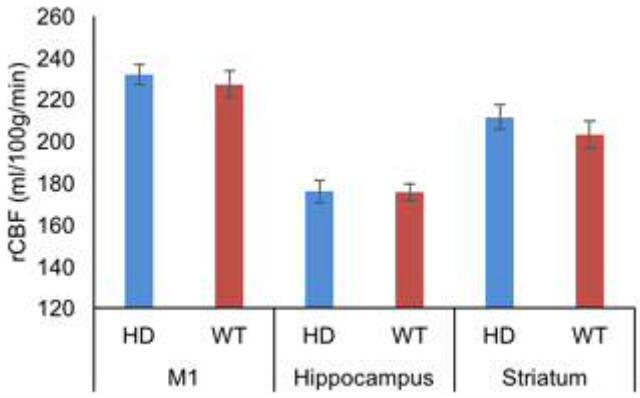


**Figure 5.8 Genotype differences in regional CBF.** CBF differences between Q175 and WT groups was not evident at 11 weeks of age in the primary motor cortex (M1), Hippocampus and Striatum. Mean ± S.E.M.

### 5.3.4.4. *Regional rCBF differences following 6-weeks wheel exposure*

Absolute rCBF was quantified within manually drawn ROIs, and averaged across experimenters. A repeated-measures ANOVA was performed with TIME (baseline vs 6weeks) and ROI (striatum vs hippocampus vs M1) as within-subject factors and Genotype and Running as between-subject factors.

As can be seen in figure 5.9., an apparent, but non-significant decrease in CBF was seen after 6 weeks (Time; F (1,21) = 3.40, p=0.08, n.s., partial $\eta^2$= 0.14), however, this did not vary between HD and WT groups (Time x Genotype; F (1,21) = 1.38, p=0.25, n.s., partial $\eta^2$= 0.06) or in runners compared to non-runners (Time x Running; F (1,21) = 1.40, n.s., p=0.25, partial $\eta^2$= 0.06), suggesting that a change over time could not be attributed to genotype or the effects of running. Exercise did not affect HD mice differently to WT animals after 6 weeks of wheel exposure (Time x Running X Genotype; F (1,21) = 1.60, p=0.22, n.s., partial $\eta^2$= 0.07) although a significant interaction between ROI and Time was observed (F (2,42) = 5.7, p=0.006, partial $\eta^2$= 0.22) whereby post hoc t-tests revealed that the decrease in CBF was driven primarily by decreases in the hippocampus over time (t (25) = 5.6, p =0.002).

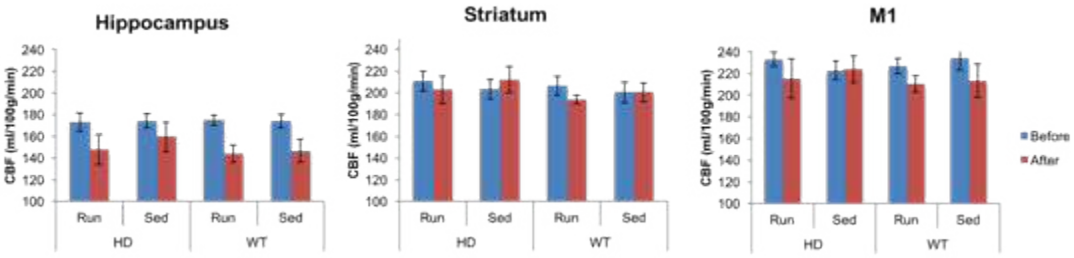


**Figure 5.9 Regional CBF (rCBF) differences across the hippocampus, M1 and striatum in running vs. non-running HD mice compared to WT controls.** Coloured bars represent CBF values before and after 6-weeks of wheel exposure in the home cage. Mean ± S.E.M.

### 5.3.4.5. *The effects of a dose response of wheel running on rCBF.*

Pearson's correlations were carried out on regions independently, to assess whether total number of rotations could predict rCBF in running HD and WT animals. As can be seen in figure 5.10, there was no evident relationship between the total number of rotations and rCBF in the hippocampus (WT (r (10) = 0.03, p=0.94, n.s.); HD (r (7) =-0.37, p=0.41, n.s), striatum (WT (r (10) =0.44, p=0.20, n.s.); HD (r (7) = 0.07, p=0.87, n.s.) or motor cortex (WT (r (10)=0.15, p=0.68, n.s.); HD (r (7)=0.20, p=0.66,

n.s.) although the strongest decoupling could be seen in the hippocampus, where running was negatively correlated with rCBF in HD mice.

## 5.3.5. Physiological monitoring

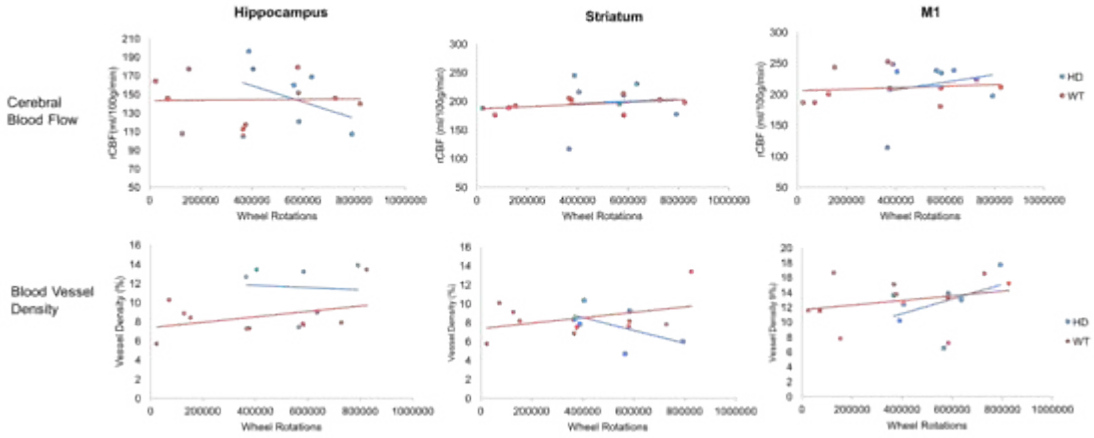


**Figure 5.10 Regional dose relationships between running distance-CBF and running distance-vessel density.** Dose response relationship between voluntary wheel running and cerebral blood flow (CBF) as measured with FAIR-EPI pASL (top row) and blood vessel density as measured using tomato lectin staining (bottom row) in the hippocampus, striatum and motor cortex (M1).

### *5.3.5.1. Anaesthetic Dose*

Isofluorane dose was targeted at 1.7% for the first scan but was adjusted to achieve stable physiological readings. Isofluorane dose was adjusted on a subject-by-subject basis, to ensure that isofluorane was consistent across scans to achieve within-subject repeatability. A repeated-measures ANOVA was performed to ensure that dose did not differ between Genotype or Running. Mean dose was 1.73±0.08% during the first scan and 1.74±0.1% during the second scan (Table 5.1). There was not a significant dose difference between scans (Time; $F(1,25) = 0.40$, $p=0.53$, n.s., partial $\eta^2= 0.02$), nor did dose vary between Genotype x Time ($F(1,25) =0.33$, $p=0.57$, n.s., partial $\eta^2= 0.01$) or Running x Time ($F(1,25) =2.6$, $p=0.12$, n.s., partial $\eta^2= 0.10$). Individual physiological parameters were explored using repeated measures ANOVAs and can be seen in Table 5.1.

| | Genotype | Group | Mean | SD | N |
|---|---|---|---|---|---|
| **Isofluorane (%) Pre** | Het | Non-running | 1.73 | 0.05 | 4 |
| | | Running | 1.72 | 0.04 | 7 |
| | | Total | 1.72 | 0.04 | 11 |
| | WT | Non-running | 1.71 | 0.04 | 8 |
| | | Running | 1.77 | 0.12 | 10 |
| | | Total | 1.74 | 0.10 | 18 |
| | Total | Non-running | 1.72 | 0.04 | 12 |
| | | Running | 1.75 | 0.10 | 17 |
| | | Total | 1.73 | 0.08 | 29 |
| **Isofluorane (%) Post** | Het | Non-running | 1.70 | 0.00 | 4 |
| | | Running | 1.77 | 0.11 | 7 |
| | | Total | 1.75 | 0.09 | 11 |
| | WT | Non-running | 1.71 | 0.04 | 8 |
| | | Running | 1.77 | 0.13 | 10 |
| | | Total | 1.74 | 0.10 | 18 |
| | Total | Non-running | 1.71 | 0.03 | 12 |
| | | Running | 1.77 | 0.12 | 17 |
| | | Total | 1.74 | 0.09 | 29 |

**Table 5.1.** Isofluorane dose (%) during CBF scans pre and post wheel exposure.

#### *5.3.5.2. Temperature*

As can be seen in Table 5.2, average temperature was ~37°C in all groups. There was no main effect of temperature between scans ($F(1,25) = 2.35$, $p=0.14$, n.s., partial $\eta^2 = 0.09$). No significant interactions were found between Running ($F(1,25) = 0.25$, $p=0.14$, n.s., partial $\eta^2 = 0.01$) or Genotype ($F(1,25) = 2.4$, $p=0.14$, n.s., partial $\eta^2 = 0.09$) across the pre- and post- exercise sessions.

#### *5.3.5.3. Pulse Rate*

Average pulse rate was slightly higher during Scan 1 519 (± 40) bpm than during Scan 2 500 (± 65), although data during scanning was very noisy. There was no difference in pulse rate ($F(1,25) = 0.90$, $p=0.18$, n.s., partial $\eta^2 = 0.07$) between scans, although it was slightly more variable in Scan 2, possibly due to the prospective targeting of anaesthetic dose. No difference was observed in pulse rate between Running ($F(1,25) = 1.10$, $p=0.30$, n.s., partial $\eta^2 = 0.04$) or Genotype ($F(1,25) = 0.26$, $p=0.62$, n.s., partial $\eta^2 = 0.01$) across the pre- and post-exercise sessions.

#### *5.3.5.4. Respiration*

There was not a significant main effect of Time on respiration ($F(1,25) = 2.7$, $p=0.11$, n.s., partial $\eta^2 = 0.10$). Non-significant interactions with RUNNING ($F(1,25) = 2.5$,

p=0.13, n.s., partial $\eta^2$= 0.06) and Genotype (F (1,25) =1.7, p=0.21, n.s., partial $\eta^2$= 0.06) suggest there were no differences between experimental groups.

| | | | Respiration (bpm) | | Temperature (°C) | | Pulse | | N |
|---|---|---|---|---|---|---|---|---|---|
| | Genotype | Group | Mean | SD | Mean | SD | Mean | SD | |
| **Pre-Exercise** | Het | Non-running | 103.96 | 14.93 | 35.89 | 1.12 | 540.78 | 69.30 | 4 |
| | | Running | 106.70 | 10.29 | 36.60 | 1.10 | 522.98 | 43.53 | 7 |
| | | Total | 105.70 | 11.50 | 36.35 | 1.11 | 529.45 | 51.56 | 11 |
| | WT | Non-running | 109.55 | 8.11 | 36.97 | 0.79 | 526.82 | 42.77 | 8 |
| | | Running | 109.76 | 7.91 | 36.78 | 0.63 | 501.45 | 37.32 | 10 |
| | | Total | 109.67 | 7.76 | 36.86 | 0.69 | 512.72 | 40.73 | 18 |
| | Total | Non-running | 107.68 | 10.50 | 36.61 | 1.01 | 531.47 | 50.21 | 12 |
| | | Running | 108.50 | 8.79 | 36.71 | 0.83 | 510.31 | 40.17 | 17 |
| | | Total | 108.16 | 9.36 | 36.67 | 0.89 | 519.07 | 45.00 | 29 |
| **Post-Exercise** | Het | Non-running | 105.59 | 9.25 | 36.38 | 0.77 | 498.00 | 72.12 | 4 |
| | | Running | 103.32 | 9.31 | 37.08 | 0.49 | 500.96 | 72.07 | 7 |
| | | Total | 104.15 | 8.89 | 36.82 | 0.67 | 499.89 | 68.41 | 11 |
| | WT | Non-running | 107.49 | 11.99 | 37.11 | 0.95 | 486.10 | 77.23 | 8 |
| | | Running | 97.50 | 11.43 | 36.63 | 1.03 | 512.28 | 57.18 | 10 |
| | | Total | 101.94 | 12.42 | 36.84 | 1.00 | 500.64 | 66.08 | 18 |
| | Total | Non-running | 106.85 | 10.75 | 36.87 | 0.93 | 490.07 | 72.45 | 12 |
| | | Running | 99.90 | 10.71 | 36.81 | 0.86 | 507.62 | 61.80 | 17 |
| | | Total | 102.78 | 11.10 | 36.84 | 0.87 | 500.36 | 65.74 | 29 |

**Table 5.2.** Respiration rate, core temperature and pulse were recorded every minute during scanning. Values reflect group mean physiological responses between GENOTYPE and GROUP and standard deviation reflects the variance between animals within the group.

#### *5.3.5.5. Effect of depth of anaesthesia on rCBF*

Depth of anaesthesia is known to influence vasodilation in the brain as well as subsequent CBF. The relationships between regional CBF values and physiological parameters including mean temperature, isofluorane dose, respiration rate and pulse rate recorded during pre-exercise and post-exercise scans, were tested using Pearson's correlation. No relationship was found between rCBF and anaesthetic dose, temperature, respiration or pulse rate during Scan 1 or Scan 2 (p values >0.5), in the M1, hippocampus or striatum. For this reason, these factors were not included as covariates in any further analyses.

### 5.3.6. Cerebrovascular Reactivity

CBF measurements displayed low SNR, such that an obvious increase in CBF following onset of the $CO_2$ challenge was not apparent. Out of 31 subjects 9 subjects showed a *decrease* in CBF in the motor cortex, 17 in the striatum and 13 in the hippocampus. Where $CO_2$ is a potent physiological stimulus, CBF is expected to increase CBF regardless of genotype and thus the present results were unexpected.

There was no interaction between HD status or running condition in any of the three regions (Genotype x Running, p>0.05), however within the striatum there appeared to be a genotype difference, whereby HD mice showed a positive elevation in CVR where WT animals showed a decrease (Genotype, F (1,27) =3.13, p=0.09, n.s., partial $\eta^2$=0.10). There was no main effect of genotype or running in any other regions (p>0.05). CVR levels were greater within the motor cortex than in subcortical regions (F (2,40) = 6.20, p = 0.01, Greenhouse-Geisser corrected for violation of sphericity).

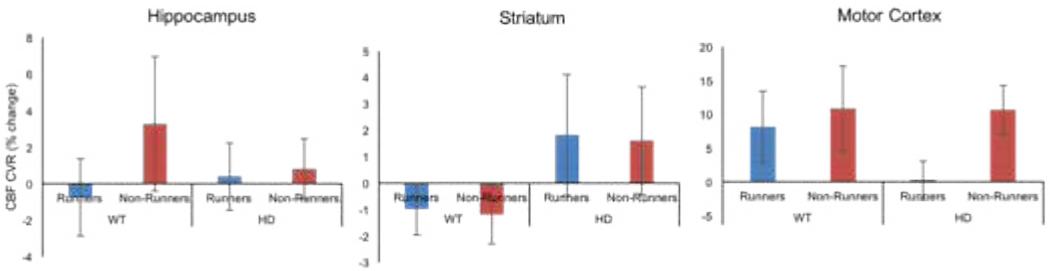


**Figure 5.11 Genotype differences in CBF CVR between running and non-running mice.** Cerebrovascular reactivity was quantified as percentage change in CBF to a 5% $CO_2$ elevation in inhaled $CO_2$. Response to hypercapnia was not consistent across animals. Variation across the group and across regions was high. Mean ± S.E.M.

## 5.3.7. Vascular density

### *5.3.7.1. Sub-regional Analysis*

*Striatum.* Visual inspection revealed that vascular density was higher in wild type animals than controls, however no obvious difference was apparent between running and non-running animals. This trend can be seen in figure 5.12, however statistical inference found no main effect Genotype (F (1,26) = 0.76, p=0.39, n.s., partial $\eta^2$= 0.03), nor an interaction with running (Running x Genotype; F (1,16) =0.012, p=0.91, n.s., partial $\eta^2$< 0.01) as hypothesised. There was also no overall effect of running (Running; (F (1.26) = 0.45, p=0.52, n.s., partial $\eta^2$= 0.20). There was however, a significant main effect of Sub region (F (2,52) = 5.1, p=0.01, n.s., partial $\eta^2$= 0.16), whereby paired t-tests revealed that on average the dorsal sub-ventricular zone (DSVZ) had a higher vascular density than the caudate putamen (CP; t (29) = 2.8,

p=0.007) and the ventral sub ventricular zone (VSVZ; t (29) = 2.3, p=0.03), with an average increase of ~7%.

*Hippocampus.* Within the hippocampus, vessel density was greater in the CA1 region of the hippocampus than the dentate gyrus (Sub region; F (1,25) = 11, p= 0.003, partial $\eta^2$ = 0.3), a difference which was not observed in Chapter 3. Vessel density did not differ within the DG, however HD animals had a greater vessel density in the CA1 than WT controls (Sub region x Genotype; F (1,25) = 5.4, p=0.03, n.s., partial $\eta^2$ = 0.18) irrespective of running. There were no differences between HD and control animals (Genotype; F (1,25) = 0.44, p=0.51, n.s., partial $\eta^2$ = 0.02). Running related differences were evident in WT mice compared to HD mice, whereby runners seemed to have a reduced vessel density compared to non-runners across both DG and CA1, whereas HD animals showed no difference in vessel density because of running (figure 5.12). This did not however, reach statistical significance (Running X Genotype; F (1,25) = 2.60, p= 0.12, n.s., partial $\eta^2$ = 0.09).

*Motor cortex.* Only one ROI was imaged within the motor cortex. As can be seen in figure 5.12, there was no interaction present to reflect a genotype moderating effect of running on vessel density (Genotype x Running; F (1,24) = 0.94, p=0.76, n.s., partial $\eta^2$= 0.04; figure 5.12). Furthermore, there was no clear difference in vessel density between running and non-running animals (Running; F (1,24) = 0.0, p=0.99, n.s., partial $\eta^2$<0.001) or between HD mice compared to controls (Genotype; F (1,24) =0.01, p = 0.99, n.s., partial $\eta^2$ < 0.001) (figure 5.12).

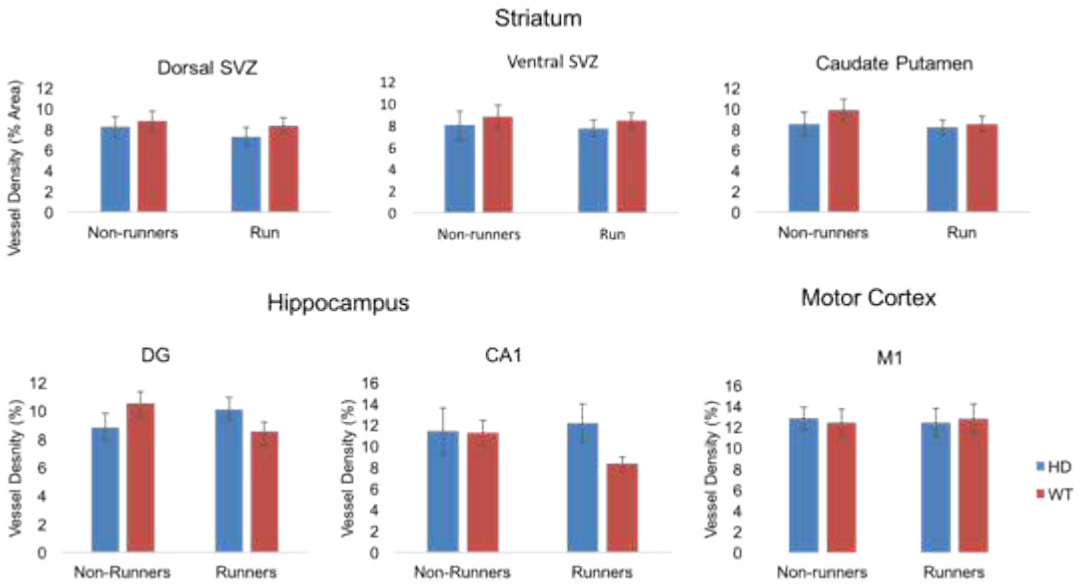


**Figure 5.12 Genotype differences in sub regional vessel density in runners vs non-runners.** Vessel density was quantified within the striatum, hippocampus and motor cortex by calculating the percentage area within each ROI that contained vessels stained by Tomato Lectin (*Lycopersicon esculentum*) using ImageJ. CP, Caudate Putamen; CA1, Cornu Ammonis of the hippocampus; DSVZ, Dorsal Sub-ventricular Zone; DG, Dentate Gyrus; M1, Primary motor cortex; VSVZ, Ventral Sub-ventricular Zone.

### *5.3.7.2. Between-region Analysis*

As no sub-regional differences were found, vessel density measurements were collapsed across each gross brain region and compared bilaterally for the striatum, hippocampus and motor cortex, with Running (running x non-running) as the between-subject variable to address whether exercise influenced vascular density differently between ROIs (Figure 5.13).

A main effect of ROI was observed whereby greater vessel density was observed in the motor cortex than the striatum or hippocampus (ROI; $F(2,26) = 22.7$, $p<0.001$, partial $\eta^2 = 0.50$). Each region differed significantly from the others (t-test; p values <0.01) where the motor cortex had the greatest vessel density, followed by the hippocampus then striatum. ROI differences in vessel density did not vary significantly with either running (ROI x Running; $F(2,46) = 0.031$, $p = 0.97$, n.s., partial $\eta^2 = 0.01$) or genotype (ROI x Genotype; $F(2, 46) = 1.01$, $p = 0.37$, n.s., partial

$\eta^2$= 0.04) or as a result of both running and genotype (ROI x Genotype X Running; F (2, 46) = 1.4, p = 0.26, n.s., partial $\eta^2$= 0.06).

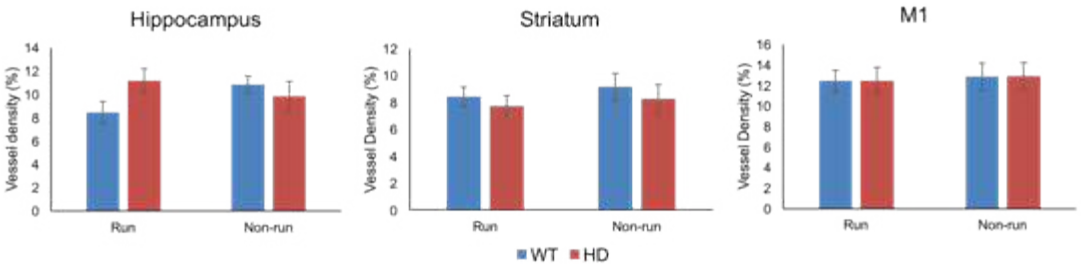


**Figure 5.13 Regional genotype differences in vessel density in runners compared to non-runners.** Gross ROI's were collapsed across sub-regions by averaging. Motor cortex had a greater vessel density than the striatum or hippocampus, with significantly lower vessel density within the striatum. This did not differ a result of running or genotype. Mean ± S.E.M.

### *5.3.7.3. The effects of a dose response of wheel running on blood vessel density*

Pearson's correlations were carried out on regions independently, to assess whether total number of rotations could predict blood vessel density in running HD and WT mice. As can be seen in figure 5.10, there was a generally positive dose-response relationship between running and vessel density in WT mice, across all regions (striatum (r (10) =0.39, p=0.26, n.s.); hippocampus (r (10) = 0.38, p=0.27); M1; (r (10) =0.27, p=0.46, n.s.). In HD mice, this relationship was not so clear. Whilst there was a weak positive relationship between running and vessel density in the motor cortex (r (7) =0.45, p=0.32, n.s.), running was negatively associated with vessel density in the striatum HD (r (7) = -0.54, p=0.27, n.s.), and absent within the hippocampus HD (r (7) =-0.21, p=0.65, n.s.).

### *5.3.7.4. Relationship between vascular density and CBF*

Pearson's correlation was used to assess whether the two vascular measurements, vascular density and CBF were related to one another. A negative trend was present in the hippocampus (r (29) = -0.3, p=0.06) that was not seen in the striatum (r (30) = 0.02, p=0.46) or motor cortex (r (28) = -0.01, p=0.48), such that increased vessel density was associated with a decline in level of CBF measured (figure 5.14).

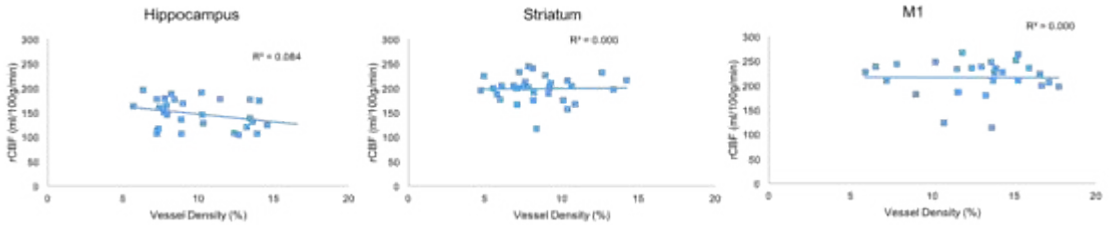


**Figure 5.14. Relationship between rCBF signal and vessel density.** A negative, but non-significant, relationship was observed within the hippocampus but no association was observed in the striatum or motor cortex (n.s).

### 5.3.8. mHTT inclusions

S830 was used to visualise cells expressing mHTT protein. Representative light microscope images of the progression of S830 immunoreactivity within the Q175/+ mouse striatum can be seen in Figure 5.15. All staining was negative in wild type animals.

S830 positive cells were marked throughout the striatum. Whilst nuclear inclusion bodies (IB's) were present in most diffusely stained cells, a proportion of positive cells showed diffuse staining throughout the cytoplasm without the presence of IBs (figure 5.15a). The total number of diffusely stained cells affected by mHTT within the striatum appeared greater in non-runners compared to runners but this was not significant (Running; $F(1,10) = 1.4$, $p=0.26$, n.s., partial $\eta^2= 0.12$; figure 5.15c), nor was there a significant interaction between Running X Cell Type; $F(1,10) = 0.2$, $p=0.71$, n.s., partial $\eta^2= 0.02$), such that there were generally more S830 positive cells in non-runners, for both IB positive and IB negative cell types.

S830 positive aggregates were also present in the neuropil (figure 5.15b) which did not appear to be located within the cell body, however number ($F(1,10) = 0.16$, $p=0.70$, n.s., partial $\eta^2= 0.02$) or inclusion size ($F(1,10) = 0.44$, $p= 0.52$, partial $\eta^2= 0.04$) did not differ significantly between running and non-running mice (figure 5.15d).

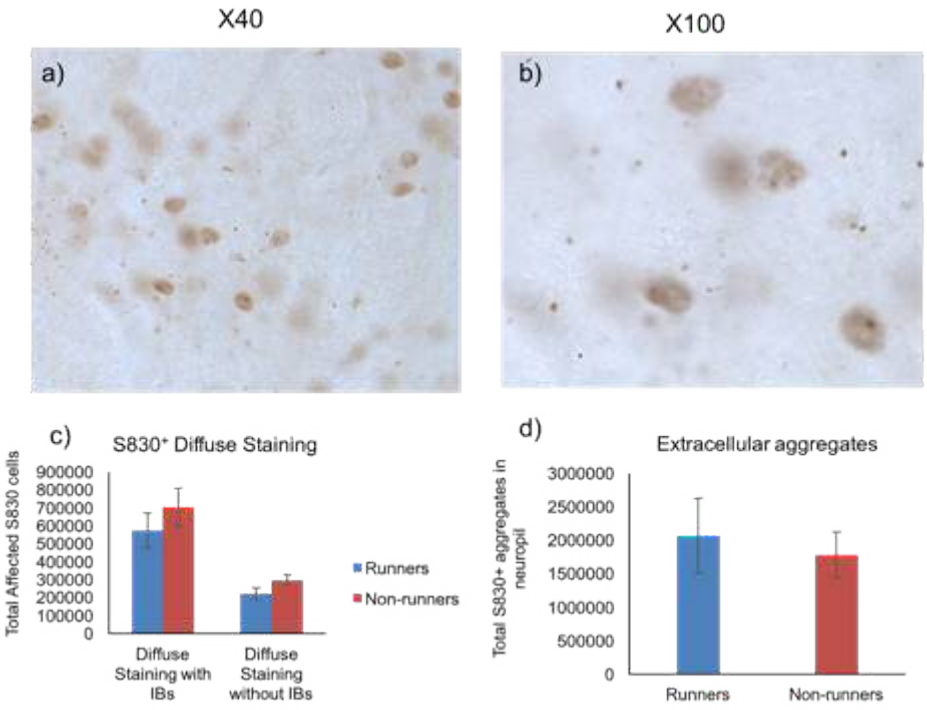


**Figure 5.15 S830 staining for mHTT expression.** Representative images from a single subject at a) x40 and b) x100 magnification. Diffuse staining was evident in all visible cells, with the majority also showing the presence of nuclear inclusion bodies (IBs). Total number of S830+ cells within the striatum (c) reveal a greater number of mHtt+ cells in the non-running mice compared to running mice for cells with IBs and cells without IBs, but this was not significant (p=0.26). Number of extracellular aggregates were also counted (d), but these did not differ significantly between groups. Mean ± S.E.M. mHtt (mutant huntingtin).

## 5.4. Discussion

### Key Findings

- Q175 mice displayed a hyperactive phenotype at 11 weeks. Running wheel activity and balance time-to-climb the balance beam was noticeably greater in Q175 mice but only the latter was significant.
- Genotype differences in CBF at baseline were not observed in Q175 mice at this early stage in the disease, although a non-significant trend suggests that CBF may be slightly higher in the striatum and motor cortex in HD mice.
- CBF did not differ significantly between groups following a 6-week voluntary running intervention.
- Blood vessel density did not increase significantly in the running group compared to the non-running group, although a trend for a dose response relationship between running and vessel density was observed.
- S830 diffuse staining for mHTT appeared lower in runners compared to non-runners, but runners had a greater number of extracellular aggregates, although this wasn't statistically significant.

In recent years, MRI has been used to characterise changes that occur within the HD brain, including changes in macro- and micro-structure. Whilst some effort has been made to assess the cerebrovascular changes that occur in patients, there has been little consensus in findings across studies, nor how cerebral blood flow (CBF) changes map onto the mechanisms occurring at a microscopic level. In the present study, we asked whether early changes in CBF can be detected at a 'pre-symptomatic' stage of the disease in a Q175 mouse model of HD, where MRI and histological techniques can be adopted. We asked whether alterations in CBF are related to vascular density, and whether 6-weeks of voluntary running, would influence outcome measures including resting CBF, vascular reactivity, vascular density, balance beam performance and expression of mHTT.

Results revealed no clear differences in cerebral blood flow in the Q175 mice at 11 weeks of age, prior to wheel exposure, although a hyperactive phenotype was evident. We did not observe any running related alterations in CBF following 6 weeks of wheel exposure, nor any clear differences between vascular density or balance beam performance, however a decrease in the number of diffuse mHTT expression in running mice, suggests that exercise may have been having a subtle effect on neuronal health that could not be detected in the cerebrovasculature at this early stage in the disease.

### 5.4.1. Behavioural Findings

Whilst it has been previously shown that exercise can improve some aspects of motor (Pang et al., 2006) and cognitive function (Harrison et al., 2013) in HD mouse models such as the R6/1 transgenic strain, the present study is the first to address the early effects of an exercise intervention in a less severe HD mouse model, the Q175 knock-in strain.

We initially set out to confirm that our HD cohort was not symptomatic at the commencement of testing. Although a thorough behavioural assessment was not feasible in the present study, voluntary wheel running and testing on the balance beam was administered, since this quick test has been found previously to be the most sensitive test of motor and cognitive function at ~3months of age in Q175 mice (Brooks et al, personal communication).

HD mice demonstrated a more hyperactive phenotype at 11 weeks than wild type control subjects, whereby they did more voluntary wheel running over the 6 weeks. Voluntary wheel running is not a typical assessment of hyperactivity, where other studies in Q175 mice have relied upon open field and climbing activity. Whereas other HD mouse models show hyperactivity in the early stage of the disease (Slow et al., 2003), this has not before been reported in the Q175 mouse model, where open field testing revealed no difference even at 2 months (Heikkinen et al., 2012).

A genotype difference in the time taken to climb the balance beam was observed, whereby HD mice climbed the beam faster than WT controls at baseline, but not after

6 weeks of wheel exposure. This too is likely to reflect a hyperactive phenotype in these animals that disappeared by 18 weeks of age. Previous research in the lab has reported a beneficial effect of exercise on the time taken for mice to turn at the end of the beam, which can be interpreted as an improvement in motor coordination (Harrison et al., 2013). The absence of any differences between HD and control animals in the time-to-turn parameter in the present experiment suggest that motor initiation and coordination was not impaired at 12 or 18 weeks in HD or WT in these Q175 mice. The absence of any differences on this task between runners and non-runners after 6 weeks of wheel exposure, therefore suggests that running did not modify cognitive or motor performance on this task at this early stage in the disease.

### 5.4.2. MRI Findings

Preclinical MRI is an under-utilised technique for assessing quantitative changes over time. The present study scanned asymptomatic subjects before and after 6-weeks of voluntary wheel running, using PASL MRI to noninvasively quantify baseline blood flow and vessel reactivity to a vasodilatory stimulus (5% $CO_{2.}$). This is the first time MRI has been used to assess blood flow in the Q175 model and in combination with their early age, such that this study was exploratory.

Previous MRI studies have observed elevations in blood volume in HD mouse models in the absence of motor dysfunction (Lin et al., 2013). However, differences in baseline cerebral blood *flow* have not been addressed. In this study, Q175 mice had a slightly higher baseline CBF at baseline (age 11 weeks) in the striatum and motor cortex compared to WT animals but this difference was not statistically significant however, even after considering differences in physiological noise due to depth of anaesthesia. It was not known whether genotype related differences would be observed at this early time point in the disease, especially since behavioural differences are not robust at this age. However, an fMRI-CBV study in transgenic R6/2 mice has shown elevated CBV compared to WT controls preceding any overt behavioural phenotypes (Cepeda-Prado et al., 2012) in addition to findings from human studies of pre-symptomatic patients in which cerebrovascular function is altered (Wolf et al., 2011).

Follow up scans after 6 weeks of exercise showed a decrease in CBF over time that was present in both runners and non-runners. Whilst it is possible that this is due to environmental enrichment, it seems more likely to be due to a decline in CBF with age or because of extraneous variables such as scanner drift and physiological instability that differed over time, rather than due to the exercise intervention itself. CBF is known to decline with age (Lu et al., 2011), although 6-weeks is unlikely to yield such a vast decrease.

Dose response relationships were also explored whereby total running wheel activity was correlated with regional CBF values. It appears a generally positive relationship was present between running and CBF, except for an apparent decoupling in HD animals within the hippocampus, such that rCBF decreased in those that ran further. Whilst CBF is generally thought to increase with fitness, directionality of results here would support the relationship reported in Chapter 2, where CBF was negatively correlated with fitness. A dose response relationship between number of rotations and vessel density was seen within the striatum, which may suggest a beneficial effect of exercise in the striatum, where running may act to reduce the apparent elevation in vessel density that has previously been reported in HD mice (Drouin-Ouellet et al., 2015; Hsiao et al., 2015; Lin et al., 2013). Although we did not observe group differences it may be that amount of running is a more sensitive independent measure, although in our case our small sample size means that interpretation of correlational analyses should be treated with caution.

Results from the cerebrovascular reactivity measure are somewhat inconclusive. Cerebrovascular reactivity is thought to be a sensitive marker of neuronal health which is thought to precede changes in structure or even baseline blood flow (Glodzik et al., 2011). The present study utilised a 5% $CO_2$ challenge which is robustly used to induce a quantitative CBF change of up to 30% (Wells et al., 2014). A previous study in R6/2 mice, aged 7 weeks, showed an impaired vascular reactivity to a similar challenge which got worse with disease progression (Hsiao et al., 2015), with no difference between HD and WT animals at a comparably early disease stage. We did not see a consistent elevation in CBF under hypercapnic conditions, where several animals showed a decrease in blood flow following gas switching to $CO_2$. Reactivity was highest in the motor cortex, with increases in CBF reaching

approximately 10%, however much lower values of <5% in the striatum and hippocampus suggest that the signal was not being adequately detected. A single TI of 1500ms was used in the present study as this was determined through piloting to yield the highest tissue perfusion signal and is in line with what has been used previously in mouse models of neurodegeneration (Wells et al., 2014). A caveat of single TI imaging is that SNR is lower, where T1 must be assumed and may underestimate the tissue perfusion signal, yielding lower CBF estimates. Nonetheless, we would still expect to see an increase in CBF during each of the challenges. With the experimental apparatus available, we were unable to measure the end-tidal gases being exhaled by our subjects, such that it was not clear how much gas was being breathed-in. Simultaneous pulse oximetry would have allowed us to measure blood gases, however this was not possible in the present study and we, like others, had to assume that mice were breathing in the air mixture as and when it was switched. Alterations in physiological parameters including respiration and heart rate following $CO_2$ switching, however, mean that we could assume that they were breathing the desired concentrations. Beyond piloting, this is the first time that this single TI method has been used within the University and as such results should be treated with caution. Further technical optimisation is required before this can be interpreted as a biomarker of cerebrovascular health as others have done.

Few MRI studies measure CBF in the diseased mouse brain, partly due to the low signal to noise ratio and the scarcity of preclinical scanners. Those that do, tend to rely on the use of dynamic contrast enhanced (DCE) MRI to exogenously increase contrast in the tissue as blood flows through the brain. DCE-MRI can also be used to estimate CBV, which is an interesting measure which has been related to vessel density (Drouin-Ouellet et al., 2015; Lin et al., 2013). ASL makes use of an endogenous signal through magnetically labelling blood, and is related to local tissue perfusion, rather than global blood volume. ASL therefore provides information about the metabolic and neuronal changes that are taking place at the level of the capillaries. Were this technique optimised more fully, it would be preferable to DCE imaging since it is non-invasive, repeatable, allows for longer scan times and does not interact with pharmacological or behavioural interventions that may be assessed. Further still, reliance on a contrast agent for measuring signal, assumed that blood brain barrier permeability is equal among subjects (Sourbron et al., 2009), however

evidence suggests that the blood-brain barrier is impaired in HD and this technique should therefore be used carefully (Drouin-Ouellet et al., 2015).

### 5.4.3. Vessel Density

Increased vessel density within the striatum and cortex has been reported in a number of HD mouse models at advanced stages of disease progression (Cisbani et al., 2013; Cisbani and Cicchetti, 2012; Franciosi et al., 2012; Lin et al., 2013). We carried out histology after 6 weeks of wheel running such that animals were aged 17-18 weeks at the time of fixation, when animals were still considered to be in the 'asymptomatic' phase. This experiment is the first to assess vessel density in an HD mouse model following an exercise intervention.

Density values were like that reported regionally in Chapter 3, with greatest density within the motor cortex. We first asked whether there was a cross-sectional difference in vessel density between HD and WT mice at this age. Following from our findings in Chapter 3 we expected to see a positive effect of running on vascular density in wild type animals. However, there was no evidence of a genotype effect within the striatum or the motor cortex, and this relationship was consistent regardless of whether animals were in the running or non-running condition. In the non-running group, WT mice seemed to have a slightly greater vessel density in the striatum although this was not significant. Interestingly, within the hippocampus, a region particularly known for running induced angiogenesis (van Praag et al., 1999b), running HD mice had increased vessel density compared to running WT controls. The difference between genotype may be explained by the increased levels of running by HD animals compared to WT because of their hyperactive phenotype. Alternatively, deficits in adult hippocampal neurogenesis have been reported in the R6/1 HD mouse model (Ransome and Hannan, 2013), such that angiogenesis in this region may be an early compensatory response by which to preserve neuronal health in that region prior to cognitive dysfunction. This would be consistent with human studies in which an increase in hippocampal blood flow has been observed in the hippocampus in pre-symptomatic HD patients (Wolf et al., 2011).

The present study was interested in the long-term effects of exercise on cerebrovasculature, with the hope of investigating its therapeutic value. In this study,

animals were culled after 5 days of exercise cessation. It is possible that vascular effects had returned to baseline by the time of fixation, which would suggest that the effects are not long-term. Indeed, evidence has shown previously that vessel density in the hippocampus can return to normal after just 24h of running cessation (Van der Borght et al., 2009). While our results from Chapter 3 suggest that differences in vascular density are observable even 5 days after running, it is possible that additional scanning and behavioural testing in this experiment introduced stress or enrichment that interfered with the vascular effects being measured.

In the present study we report vascular density, but due to time constraints were unable to measure other morphological measures, that have previously been shown to be altered in HD mouse models, including lumen diameter, vessel wall thickness and branching (Franciosi et al., 2012; Lin et al., 2013). Given that changes in vessel density were not clear in the present study, we hypothesised that it may be too early to detect changes in these parameters. Time constraints meant that we were unable to carry out investigations into the subtypes of vessel being measured. Tomato Lectin stains endothelial cells indiscriminately, and therefore stains all vessels. Evidence from Lin et al. (2013) observed a dichotomy between the type of blood vessels that are affected in HD, namely capillaries versus arteries by co-staining tissue with an antibody that binds to the smooth muscle actin in the vessel walls of arteries. They found that whilst microvascular density was increased in R6/2 HD mice, whilst the number of arteries were decreased, from an early disease stage, prior to behavioural impairment. Where vessel density is deemed to be both a positive hallmark of exercise, but a pathogenic feature of HD, it is important to understand the *type* of vessel being assessed. I hypothesis that it may be that the type of angiogenesis being measured because of exercise that is important. Whilst exercise may lead to increased arteriogenesis (the growth and widening of arteries), growth of immature capillaries in the case of HD would have the same net effect on measures of vascular density, both of which fall under the term ‘angiogenesis’. It is known that CBF is primarily influenced by increases in capillary density and vessels that lack smooth muscle. CBF should then be influenced more heavily by small vessels, whereas measures more typical measures reporting CBV, reflects a global difference in blood volume, regardless of vessel subtype.

A negative association was observed between hippocampal CBF and vessel density, suggestive of a decline in CBF with increased density. We can speculate that this may reflect an efficiency of cerebral perfusion, such that an increased capillary density could increase the rate of oxygen extraction in the tissue bed, leading to an apparent reduction in the CBF signal. Why this relationship was only observable in the hippocampus and not the cortex or striatum however, remains unclear.

### 5.4.4. Intracellular inclusions

S830 was used to visualise cells expressing mHTT in the striatum using well established methods within the lab (Bayram-Weston et al., 2016). Compared to runners, non-runners had a greater number of diffusely stained cells with and without IBs than runners, whilst runners demonstrated a greater number of extracellular aggregates, although neither of these results reached statistical significance.

Neuronal inclusions are typically deemed problematic for the cells in which they are located, causing significant changes in cell structure, trapping and interfering with the normal production of other proteins such as the CREB-binding protein (CRB), and eventually becoming toxic to the nerve cell. An array of evidence has shown that aggregates located in the nuclei (inclusion bodies; IBs) can block transcription, and other cellular processes such as neuronal axonal transport and impair major protein degradation pathways including the ubiquitin-proteasome system (UPS) and autophagy which under normal circumstances would acts to destroy affected cells (Kirkin et al., 2009). Albeit non-significant, running mice in this chapter had a reduction in the number of IBs compared to non-running mice, suggestive that exercise may ameliorate one or more of these processes, thereby reducing mHTT build up in the cell.

Whether IBs are a cause or a result of HD pathology is still not clear, and there is a large amount of evidence to suggest that IB formation may be protective (Arrasate and Finkbeiner, 2012). There is a mounting array of evidence to support the idea that aggregates do not cause HD, but reflect an attempt by cells to isolate toxic cell fragments, to prevent these fragments from causing too much harm . Slow et al. (2005) found that HD mice with frequent, widespread aggregates did not display any evidence of behavioural abnormality, neuronal dysfunction or degeneration,

indicating that HTT aggregation may not be sufficient to cause neurodegeneration. Further evidence has proposed that IB formation may be neuro*protective* since it reduces the amount of toxic diffuse mHTT throughout the cytoplasm, acting as a cellular 'coping mechanism' to temporarily cluster toxic fragments before they are degraded by the proteasome (Arrasate and Finkbeiner, 2012). Diffuse forms of polyQ-expanded HTT could in fact be the principal toxic species, and that their levels, rather than inclusion bodies themselves, govern neuronal survival (Arrasate et al., 2004). In their study, Cox proportional hazard analysis was used, and found that levels of diffuse HTT staining in neurons on the first day after transfection were correlated significantly and negatively with neuronal lifespan whereas IB load did not predict neuronal death.

In this chapter, diffuse cells were counted and grouped according to those with or without IBs, and it appeared that the largest difference between runners and non-runners, was in the number of diffuse cells *without* IBs. This could suggest that exercise acts by decreasing the amount of toxic mHTT in the cytoplasm. It was also found that runners displayed an elevated (but non-significant) number of protein aggregates that appeared to occur outside the cytoplasm, within the extracellular space. It is possible to speculate that exercise may protect against the damaging effects of mHTT through better cell clearance mechanisms(e.g. lysosomal clearance and autophagy), and could be a neuroprotective hallmark of voluntary running on mHTT expression.

Together these visual, but non-significant, trends hint towards an alteration in mHTT aggregation even after 6 weeks of running, whereby exercise may act 1) by reducing the number of mHTT affected cells by modulating Htt levels, and 2) increasing the level of protein aggregation (IBs) as a 'coping mechanism' by modulating the propensity to mis-fold and 3) improving mechanisms underlying clearance of toxic fragments leading to an elevation in extracellular protein aggregates. Whilst these are interesting speculations, interpreting these preliminary findings is premature and further work is needed to elucidate the cellular mechanisms underlying neuronal protein aggregation, in particular whether IBs are toxic, incidental, or part of an important coping response, and how exercise might work to mediate these processes.

A caveat of the present study, is that we were unable to co-localise the type of cells which were expressing mHTT. Recent evidence has shownt hat mHTT is expressed in all apsects of the neurovascular unit, including the basal membrane sheaths of small and large caliber vessels as well as the nuclei of cells imbedded within the basal membrane including endothelial cells, smooth muscle cells and perivascualar macrophages (Drouin-Ouellet et al., 2015) in R6/2 mice. Mutant HTT can impair mitochondrial integrity and/or trafficking (Chang et al., 2006) and induce oxidative stress, which may affect the physiology of cells forming the cerebral vasculature and influence small vessel growth. Exercise is known to reduce oxidative stress (Durrant et al., 2009), and may therefore protect vulnerable cells from mHTT accumulation. Further work would consider using fluorescence microscopy to co-localise mHTT markers with neurovascular markers such that the benefit of exercise on mHTT within specific cells known can be explored.

### 5.4.5. General Limitations

Small sample sizes in this study mean that results should be treated with caution and used as a stepping stone from which to probe these questions further. Whereas group and genotype differences were not significant, low power may have masked some interesting effects. The present study was limited by the number of individual running wheels, such that greater numbers were not feasible. Previous studies have used alternative designs such as group housing with a single wheel or by limiting the amount of daily running (Harrison et al., 2013), however we wished to measure individual running activity and limit fighting such that this was not an option.

This is the first time many of these questions have been asked of a Q175 mouse model and thus it was unknown what age we would expect to see changes in vascular function. We chose young adulthood so that our cohort could be compared to that used in Chapter 3 and because we wanted to investigate differences within an early time-window, prior to obvious cognitive and motor impairment, such that results could be analogous to those measured in our pre/early-symptomatic HD patients in Chapter 4. Whilst we had initially planned to repeat the same experiment in a cohort of Q175 littermates at 1 year of age, time-restrictions meant that this was not feasible. At 1 year, we would expect obvious cognitive and motor impairment in this mouse model (Heikkinen et al., 2012) and perhaps more exacerbated differences

in cerebrovascular function. This work is taking place, but cannot be presented within the scope of this thesis.

### 5.4.6. Conclusion

At 11-weeks of age, prior to voluntary wheel exposure, Q175 mice did not show elevations in cerebral blood flow or vessel density compared to wild-type mice as hypothesised. We conclude that this is likely due to the early stage of disease in which they were tested. A six-week running intervention did not yield clear differences in vessel density as expected according to our previous experiment in Chapter 3. A decline in CBF over time was seen in all animals, but was not influenced by genotype or running. Technical development of the cerebrovascular reactivity MRI pipeline is necessary before conclusions can be made regarding vascular function. Future work will repeat this study in an older Q175 cohort to confirm that vascular function is jeopardised in these animals and larger sample sizes will be adopted for statistical power.

# Chapter 6

# General Discussion

Cerebrovascular health is essential for efficient neuronal function. Identifying mediators of cerebrovascular health may provide us with therapeutic targets by which to delay cognitive and neuronal deterioration in healthy aging and disease. The aim of this thesis was to investigate the link between cardiorespiratory fitness and cerebrovascular health in young adulthood and in Huntington's disease, both in humans and in mice. The purpose of addressing this question in two species was to allow for bi-directional translation, in which insight into the human brain was motivation for translational research in mouse models whilst increased biological specificity gained from animal work could inform interpretation of current research and motivation for future research in humans.

## 6.1. Summary of findings

In Chapter 2, PASL was used to measure resting cerebral blood flow, arterial compliance and cerebrovascular reactivity in a sample of highly fit male adults, which are known markers of cerebrovascular health. The key finding from this study, was that cardiorespiratory fitness ( $O_{2MAX}$) was positively associated with arterial compliance. This is the first time the relationship between fitness and arterial compliance has been addressed using MRI measures, and is suggestive of improved cerebrovascular health even in young adulthood. The finding that $O_{2MAX}$ negatively predicted resting CBF was counter-intuitive, where higher CBF is typically associated with improved cerebrovascular health. In line with this, a negative trend was also observed between $O_{2MAX}$ and CVR, but this was not significant. Despite fitness-related differences in cerebrovascular parameters, there was no association between $O_{2MAX}$ and performance on cognitive tasks that have been previously associated with fitness in aged participants.

In Chapter 3, healthy young adult mice underwent a six-week running wheel intervention to replicate previous findings of exercise-induced angiogenesis, that might help explain the cerebrovascular differences observed in Chapter 2. Increased vessel density was observed in running mice, within all regions studied 5 days after running cessation. The greatest changes were seen in the striatum, a region that is rarely examined, but is largely involved in executive cognitive performance, and the hippocampus, known to decline in ageing. These findings corroborate and extend the existing literature whereby vascular changes appeared more stable than previously thought, lasting up to 5 days after exercise cessation.

In Chapter 4, I aimed to address whether exercise may be a clinically useful intervention in patients with Huntington's Disease. This is the first time an MRI study has addressed the relationship between cardiorespiratory fitness and the HD brain. It was found that resting CBF and CVR were generally lower in HD patients than controls, even when correcting for partial volume effects that are likely to be important in the atrophying HD brain. However, unlike previous studies, these differences were not significant. Disease burden and symptom severity was associated with a decrease in whole-brain CBF. However, elevated CBF in functionally relevant regions including the frontal cortex and thalamus was associated with worse disease outcomes. Fundamental to our aims was whether HD patients differed from controls in their response to higher cardiorespiratory fitness. $O_{2PEAK}$ was not associated with cognitive performance in controls or HD patients. $O_{2PEAK}$ did not appear to predict CBF or CVR across subjects, although negative trends were observed in a whole brain ROI, as in Chapter 2. An interaction in the left caudate was found in which $O_{2PEAK}$ predicted higher CBF in controls, but lower CBF in HD patients. Overall, these results do not provide clear support for the benefits of fitness in HD. The interaction observed in the caudate may suggest fitness is able to jeopardise cerebrovascular function, or even perhaps the existence of a compensatory response in a key region known to be particularly affected in HD.

In Chapter 5, the study performed in Chapter 3 was replicated in a transgenic Q175 HD mouse- line prior to onset of typical disease-related cognitive and behavioural impairments. This age was chosen to be analogous to pre-/early-symptomatic patients examined in Chapter 4. Behavioural, histological and PASL outcome

measures were used. No differences in CBF or CBF CVR were observed at baseline or after 6 weeks of wheel running between HD mice and controls. Vessel density was not elevated in running mice as was reported in Chapter 3, nor were there any clear genotype differences. The most intriguing effect was the observation that diffuse mHTT expression in the striatum was greater in non-running HD mice than controls, although this was not statistically significant. This is the first study to assess the benefits of exercise in an HD mouse model using MRI. However, it may be too early into the disease to detect cerebrovascular deficits, such that the benefits of exercise could not be observed.

## 6.2. Is physical activity related to improved cerebrovascular health in healthy young humans and mice?

It is suggested that aerobic fitness is predictive of better cerebrovascular health and reduced risk of cognitive decline. However, there has been little evidence to suggest whether these changes occur as early as young adulthood. Chapters 2 and 3 aimed to address this question in humans and mice respectively, providing promising evidence that improvements in cerebrovascular function *can* be detected early in the lifespan. Chapter 2 addressed this in humans, using a cross-sectional measure of aerobic fitness ( $O_{2MAX}$) as a surrogate measure, where causality following an exercise intervention was not assessed. Chapter 3 addressed this in mice, by investigating vessel density in mice who had undergone 6 weeks of voluntary wheel running.

A clear benefit to cerebrovascular health was observed in Chapter 2, whereby fitter individuals appeared to have better arterial compliance. The importance of arteries in protecting the capillary bed by buffering pulsatile blood arising from the heart, has been proposed previously (Poels et al., 2012), and systemic arterial compliance has been linked to cognitive function (Davenport et al., 2012). Here we demonstrate this link for the first time in *cerebral* arteries. Evidence for early cerebrovascular changes in aerobically fit adults, provides a promising mechanism by which physical activity can mediate cerebral health and preserve cognition later in life. Physical training is thought to drive adaptation and arterial remodelling of the endothelial and smooth

muscle cells via changes in hemodynamic and shear stress patterns (Newcomer et al., 2011). In the absence of time, it was not possible to probe this mechanism further in the healthy young mice in Chapter 3. Planned work to extend these results will examine expression of smooth muscle actin in the major cerebral arteries in the mouse brain, to validate the link between arterial remodelling of smooth muscle cells because of exercise. This would help to shed light on the mechanisms underpinning elevated arterial compliance observed in Chapter 2.

It was also found that vessel density was increased in young adult mice. This can also be taken as evidence that exercise can improve cerebrovascular health. This finding corroborates previous studies and supports literature in humans that have identified an increase in CBF with fitness and following an exercise intervention. Vessel density is thought to reflect angiogenesis which, when new vessels function properly, provides greater surface area from which oxygen and nutrients can perfuse into the tissue. How this corresponds to the findings in Chapter 2, that CBF was lower in fitter subjects is not clear.

In Chapter 2, the findings that CBF was reduced in fitter subjects was unexpected. Where CBF (MCAv) and CVR are typically thought to increase with fitness (Bailey et al., 2013), reductions in these measures are usually thought to be a pathological biomarker. In the present context, it is unlikely that this is a pathological process and the possibility that this may in fact be an *adaptive* process is discussed. This study utilised a cohort with an unusually high range of cardiorespiratory fitness, such that altered vascular response, may be protective to those that engage in physical activity regularly. Possible adaptive mechanisms discussed, include increased efficiency of oxygen extraction in these highly-trained subjects. Work within the lab provides preliminary evidence for a link between fitness and enhanced oxygen extraction and planned work will extend this investigation in a wider cohort.

Whether the findings of reduced CBF in Chapter 2 can be reconciled with the increased angiogenesis reported in Chapter 3 is unknown. Typically, angiogenesis has been associated with a concomitant elevation in cerebral blood volume in preclinical studies (Swain et al., 2003), although it has been observed that the

relationship between angiogenesis and cerebral blood flow are not always tightly coupled (Vogel et al., 2004).

## 6.3. Is physical activity related to improved cerebrovascular health in pre-/early-symptomatic HD patients and in transgenic HD mice?

Chapter 4 is the first PASL study to address the benefits of fitness on cerebrovascular health in the HD brain, whilst Chapter 5 is the first study to address the benefits of exercise on cerebrovascular health in an HD mouse model. However, no convincing evidence was observed by which to claim any beneficial effects of exercise on cerebrovascular health in the preHD stages examined.

### *6.3.1. Fitness might alter CBF in the caudate nucleus differently for patients and controls.*

In Chapter 4, interesting differences were found between HD patients and controls in aspects of cognition, mood and differences in perfusion, however, the primary interest was in the moderating effect of cardiorespiratory fitness. The most interesting observation was in the left caudate nucleus. Firstly, it was observed that this region showed a reduction in resting CBF relative to controls, although this only approached statistical significance. Secondly, a group interaction with fitness in the same region unveiled an interesting pattern of results, whereby $O_{2MAX}$ predicated a higher CBF in the controls, but a lower CBF in HD patients. Of course, this is a cross-sectional study, such that CBF differences cannot reflect 'change' as a result of HD, however this relationship was deemed worthy of further exploration.

Unlike the highly fit subjects studied in Chapter 2, an observed elevation in CBF with fitness is in line with what has been reported previously in the general population (Ainslie et al., 2008). Conversely, what causes hypoperfusion in the caudate in HD because of exercise is less clear and motivated further investigation in Chapter 5. Vessel density in an HD mouse model was measured to assess whether this CBF interaction in the patient brain could be explained by a reduction in vessel density. Although caudate vessel density appeared lower in HD mice than controls, this was not significant at baseline and did not appear to interact with running.

Metabolic function has been shown to be reduced in Huntington's disease, where mitochondrial dysfunction and glucose metabolism have been observed in the caudate (Browne et al., 1997). It is possible that people with HD do not benefit from exercise in the same way as controls, where metabolic function is already under stress from the disease, leading to hypoperfusion in fitter subjects. This is in line with previous reports of the negative effects of exercise in HD mice (Potter et al., 2010). These results are only speculative and it is acknowledged that this relationship is not causal and may mask the same underlying factor which is that HD severity is associated with lower fitness levels and reduced CBF.

### *6.3.2. Running wheel activity does not influence cerebrovascular health in early-stage HD mice or wild-type controls.*

Contrary to the findings in Chapter 4, running Q175 mice in Chapter 5 did not show any differences in CBF, CVR or angiogenesis compared to runners following 6 weeks of wheel exposure. It was hypothesised that diseased mice would have higher vessel density than wild-type controls, which would be reflected in a higher level of resting CBF, although this difference was not significant in this study. Because this is the first time such a study has been performed, we were unsure whether exercise would increase or decrease vessel density or CBF. No differences were seen between runners and non-runners on any of the measures assessed, and this did not interact with group. It is possible that our measures were at ceiling levels and thus the running intervention did not yield an effect on the observed cerebrovascular measures in this cohort. Whilst the benefits of exercise were not detected in this study, neither were there any negative effects of exercise on cerebrovascular health.

Homozygous Q175 mice were adopted as the model of interest. This transgenic model is known to have a relatively long disease progression, which was of interest in this study where a longitudinal aspect was initially planned. Assessment at later time-points was not feasible and it is possible, therefore, that mice were too far from disease onset such that differences in CBF, CVR or angiogenesis did not differ from wild-type controls. Planned work will repeat this experiment in subjects from the same litter at >1 year of age, where behavioural symptoms are evident, to address the benefits of exercise in these animals. It is unknown whether hypoperfusion is

evident in HD mice prior to symptom onset although reports have shown that heterozygous Q175 mice display significant atrophy in the striatum and cortex by 4 months (Heikkinen et al., 2012) and behavioural differences by 12 weeks (Brooks et al; unpublished). Future work would consider repeating the first scan closer to symptom onset where the efficacy of exercise may be observed in the behavioural and cerebrovascular outcome measures by the second time-point. BrdU analysis will also be carried out to investigate differences in endothelial growth that can be directly attributed to the running intervention.

## 6.4. Can PASL measures be considered reliable cerebrovascular biomarkers in humans and in mice?

Advances in arterial spin labelling have come on greatly over the last 20 years and there are a variety of labelling sequences and acquisition strategies that offer different benefits. A number of well validated, but also novel measurements were adopted to measure cerebrovascular health in the present thesis. A biomarker can be defined as a characteristic by which a particular pathological or physiological process/disease can be identified. In this respect, a reliable MRI biomarker is one that has been well validated and taps into a particular process characteristic of cerebrovascular health. The measurements used in this thesis will be discussed in turn with regard to the above definition.

### *6.4.1. Arterial Compliance*

Measurement of arterial compliance in Chapter 2 employed short inversion time PASL to map arterial blood volume at different phases of the cardiac cycle. This is a recently developed technique such that, at time of scanning, this was the second study to apply it for measuring cerebrovascular health. This technique has since been validated by a number of studies (Warnert et al., 2015a, 2015b) and ongoing work is validating this measure in the Huntington's Disease cohort studied here, where time did not permit its inclusion in this thesis.

Regarding the specificity of the measurement, the direction of the results observed using this measure so far, correspond to physiologically meaningful changes that

would be hypothesised in the groups tested. Compliance is thought to increase in systemic arteries with physical activity (Tanaka et al., 1998), to play an important role in increasing cerebrovascular resistance (Warnert et al., 2015a), and to mediate arterial remodelling in response to altered patterns of shear stress (Newcomer et al., 2011). These mechanisms work to prevent capillary damage by increasing the capability to buffer pulsatile flow arising from the heart. Further validation is needed in aged and diseased patients; however, this measure can be considered a promising cerebrovascular biomarker.

### *6.4.2. Resting CBF*

CBF can be influenced by a number of underlying factors and as such, does not provide definitive information about a particular pathological process. CBF appears to be lower in young healthy athletes and also in Huntington's Disease. Whether a reduction in CBF is pathological or adaptive is not clear, and may depend upon disease/fitness status in a complex way. As such, resting CBF may not be a good biomarker of disease, but rather a surrogate marker of vascular function.

Resting CBF in humans was acquired and analysed using well established methods within the lab, using a multi-inversion time spiral readout gradient echo sequence and FSL BASIL for CBF quantification (Chappell et al., 2009). The same methods were used in both human chapters, however, the number and spacing of inversion times in Chapter 4 was chosen to minimise scan time for patients. As a result, it is possible that SNR may be slightly lower in Chapter 4 than Chapter 2, where fewer repetitions meant averaging of the signal may have been noisier. Nonetheless, all perfusion values were within the range reported elsewhere. Inflated PVC corrected values were also in the expected range (Chappell et al., 2011) such that resting CBF values were considered reliable in the human studies.

Preclinical imaging of resting CBF was acquired using a FAIR EPI sequence (Kim, 1995). This is the default sequence in Bruker's ParaVision 5 software and has been validated in mice (Leithner et al., 2010). This sequence used a total of 13 TIs to model T1 relaxation, which is more robust than the 5 TIs used in the FAIR-EPI sequence used to assess CBF in the R6/2 mice (Hsiao et al., 2015). A repeatability study conducted prior to scanning, tested repeatability of CBF estimates on separate

days (data not reported). This pilot study also explored whether CBF estimates were affected by the number of TIs used to model T1 relaxation. Analysis was performed on 24 (recommended by Bruker), 12, or 9 inversion times. Coefficients of variability for between-subject scans were 0.2-21.8%, which is higher than the variability estimates expected between scans in humans (~3.5%; Tancredi et al., 2015). However, between subject differences were found to vary greatly with depth of anaesthesia. It was also found that a CBF model with 12 TIs did not differ from CBF estimates modelled with 24TIs. In reaction to these findings, scan time was reduced in Chapter 5 by measuring 13 TI's with an emphasis on controlling variability in anaesthesia between scans to maximise within-subject reliability. Nonetheless, where anaesthesia is a vasodilator, reliability of ASL in preclinical scanning is an inherent challenge and it is not known whether the HD mouse model would respond differently to wild-type animals. Further validation of this sequence is needed is healthy and diseased mice.

### *6.4.3. Cerebrovascular reactivity*

CVR is thought to be a more sensitive marker of cerebrovascular health than resting CBF. Regulation of CBF in response to vasoactive stimuli, reflects efficiency of the vasculature, and implicates a number of well-established mechanisms. Where CVR is jeopardised, quantifying CVR with MRI may be useful for tracking disease progression and targeting treatments and further research. Nonetheless, the biological specificity of this method remains limited.

In Chapters' 2 and 4, cerebrovascular reactivity was measured in response to a breath-hold task. Whilst the breath-hold is not the most robust challenge for manipulating arterial $CO_2$ (Tancredi and Hoge, 2013), we deemed it worthy of investigation in patients due to its ease of use by patients. Chapter 2 measured reactivity of the BOLD response in addition to the CBF response which has notoriously low SNR, but contains more specific information regarding the origin of the signal. Established methods were used (Bright and Murphy, 2013) and it was found that the BOLD and CBF CVR responses were closely related, despite increased noise in the CBF time-series. Because CVR measurements aligned with the findings of previous studies, it was deemed a reliable measure for use in HD patients in Chapter 4. In this study, absolute CBF CVR but not BOLD CVR was

reported. Data from this study was not what was expected, whereby several subjects showed a negative CBF response, particularly in the HD group. These findings are discussed in more depth in Chapter 4, however it does a raise questions as to the reliability of the data. Whilst it would be expected that HD patients have lower CBF than controls (Hsiao et al., 2015), ongoing work is being carried out to establish whether CBF CVR in response to a breath-hold challenge is a reliable biomarker of cerebrovascular health.

In Chapter 5, relative CBF change was measured in response to a hypercapnic challenge (5% $CO_2$). FAIR-EPI parameters adopted were similar to those used previously (Wells et al., 2014), however this is the first time this sequence or a gas challenge has been used within Cardiff University and, as such, has not been previously validated. A negative CVR was also observed in many animal subjects and overall CVR appeared elevated in HD mice and reduced in wild-type animals. This is contrary to the findings observed in HD patients in Chapter 4 or previous scientific reports (Hsiao et al., 2015). Due to time limitations, further exploration of the data was not performed, such that CVR results in Chapter 5 should be treated as preliminary.

## 6.5. Can exercise be reliably recommended as a prophylactic to deterioration of cognitive function?

The present studies provide little evidence to support the link between exercise and improved cognitive function. This is not to say that exercise does not yield benefits in mood and cognition, but that this could not be detected in the present studies.

Evidence in rodent models have reported improvements on tasks including Pattern Separation (Creer et al., 2010a), Morris Water Maze (van Praag et al., 1999; spatial working memory), T-maze (Harrison et al., 2013; procedural and reversal learning); Forced Swim Test (Duman et al., 2009; depressive symtoms), Wisconsin General Testing Apparatus (Rhyu et al., 2010; rule learning), Radial Arm Maze (Anderson et al., 2000; spatial memory) and Passive Avoidance (Radák et al., 2001; Long-term memory). Cognitive function was not measured in the rodent studies within this

thesis, in part due to the long-period of training necessary for complex behavioural assessment on operant tasks.

As described in Chapter 2, there is little available evidence in the literature to support a link between fitness and/or exercise and cognition in young adults, possibly because cognitive performance is at ceiling level. The largest effect sizes are in elderly participants, where lifelong exercise is associated with better cognitive performance on tasks of executive functioning (Colcombe and Kramer, 2003). Whether exercise is beneficial earlier in the lifespan is still a relevant question, where detection of cognitive deficits later in life may be too late to begin exercising. It is likely that many of the cognitive tests, including those in Chapter 2, are not sensitive enough to detect the small effect sizes expected as a result of exercise. Visual trends were observed between $VO_{2PEAK}$ and cognitive performance in HD patients, on a number of the cognitive tasks, and these relationships appeared stronger than in controls. It could be that because cognitive performance is not at ceiling levels in patients, the influence of mediators such as fitness become more apparent. Although interactions between group and fitness were not significant in these patients, it is possible that this relationship would become stronger as the disease progresses.

Research has proposed that maximal gains come from a combination of exercise and brain 'training' in order to gain the cognitive benefits from exercise (Lauenroth et al., 2016). Future exercise interventions within the Cardiff HD Centre will consider incorporate brain training exercises to maximise the functional benefits. Development of more sensitive measures of cognitive function are needed before exercise can be reliably recommended as a prophylactic to deterioration of cognitive function.

## 6.6. Practical considerations for exercise prescription in people with Huntington's Disease

The view that exercise is good for the body and the mind is by no means novel. Despite the vast amount of research demonstrating the importance of physical activity, 20million UK adults are classified as physically inactive according to the 2017 report by the British Heart Foundation. Even healthy gene negative individuals

struggle to meet the recommended goal of 150 minutes of moderate intensity exercise per week, so it is important to consider how best to encourage uptake of physical activity in HD patients where barriers may be even more severe.

### *6.6.1. Exercise in HD*

Just a few of the specific challenges that should be considered when recommending exercise to people with HD include, low mood, apathy, self-confidence, degree of mobility, difficulty with balance, level of supervision and risk of falls. It is also worth noting that it is unknown whether vigorous exercise is beneficial in people, where metabolic and immune function may already be compromised by the disease. For example, in the RCT conducted by Quinn et al (2016a), HD participants who a supported multi-modal exercise programme had substantial weight loss when assessed at 13 weeks, which is not ideal in this population where there is a propensity for weight loss as the disease progresses. With these challenges in mind it is unlikely that a 'one size fits all' approach would work, and that recommended activity should be tailored according to the clinical presentation of the individual. Findings from the RCT from Quinn et al (2016a) demonstrated that people with HD could exercise safely in an aerobic zone and conduct progressive strengthening exercises, even in the presence of advanced motor impairments. In their study, retention was attributed to the support structure in which a trainer was available to monitor that the program was being conducted, to provide support and encouragement and to facilitate adherence.

A number of referral schemes are available, which run active groups for people suffering (or have suffered) from a wide range of conditions. Whilst such schemes are a fantastic idea, symptomatic HD patients may be prevented from tapping into these resources without the assistance of a carer or trained physiotherapist. A recent study at Cardiff assessed the feasibility and uptake of a fortnightly HD walking group. Patient feedback from this study revealed that patients felt uncomfortable taking part in organised activities that might draw attention to their disease, and that they had trouble committing to a time and a place (personal communication with Una Jones from Active HD). Continued efforts are needed to 1) normalise public attitudes towards patients with neurological conditions such as HD, so that they are not deterred from attending group exercise sessions and 2) provide specific training to

exercise instructors such that exercises may be tailored to suit individual needs based upon an understanding of disease features.

Recommending physical activity early in life is preferential, regardless of gene status, as the life-long effects are likely to be cumulative. In the case of HD, introducing exercise into their daily routine early in the disease process may have several additional advantages. For example, where perseverative symptoms are typical as the disease progresses, introducing physical activity into a patient's routine later in the disease may be particularly challenging, and require more motivation from the carer. Introducing physical activity earlier in life, before symptoms manifest, may have better uptake, provide additional benefits and have greater longevity in terms of persevering with the exercise as the disease progresses. There remains a lack of clear-cut research in humans that demonstrates the benefits of exercise, although evidence from this study found that self-reported quality of life was higher in fitter subjects. Feedback from patients studied in Chapter 4 suggested that they were reluctant to introduce additional complexity into their lives as they did not believe it would have much direct benefit on their physical prognosis. Longitudinal studies in pre-symptomatic patients are warranted to explore the lasting benefits of exercising and combined with sensitive outcome measures so that the benefits can be captured and conveyed to patients in a convincing way.

### *6.6.2. Exercise Mimetics*

Where exercise prescription in HD is inherently challenging, pharmacological compounds that mimic systemic and central effects of exercise, 'exercise mimetics' is appealing. *In vivo* and *in vitro* research has identified metabolic networks of transcriptional activators and interconnected enzymes known to be implicated in muscle metabolism such as the AMPK-SIRT1-PGC-1$\alpha$ pathway in response to exercise (Guerrieri et al., 2017). The most well-known of these compounds are metformin, GW501516 and AICAR (5-Aminoimidazole-4-carboxa-mide ribonucleotide). AICAR is the analog of AMP and intermediate metabolite of the purine synthesis pathway and has been found to affect many organs and regulate a range of metabolic processes by replicating some of the effects of exercise e.g. increasing glucose transporter type-4 (GLUT-4), hexokinase activity, resting glycogen content and muscle mitochondria numbers (Lauritzen et al., 2013; Sánchez

et al., 2013). AICAR has also reported to increase angiogenesis and vascularization by inducing VEGFa expression in muscle, in a similar way to exercise (Ouchi et al., 2005). It is currently unclear however, to what extent this compound can cross the blood brain barrier. Short-term but not long-term treatment has been found to increase BDNF levels, neuronal proliferation and spatial memory in the dentate gyrus (Kobilo et al., 2011), but this effect was not stable after 14 days where AICAR appears to upregulate expression of apoptotic genes and inflammatory cytokine interleukin-1β (Guerrieri and van Praag, 2015). Dietary supplements such as resveratrol and (-) epicatechin (van Praag et al., 2007) have found similar benefits to exercise in mice with evidence demonstrating improved spatial memory, increased dentate granule cell spine density, neurogenesis, hippocampal vascularization, neuroprotection following ischemia and expression of genes implicated in synaptic plasticity (Guerrieri et al., 2017).

A mounting array of evidence has shown the benefits of resveratrol in *in vitro* and *in vivo* models of Huntington's Disease, in which function of the principal metabolic regulator, peroxisome proliferator-activated receptor gamma coactivator-1α (PGC-1α), is significantly impaired. Resveratrol has been shown to rescue mutant polyglutamine–specific cell death in cultured striatal neuronal cells derived from Hdh Q111 knock-in mice via Sir2 activation (Parker et al., 2005). Furthermore, treatment with Resveratrol for 45 days (5days/week) in N171-82Q HD transgenic HD mice, yielded a significant elevation of PGC-1α and NRF-1 mRNA expression was reported in the cortex, but not striatum, nor was it related to striatal atrophy or motor function (Ho et al., 2010). Together, an increasing understanding of the functioning of metabolic pathways implicated in both Huntington's disease and physical exercise, appear to be converging on similar pharmacological targets. Drugs that mimic systemic and central effects of exercise are promising as they remove multiple challenges associated with exercising, however care should be taken, since the cacophony of benefits associated by exercise may not be recreated by a pill alone. The effects of exercise-mimetics on central versus peripheral systems is currently limiting the viability of these pharmacological alternatives (Guerrieri et al., 2017) and the effects of such compounds on cerebrovascular function is needed.

## 6.7. Theoretical and practical considerations.

### *6.7.1. Sample size*

Neuroimaging studies are costly, time-consuming and strict criteria exist for participant inclusion. It is acknowledged that the sample sizes adopted in all the studies presented in this thesis are small. Where correlational analysis and multifactorial designs are used, it is possible that some of the results in this study may be hampered by this low statistical power. Nonetheless, these practical challenges were unavoidable given the timescale and budget. Participants in Chapter 2 were recruited from an existing cohort at the University of South Wales, of which only 11 participants were eligible to take part in the follow up MRI study at Cardiff University and it was not possible to extend the study. Recruitment of participants in Chapter 4, was impressive given the number of exclusion criteria present in this study and the time commitment required of these patients, however further recruitment was prevented due to closure of the MRI scanner. Animal studies were also limited in power due to limited number of running wheels, housing costs and longitudinal MRI costs.

### *6.7.2. Assessment of cardiorespiratory fitness*

$O_{2MAX}$ is currently considered to be the 'gold-standard' measure of cardiorespiratory fitness, however a few practical issues were raised in the present study. Future work should consider using a semi-recumbent cycle ergometer to maximise safety in those who have balance issues. As mentioned in Chapter 4, participants struggled to push through the steep load transitions, where it appeared that muscle fatigue and/or motivation caused them to terminate exercise before they reached their aerobic threshold. Previous studies have used predictive $O_{2MAX}$ tests where symptomatic patients were unable to complete a full protocol (Quinn et al., 2016b). The present study included all subjects, regardless of whether they completed a valid test, reporting the peak $O_2$ at the point of subjective exhaustion since exclusion of patients who did not complete a valid test would have resulted in even lower power. It is possible that the reliability of this measure may have influenced the results of this study, however in the absence of a strong alternative, $O_{2PEAK}$ was the most informative available measure of cardiorespiratory fitness.

### 6.7.3. Correction of partial volume effects

Atrophy was visible in many HD patients such that a corrective step was included in our analysis to minimise partial volume effects. Other ASL studies in HD have used corrective measures, by spatial erosion of subcortical masks or by including cortical thickness as a co-variate (Chen et al., 2012), however this is not a robust way to remove intra-voxel partial-volume effects. The current measure used a Bayesian approach which employs a probabilistic kinetic curve analysis, using adaptive spatial priors and has therefore been found to preserve spatial detail better than the more standard linear regression approach (Chappell et al., 2011). Inflation of CBF estimates in HD subjects than controls was found, suggesting that PVC should be recommended as a critical step in all ASL analysis, especially in those where atrophy is hypothesised. Cortical thickness and volumetric differences were not reported in this thesis, however planned analysis is underway to assess atrophy and will also cross-reference these volumetric differences with the degree of partial volume correction observed.

### 6.7.4. Cross-species translation

Translation between the human and rodent findings in this thesis is a challenge and it is acknowledged that very different designs were used to probe the question of physical activity. It is possible to measure $O_{2MAX}$ in rodents , using calorimetry in metabolic treadmill chambers (Schefer and Talan, 1996), and studies have yielded similar age-related alterations in $O_{2MAX}$ as human studies. This requires a complex setup and is considered extremely stressful for the animal, which in this study would likely interfere with our outcome measurements, particularly in HD mice. Alternatively, an interventional design could have been used in the human study to assess the effects of a long-term exercise intervention. Such interventions are time consuming and costly, such that it was deemed sensible to assess the relationship with fitness in a cross-sectional design as a proof of principle study prior to developing an intervention. It is also unknown how long an intervention would need to be in order to detect cerebral benefits, and study retention over long periods could be extremely challenging in HD patients. Plans are currently ongoing to include a neuroimaging arm into an exercise randomised controlled trial in HD patients.

In planning these experiments, age of the rodent cohorts was chosen to be as analogous as possible to the human cohorts. A young-adult age (8 weeks) was chosen in Chapter 3 and Chapter 5, albeit slightly older in Chapter 5 (10 weeks). Time of onset in the HD condition is dependent upon several factors, particularly CAG repeat length, which can influence the age of disease onset. Pre-symptomatic patients varied in age, whereas all mice were the same age and expected to have a similar age of disease onset. Because the human condition is so heterogeneous, translating disease stage across species is a practical challenge and should be considered carefully in future studies.

## 6.8. Concluding Remarks

The research undertaken in this thesis explored the benefits of physical activity on markers of cerebrovascular health in both humans and mice. Clinical application of exercise as a therapeutic was explored by addressing this question in Huntington's Disease, both in HD patients and in a transgenic HD mouse model. It is not known at exactly what stage cerebrovascular function becomes jeopardised in Huntington's disease. However, evidence in young healthy adult subjects suggests that the benefits of exercise on cerebrovascular health can begin early in life. Whether these benefits of exercise translate to improved cerebrovascular health in HD, however, remains unknown. Future work should aim to incorporate ASL imaging into longitudinal exercise studies in HD patients, such that its efficacy for identifying the progression of cerebrovascular decline can be explored in the same subjects. Where thorough fitness tests may not be feasible in HD, it is also recommended that a self-reported measure of physical activity, or activity monitoring, be assessed in all neuroimaging studies such that the importance of physical activity as a covariate can be explored. The findings in the present thesis attempt to bridge the gap between preclinical and clinical understanding of the importance of exercise in healthy subjects and in those with HD. Addressing the complex mechanisms in preclinical models is essential in unpacking the relevance of changes seen in humans and the emphasis on collaboration between preclinical and clinical imaging centres should be promoted.

# References

Aaslid, R., Lindegaard, K.F., Sorteberg, W., Nornes, H., 1989. Cerebral autoregulation dynamics in humans. Stroke. 20, 45–52. doi:10.1161/01.STR.20.1.45

Aguiar, A.S., Speck, A.E., Prediger, R.D.S., Kapczinski, F., Pinho, R.A., 2008. Downhill training upregulates mice hippocampal and striatal brain-derived neurotrophic factor levels. J. Neural Transm. 115, 1251–1255. doi:10.1007/s00702-008-0071-2

Agulhon, C., Petravicz, J., McMullen, A.B., Sweger, E.J., Minton, S.K., Taves, S.R., Casper, K.B., Fiacco, T.A., McCarthy, K.D., 2008. What Is the Role of Astrocyte Calcium in Neurophysiology? Neuron 59, 932–946. doi:10.1016/j.neuron.2008.09.004

Ainslie, P.N., Ashmead, J.C., Ide, K., Morgan, B.J., Poulin, M.J., 2005. Differential responses to CO2 and sympathetic stimulation in the cerebral and femoral circulations in humans. J. Physiol. 566, 613–624. doi:10.1113/jphysiol.2005.087320

Ainslie, P.N., Cotter, J.D., George, K.P., Lucas, S., Murrell, C., Shave, R., Thomas, K.N., Williams, M.J. a, Atkinson, G., 2008. Elevation in cerebral blood flow velocity with aerobic fitness throughout healthy human ageing. J. Physiol. 586, 4005–10. doi:10.1113/jphysiol.2008.158279

Ainslie, P.N., Hoiland, R.L., 2014. Transcranial Doppler ultrasound: Valid, invalid, or both? J. Appl. Physiol. 117, 1081–1083. doi:10.1152/japplphysiol.00854.2014

Al-Jarrah, M., Jamous, M., Al Zailaey, K., Bweir, S.O., 2010. Endurance exercise training promotes angiogenesis in the brain of chronic/progressive mouse model of parkinson's disease. NeuroRehabilitation 26, 369–373. doi:10.3233/NRE-2010-0574

Allen, A., Messier, C., 2013. Plastic changes in the astrocyte GLUT1 glucose transporter and beta-tubulin microtubule protein following voluntary exercise in mice. Behav. Brain Res. 240, 95–102. doi:10.1016/j.bbr.2012.11.025

Altschuler, E.L., 2006. Strenuous, intensive, long-term exercise does not prevent or delay the onset of Huntington's disease. Med. Hypotheses 67, 1429–1430. doi:10.1016/j.mehy.2006.04.068

Anderson, B.J., Rapp, D.N., Baek, D.H., McCloskey, D.P., Coburn-Litvak, P.S., Robinson, J.K., 2000. Exercise influences spatial learning in the radial arm maze. Physiol. Behav. 70, 425–429. doi:10.1016/S0031-9384(00)00282-1

Anderson, K.E., Gehl, C.R., Ph, D., Marder, K.S., Leigh, J., Paulsen, J.S., Group, S., 2011. Comorbidities of obsessive and compulsive symptoms in Huntington disease 198, 334–338. doi:10.1097/NMD.0b013e3181da852a.Comorbidities

Apostol, B.L., Simmons, D.A., Zuccato, C., Illes, K., Pallos, J., Casale, M., Conforti, P., Ramos, C., Roarke, M., Kathuria, S., Cattaneo, E., Marsh, J.L., Michels, L., 2008. Molecular and Cellular Neuroscience CEP-1347 reduces mutant huntingtin-associated neurotoxicity and restores BDNF levels in R6 / 2 mice 39, 8–20. doi:10.1016/j.mcn.2008.04.007

Arning, L., Epplen, J.T., 2013. Genetic modifiers in Huntington ' s disease : fiction or fact ? 171–172. doi:10.1007/s10048-013-0365-x

Arrasate, M., Finkbeiner, S., 2012. Protein aggregates in Huntington's disease. Exp. Neurol. 238, 1–11. doi:10.1016/j.expneurol.2011.12.013

Arrasate, M., Mitra, S., Schweitzer, E.S., Segal, M.R., Finkbeiner, S., 2004. Inclusion body formation reduces levels of mutant huntingtin and the risk of neuronal death. Nature 431, 805–10. doi:10.1038/nature02998

Aspenes, S.T., Nilsen, T.O.M.I.L., Skaug, E.-A., Bertheussen, G.R.O.F., Ellingsen, Ø., Vatten, L., Wisloff, U., 2011. Peak oxygen uptake and cardiovascular risk factors in 4631 healthy women and men. Med. Sci. Sport. Exerc. 43, 1465–1473. doi:10.1249/MSS.0b013e31820ca81c

Atwal, R.S., Desmond, C.R., Caron, N., Maiuri, T., Xia, J., Sipione, S., Truant, R., 2011. Kinase inhibitors modulate huntingtin cell localization and toxicity. Nat. Chem. Biol. 7, 452–453. doi:10.1038/nchembio.582

Aylward, E.H., 2007. Change in MRI striatal volumes as a biomarker in preclinical Huntington's disease. Brain Res. Bull. 72, 152–158. doi:10.1016/j.brainresbull.2006.10.028

Bahar-Fuchs, A., Clare, L., Woods, B., 2013. Cognitive training and cognitive rehabilitation for persons with mild to moderate dementia of the Alzheimer's or vascular type: a review. Alzheimers. Res. Ther. 5, 35. doi:10.1186/alzrt189

Bailey, D.M., Marley, C.J., Brugniaux, J. V, Hodson, D., New, K.J., Ogoh, S., Ainslie, P.N., 2013. Elevated aerobic fitness sustained throughout the adult lifespan is associated with improved cerebral hemodynamics. Stroke. 44, 3235–8. doi:10.1161/STROKEAHA.113.002589

Banderro, G.F., LaManna, J.C., 2011. Hypoxia-induced angiogenesis is delayed in aging mouse brain. Brain Res. 4, 50–60. doi:10.1126/scisignal.2001449.Engineering

Bank, A.J., Wang, H., Holte, J.E., Mullen, K., Shammas, R., Kubo, S.H., 1996. Contribution of Collagen, Elastin, and Smooth Muscle to In Vivo Human Brachial Artery Wall Stress and Elastic Modulus. Circulation 94, 1–18.

Barker, R.A., Mason, S.L., Harrower, T.P., Swain, R.A., Ho, A.K., Sahakian, B.J., Mathur, R., Elneil, S., Thornton, S., Hurrelbrink, C., Armstrong, R.J., Tyers, P., Smith, E., Carpenter, A., Piccini, P., Tai, Y.F., Brooks, D.J., Pavese, N., Watts, C., Pickard, J.D., Rosser, A.E., Dunnett, S.B., 2013. The long-term safety and efficacy of bilateral transplantation of human fetal striatal tissue in patients with mild to moderate Huntington's disease. J Neurol Neurosurg Psychiatry 84, 657–665. doi:10.1136/jnnp-2012-302441

Barnes, J.N., Taylor, J.L., Kluck, B.N., Johnson, C.P., Joyner, M.J., 2013. Cerebrovascular reactivity is associated with maximal aerobic capacity in healthy older adults. J. Appl. Physiol. 114, 1383–7. doi:10.1152/japplphysiol.01258.2012

Basterfield, L., Lumley, L.K., Mathers, J.C., 2009. Wheel running in female C57BL/6J mice: impact of oestrus and dietary fat and effects on sleep and body mass. Int. J. Obes. (Lond). 33, 212–218. doi:10.1038/ijo.2008.253

Batchelor, T.T., Duda, D.G., Di Tomaso, E., Ancukiewicz, M., Plotkin, S.R., Gerstner, E., Eichler, A.F., Drappatz, J., Hochberg, F.H., Benner, T., Louis, D.N., Cohen, K.S., Chea, H., Exarhopoulos, A., Loeffler, J.S., Moses, M.A., Ivy, P., Sorensen, A.G., Wen, P.Y., Jain, R.K., 2010. Phase II study of cediranib, an oral pan-vascular endothelial growth factor receptor tyrosine kinase inhibitor, in patients with recurrent glioblastoma. J. Clin. Oncol. 28, 2817–2823. doi:10.1200/JCO.2009.26.3988

Bayram-Weston, Z., Jones, L., Dunnett, S.B., Brooks, S.P., 2016. Comparison of mHTT Antibodies in Huntington's Disease Mouse Models Reveal Specific Binding Profiles and Steady-State Ubiquitin Levels with Disease Development. PLoS One 11, e0155834. doi:10.1371/journal.pone.0155834

Beck, H., Plate, K.H., 2009. Angiogenesis after cerebral ischemia. Acta Neuropathol. 117, 481–496. doi:10.1007/s00401-009-0483-6

Beglinger, L.J., Adams, W.H., Langbehn, D., Fiedorowicz, J.G., Jorge, R., Biglan, K., Caviness, J., Olson, B., Robinson, R.G., Paulsen, J.S., 2015. Results of the Citalopram to Enhance Cognition in Huntington Disease Trial. Mov. Disord. 29, 401–405. doi:10.1002/mds.25750.Results

Behrens, T.E.J., Woolrich, M.W., Smith, S.M., Boulby, P.A., Barker, G.J., Sillery, E.L., Sheehan, K., Ciccarelli, O., Thompson, A.J., Brady, J.M., Matthews, P.M., 2003. Non-invasive mapping of connections between human thalamus and cortex using diffusion imaging. Nat. Neurosci. 6, 750–757.

Bekar, L.K., Wei, H.S., Nedergaard, M., 2012. The locus coeruleus-norepinephrine network optimizes coupling of cerebral blood volume with oxygen demand. J. Cereb. Blood Flow Metab. 32, 2135–45. doi:10.1038/jcbfm.2012.115

Bell, R.D., Winkler, E.A., Sagare, A.P., Singh, I., Larue, B., Deane, R., Zlokovic, B. V, 2011. Pericytes control key neurovascular functions and neuronal phenotype in the adult brain and during brain aging Robert 68, 409–427. doi:10.1016/j.neuron.2010.09.043.Pericytes

Benn, C.L., Butler, R., Mariner, L., Nixon, J., Moffitt, H., Mielcarek, M., Bates, G.P., 2009. Genetic Knock-Down of HDAC7 Does Not Ameliorate Disease Pathogenesis in the R6 / 2 Mouse Model of Huntington ' s Disease 4, 6–14. doi:10.1371/journal.pone.0005747

Bernardi, C., Tramontina, A.C., Nardin, P., Biasibetti, R., Costa, A.P., Vizueti, A.F., Batassini, C., Tortorelli, L.S., Wartchow, K.M., Dutra, M.F., Bobermin, L., Sesterheim, P., Quincozes-Santos, A., De Souza, J., Gonçalves, C.A., 2013. Treadmill exercise induces hippocampal astroglial alterations in rats. Neural Plast. 2013. doi:10.1155/2013/709732

Biedermann, S., Fuss, J., Zheng, L., Sartorius, A., Falfán-Melgoza, C., Demirakca, T., Gass, P., Ende, G., Weber-Fahr, W., 2012. In vivo voxel based morphometry: detection of increased hippocampal volume and decreased glutamate levels in exercising mice. Neuroimage 61, 1206–12. doi:10.1016/j.neuroimage.2012.04.010

Birn, R.M., Murphy, K., Handwerker, D. a, Bandettini, P. a, 2009. fMRI in the presence of task-correlated breathing variations. Neuroimage 47, 1092–104. doi:10.1016/j.neuroimage.2009.05.030

Biron, K.E., Dickstein, D.L., Gopaul, R., Jefferies, W.A., 2011. Amyloid triggers extensive cerebral angiogenesis causing blood brain barrier permeability and hypervascularity in alzheimer's disease. PLoS One 6. doi:10.1371/journal.pone.0023789

Black, J.E., Isaacs, K.R., Anderson, B.J., Alcantara, a a, Greenough, W.T., 1990. Learning causes synaptogenesis, whereas motor activity causes angiogenesis, in cerebellar cortex of adult rats. Proc. Natl. Acad. Sci. U. S. A. 87, 5568–72.

Bloor, C.M., 2005. Angiogenesis during exercise and training. Angiogenesis 8, 263–71. doi:10.1007/s10456-005-9013-x

Bohanna, I., Georgiou-Karistianis, N., Hannan, A.J., Egan, G.F., 2008. Magnetic resonance imaging as an approach towards identifying neuropathological biomarkers for Huntington's disease. Brain Res. Rev. 58, 209–225. doi:10.1016/j.brainresrev.2008.04.001

Borg, E., Kaijser, L., 2006. A comparison between three rating scales for perceived exertion and two different work tests. Scand. J. Med. Sci. Sport. 16, 57–69. doi:10.1111/j.1600-0838.2005.00448.x

Borghammer, P., 2012. Perfusion and metabolism imaging studies In Parkinson' s disease. Dan. Med. J. 59, B4466.

Bright, M.G., Murphy, K., 2013. Reliable quantification of BOLD fMRI cerebrovascular reactivity despite poor breath-hold performance. Neuroimage 83, 559–68. doi:10.1016/j.neuroimage.2013.07.007

Brooks, S., Higgs, G., Jones, L., Dunnett, S.B., 2012. Longitudinal analysis of the behavioural phenotype in Hdh(CAG)150 Huntington's disease knock-in mice. Brain Res. Bull. 88, 182–8. doi:10.1016/j.brainresbull.2010.05.004

Brown, A.D., McMorris, C. a, Longman, R.S., Leigh, R., Hill, M.D., Friedenreich, C.M., Poulin, M.J., 2010. Effects of cardiorespiratory fitness and cerebral blood flow on cognitive outcomes in older women. Neurobiol. Aging 31, 2047–57. doi:10.1016/j.neurobiolaging.2008.11.002

Brown, G.C., 2007. Mechanisms of inflammatory neurodegeneration: iNOS and NADPH oxidase. Biochem Soc Trans 35, 1119–1121. doi:10.1042/BST0351119

Brown, J., Cooper-Kuhn, C.M., Kempermann, G., Van Praag, H., Winkler, J., Gage, F.H., Kuhn, H.G., 2003. Enriched environment and physical activity stimulate hippocampal but not olfactory bulb neurogenesis. Eur. J. Neurosci. 17, 2042–2046. doi:10.1046/j.1460-9568.2003.02647.x

Browne, S.E., Bowling, A.C., Macgarvey, U., Baik, M.J., Berger, S.C., Muqit, M.M.K., Bird, E.D., Beal, M.F., 1997. Oxidative Damage and Metabolic Dysfunction in HGntington ' s Disease : Selective Vulnerability of the Basal Ganglia 646–653.

Brun, J.F., Bouchahda, C., Chaze, D., Benhaddad, A.A., Micallef, J.P., Mercier, J., 2000. The paradox of hematocrit in exercise physiology : which is the " normal " range from an hemorheologist ' s viewpoint ? 22, 287–303.

Busse, M., Hughes, G., Wiles, C., Rosser, A., 2008. Use of hand-held dynamometry in the evaluation of lower limb muscle strength in people with Huntington's disease. J. Neurol. 255, 1534–1540. doi:10.1007/s00415-008-0964-x

Busse, M., Quinn, L., Debono, K., Jones, K., Collett, J., Playle, R., Kelly, M., Simpson, S., Backx, K., Wasley, D., Dawes, H., Rosser, A., 2013. A randomized feasibility study of a 12-week community-based exercise program for people with Huntington's disease. J. Neurol. Phys. Ther. 37, 149–58. doi:10.1097/NPT.0000000000000016

Busse, M.E., Wiles, C.M., Rosser, A.E., 2009. Mobility and falls in people with Huntington's disease. J. Neurol. Neurosurg. Psychiatry 80, 88–90. doi:10.1136/jnnp.2008.147793

Busse, R., Fleming, I., 2003. Regulation of endothelium-derived vasoactive autacoid production by hemodynamic forces. Trends Pharmacol. Sci. 24, 24–29. doi:10.1016/S0165-6147(02)00005-6

Buxton, R.B., Frank, L.R., Wong, E.C., Siewert, B., Warach, S., Edelman, R.R., 1998. A general kinetic model for quantitative perfusion imaging with arterial spin labeling. Magn. Reson. Med. 40, 383–396. doi:10.1002/mrm.1910400308

Buxton, R.B., Uludağ, K., Dubowitz, D.J., Liu, T.T., 2004. Modeling the hemodynamic response to brain activation. Neuroimage 23 Suppl 1, S220-33. doi:10.1016/j.neuroimage.2004.07.013

Cantin, S., Villien, M., Moreaud, O., Tropres, I., Keignart, S., Chipon, E., Bas, J. Le, 2011. NeuroImage Impaired cerebral vasoreactivity to CO 2 in Alzheimer ' s disease using BOLD fMRI. Neuroimage 58, 579–587. doi:10.1016/j.neuroimage.2011.06.070

Carmignoto, G., Gómez-Gonzalo, M., 2010. The contribution of astrocyte signalling to neurovascular coupling. Brain Res. Rev. 63, 138–48. doi:10.1016/j.brainresrev.2009.11.007

Carrera, E., Kim, D.J., Castellani, G., Zweifel, C., Smielewski, P., Pickard, J.D., Czosnyka, M., 2011. Effect of Hyper- and Hypocapnia on Cerebral Arterial Compliance in Normal Subjects. J. Neuroimaging 21, 121–125. doi:10.1111/j.1552-6569.2009.00439.x

Cepeda-Prado, E., Popp, S., Khan, U., Stefanov, D., Rodriguez, J., Menalled, L., Dow-Edwards, D., Small, S., Moreno, H., 2012. R6/2 Huntington's disease Mice Develop Early and Progressive Abnormal Brain Metabolism and Seizures. J. Neurosci. 32, 6456–6467. doi:10.1523/JNEUROSCI.0388-12.2012.R6/2

Chaddock, L., Erickson, K.I., Prakash, R.S., VanPatter, M., Voss, M.W., Pontifex, M.B., Raine, L.B., Hillman, C.H., Kramer, A.F., 2010. Basal ganglia volume is associated with aerobic fitness in preadolescent children. Dev. Neurosci. 32, 249–56. doi:10.1159/000316648

Chang, D.T.W., Rintoul, G.L., Pandipati, S., Reynolds, I.J., 2006. Mutant huntingtin aggregates impair mitochondrial movement and trafficking in cortical neurons 22, 388–400. doi:10.1016/j.nbd.2005.12.007

Chapman, S.B., Aslan, S., Spence, J.S., DeFina, L.F., Keebler, M.W., Didehbani, N., Lu, H., 2013. Shorter term aerobic exercise improves brain, cognition, and cardiovascular fitness in aging. Front. Aging Neurosci. 5, 1–9. doi:10.3389/fnagi.2013.00075

Chappell, M.A., Groves, A.R., MacIntosh, B.J., Donahue, M.J., Jezzard, P., Woolrich, M.W., 2011. Partial volume correction of multiple inversion time arterial spin labeling MRI data. Magn. Reson. Med. 65, 1173–1183. doi:10.1002/mrm.22641

Chappell, M.A., Groves, A.R., Whitcher, B., Woolrich, M.W., 2009. Variational Bayesian Inference for a Nonlinear Forward Model 57, 223–236.

Chen, J.J., Rosas, H.D., Salat, D.H., 2011. Age-Associated Reductions in Cerebral Blood Flow Are Independent from Regional Atrophy. Neuroimage 4, 468–478. doi:10.1126/scisignal.2001449.Engineering

Chen, J.J., Salat, D.H., Rosas, H.D., 2012. Complex relationships between cerebral blood flow and brain atrophy in early Huntington's disease. Neuroimage 59, 1043–51. doi:10.1016/j.neuroimage.2011.08.112

Chen, J.J., Wieckowska, M., Meyer, E., Pike, G.B., 2008. Cerebral blood flow measurement using fMRI and PET: A cross-validation study. Int. J. Biomed. Imaging 2008. doi:10.1155/2008/516359

Chen, Y.F., Wang, D.J.J., Detre, John, A., 2011. Test-Retest Reliability of Arterial Spin Labeling with Common Labeling Strategies. J. Magn. Reson. Imaging 33, 940–949. doi:10.1002/jmri.22345.Test-Retest

Church, T.S., Gill, T.M., Newman, A.B., Blair, S.N., Earnest, C.P., Pahor, M., 2008. Maximal fitness testing in sedentary elderly at substantial risk of disability: LIFE-P study experience. J. Aging Phys. Act. 16, 408–415.

Cisbani, G., Cicchetti, F., 2012. An in vitro perspective on the molecular mechanisms underlying mutant huntingtin protein toxicity. Cell Death Dis. 3, e382. doi:10.1038/cddis.2012.121

Cisbani, G., Freeman, T.B., Soulet, D., Saint-Pierre, M., Gagnon, D., Parent, M., Hauser, R.A., Barker, R.A., Cicchetti, F., 2013. Striatal allografts in patients with Huntington's disease: Impact of diminished astrocytes and vascularization on graft viability. Brain 136, 433–443. doi:10.1093/brain/aws359

Clark, P.J., Brzezinska, W.J., Puchalski, E.K., Krone, D.A., Rhodes, Justin, S., 2009. Functional Analysis of Neurovascular Adaptations to Exercise in the Dentate Gyrus of Young Adult Mice Associated With Cognitive Gain. Hippocampus 19, 937–950. doi:10.1002/hipo.20543.Functional

Colcombe, S., Kramer, A.F., 2003. Fitness effects on the cognitive function of older adults: a meta-analytic study. Psychol. Sci. 14, 125–30.

Colcombe, S.J., Erickson, K.I., Scalf, P.E., Kim, J.S., Prakash, R., Mcauley, E., Elavsky, S., Marquez, D.X., Hu, L., Kramer, A.F., 2006. Brain Volume in Aging Humans 61, 1166–1170.

Colcombe, S.J., Kramer, A.F., Erickson, K.I., Scalf, P., McAuley, E., Cohen, N.J., Webb, A., Jerome, G.J., Marquez, D.X., Elavsky, S., 2004. Cardiovascular fitness, cortical plasticity, and aging. Proc. Natl. Acad. Sci. 101, 3316–3321. doi:10.1073/pnas.0400266101

Conforti, P., Zuccato, C., Gaudenzi, G., Ieraci, A., Camnasio, S., Buckley, N.J., C, M., Cotelli, F., Contini, A., Cattaneo, E., 2013. Binding of the repressor complex REST-mSIN3b by small molecules restores neuronal gene transcription in Huntington's disease models. J. Neurochem. 127, 22–35. doi:10.1111/jnc.12348

Coskran, T.M., Morton, D., Menniti, F.S., Adamowicz, W.O., Kleiman, R.J., Ryan, A.M., Strick, C.A., Schmidt, C.J., Stephenson, D.T., 2006. Immunohistochemical Localization of Phosphodiesterase 10A in Multiple Mammalian Species The Journal of Histochemistry & Cytochemistry 54, 1205–1213. doi:10.1369/jhc.6A6930.2006

Cotman, C.W., Berchtold, N.C., Christie, L.-A., 2007. Exercise builds brain health: key roles of growth factor cascades and inflammation. Trends Neurosci. 30, 464–72. doi:10.1016/j.tins.2007.06.011

Cox, R., 1996. AFNI: Software for analysis and visualization of functional magnetic resonance neuroimages. Comput Biomed Res 29, 162–173.

Craig, C.L., Marshall, A.L., Sjostrom, M., Bauman, A.E., Booth, M.L., Ainsworth, B.E., Pratt, M., Ekelund, U., Yngve, A., Sallis, J.F., Oja, P., 2003. International physical activity questionnaire: 12-Country reliability and validity. Med. Sci. Sports Exerc. 35, 1381–1395. doi:10.1249/01.MSS.0000078924.61453.FB

Creer, D.J., Romberg, C., Saksida, L.M., van Praag, H., Bussey, T.J., 2010a. Running enhances spatial pattern separation in mice. Proc. Natl. Acad. Sci. U. S. A. 107, 2367–72. doi:10.1073/pnas.0911725107

Creer, D.J., Romberg, C., Saksida, L.M., van Praag, H., Bussey, T.J., 2010b. Running enhances spatial pattern separation in mice. Proc. Natl. Acad. Sci. U. S. A. 107, 2367–72. doi:10.1073/pnas.0911725107

Damiano, M., Galvan, L., Déglon, N., Brouillet, E., 2010. Mitochondria in Huntington's disease. Biochim. Biophys. Acta - Mol. Basis Dis. 1802, 52–61. doi:10.1016/j.bbadis.2009.07.012

Davenport, M.H., Hogan, D.B., Eskes, G. a, Longman, R.S., Poulin, M.J., 2012. Cerebrovascular reserve: the link between fitness and cognitive function? Exerc. Sport Sci. Rev. 40, 153–8. doi:10.1097/JES.0b013e3182553430

Dawes, H., Collett, J., Debono, K., Quinn, L., Jones, K., Kelson, M., Simpson, S., Playle, R., Backx, K., Wasley, D., Nemeth, A., Rosser, a, Izardi, H., Busse, M., 2014. Exercise testing and training in people with Huntington's disease. Clin. Rehabil. 0269215514540921-. doi:10.1177/0269215514540921

Deckel, A.W., 2002. Altered neuronal nitric oxide synthase expression contributes to disease progression in Huntington ' s disease transgenic mice 939, 76–86.

Deckel, A.W., Weiner, R., Szigeti, D., Clark, V., Vento, J., 2000. Altered Patterns of

Regional Cerebral Blood Flow in Patients with Huntington ' s or Motor Activation Disease : A SPECT Study During Rest and Cognitive 773–780.
Deng, Y.P., Albin, R.L., Penney, J.B., Young, A.B., Anderson, K.D., Reiner, A., 2004. Differential loss of striatal projection systems in Huntington's disease: A quantitative immunohistochemical study. J. Chem. Neuroanat. 27, 143–164. doi:10.1016/j.jchemneu.2004.02.005
Detre, J. a., Leigh, J.S., Williams, D.S., Koretsky, A.P., 1992. Perfusion imaging. Magn. Reson. Med. 23, 37–45. doi:10.1002/mrm.1910230106
Ding, Y.-H., Li, J., Zhou, Y., Rafols, J. a, Clark, J.C., Ding, Y., 2006. Cerebral angiogenesis and expression of angiogenic factors in aging rats after exercise. Curr. Neurovasc. Res. 3, 15–23.
Döbrössy, M.D., Dunnett, S.B., 2006. Morphological and cellular changes within embryonic striatal grafts associated with enriched environment and involuntary exercise. Eur. J. Neurosci. 24, 3223–33. doi:10.1111/j.1460-9568.2006.05182.x
Domínguez, J.F., Egan, G.F., Gray, M.A., Poudel, G.R., Churchyard, A., Chua, P., Stout, J.C., Georgiou-Karistianis, N., 2013. Multi-Modal Neuroimaging in Premanifest and Early Huntington's Disease: 18 Month Longitudinal Data from the IMAGE-HD Study. PLoS One 8, 16–22. doi:10.1371/journal.pone.0074131
Douaud, G., Gaura, V., Ribeiro, M.J., Lethimonnier, F., Maroy, R., Verny, C., Krystkowiak, P., Damier, P., Bachoud-Levi, A.C., Hantraye, P., Remy, P., 2006. Distribution of grey matter atrophy in Huntington's disease patients: A combined ROI-based and voxel-based morphometric study. Neuroimage 32, 1562–1575. doi:10.1016/j.neuroimage.2006.05.057
Drake, C.T., Iadecola, C., 2007. The role of neuronal signaling in controlling cerebral blood flow. Brain Lang. 102, 141–152. doi:10.1016/j.bandl.2006.08.002
Drouin-Ouellet, J., Sawiak, S.J., Cisbani, G., Lagacé, M., Kuan, W.L., Saint-Pierre, M., Dury, R.J., Alata, W., St-Amour, I., Mason, S.L., Calon, F., Lacroix, S., Gowland, P.A., Francis, S.T., Barker, R.A., Cicchetti, F., 2015. Cerebrovascular and blood-brain barrier impairments in Huntington's disease: Potential implications for its pathophysiology. Ann. Neurol. 78, 160–177. doi:10.1002/ana.24406
Duff, K., Paulsen, J., Mills, J., Beglinger, L.J., Moser, D.J., Smith, M.M., Langbehn, D., Stout, J., Queller, S., Harrington, D.L., 2010. Mild cognitive impairment in prediagnosed Huntington disease. Neurology 75, 500–507. doi:10.1212/WNL.0b013e3181eccfa2
Duff, K., Paulsen, J.S., Beglinger, L.J., Langbehn, D.R., Stout, J.C., 2007. Psychiatric Symptoms in Huntington's Disease before Diagnosis: The Predict-HD Study. Biol. Psychiatry 62, 1341–1346. doi:10.1016/j.biopsych.2006.11.034
Duijn, E. Van, Craufurd, D., Hubers, A.A.M., Giltay, E.J., Bonelli, R., Rickards, H., Anderson, K.E., Walsem, M.R. Van, Mast, R.C. Van Der, Orth, M., Landwehrmeyer, G.B., 2014. Neuropsychiatric symptoms in a European Huntington ' s disease cohort ( REGISTRY ) 1411–1418. doi:10.1136/jnnp-2013-307343
Duijn, E. Van, Ph, D., Reedeker, N., Giltay, E.J., Roos, R. a C., Mast, R.C. Van Der, 2010. Correlates of Apathy in Huntington ' s Disease. J. Neuropsychiatry Clin. Neurosci. 287–294.
Dukart, J., Bertolino, A., 2014. When Structure Affects Function – The Need for Partial Volume Effect Correction in Functional and Resting State Magnetic

Resonance Imaging Studies 1–18. doi:10.1371/journal.pone.0114227
Duman, C.H., Schlesinger, L., Russell, D.S., Duman, R.S., 2009. Voluntary Exercise Produces Antidepressant and Anxiolytic Behavioral Effects in Mice. Brain Res. 1199, 148–158.
Dunnett, S.B., Rosser, A.E., 2014. Challenges for taking primary and stem cells into clinical neurotransplantation trials for neurodegenerative disease. Neurobiol. Dis. 61, 79–89. doi:10.1016/j.nbd.2013.05.004
Dupuy, O., Gauthier, C.J., Fraser, S. a, Desjardins-Crèpeau, L., Desjardins, M., Mekary, S., Lesage, F., Hoge, R.D., Pouliot, P., Bherer, L., 2015. Higher levels of cardiovascular fitness are associated with better executive function and prefrontal oxygenation in younger and older women. Front. Hum. Neurosci. 9, 66. doi:10.3389/fnhum.2015.00066
Durrant, J.R., Seals, D.R., Connell, M.L., Russell, M.J., Lawson, B.R., Folian, B.J., Donato, A.J., Lesniewski, L. a, 2009. Voluntary wheel running restores endothelial function in conduit arteries of old mice: direct evidence for reduced oxidative stress, increased superoxide dismutase activity and down-regulation of NADPH oxidase. J. Physiol. 587, 3271–85. doi:10.1113/jphysiol.2009.169771
Dusak, A., Kamasak, K., Goya, C., Adin, M.E., Elbey, M.A., Bilici, A., 2013. Arterial distensibility in patients with ruptured and unruptured intracranial aneurysms: is it a predisposing factor for rupture risk? Med. Sci. Monit. 19, 703–9. doi:10.12659/MSM.889032
Edelman, R.R., Chen, Q., 1998. EPISTAR MRI: multislice mapping of cerebral blood flow. Magn. Reson. Med. 40, 800–805. doi:10.1002/mrm.1910400603
Edvardsen, E., Hem, E., Anderssen, S.A., 2014. End criteria for reaching maximal oxygen uptake must be strict and adjusted to sex and age: A cross-sectional study. PLoS One 9, 18–20. doi:10.1371/journal.pone.0085276
Ekstrand, J., Hellsten, J., Tingström, A., 2008. Environmental enrichment, exercise and corticosterone affect endothelial cell proliferation in adult rat hippocampus and prefrontal cortex. Neurosci. Lett. 442, 203–7. doi:10.1016/j.neulet.2008.06.085
Epping, E.A., Mills, J.A., Beglinger, L.J., Fierdorwiczm J G, Crauford, D., Smith, M.M., Groves, M., Bijanki, K.R., Downing, N., Williams, J.K., Long, J.D., Paulsen, J.S., 2014. Characterization of Depression in Prodromal Huntington Disease in the Neurobiological Predictors of HD (PREDICT-HD) Study. J. Psychiatr. Res. 47, 380–392. doi:10.1016/j.jpsychires.2013.05.026
Erickson, K.I., Voss, M.W., Prakash, R.S., Basak, C., Szabo, A., Chaddock, L., Kim, J.S., Heo, S., Alves, H., White, S.M., Wojcicki, T.R., Mailey, E., Vieira, V.J., Martin, S. a, Pence, B.D., Woods, J. a, McAuley, E., Kramer, A.F., 2011. Exercise training increases size of hippocampus and improves memory. Proc. Natl. Acad. Sci. U. S. A. 108, 3017–22. doi:10.1073/pnas.1015950108
Escartin, C., Murai, K.K., 2014. Imaging and monitoring astrocytes in health and disease. Front. Cell. Neurosci. 8, 74. doi:10.3389/fncel.2014.00074
Evans, S.J.W., Douglas, I., Rawlins, M.D., Wexler, N.S., Tabrizi, S.J., Smeeth, L., 2013. Prevalence of adult Huntington's disease in the UK based on diagnoses recorded in general practice records. J. Neurol. Neurosurg. Psychiatry 84, 1156–60. doi:10.1136/jnnp-2012-304636
Fabel, K., Fabel, K., Tam, B., Kaufer, D., Baiker, A., Simmons, N., Kuo, C.J., Palmer, T.D., Elisa, S., 2003. VEGF is necessary for exercise-induced adult hippocampal neurogenesis 18. doi:10.1046/j.1460-9568.2003.03041.x
Fabre, C., Chamari, K., Mucci, P., Massé-Biron, J., Préfaut, C., 2002. Improvement

of cognitive function by mental and/or individualized aerobic training in healthy elderly subjects. Int. J. Sports Med. 23, 415–421. doi:10.1055/s-2002-33735

Faraci, F.M., Heistad, D.D., 1998. Regulation of the cerebral circulation: role of endothelium and potassium channels. Physiol. Rev. 78, 53–97.

Farkas, E., Luiten, P.G.., 2001. Cerebral microvascular pathology in aging and Alzheimer's disease, Progress in Neurobiology. doi:10.1016/S0301-0082(00)00068-X

Feigin, A., Tang, C., Ma, Y., Mattis, P., Zgaljardic, D., Guttman, M., Paulsen, J.S., Dhawan, V., Eidelberg, D., 2014. Thalamic metabolism and symptom onset in preclinical Huntington's disease. Brain 67, 223–230. doi:10.1038/ja.2013.113.Venturicidin

Fernando, M.S., Simpson, J.E., Matthews, F., Brayne, C., Lewis, C.E., Barber, R., Kalaria, R.N., Forster, G., Esteves, F., Wharton, S.B., Shaw, P.J., O'Brien, J.T., Ince, P.G., 2006. White matter lesions in an unselected cohort of the elderly: Molecular pathology suggests origin from chronic hypoperfusion injury. Stroke 37, 1391–1398. doi:10.1161/01.STR.0000221308.94473.14

Ferré, J.-C., Bannier, E., Raoult, H., Mineur, G., Carsin-Nicol, B., Gauvrit, J.-Y., 2013. Arterial spin labeling (ASL) perfusion: Techniques and clinical use. Diagn Interv Imaging 94, epub ahead of print. doi:10.1016/j.diii.2013.06.010

Ferris, L.T., Williams, J.S., Shen, C.-L., 2007. The effect of acute exercise on serum brain-derived neurotrophic factor levels and cognitive function. Med. Sci. Sports Exerc. 39, 728–34. doi:10.1249/mss.0b013e31802f04c7

Figley, C.R., Stroman, P.W., 2011. The role(s) of astrocytes and astrocyte activity in neurometabolism, neurovascular coupling, and the production of functional neuroimaging signals. Eur. J. Neurosci. 33, 577–88. doi:10.1111/j.1460-9568.2010.07584.x

Fisher, J.P., Hartwich, D., Seifert, T., Olesen, N.D., McNulty, C.L., Nielsen, H.B., van Lieshout, J.J., Secher, N.H., 2013. Cerebral perfusion, oxygenation and metabolism during exercise in young and elderly individuals. J. Physiol. 591, 1859–70. doi:10.1113/jphysiol.2012.244905

Fleenor, B.S., Marshall, K.D., Durrant, J.R., Lesniewski, L. a, Seals, D.R., 2010. Arterial stiffening with ageing is associated with transforming growth factor-β1-related changes in adventitial collagen: reversal by aerobic exercise. J. Physiol. 588, 3971–3982. doi:10.1113/jphysiol.2010.194753

Franciosi, S., Ryu, J.K., Shim, Y., Hill, A., Connolly, C., Hayden, M.R., Mclarnon, J.G., Leavitt, B.R., 2012. Neurobiology of Disease Age-dependent neurovascular abnormalities and altered microglial morphology in the YAC128 mouse model of Huntington disease. Neurobiol. Dis. 45, 438–449. doi:10.1016/j.nbd.2011.09.003

Gallichan, D., Jezzard, P., 2009. Variation in the Shape of Pulsed Arterial Spin Labeling Kinetic Curves across the Healthy Human Brain and Its Implications for CBF Quantification 695, 686–695. doi:10.1002/mrm.21886

Gauthier, C.J., Lefort, M., Mekary, S., Desjardins-Crépeau, L., Skimminge, a., Iversen, P., Madjar, C., Desjardins, M., Lesage, F., Garde, E., Frouin, F., Bherer, L., Hoge, R.D., 2014a. Hearts and minds: linking vascular rigidity and aerobic fitness with cognitive aging. Neurobiol. Aging. doi:10.1016/j.neurobiolaging.2014.08.018

Gauthier, C.J., Lefort, M., Mekary, S., Desjardins-Crépeau, L., Skimminge, a., Iversen, P., Madjar, C., Desjardins, M., Lesage, F., Garde, E., Frouin, F., Bherer, L., Hoge, R.D., 2014b. Hearts and minds: linking vascular rigidity and aerobic fitness with cognitive aging. Neurobiol. Aging 36, 304–314.

doi:10.1016/j.neurobiolaging.2014.08.018
Gee, M.S., Procopio, W.N., Makonnen, S., Feldman, M.D., Yeilding, N.M., Lee, W.M.F., 2003. Tumor vessel development and maturation impose limits on the effectiveness of anti-vascular therapy. Am. J. Pathol. 162, 183–193. doi:10.1016/S0002-9440(10)63809-6
George, J.D., Fellingham, G.W., Fisher, a G., 1998. A modified version of the Rockport Fitness Walking Test for college men and women. Res. Q. Exerc. Sport 69, 205–9. doi:10.1080/02701367.1998.10607685
Germuska, M., Merola, A., Murphy, K., Babic, A., Richmond, L., Khot, S., Hall, J.E., Wise, R.G., 2016. A new framework for dual calibrated estimation of OEF R2v1.
Gianfriddo, M., Melani, A., Turchi, D., Giovannini, M.G., Pedata, F., 2004. Adenosine and glutamate extracellular concentrations and mitogen-activated protein kinases in the striatum of Huntington transgenic mice . Selective antagonism of adenosine A 2A receptors reduces transmitter outflow 17, 77–88. doi:10.1016/j.nbd.2004.05.008
Girotti, F., Marano, R., Soliveri, P., Geminiani, G., Scigliano, G., 1988. Relationship between motor and cognitive disorders in Huntington's disease. J. Neurol. 235, 454–457. doi:10.1007/BF00314246
Glodzik, L., Rusinek, H., Brys, M., Tsui, W.H., Switalski, R., Mosconi, L., Mistur, R., Pirraglia, E., de Santi, S., Li, Y., Goldowsky, A., de Leon, M.J., 2011. Framingham cardiovascular risk profile correlates with impaired hippocampal and cortical vasoreactivity to hypercapnia. J. Cereb. Blood Flow Metab. 31, 671–679. doi:10.1038/jcbfm.2010.145
Glover, G.H., Li, T.Q., Ress, D., 2000. Image-based method for retrospective correction of physiological motion effects in fMRI: RETROICOR. Magn. Reson. Med. 44, 162–7.
Golay, X., Stuber, M., Pruessmann, K.P., Meier, D., Boesiger, P., 1999. Transfer insensitive labeling technique (TILT): Application to multislice functional perfusion imaging. J. Magn. Reson. Imaging 9, 454–461. doi:10.1002/(SICI)1522-2586(199903)9:3<454::AID-JMRI14>3.0.CO;2-B
Goodwin, V.A., Richards, S.H., Taylor, R.S., Taylor, A.H., Campbell, J.L., 2008. The effectiveness of exercise interventions for people with Parkinson's disease: A systematic review and meta-analysis. Mov. Disord. 23, 631–640. doi:10.1002/mds.21922
Gould, E., Beylin, a, Tanapat, P., Reeves, a, Shors, T.J., 1999. Learning enhances adult neurogenesis in the hippocampal formation. Nat. Neurosci. 2, 260–5. doi:10.1038/6365
Green, D.J., Bilsborough, W., Naylor, L.H., Reed, C., Wright, J., O'Driscoll, G., Walsh, J.H., 2005. Comparison of forearm blood flow responses to incremental handgrip and cycle ergometer exercise: relative contribution of nitric oxide. J. Physiol. 562, 617–628. doi:10.1113/jphysiol.2004.075929
Green, D.J., Maiorana, A., O'Driscoll, G., Taylor, R., 2004. Effect of exercise training on endothelium-derived nitric oxide function in humans. J. Physiol. 561, 1–25. doi:10.1113/jphysiol.2004.068197
Guan, J., Pavlovic, D., Dalkie, N., Waldvogel, H.J., O'Carroll, S.J., Green, C.R., Nicholson, L.F.B., 2013. Vascular degeneration in parkinsons disease. Brain Pathol. 23, 154–164. doi:10.1111/j.1750-3639.2012.00628.x
Guerrieri, D., Moon, H.Y., Van Praag, H., 2017. Exercise in a pill: the latest on exercise-mimetics 2, 153–169. doi:10.3233/BPL-160043
Guerrieri, D., van Praag, H., 2015. Exercise-mimetic AICAR transiently benefits

brain function. Oncotarget 6, 18293–18313. doi:10.18632/oncotarget.4715
Guiney, H., Lucas, S.J., Cotter, J.D., Machado, L., 2014. Neuropsychology Evidence Cerebral Blood-Flow Regulation Mediates Exercise – Cognition Links in Healthy Young Adults Evidence Cerebral Blood-Flow Regulation Mediates Exercise – Cognition Links in Healthy Young Adults. Neuropsychology 29, 1–9. doi:10.1037/neu0000124
Haber, S.N., 2003. The primate basal ganglia: Parallel and integrative networks. J. Chem. Neuroanat. 26, 317–330. doi:10.1016/j.jchemneu.2003.10.003
Hall, C.N., Reynell, C., Gesslein, B., Hamilton, N.B., Mishra, A., Sutherland, B.A., O'Farrell, F.M., Buchan, A.M., Lauritzen, M., Attwell, D., 2014. Capillary pericytes regulate cerebral blood flow in health and disease. Nature 508, 55–60. doi:10.1038/nature13165
Hall, J.M., Vetreno, R.P., Savage, L.M., 2013. Differential cortical neurotrophin and cytogenetic adaptation after voluntary exercise in normal and amnestic rats. Neuroscience 258C, 131–146. doi:10.1016/j.neuroscience.2013.10.075
Hansen, A.L., Johnsen, B.H., Sollers, J.J., Stenvik, K., Thayer, J.F., 2004. Heart rate variability and its relation to prefrontal cognitive function: The effects of training and detraining. Eur. J. Appl. Physiol. 93, 263–272. doi:10.1007/s00421-004-1208-0
Harris, G.J., Codori, A.M., Lewis, R.F., Schmidt, E., Bedi, A., Brandt, J., 1999. Reduced basal ganglia blood flow and volume in pre-symptomatic, gene-tested persons at-risk for Huntington's disease. Brain 122, 1667–1678. doi:10.1093/brain/122.9.1667
Harrison, D.J., Busse, M., Openshaw, R., Rosser, A.E., Dunnett, S.B., Brooks, S.P., 2013. Exercise attenuates neuropathology and has greater benefit on cognitive than motor deficits in the R6/1 Huntington's disease mouse model. Exp. Neurol. 248, 457–69. doi:10.1016/j.expneurol.2013.07.014
Hasselbalch, S.G., Oberg, G., Sorensen, S.A., Andersen, A.R., Waldemar, G., Schmidt, J.F., Fenger, K., Paulson, O.B., 1992. Reduced regional cerebral blood flow in Huntington's disease studied by SPECT. J.Neurol.Neurosurg.Psychiatry 55, 1018–1023. doi:10.1136/jnnp.55.11.1018
Hayden, M.R., Leavitt, B.R., Yasothan, U., Kirkpatrick, P., 2009. Tetrabenazine 8, 17–18. doi:10.1038/nrd2784
Heikkinen, T., Lehtimäki, K., Vartiainen, N., Puoliväli, J., Hendricks, S.J., Glaser, J.R., Bradaia, A., Wadel, K., Touller, C., Kontkanen, O., Yrjänheikki, J.M., Buisson, B., Howland, D., Beaumont, V., Munoz-Sanjuan, I., Park, L.C., 2012. Characterization of Neurophysiological and Behavioral Changes, MRI Brain Volumetry and 1H MRS in zQ175 Knock-In Mouse Model of Huntington's Disease. PLoS One 7. doi:10.1371/journal.pone.0050717
Hendelman, D., Miller, K., Baggett, C., Debold, E., Freedson, P., 2000. Validity of accelerometry for the assessment of moderate intensity physical activity in the field. Med. Sci. Sport. Exerc. 32, 442–449.
Hennenlotter, A., Schroeder, U., Erhard, P., Haslinger, B., Stahl, R., Weindl, A., Von Einsiedel, H.G., Lange, K.W., Ceballos-Baumann, A.O., 2004. Neural correlates associated with impaired disgust processing in pre-symptomatic Huntington's disease. Brain 127, 1446–1453. doi:10.1093/brain/awh165
Henry, J.D., Crawford, J.R., Phillips, L.H., 2005. A meta-analytic review of verbal fluency deficits in Huntington's disease. Neuropsychology 19, 243–252. doi:10.1037/0894-4105.19.2.243
Herbst, E. a. F., Holloway, G.P., 2015. Exercise training normalizes mitochondrial respiratory capacity within the striatum of the R6/1 model of Huntington's

disease. Neuroscience 303, 515–523. doi:10.1016/j.neuroscience.2015.07.025
Herscovitch, P., Raichle, M.E., 1985. What is the correct value for the brain--blood partition coefficient for water? J. Cereb. Blood Flow Metab. 5, 65–69. doi:10.1038/jcbfm.1985.9
Hill, R.A., Tong, L., Yuan, P., Murikinati, S., Gupta, S., Grutzendler, J., 2015. Regional Blood Flow in the Normal and Ischemic Brain Is Controlled by Arteriolar Smooth Muscle Cell Contractility and Not by Capillary Pericytes. Neuron 87, 95–110. doi:10.1016/j.neuron.2015.06.001
Hillman, C.H., Erickson, K.I., Kramer, A.F., 2008. Be smart, exercise your heart: exercise effects on brain and cognition. Nat. Rev. Neurosci. 9, 58–65. doi:10.1038/nrn2298
Hillman, C.H., Motl, R.W., Pontifex, M.B., Posthuma, D., Stubbe, J.H., Boomsma, D.I., de Geus, E.J.C., 2006. Physical activity and cognitive function in a cross-section of younger and older community-dwelling individuals. Health Psychol. 25, 678–687. doi:10.1037/0278-6133.25.6.678
Ho, A.K., Sahakian, B.J., Brown, R.G., Barker, R.A., Hodges, J.R., Ane, M.N., Snowden, J., Thompson, J., Esmonde, T., Gentry, R., Moore, J.W., Bodner, T., The, N.-H.D.C., 2003. Profile of cognitive progression in early Huntington's disease. Neurology 61, 1702–1706. doi:10.1212/01.WNL.0000098878.47789.BD
Ho, D.J., Calingasan, N.Y., Wille, E., Dumont, M., Beal, M.F., 2010. Resveratrol protects against peripheral deficits in a mouse model of Huntington's disease. Exp. Neurol. 225, 74–84. doi:10.1016/j.expneurol.2010.05.006
Hockly, E., Cordery, P.M., Woodman, B., Mahal, A., Van Dellen, A., Blakemore, C., Lewis, C.M., Hannan, A.J., Bates, G.P., 2002. Environmental enrichment slows disease progression in R6/2 Huntington's disease mice. Ann. Neurol. 51, 235–242. doi:10.1002/ana.10094
Hoge, R.D., Atkinson, J., Gill, B., Crelier, G.R., Marrett, S., Pike, G.B., 1999. Linear coupling between cerebral blood flow and oxygen consumption in activated human cortex. Proc. Natl. Acad. Sci. U. S. A. 96, 9403–9408. doi:VL - 96
Holdsworth, D.W., Norley, C.J.D., Frayne, R., Steinman, D.A., Rutt, B.K., 1999. Characterization of common carotid artery blood-flow waveforms in normal human subjects Characterization of common carotid artery blood-flow waveforms in normal human subjects. Physiol. Meas. 20, 219–240. doi:10.1063/1.3607435
Hossmann, K. a., 1994. Viability thresholds and the penumbra of focal ischemia. Ann. Neurol. 36, 557–565. doi:10.1002/ana.410360404
Howley, E.T., Bassett, D.R., Welch, H.G., 1995. Criteria for maximal oxygen uptake: review and commentary. Med. Sci. Sports Exerc. doi:10.1249/00005768-199509000-00009
Hsiao, H.Y., Chen, Y.C., Huang, C.H., Chen, C.C., Hsu, Y.H., Chen, H.M., Chiu, F.L., Kuo, H.C., Chang, C., Chern, Y., 2015. Aberrant astrocytes impair vascular reactivity in Huntington disease. Ann. Neurol. 78, 178–192. doi:10.1002/ana.24428
Hughes, T.M., Craft, S., Lopez, O.L., Medicine, G., Forest, W., 2015. HHS Public Access 5, 121–135. doi:10.2217/nmt.14.53.Review
Huntington's Study Group, 2017. Effect of Deutetrabenazine on Chorea Among Patients With Huntington Disease A Randomized Clinical Trial. JAMA 316, 40–50. doi:10.1001/jama.2016.8655
Huntington Study Group, 2006. Tetrabenazine as antichorea therapy in Huntington

disease A randomized controlled trial. Neurology 66, 366–372.
Iadecola, C., 2004. Neurovascular regulation in the normal brain and in Alzheimer's disease. Nat. Rev. Neurosci. 5, 347–60. doi:10.1038/nrn1387
Iadecola, C., Gorelick, P.B., 2004. Hypertension, Angiotensin, and Stroke: Beyond Blood Pressure. Stroke 35, 348–350. doi:10.1161/01.STR.0000115162.16321.AA
Isaacs, K.R., Anderson, B.J., Alcantara, a a, Black, J.E., Greenough, W.T., 1992. Exercise and the brain: angiogenesis in the adult rat cerebellum after vigorous physical activity and motor skill learning. J. Cereb. Blood Flow Metab. 12, 110–9. doi:10.1038/jcbfm.1992.14
Jackson, A.S., Sui, X., Hébert, J.R., Church, T.S., Blair, S.N., 2009. Role of lifestyle and aging on the longitudinal change in cardiorespiratory fitness. Arch. Intern. Med. 169, 1781–7. doi:10.1001/archinternmed.2009.312
Jellinger, K.A., 2010. Prevalence and impact of cerebrovascular lesions in Alzheimer and lewy body diseases. Neurodegener. Dis. 7, 112–115. doi:10.1159/000285518
Jenkinson, M., Bannister, P., Brady, M., Smith, S., 2002. Improved Optimization for the Robust and Accurate Linear Registration and Motion Correction of Brain Images. Neuroimage 17, 825–841. doi:10.1006/nimg.2002.1132
Jenkinson, M., Smith, S.M., 2001. A global optimization method for robust affine registration of brain images. Med. Imaging Anal. 5, 143–156.
Jennings, J.R., Heim, A.F., Kuan, D.C.-H., Gianaros, P.J., Muldoon, M.F., Manuck, S.B., 2013. Use of total cerebral blood flow as an imaging biomarker of known cardiovascular risks. Stroke 44, 2480–5. doi:10.1161/STROKEAHA.113.001716
Jiang, Q., Zheng, G.Z., Guang, L.D., Zhang, L., Ewing, J.R., Wang, L., Zhang, R., Li, L., Lu, M., Meng, H., Arbab, A.S., Hu, J., Qing, J.L., Nejad D, S.P., Athiraman, H., Chopp, M., 2005. Investigation of neural progenitor cell induced angiogenesis after embolic stroke in rat using MRI. Neuroimage 28, 698–707. doi:10.1016/j.neuroimage.2005.06.063
Jilani, S.M., Murphy, T.J., Thai, S.N.M., Eichmann, A., Alva, J. a, Iruela-Arispe, M.L., 2003. Selective binding of lectins to embryonic chicken vasculature. J. Histochem. Cytochem. 51, 597–604. doi:10.1177/002215540305100505
Jr, W.J.M., Bartus, R.T., Siff, J., Davis, C.S., Lozano, A., Boulis, N., Vitek, J., Stacy, M., Turner, D., Verhagen, L., Bakay, R., Watts, R., Guthrie, B., Jankovic, J., Simpson, R., Tagliati, M., Alterman, R., Stern, M., Baltuch, G., Starr, P.A., Larson, P.S., Ostrem, J.L., Nutt, J., Kieburtz, K., Kordower, J.H., Olanow, C.W., 2010. Gene delivery of AAV2-neurturin for Parkinson ' s disease : a double-blind , randomised , controlled trial 9. doi:10.1016/S1474-4422(10)70254-4
Kamijo, K., Takeda, Y., 2010. Regular physical activity improves executive function during task switching in young adults. Int. J. Psychophysiol. 75, 304–311. doi:10.1016/j.ijpsycho.2010.01.002
Kang, H.M., Sohn, I., Jung, J., Jeong, J.W., Park, C., 2015. Age-related changes in pial arterial structure and blood flow in mice. Neurobiol. Aging 37, 161–170. doi:10.1016/j.neurobiolaging.2015.09.008
Kawashima, H., Sueyoshi, S., Li, H., Yamamoto, K., Osawa, T., 1990. Carbohydrate binding specificities of several poly- N -acetyllactosamine-binding lectins. Glycoconj. J. 7, 323–334.
Kempermann, G., Kuhn, H.G., Gage, F.H., 1997. More hippocampal neuons in adult mice livign in anenriched environment. Nature 386, 493–495.

Khalil, H., Quinn, L., van Deursen, R., Dawes, H., Playle, R., Rosser, A., Busse, M., 2013a. What effect does a structured home-based exercise programme have on people with Huntington's disease? A randomized, controlled pilot study. Clin. Rehabil. 27, 646–58. doi:10.1177/0269215512473762

Khalil, H., Quinn, L., van Deursen, R., Dawes, H., Playle, R., Rosser, A., Busse, M., 2013b. What effect does a structured home-based exercise programme have on people with Huntington's disease? A randomized, controlled pilot study. Clin. Rehabil. 27, 646–58. doi:10.1177/0269215512473762

Kim, S.G., 1995. Quantification of Relative Cerebral Blood-Flow Change by Flow-Sensitive Alternating Inversion-Recovery (FAIR) Technique - Application to Functional Mapping. Magn. Reson. Med. 34, 293–301. doi:DOI 10.1002/mrm.1910340303

Kim, Y.-M., Ji, E.-S., Kim, S.-H., Kim, T.-W., Ko, I.-G., Jin, J.-J., Kim, C.-J., Kim, T.-W., Kim, D.-H., 2015. Treadmill exercise improves short-term memory by enhancing hippocampal cell proliferation in quinolinic acid-induced Huntington's disease rats. J. Exerc. Rehabil. 11, 5–11. doi:10.12965/jer.150182

Kirkin, V., Mcewan, D.G., Novak, I., Dikic, I., 2009. Review A Role for Ubiquitin in Selective Autophagy. Mol. Cell 34, 259–269. doi:10.1016/j.molcel.2009.04.026

Kirkwood, S.C., Siemers, E., Hodes, M.E., Conneally, P.M., Christian, J.C., Foroud, T., 2000. Subtle changes among presymptomatic carriers of the Huntington's disease gene. J. Neurol. Neurosurg. Psychiatry 69, 773–779. doi:10.1136/jnnp.69.6.773

Kiselev, V.G., 2005. Transverse relaxation effect of MRI contrast agents: A crucial issue for quantitative measurements of cerebral perfusion. J. Magn. Reson. Imaging 22, 693–696. doi:10.1002/jmri.20452

Kitamura, A., Kubota, H., Pack, C., Matsumoto, G., Hirayama, S., Takahashi, Y., Kimura, H., Kinjo, M., Morimoto, R.I., Nagata, K., 2006. Cytosolic chaperonin prevents polyglutamine toxicity with altering the aggregation state. Nat. Cell Biol. 8. doi:10.1038/ncb1478

Kleim, J.A., Cooper, N.R., VandenBerg, P.M., 2002. Exercise induces angiogenesis but does not alter movement representations within rat motor cortex. Brain Res. 934, 1–6. doi:10.1016/S0006-8993(02)02239-4

Kobilo, T., Yuan, C., van Praag, H., 2011. Endurance factors improve hippocampal neurogenesis and spatial memory in mice. Learn. Mem. 18, 103–7. doi:10.1101/lm.2001611

Kordasiewicz, H.B., Stanek, L.M., Wancewicz, E. V, Mazur, C., Melissa, M., Pytel, K. a, Artates, J.W., Weiss, A., Cheng, S.H., Shihabuddin, L.S., Hung, G., Bennett, C.F., Cleveland, D.W., 2012. Sustained therapeutic reversal of Huntington's disease by transient repression of huntingtin synthesis. Neuron 74, 1031–1044. doi:10.1016/j.neuron.2012.05.009.Sustained

Kullmann, D.M., Asztely, F., 1998. Extrasynaptic glutamate spillover in the hippocampus: Evidence and implications. Trends Neurosci. 21, 8–14. doi:10.1016/S0166-2236(97)01150-8

Kuroda, S., Houkin, K., Kamiyama, H., Mitsumori, K., Iwasaki, Y., Abe, H., Yonas, H., Wechsler, L.R., Nemoto, E., Pindzola, R., 2001. Long-Term Prognosis of Medically Treated Patients With Internal Carotid or Middle Cerebral Artery Occlusion: Can Acetazolamide Test Predict It? Stroke 32, 2110–2116. doi:10.1161/hs0901.095692

Kwong, K.K., Chesler, D.A., Weisskoff, R.M., Donahue, K.M., Davis, T.L., Ostergaard, L., Campbell, T.A., Rosen, B.R., 1995. MR perfusion studies with

T1-weighted echo planar imaging. Magn. Reson. Med. 34, 878–887. doi:10.1002/mrm.1910340613

Labbadia, J., Novoselov, S.S., Bett, J.S., Weiss, A., Paganetti, P., Bates, G.P., Cheetham, M.E., 2012. modification of high molecular weight complexes 1180–1196. doi:10.1093/brain/aws022

LaManna, J.C., Chavez, J.C., Pichiule, P., 2004. Structural and functional adaptation to hypoxia in the rat brain. J. Exp. Biol. 207, 3163–3169. doi:10.1242/jeb.00976

Landwehrmeyer, G.B., Dubois, B., Ye, J.G. De, Kremer, B., Gaus, W., Kraus, P.H., Przuntek, H., Dib, M., Doble, A., Fischer, W., Ludolph, A.C., 2007. Riluzole in Huntington ' s Disease : A 3-Year, Randomized Controlled Study. Ann. Neurol. 4, 262–272. doi:10.1002/ana.21181

Langbehn, D.R., Brinkman, R.R., Falush, D., Paulsen, J.S., Hayden, M.R., 2004. A new model for prediction of the age of onset and penetrance for Huntington ' s disease based on CAG length. Clin. Genet. 65, 267–277. doi:10.1111/j.1399-0004.2004.00241.x

Langbehn, D.R., Hayden, M., Paulsen, J.S., Group, P.-H.I. of the H.S., 2011. CAG-Repeat Length and the Age of Onset in Huntington Disease (HD): A Review and Validation Study of Statistical Approaches. Am. J. Med. Genet. Part B Neuropsychiatr. Genet. 153B, 397–408. doi:10.1002/ajmg.b.30992.CAG-Repeat

Lange, H., Thorner, G., Hopf, A., Schroder, K.F., 1976. Morphometric studies of the neuropathological changes in choreatic diseases. J. Neurol. Sci. 28, 401–425. doi:10.1016/0022-510X(76)90114-3

Lassen, N.A., 1959. Cerebral Blood Flow and Oxygen Consumption in Man. Physiol. Rev. 39, 183–238.

Lauenroth, A., Ioannidis, A.E., Teichmann, B., 2016. Influence of combined physical and cognitive training on cognition: a systematic review. BMC Geriatr. 16, 141–154. doi:10.1186/s12877-016-0315-1

Laurent, S., Alivon, M., Beaussier, H., Boutouyrie, P., 2012. Aortic stiffness as a tissue biomarker for predicting future cardiovascular events in asymptomatic hypertensive subjects. Ann. Med. 44, S93–S97. doi:10.3109/07853890.2011.653398

Lauritzen, H.P.M.M., Brandauer, J., Schjerling, P., Koh, H.J., Treebak, J.T., Hirshman, M.F., Galbo, H., Goodyear, L.J., 2013. Contraction and AICAR stimulate IL-6 vesicle depletion from skeletal muscle fibers in vivo. Diabetes 62, 3081–3092. doi:10.2337/db12-1261

Leenders, K.L., Perani, D., Lammertsma, A.A., Heather, J.D., Buckingham, P., Healy, M.J.R., Gibbs, J.M., Wise, R.J.S., Hatazawa, J., Herold, S., Beaney, R.P., Brooks, D.J., Spinks, T., Rhodes, C., Frackowiak, R.S.J., Jones, T., 1990. CEREBRAL BLOOD FLOW , BLOOD VOLUME AND OXYGEN UTILIZATION NORMAL VALUES AND EFFECT OF AGE. Brain 113, 27–47.

Leithner, C., Gertz, K., Schröck, H., Priller, J., Prass, K., Steinbrink, J., Villringer, A., Endres, M., Lindauer, U., Dirnagl, U., Royl, G., 2008. A flow sensitive alternating inversion recovery (FAIR)-MRI protocol to measure hemispheric cerebral blood flow in a mouse stroke model. Exp. Neurol. 210, 118–127. doi:10.1016/j.expneurol.2007.10.003

Leithner, C., Royl, G., Offenhauser, N., Füchtemeier, M., Kohl-Bareis, M., Villringer, A., Dirnagl, U., Lindauer, U., 2010. Pharmacological uncoupling of activation induced increases in CBF and CMRO2. J. Cereb. Blood Flow Metab. 30, 311–322. doi:10.1038/jcbfm.2009.211

Li, J., Ding, Y.H., Rafols, J.A., Lai, Q., McAllister, J.P., Ding, Y., 2005. Increased astrocyte proliferation in rats after running exercise. Neurosci. Lett. 386, 160–164. doi:10.1016/j.neulet.2005.06.009

Li, Y., Shen, Q., Huang, S., Li, W., Muir, E.R., Long, J., Duong, T.Q., 2015. Cerebral angiography, blood flow and vascular reactivity in progressive hypertension. Neuroimage 111, 329–337. doi:10.1016/j.neuroimage.2015.02.053

Lin, C.-Y., Hsu, Y.-H., Lin, M.-H., Yang, T.-H., Chen, H.-M., Chen, Y.-C., Hsiao, H.-Y., Chen, C.-C., Chern, Y., Chang, C., 2013. Neurovascular abnormalities in humans and mice with Huntington's disease. Exp. Neurol. 250, 20–30. doi:10.1016/j.expneurol.2013.08.019

Liu, J.Z., Dai, T.H., Sahgal, V., Brown, R.W., Yue, G.H., 2002. Nonlinear cortical modulation of muscle fatigue: a functional MRI study. Brain Res. 957, 320–9.

Liu, T.T., Wong, E.C., 2005. A signal processing model for arterial spin labeling functional MRI. Neuroimage 24, 207–15. doi:10.1016/j.neuroimage.2004.09.047

Liu, Y., Zhu, X., Feinberg, D., Guenther, M., Gregori, J., Weiner, M.W., Schuff, N., 2011. Arterial Spin Labeling MRI Study of Age and Gender Effects on Brain Perfusion Hemodynamics 0, 1–11. doi:10.1002/mrm.23286

Lobsiger, C.S., Cleveland, D.W., 2011. Glial cells as intrinsic components of non-cell autonomous neurodegenerative disease. Nat. Neurosci. 10, 1355–1360. doi:10.1038/nn1988.Glial

Lombardi, M.S., Jaspers, L., Spronkmans, C., Gellera, C., Taroni, F., Di, E., Di, S., Kaemmerer, W.F., 2009. A majority of Huntington ' s disease patients may be treatable by individualized allele-speci fi c RNA interference. Exp. Neurol. 217, 312–319. doi:10.1016/j.expneurol.2009.03.004

Lopez-Lopez, C., LeRoith, D., Torres-Aleman, I., 2004. Insulin-like growth factor I is required for vessel remodeling in the adult brain. Proc. Natl. Acad. Sci. U. S. A. 101, 9833–9838. doi:10.1073/pnas.0400337101

Lu, H., Clingman, C., Golay, X., van Zijl, P.C.M., 2004. Determining the longitudinal relaxation time (T1) of blood at 3.0 Tesla. Magn. Reson. Med. 52, 679–82. doi:10.1002/mrm.20178

Lu, H., Xu, F., Rodrigue, K.M., Kennedy, K.M., Cheng, Y., Flicker, B., Hebrank, A.C., Uh, J., Park, D.C., 2011. Alterations in cerebral metabolic rate and blood supply across the adult lifespan. Cereb. Cortex 21, 1426–1434. doi:10.1093/cercor/bhq224

Luh, W.M., Wong, E.C., Bandettini, P. a., Hyde, J.S., 1999. QUIPSS II with thin-slice TI1Q periodic saturation: A method for improving accuracy of quantitative perfusion imaging using pulsed arterial spin labeling. Magn. Reson. Med. 41, 1246–1254. doi:10.1002/(SICI)1522-2594(199906)41:6<1246::AID-MRM22>3.0.CO;2-N

Ma, Y., Eidelberg, D., 2015. Functional Imaging of Cerebral Blood Flow and Glucose Metabolism in Parkinson's Disease and Huntington's Disease. Mol. Imaging Biol. 2, 223–233. doi:10.14440/jbm.2015.54.A

Mairbäurl, H., 2013. Red blood cells in sports: Effects of exercise and training on oxygen supply by red blood cells. Front. Physiol. 4 NOV, 1–13. doi:10.3389/fphys.2013.00332

Marais, L., Stein, D.J., Daniels, W.M.U., 2009. Exercise increases BDNF levels in the striatum and decreases depressive-like behavior in chronically stressed rats. Metab. Brain Dis. 24, 587–597. doi:10.1007/s11011-009-9157-2

Marshall, R.S., Lazar, R.M., 2011. Pumps, aqueducts, and drought management:

Vascular physiology in vascular cognitive impairment. Stroke 42, 221–226. doi:10.1161/STROKEAHA.110.595645

Marzinzik, F., Wahl, M., Schneider, G., Kupsch, A., Curio, G., Klostermann, F., 2008. The Human Thalamus is Crucially Involved in Executive Control Operations 1903–1914.

Mattis, V.B., Svendsen, S.P., Ebert, A., Svendsen, C.N., King, A.R., Casale, M., Winokur, S.T., Batugedara, G., Vawter, M., Peter, J., Gillis, T., Mysore, J., Li, J., Seong, I., Shen, Y., Arbez, N., Juopperi, T., Ratovitski, T., Chiang, J.H., Kim, R., Chighladze, E., Watkin, E., Zhong, C., Makri, G., Cole, R.N., 2013. Induced Pluripotent Stem Cells from Patients with Huntington's Disease Show CAG-Repeat-Expansion-Associated Phenotypes. Cell Stem Cell 11, 264–278. doi:10.1016/j.stem.2012.04.027.Induced

Mazzocchi-Jones, D., D??br??ssy, M., Dunnett, S.B., 2009. Embryonic striatal grafts restore bi-directional synaptic plasticity in a rodent model of Huntington's disease. Eur. J. Neurosci. 30, 2134–2142. doi:10.1111/j.1460-9568.2009.07006.x

Menalled, L.B., 2005. Knock-in mouse models of Huntington's disease. NeuroRx 2, 465–470. doi:10.1602/neurorx.2.3.465

Menalled, L.B., Kudwa, A.E., Miller, S., Fitzpatrick, J., Watson-Johnson, J., Keating, N., Ruiz, M., Mushlin, R., Alosio, W., McConnell, K., Connor, D., Murphy, C., Oakeshott, S., Kwan, M., Beltran, J., Ghavami, A., Brunner, D., Park, L.C., Ramboz, S., Howland, D., 2012. Comprehensive Behavioral and Molecular Characterization of a New Knock-In Mouse Model of Huntington's Disease: ZQ175. PLoS One 7. doi:10.1371/journal.pone.0049838

Merola, A., Murphy, K., Stone, A.J., Germuska, M. a, Griffeth, V.E.M., Blockley, N.P., Buxton, R.B., Wise, R.G., 2016. Measurement of oxygen extraction fraction ( OEF ): an optimised BOLD signal model for use with hypercapnic and hyperoxic calibration. Neuroimage 5–6. doi:10.1016/j.neuroimage.2016.01.021

Micó-Amigo, M.E., Kingma, I., Ainsworth, E., Walgaard, S., Niessen, M., van Lummel, R.C., van Dieën, J.H., 2016. A novel accelerometry-based algorithm for the detection of step durations over short episodes of gait in healthy elderly. J. Neuroeng. Rehabil. 13, 38. doi:10.1186/s12984-016-0145-6

Milman, U., Atias, H., Weiss, A., Mirelman, A., Hausdorff, J.M., 2014. Can cognitive remediation improve mobility in patients with parkinson's disease? Findings from a 12 week pilot study. J. Parkinsons. Dis. 4, 37–44. doi:10.3233/JPD-130321

Mitchell, G.F., Gudnason, V., Launer, L.J., Aspelund, T., Harris, T.B., 2008. Hemodynamics of increased pulse pressure in older women in the community-based age, gene/environment susceptibility-Reykjavik study. Hypertension 51, 1123–1128. doi:10.1161/HYPERTENSIONAHA.107.108175

Mitchell, G.F., Van Buchem, M. a., Sigurdsson, S., Gotal, J.D., Jonsdottir, M.K., Kjartansson, Ó., Garcia, M., Aspelund, T., Harris, T.B., Gudnason, V., Launer, L.J., 2011. Arterial stiffness, pressure and flow pulsatility and brain structure and function: The Age, Gene/Environment Susceptibility-Reykjavik Study. Brain 134, 3398–3407. doi:10.1093/brain/awr253

Miyachi, M., Donato, A.J., Yamamoto, K., Takahashi, K., Gates, P.E., Moreau, K.L., Tanaka, H., 2003. Greater age-related reductions in central arterial compliance in resistance-trained men. Hypertension 41, 130–135. doi:10.1161/01.HYP.0000047649.62181.88

Mo, C., Hannan, A.J., Renoir, T., 2015. Environmental factors as modulators of

neurodegeneration: Insights from gene–environment interactions in Huntington's disease. Neurosci. Biobehav. Rev. 52, 178–192. doi:10.1016/j.neubiorev.2015.03.003
Moulton, C.D., Mrcp, M.A., 2014. of Pharmacological Treatments for Depressive Symptoms in Huntington ' s Disease 29, 1556–1561. doi:10.1002/mds.25980
Mujika, I., Padilla, S., 2001. Cardiorespiratory and metabolic characteristics of detraining in humans. Med. Sci. Sports Exerc. 33, 413–21.
Muramatsu, F., Kidoya, H., Naito, H., Sakimoto, S., Takakura, N., 2013. microRNA-125b inhibits tube formation of blood vessels through translational suppression of VE-cadherin. Oncogene 32, 414–21. doi:10.1038/onc.2012.68
Murphy, K., Harris, A.D., Diukova, A., Evans, C.J., Lythgoe, D.J., Zelaya, F., Wise, R.G., 2011a. Pulsed arterial spin labeling perfusion imaging at 3 T: estimating the number of subjects required in common designs of clinical trials. Magn. Reson. Imaging 29, 1382–9. doi:10.1016/j.mri.2011.02.030
Murphy, K., Harris, A.D., Wise, R.G., 2011b. Robustly measuring vascular reactivity differences with breath-hold: Normalising stimulus-evoked and resting state BOLD fMRI data. Neuroimage 54, 369–379. doi:10.1016/j.neuroimage.2010.07.059
Murrell, C.J., Cotter, J.D., Thomas, K.N., Lucas, S.J.E., Williams, M.J.A., Ainslie, P.N., 2013. Cerebral blood flow and cerebrovascular reactivity at rest and during sub-maximal exercise: Effect of age and 12-week exercise training. Age (Omaha). 35, 905–920. doi:10.1007/s11357-012-9414-x
Myllylä, T., Korhonen, V., Vihriälä, E., Sorvoja, H., Hiltunen, T., Tervonen, O., Kiviniemi, V., 2012. Human heart pulse wave responses measured simultaneously at several sensor placements by two MR-compatible fibre optic methods. J. Sensors 2012. doi:10.1155/2012/769613
Neeper, S. a, Gómez-Pinilla, F., Choi, J., Cotman, C.W., 1996. Physical activity increases mRNA for brain-derived neurotrophic factor and nerve growth factor in rat brain. Brain Res. 726, 49–56.
Nelson, M.D., Petersen, S.R., Dlin, R.A., 2010. Effects of age and counseling on the cardiorespiratory response to graded exercise. Med. Sci. Sports Exerc. 42, 255–264. doi:10.1249/MSS.0b013e3181b0e534
Newcomer, S.C., Thijssen, D.H.J., Green, D.J., 2011. Effects of exercise on endothelium and endothelium/smooth muscle cross talk: role of exercise-induced hemodynamics. J. Appl. Physiol. 111, 311–320. doi:10.1152/japplphysiol.00033.2011
O'Callaghan, C., Bertoux, M., Hornberger, M., 2014. Beyond and below the cortex: the contribution of striatal dysfunction to cognition and behaviour in neurodegeneration. J. Neurol. Neurosurg. Psychiatry 85, 371–8. doi:10.1136/jnnp-2012-304558
O'Connor, J.P.B., Tofts, P.S., Miles, K.A., Parkes, L.M., Thompson, G., Jackson, A., 2011. Dynamic contrast-enhanced imaging techniques: CT and MRI. Br. J. Radiol. 84. doi:10.1259/bjr/55166688
O'Rourke, M.F., Hashimoto, J., 2007. Mechanical Factors in Arterial Aging. A Clinical Perspective. J. Am. Coll. Cardiol. 50, 1–13. doi:10.1016/j.jacc.2006.12.050
O'Rourke, M.F., Safar, M.E., 2005. Relationship Between Aortic Stiffening and Microvascular Disease in Brain and Kidney: Cause and Logic of Therapy. Hypertension 46, 200–204. doi:10.1161/01.HYP.0000168052.00426.65
O'Suilleabhain, P., Dewey, Jr, R.B., 2003. A Randomized Trial of Amantadine in Huntington Disease. Arch. Neurol. 60, 996–998.

Ogoh, S., Ainslie, P.N., 2009. Cerebral blood flow during exercise : mechanisms of regulation 107, 1370–1380. doi:10.1152/japplphysiol.00573.2009.
Ondo, W.G., Mejia, N.I., Hunter, C.B., 2007. A pilot study of the clinical efficacy and safety of memantine for Huntington's disease. Parkinsonism Relat. Disord. 13, 453–4. doi:10.1016/j.parkreldis.2006.08.005
Orth, M., Handley, O.J., Schwenke, C., Dunnett, S.B., Wild, E.J., Tabrizi, S.J., Landwehrmeyer, G.B., 2011. Observing Huntington's disease: the European Huntington's Disease Network's REGISTRY. J. Neurol. Neurosurg. Psychiatry 82, 1409–12. doi:10.1136/jnnp.2010.217513
Ouchi, N., Shibata, R., Walsh, K., 2005. AMP-activated protein kinase signaling stimulates VEGF expression and angiogenesis in skeletal muscle. Circ. Res. 96, 838–846. doi:10.1161/01.RES.0000163633.10240.3b
Owen, A.M., McMillan, K.M., Laird, A.R., Bullmore, E., 2005. N-back working memory paradigm: a meta-analysis of normative functional neuroimaging studies. Hum. Brain Mapp. 25, 46–59. doi:10.1002/hbm.20131
Palmer, T.D., Willhoite, A.R., Gage, F.H., 2000. Vascular Niche for Adult Hippocampal 494, 479–494.
Pang, T.Y.C., Stam, N.C., Nithianantharajah, J., Howard, M.L., Hannan, A.J., 2006. Differential effects of voluntary physical exercise on behavioral and brain-derived neurotrophic factor expression deficits in huntington's disease transgenic mice. Neuroscience 141, 569–584. doi:10.1016/j.neuroscience.2006.04.013
Papp, K. V., Snyder, P.J., Mills, J.A., Duff, K., Westervelt, H.J., Long, J.D., Lourens, S., Paulsen, J.S., 2013. Measuring executive dysfunction longitudinally and in relation to genetic burden, brain volumetrics, and depression in prodromal huntington disease. Arch. Clin. Neuropsychol. 28, 156–168. doi:10.1093/arclin/acs105
Papworth, M., Kolasinska, P., Minczuk, M., 2006. Designer zinc-finger proteins and their applications 366, 27–38. doi:10.1016/j.gene.2005.09.011
Pardo Di, A., Maglione, V., Alpaugh, M., Horkey, M., Atwal, R.S., Sassone, J., 2012. Ganglioside GM1 induces phosphorylation of mutant huntingtin and restores normal motor behavior in Huntington disease mice. PNAS 109, 1–6. doi:10.1073/pnas.1114502109
París, A.P., Saleta, H.G., de la Cruz Crespo Maraver, M., Silvestre, E., Freixa, M.G., Torrellas, C.P., Pont, S.A., Nadal, M.F., Garcia, S.A., Bartolomé, M.V.P., Fernández, V.L., Bayés, À.R., 2011. Blind randomized controlled study of the efficacy of cognitive training in Parkinson's disease. Mov. Disord. 26, 1251–1258. doi:10.1002/mds.23688
Parker, J.A., Arango, M., Abderrahmane, S., Lambert, E., Tourette, C., Catoire, H., Néri, C., 2005. Resveratrol rescues mutant polyglutamine cytotoxicity in nematode and mammalian neurons. Nat. Genet. 37, 349–350. doi:10.1038/ng1534
Patenaude, B., Smith, S.M., Kennedy, D.N., Jenkinson, M., 2012. A Bayesian model of shape and appearance for subcortical brain segmentation. Neuroimage 56, 907–922. doi:10.1016/j.neuroimage.2011.02.046.A
Paulsen, J.S., 2011. Cognitive impairment in Huntington disease: Diagnosis and treatment. Curr. Neurol. Neurosci. Rep. 11, 474–483. doi:10.1007/s11910-011-0215-x
Paulsen, J.S., Langbehn, D.R., Stout, J.C., Aylward, E., Ross, C. a, Nance, M., Guttman, M., Johnson, S., MacDonald, M., Beglinger, L.J., Duff, K., Kayson, E., Biglan, K., Shoulson, I., Oakes, D., Hayden, M., 2008. Detection of

Huntington's disease decades before diagnosis: the Predict-HD study. J. Neurol. Neurosurg. Psychiatry 79, 874–880. doi:10.1136/jnnp.2007.128728

Paulsen, J.S., Long, J.D., Ross, C.A., Harrington, D.L., Erwin, C.J., Williams, J.K., Westervelt, H.J., Johnson, H.J., Aylward, E.H., Zhang, Y., Bockholt, H.J., Barker, R.A., 2014. Prediction of manifest huntington's disease with clinical and imaging measures: A prospective observational study. Lancet Neurol. 13, 1193–1201. doi:10.1016/S1474-4422(14)70238-8

Paulsen, J.S., Wang, C., Duff, K., Barker, R., Nance, M., Beglinger, L., Moser, D., Williams, J.K., Simpson, S., Langbehn, D., Kammen, D.P. Van, 2010. Challenges assessing clinical endpoints in early Huntington disease. Mov. Disord. 25, 2595–2603. doi:10.1002/mds.23337.Challenges

Paulsen, J.S., Zimbelman, J.L., Hinton, S.C., Langbehn, D.R., Leveroni, C.L., Benjamin, M.L., Reynolds, N.C., Rao, S.M., 2004. fMRI Biomarker of Early Neuronal Dysfunction in Presymptomatic Huntington ' s Disease 51358, 1715–1721.

Penney, J.B., Vonsattel, J., E, M.M., Gusella, J.F., Myers, R.H., 1997. CAG Repeat Number Governs the Development Rate of Pathology in Huntington's Disease. Ann. Neurol. 41, 3696–3699.

Pereira, A.C., Huddleston, D.E., Brickman, A.M., Sosunov, A. a, Hen, R., McKhann, G.M., Sloan, R., Gage, F.H., Brown, T.R., Small, S. a, 2007. An in vivo correlate of exercise-induced neurogenesis in the adult dentate gyrus. Proc. Natl. Acad. Sci. U. S. A. 104, 5638–43. doi:10.1073/pnas.0611721104

Peterson, E.C., Wang, Z., Britz, G., 2011. Regulation of cerebral blood flow. Int. J. Vasc. Med. 2011. doi:10.1155/2011/823525

Poels, M.M.F., Zaccai, K., Verwoert, G.C., Vernooij, M.W., Hofman, A., Van Der Lugt, A., Witteman, J.C.M., Breteler, M.M.B., Mattace-Raso, F.U.S., Ikram, M.A., 2012. Arterial stiffness and cerebral small vessel disease: The rotterdam scan study. Stroke 43, 2637–2642. doi:10.1161/STROKEAHA.111.642264

Potter, M.C., Yuan, C., Ottenritter, C., Mughal, M., van Praag, H., 2010. Exercise is not beneficial and may accelerate symptom onset in a mouse model of Huntington's disease. PLos Curr. 2, 1–23. doi:10.1371/currents.RRN1201.Authors

Prichard, J., Rothman, D., Novotny, E., Petroff, O., Kuwabara, T., Avison, M., Howseman, A., Hanstock, C., Shulman, R., 1991. Lactate rise detected by 1H NMR in human visual cortex during physiologic stimulation. Proc. Natl. Acad. Sci. U. S. A. 88, 5829–31. doi:10.1073/pnas.88.13.5829

Prins, N.D., Van Dijk, E.J., Den Heijer, T., Vermeer, S.E., Jolles, J., Koudstaal, P.J., Hofman, A., Breteler, M.M.B., 2005. Cerebral small-vessel disease and decline in information processing speed, executive function and memory. Brain 128, 2034–2041. doi:10.1093/brain/awh553

Quinn, L., Hamana, K., Kelson, M., Dawes, H., Collett, J., Townson, J., Roos, R., van der Plas, A.A., Reilmann, R., Frich, J.C., Rickards, H., Rosser, A., Busse, M., 2016a. A randomized, controlled trial of a multi-modal exercise intervention in Huntington's disease. Parkinsonism Relat. Disord. 31, 46–52. doi:10.1016/j.parkreldis.2016.06.023

Quinn, L., Hamana, K., Kelson, M., Dawes, H., Collett, J., Townson, J., Roos, R., van der Plas, A., Reilmann, R., Frich, J., Rickards, H., Rosser, A., Busse, M., 2016b. A randomized, controlled trial of a multi-modal exercise intervention in Huntington's disease. Parkinsonism Relat. Disord. 1–7. doi:10.1016/j.parkreldis.2016.06.023

Quinn, L., Rao, A., 2002. Physical Therpay for Peoplewith Huntington's Disease:

Current perspectives and Case Report. Neurol. Rep. 26, 145–153.
Quinn, L., Rosser, A., Busse, M., 2013. Movement Disorders Huntington ' s Disease Critical Features in the Development of Exercise-based Interventions for People with Huntington ' s Disease 10–13.
Radák, Z., Kaneko, T., Tahara, S., Nakamoto, H., Pucsok, J., Sasvári, M., Nyakas, C., Goto, S., 2001. Regular exercise improves cognitive function and decreases oxidative damage in rat brain. Neurochem. Int. 38, 17–23. doi:10.1016/S0197-0186(00)00063-2
Ransome, M.I., Hannan, A.J., 2013. Impaired basal and running-induced hippocampal neurogenesis coincides with reduced Akt signaling in adult R6/1 HD mice. Mol. Cell. Neurosci. 54, 93–107. doi:10.1016/j.mcn.2013.01.005
Rattray, I., Smith, E., Gale, R., Matsumoto, K., Bates, G.P., Modo, M., 2013. Correlations of Behavioral Deficits with Brain Pathology Assessed through Longitudinal MRI and Histopathology in the R6/2 Mouse Model of HD. PLoS One 8, e60012. doi:10.1371/journal.pone.0060012
Ravikumar, B., Vacher, C., Berger, Z., Davies, J.E., Luo, S., Oroz, L.G., Scaravilli, F., Easton, D.F., Duden, R., Kane, C.J.O., Rubinsztein, D.C., 2004. Inhibition of mTOR induces autophagy and reduces toxicity of polyglutamine expansions in fly and mouse models of Huntington disease 36, 585–595. doi:10.1038/ng1362
Renoir, T., Pang, T.Y.C., Mo, C., Chan, G., Chevarin, C., Lanfumey, L., Hannan, A.J., 2013. Differential effects of early environmental enrichment on emotionality related behaviours in Huntington's disease transgenic mice. J. Physiol. 591, 41–55. doi:10.1113/jphysiol.2012.239798
Rhyu, I.J., Bytheway, J. a, Kohler, S.J., Lange, H., Lee, K.J., Boklewski, J., McCormick, K., Williams, N.I., Stanton, G.B., Greenough, W.T., Cameron, J.L., 2010. Effects of aerobic exercise training on cognitive function and cortical vascularity in monkeys. Neuroscience 167, 1239–48. doi:10.1016/j.neuroscience.2010.03.003
Rietberg, M.B., Brooks, D., Uitdehaag, Bernar, M.J., Kwakkel, G., 2005. Exercise therapy for multiple sclerosis. Cochrane Database Syst. Rev. doi:10.1002/14651858.CD003980.pub2
Rivard, A., Fabre, J.E., Silver, M., Chen, D., Murohara, T., Kearney, M., Magner, M., Asahara, T., Isner, J.M., 1999. Age-dependent impairment of angiogenesis. Circulation 99, 111–20. doi:10.1161/01.CIR.99.1.111
Robertson, R.T., Levine, S.T., Haynes, S.M., Gutierrez, P., Baratta, J.L., Tan, Z., Longmuir, K.J., 2014. Use of labeled tomato lectin for imaging vasculature structures. Histochem. Cell Biol. 143, 225–234. doi:10.1007/s00418-014-1301-3
Rohrer, D., Salmon, D.P., Wixted, J.T., Paulsen, J.S., 1999. The disparate effects of Alzheimer's disease and Huntington's disease on semantic memory. Neuropsychology 13, 381–388. doi:10.1037/0894-4105.13.3.381
Roman, G.C., Kalaria, R.N., 2006. Vascular determinants of cholinergic deficits in Alzheimer disease and vascular dementia. Neurobiol. Aging 27, 1769–1785. doi:10.1016/j.neurobiolaging.2005.10.004
Rosas, H.D., Koroshetz, W.J., Chen, Y.I., Skeuse, C., Vangel, M., Cudkowicz, M.E., Caplan, K., Marek, K., Seidman, L.J., Makris, N., Jenkins, B.G., Goldstein, J.M., 2003. Evidence for more widespread cerebral pathology in early HD: an MRI-based morphometric analysis. Neurology 60, 1615–1620. doi:10.1212/WNL.62.3.523-a
Rosenstein, J.M., Mani, N., Silverman, W.F., Krum, J.M., 1998. Patterns of brain

angiogenesis after vascular endothelial growth factor administration in vitro and in vivo. Proc. Natl. Acad. Sci. U. S. A. 95, 7086–91.

Ross, C.A., Aylward, E.H., Wild, E.J., Langbehn, D.R., Jeffrey, D., Warner, J.H., Scahill, R.I., Leavitt, B.R., Stout, J.C., Paulsen, J.S., Unschuld, P.G., Wexler, A.R., Margolis, R.L., Tabrizi, S.J., 2014. Huntington disease: natural history, biomarkers and prospects for therapeutics Christopher A. Ross, Elizabeth H. Aylward, Edward J. Wild, Douglas R. Langbehn, Jeffrey D. Long, John H. Warner, Rachael I. Scahill, Blair R. Leavitt, Julie C. Stout, Jane S. P.

Ruitenberg, A., Den Heijer, T., Bakker, S.L.M., Van Swieten, J.C., Koudstaal, P.J., Hofman, A., Breteler, M.M.B., 2005. Cerebral hypoperfusion and clinical onset of dementia: The Rotterdam Study. Ann. Neurol. 57, 789–794. doi:10.1002/ana.20493

Sagare, A.P., Bell, R.D., Zlokovic, B. V., 2012. Neurovascular dysfunction and faulty amyloid beta-peptide clearance in Alzheimer disease. Cold Spring Harb. Perspect. Med. 2, 1–17. doi:10.1101/cshperspect.a011452

Sahay, A., Scobie, K.N., Hill, A.S., O'Carroll, C.M., Kheirbek, M. a, Burghardt, N.S., Fenton, A. a, Dranovsky, A., Hen, R., 2011. Increasing adult hippocampal neurogenesis is sufficient to improve pattern separation. Nature 472, 466–70. doi:10.1038/nature09817

Saint-Geniez, M., D'Amore, P.A., 2004. Development and pathology of the hyaloid, choroidal and retinal vasculature. Int. J. Dev. Biol. 48, 1045–1058. doi:10.1387/ijdb.041895ms

Sallis, J.F., Saelens, B.E., 2000. Assessment of physical activity by self-report: status, limitations, and future directions. Res Q Exerc Sport 71, S1-14. doi:10.1080/02701367.2000.11082780

Sánchez, J., Nozhenko, Y., Palou, A., Rodríguez, A.M., 2013. Free fatty acid effects on myokine production in combination with exercise mimetics. Mol. Nutr. Food Res. 57, 1456–1467. doi:10.1002/mnfr.201300126

Sandrock, M., Schulze, C., Schmitz, D., Dickhuth, H.-H., Schmidt-Trucksaess, a, 2008. Physical activity throughout life reduces the atherosclerotic wall process in the carotid artery. Br. J. Sports Med. 42, 839–44. doi:10.1136/bjsm.2007.040014

Santisakultarm, T.P., Cornelius, N.R., Nishimura, N., Schafer, a. I., Silver, R.T., Doerschuk, P.C., Olbricht, W.L., Schaffer, C.B., 2012. In vivo two-photon excited fluorescence microscopy reveals cardiac- and respiration-dependent pulsatile blood flow in cortical blood vessels in mice. AJP Hear. Circ. Physiol. 302, H1367–H1377. doi:10.1152/ajpheart.00417.2011

Schallert, T., 2006. Behavioral Tests for Preclinical Intervention Assessment. NeuroRx 3, 497–504. doi:10.1016/j.nurx.2006.08.001

Schefer, V., Talan, M.I., 1996. Oxygen Consumption in Adult and Aged C57/BL6J Mice During Acue Treadmill Exercise of Different Intensity. Exp. Gerentology 31, 387–392.

Schummers, J., Yu, H., Sur, M., 2008. Tuned responses of astrocytes and their influence on hemodynamic signals in the visual cortex. Science 320, 1638–43. doi:10.1126/science.1156120

Segal, S.S., 2000. Integration of blood flow control to skletal muscle: key role of feed arteries. Acta Physiol. Scand. 168, 511–518.

Sešok, S., Bolle, N., Kobal, J., Bucik, V., Vodušek, D.B., 2014. Cognitive function in early clinical phase huntington disease after rivastigmine treatment. Psychiatr. Danub. 26, 239–48.

Sharpe, K., 2002. Development of reference ranges in elite athletes for markers of

altered erythropoiesis. Haematologica 1248–1257.
Shi, L.H., Luo, F., Woodward, D.J., Chang, J.Y., 2004. Neural responses in multiple basal ganglia regions during spontaneous and treadmill locomotion tasks in rats. Exp. Brain Res. 157, 303–314. doi:10.1007/s00221-004-1844-y
Silvestrini, M., Pasqualetti, P., Baruffaldi, R., Bartolini, M., Handouk, Y., Matteis, M., Moffa, F., 2006. Cerebrovascular Reactivity and Cognitive Decline in Patients With Alzheimer Disease. doi:10.1161/01.STR.0000206439.62025.97
Simmons, D.A., Belichenko, N.P., Yang, T., Condon, C., Monbureau, M., Shamloo, M., Jing, D., Massa, S.M., Longo, F.M., 2013. Neurobiology of Disease A Small Molecule TrkB Ligand Reduces Motor Impairment and Neuropathology in R6 / 2 and BACHD Mouse Models of Huntington ' s Disease 33, 18712–18727. doi:10.1523/JNEUROSCI.1310-13.2013
Skillings, E.A., Wood, N.I., Morton, A.J., 2014. Beneficial effects of environmental enrichment and food entrainment in the R6/2 mouse model of Huntington's disease. Brain Behav. 4, 675–686. doi:10.1002/brb3.235
Slessarev, M., Han, J., Mardimae, A., Prisman, E., Preiss, D., Volgyesi, G., Ansel, C., Duffin, J., Fisher, J.A., 2007. Prospective targeting and control of end-tidal CO 2 and O 2 concentrations 3, 1207–1219. doi:10.1113/jphysiol.2007.129395
Slow, E.J., Graham, R.K., Osmand, A.P., Devon, R.S., Lu, G., Deng, Y., Pearson, J., Vaid, K., Bissada, N., Wetzel, R., Leavitt, B.R., Hayden, M.R., 2005. Absence of behavioral abnormalities and neurodegeneration in vivo despite widespread neuronal huntingtin inclusions 102.
Slow, E.J., van Raamsdonk, J., Rogers, D., Coleman, S.H., Graham, R.K., Deng, Y., Oh, R., Bissada, N., Hossain, S.M., Yang, Y.Z., Li, X.J., Simpson, E.M., Gutekunst, C.A., Leavitt, B.R., Hayden, M.R., 2003. Selective striatal neuronal loss in a YAC128 mouse model of Huntington disease. Hum. Mol. Genet. 12, 1555–1567. doi:10.1093/hmg/ddg169
Smith, A.M., Spiegler, K.M., Sauce, B., Wass, C.D., Sturzoiu, T., Matzel, L.D., 2013. Voluntary aerobic exercise increases the cognitive enhancing effects of working memory training. Behav. Brain Res. 256, 626–35. doi:10.1016/j.bbr.2013.09.012
Smith, G.A., Rocha, E.M., McLean, J.R., Hayes, M.A., Izen, S.C., Isacson, O., Hallett, P.J., 2014. Progressive axonal transport and synaptic protein changes correlate with behavioral and neuropathological abnormalities in the heterozygous Q175 KI mouse model of Huntington's disease. Hum. Mol. Genet. 23, 4510–4527. doi:10.1093/hmg/ddu166
Smith, M.A., Brandt, J., Shadmehr, R., 2000. Motor Disorder in Huntington's Disease Begins as a Dysfunction in Error Feedback Control 403, 544–549. doi:10.1038/35000576.Motor
Smith, M.R., Syed, A., Lukacsovich, T., Purcell, J., Barbaro, B.A., Shane, A., Wei, S.R., Pollio, G., Magnoni, L., Scali, C., Massai, L., Franceschini, D., Camarri, M., Gianfriddo, M., Diodato, E., Thomas, R., Gokce, O., Tabrizi, S.J., Caricasole, A., Landwehrmeyer, B., Menalled, L., Murphy, C., Ramboz, S., Luthi-carter, R., Westerberg, G., Marsh, J.L., 2014. A potent and selective Sirtuin 1 inhibitor alleviates pathology in multiple animal and cell models of Huntington ' s disease 23, 2995–3007. doi:10.1093/hmg/ddu010
Smith, P.J., Blumenthal, J.A., Hoffman, B.M., Strauman, T.A., Welsh-bohmer, K., Jeffrey, N., Sherwood, A., 2011. NIH Public Access 72, 239–252. doi:10.1097/PSY.0b013e3181d14633.Aerobic
Smith, S.M., 2002. Fast robust automated brain extraction. Hum. Brain Mapp. 17,

143–55. doi:10.1002/hbm.10062
Smith, S.M., Brady, J., 1997. SUSAN - a new approach to low level image processing.
Sourbron, S., Ingrisch, M., Siefert, A., Reiser, M., Herrmann, K., 2009. Quantification of cerebral blood flow, cerebral blood volume, and blood-brain-barrier leakage with DCE-MRI. Magn. Reson. Med. 62, 205–17. doi:10.1002/mrm.22005
Stark, S.M., Yassa, M. a, Lacy, J.W., Stark, C.E.L., 2013. A task to assess behavioral pattern separation (BPS) in humans: Data from healthy aging and mild cognitive impairment. Neuropsychologia 51, 2442–9. doi:10.1016/j.neuropsychologia.2012.12.014
Stern, Y., 2009. Cognitive reserve. Neuropsychologia 47, 2015–2028. doi:10.1016/j.neuropsychologia.2009.03.004
Stobart, J.L., Anderson, C.M., 2013. Multifunctional role of astrocytes as gatekeepers of neuronal energy supply. Front. Cell. Neurosci. 7, 38. doi:10.3389/fncel.2013.00038
Stoquart-ElSankari, S., Balédent, O., Gondry-Jouet, C., Makki, M., Godefroy, O., Meyer, M.-E., 2007. Aging effects on cerebral blood and cerebrospinal fluid flows. J. Cereb. Blood Flow & Metab. 27, 1563–1572. doi:10.1038/sj.jcbfm.9600462
Storer, T., Davis, J., Caiozzo, V., 1990. Accurate prediction of VO2max in cycle ergometry. - PubMed - NCBI. Med Sci Sport. Exerc. 22, 704–12.
Stout, J.C., Paulson, J.S., Queller, S., Solomon, A.C., Whitlock, K.B., Campbell, C.J., Carlozzi, N.E., Duff, K., Beglinger, L.J., Langbehn, D.R., Johnson, S.A., Biglan, K.M., Aylward, E.H., 2011. Neurocognitive Signs in Prodromal Huntington's Disease. Neuropsychology 25, 1–14. doi:10.1037/a0020937.
Stranahan, A.M., Khalil, D., Gould, E., 2007. Running Induces Widespread Structural Alterations in the Hippocampus and Entorhinal Cortex. Hippocampus 17, 1017–1022. doi:10.1002/hipo.20348.Running
Swain, R.., Harris, a. ., Wiener, E.., Dutka, M.., Morris, H.., Theien, B.., Konda, S., Engberg, K., Lauterbur, P.., Greenough, W.., 2003. Prolonged exercise induces angiogenesis and increases cerebral blood volume in primary motor cortex of the rat. Neuroscience 117, 1037–1046. doi:10.1016/S0306-4522(02)00664-4
Tabara, Y., Yuasa, T., Oshiumi, a, Kobayashi, T., Miyawaki, Y., Miki, T., Kohara, K., 2007. Effect of acute and long-term aerobic exercise on arterial stiffness in the elderly. Hypertens.Res. 30, 895–902. doi:10.1291/hypres.30.895
Tabrizi, S.J., Langbehn, D.R., Leavitt, B.R., Roos, R.A., Durr, A., Craufurd, D., Kennard, C., Hicks, S.L., Fox, N.C., Scahill, R.I., Borowsky, B., Tobin, A.J., Rosas, H.D., Johnson, H., Reilmann, R., Landwehrmeyer, B., Stout, J.C., 2009. Biological and clinical manifestations of Huntington's disease in the longitudinal TRACK-HD study: cross-sectional analysis of baseline data. Lancet Neurol. 8, 791–801. doi:10.1016/S1474-4422(09)70170-X
Tabrizi, S.J., Scahill, R.I., Owen, G., Durr, A., Leavitt, B.R., Roos, R.A., Borowsky, B., Landwehrmeyer, B., Frost, C., Johnson, H., Craufurd, D., Reilmann, R., Stout, J.C., Langbehn, D.R., 2013. Predictors of phenotypic progression and disease onset in premanifest and early-stage Huntington's disease in the TRACK-HD study: Analysis of 36-month observational data. Lancet Neurol. 12, 637–649. doi:10.1016/S1474-4422(13)70088-7
Tanaka, H., DeSouza, C. a, Seals, D.R., 1998. Absence of age-related increase in central arterial stiffness in physically active women. Arterioscler. Thromb.

Vasc. Biol. 18, 127–132. doi:10.1161/01.ATV.18.1.127
Tanaka, H., Dinenno, F. a, Monahan, K.D., Clevenger, C.M., DeSouza, C. a, Seals, D.R., 2000. Aging, habitual exercise, and dynamic arterial compliance. Circulation 102, 1270–1275. doi:10.1161/01.CIR.102.11.1270
Tancredi, F.B., Hoge, R.D., 2013. Comparison of cerebral vascular reactivity measures obtained using breath-holding and CO2 inhalation. J. Cereb. Blood Flow Metab. 33, 1066–74. doi:10.1038/jcbfm.2013.48
Tancredi, F.B., Lajoie, I., Hoge, R.D., 2015. Test-retest reliability of cerebral blood flow and blood oxygenation level-dependent responses to hypercapnia and hyperoxia using dual-echo pseudo-continuous arterial spin labeling and step changes in the fractional composition of inspired gases. J. Magn. Reson. Imaging 1–14. doi:10.1002/jmri.24878
Taylor, D.M., Moser, R., Régulier, E., Breuillaud, L., Dixon, M., Beesen, A.A., Elliston, L., Fatima, M. De, Santos, S., Kim, J., Goldstein, D.R., Ferrante, R.J., Luthi-carter, R., 2013. MAP Kinase Phosphatase 1 (MKP-1/DUSP1) is Neuroprotective in Huntington's Disease Via Additive Effects of JNK and p38 Inhibition. J. Neurosci. 33, 2313–2325. doi:10.1523/JNEUROSCI.4965-11.2013.MAP
Thiele, R.H., Nemergut, E.C., Lynch, C., 2011. The clinical implications of isolated alpha1 adrenergic stimulation. Anesth. Analg. 113, 297–304. doi:10.1213/ANE.0b013e3182120ca5
Thomas, A.G., Dennis, A., Bandettini, P. a, Johansen-Berg, H., 2012. The effects of aerobic activity on brain structure. Front. Psychol. 3, 86. doi:10.3389/fpsyg.2012.00086
Thomas, B., Liu, P., Aslan, S., King, K., van Osch, M.J.P., Lu, H., 2013a. Physiologic underpinnings of negative BOLD cerebrovascular reactivity in brain ventricles. Neuroimage 83, 505–512. doi:10.1126/scisignal.2001449.Engineering
Thomas, B., Yezhuvath, U., Tseng, B., Liu, P., Levine, B., Zhang, R., Lu, H., 2013b. Life-long aerobic exercise preserved baseline cerebral blood flow but reduced vascular reactivity to CO2. J. Magn. Reson. Imaging 38, 1177–83. doi:10.1002/jmri.24090
Threlfell, S., West, A.R., 2014. Review: Modulation of striatal neuron activity by cyclic nucleotide signaling and phosphodiesterase inhibition Sarah. Basal Ganglia 3, 137–146. doi:10.1016/j.baga.2013.08.001.Review
Townsend, N., Wickramasinghe, K., Williams, J., Bhatnagar, P., Rayner, M., 2015. Physical activity statistics. Br. Hear. Found. 1–128.
Trangmar, S.J., Chiesa, S.T., Stock, C.G., Kalsi, K.K., Secher, N.H., González-Alonso, J., 2014. Dehydration affects cerebral blood flow but not its metabolic rate for oxygen during maximal exercise in trained humans. J. Physiol. 592, 3143–60. doi:10.1113/jphysiol.2014.272104
Trejo, L., Carro, E., Torres-alema, I., 2001. Circulating Insulin-Like Growth Factor I Mediates Exercise-Induced 21, 1628–1634.
Trembath, M.K., Horton, Z. a, Tippett, L., Hogg, V., Collins, V.R., Churchyard, A., Velakoulis, D., Roxburgh, R., Delatycki, M.B., 2010. A retrospective study of the impact of lifestyle on age at onset of Huntington disease. Mov. Disord. 25, 1444–1450. doi:10.1002/mds.23108
Udo, H., Yoshida, Y., Kino, T., Ohnuki, K., Mizunoya, W., Mukuda, T., Sugiyama, H., 2008. Enhanced Adult Neurogenesis and Angiogenesis and Altered Affective Behaviors in Mice Overexpressing Vascular Endothelial Growth Factor 120. J. Neurosci. 28, 14522–14536. doi:10.1523/JNEUROSCI.3673-

08.2008
Vaitkevicius, P. V, Fleg, J.L., Engel, J.H., O'Connor, F.C., Wright, J.G., Lakatta, L.E., Yin, F.C., Lakatta, E.G., 1993. Effects of age and aerobic capacity on arterial stiffness in healthy adults. Circulation 88, 1456–1462. doi:10.1161/01.CIR.88.4.1456
van Dellen, A., Cordery, P.M., Spires, T.L., Blakemore, C., Hannan, A.J., 2008. Wheel running from a juvenile age delays onset of specific motor deficits but does not alter protein aggregate density in a mouse model of Huntington's disease. BMC Neurosci. 9, 34. doi:10.1186/1471-2202-9-34
van Dellen, a, Blakemore, C., Deacon, R., York, D., Hannan, a J., 2000. Delaying the onset of Huntington's in mice. Nature 404, 721–722. doi:10.1038/35008142
Van der Borght, K., Kóbor-Nyakas, D.E., Klauke, K., Eggen, B.J.L., Nyakas, C., Van der Zee, E. a, Meerlo, P., 2009. Physical exercise leads to rapid adaptations in hippocampal vasculature: temporal dynamics and relationship to cell proliferation and neurogenesis. Hippocampus 19, 928–36. doi:10.1002/hipo.20545
van Duijn, E., Kingma, E.M., van der Mast, R.C., 2007. Psychopathology in verified Huntington's disease gene carriers. J Neuropsychiatry Clin Neurosci 19, 441–448. doi:10.1176/appi.neuropsych.19.4.441
Van Duijn, E., Reedeker, N., Giltay, E.J., Eindhoven, D., Roos, R.A.C., Van Der Mast, R.C., 2013. Course of irritability, depression and apathy in Huntington's disease in relation to motor symptoms during a two-year follow-up period. Neurodegener. Dis. 13, 9–16. doi:10.1159/000343210
Van Praag, H., 2008. Neurogenesis and exercise: Past and future directions. NeuroMolecular Med. 10, 128–140. doi:10.1007/s12017-008-8028-z
van Praag, H., Christie, B.R., Sejnowski, T.J., Gage, F.H., 1999a. Running enhances neurogenesis, learning, and long-term potentiation in mice. Proc. Natl. Acad. Sci. U. S. A. 96, 13427–31.
van Praag, H., Kempermann, G., Gage, F.H., 1999b. Running increases cell proliferation and neurogenesis in the adult mouse dentate gyrus. Nat. Neurosci. 2, 266–270. doi:10.1038/6368
van Praag, H., Lucero, M.J., Yeo, G.W., Stecker, K., Heivand, N., Zhao, C., Yip, E., Afanador, M., Schroeter, H., Hammerstone, J., Gage, F.H., 2007. Plant-Derived Flavanol (-)Epicatechin Enhances Angiogenesis and Retention of Spatial Memory in Mice. J. Neurosci. 27, 5869–5878. doi:10.1523/JNEUROSCI.0914-07.2007
van Praag, H., Shubert, T., Zhao, C., Gage, F.H., 2005. Exercise enhances learning and hippocampal neurogenesis in aged mice. J. Neurosci. 25, 8680–5. doi:10.1523/JNEUROSCI.1731-05.2005
Vazey, E.M., Connor, B., 2010. Differential fate and functional outcome of lithium chloride primed adult neural progenitor cell transplants in a rat model of Huntington disease. Stem Cell Res. Ther. 1, 41. doi:10.1186/scrt41
Vital, T.M., Stein, A.M., Coelho, F.G. de M., Arantes, F.J., Teodorov, E., Santos-Galduróz, R.F., 2014. Physical exercise and vascular endothelial growth factor (VEGF) in elderly: A systematic review. Arch. Gerontol. Geriatr. 59, 234–239. doi:10.1016/j.archger.2014.04.011
Voelcker-Rehage, C., Godde, B., Staudinger, U.M., 2010. Physical and motor fitness are both related to cognition in old age. Eur. J. Neurosci. 31, 167–176. doi:10.1111/j.1460-9568.2009.07014.x
Vogel, J., Gehrig, M., Kuschinsky, W., Marti, H.H., 2004. Massive inborn

angiogenesis in the brain scarcely raises cerebral blood flow. J. Cereb. Blood Flow Metab. 24, 849–859. doi:10.1097/01.WCB.0000126564.89011.11
Vonsattel, J.P.G., DiFiglia, M., 1998. Huntington's Disease. J. Neuropathol. Exp. Neurol. 1, 369–384. doi:http://dx.doi.org/10.1097/00005072-199805000-00001
Voss, M.W., Vivar, C., Kramer, A.F., van Praag, H., 2013. Bridging animal and human models of exercise-induced brain plasticity. Trends Cogn. Sci. 17, 525–544. doi:10.1016/j.tics.2013.08.001
Waddoups, L., Wagner, D., Fallon, J., Heath, E., 2008. Validation of a single-stage submaximal treadmill walking test. J. Sports Sci. 26, 491–7. doi:10.1080/02640410701591425
Wälchli, T., Mateos, J.M., Weinman, O., Babic, D., Regli, L., Hoerstrup, S.P., Gerhardt, H., Schwab, M.E., Vogel, J., 2014. Quantitative assessment of angiogenesis, perfused blood vessels and endothelial tip cells in the postnatal mouse brain. Nat. Protoc. 10, 53–74. doi:10.1038/nprot.2015.002
Warburton, D.E.R., Nicol, C.W., Bredin, S.S.D., 2006. Health benefits of physical activity: the evidence. CMAJ 174, 801–9. doi:10.1503/cmaj.051351
Warnert, E.A., Murphy, K., Hall, J.E., Wise, R.G., 2014. Noninvasive assessment of arterial compliance of human cerebral arteries with short inversion time arterial spin labeling. J. Cereb. Blood Flow Metab. 35, 461–468. doi:10.1038/jcbfm.2014.219
Warnert, E.A.H., Hall, J.E., Wise, R.G., 2014a. Arterial compliance of the middle cerebral artery measured with short inversion time pulsed arterial spin labelling. Proc Intl Soc Mag Reson Med 35, 4574. doi:10.1038/jcbfm.2014.219
Warnert, E.A.H., Harris, A.D., Murphy, K., Saxena, N., Tailor, N., Jenkins, N.S., Hall, J.E., Wise, R.G., 2014b. In vivo assessment of human brainstem cerebrovascular function: a multi-inversion time pulsed arterial spin labelling study. J. Cereb. Blood Flow Metab. 34, 956–63. doi:10.1038/jcbfm.2014.39
Warnert, E.A.H., Hart, E.C., Hall, J.E., Murphy, K., Wise, R.G., 2015a. The major cerebral arteries proximal to the Circle of Willis contribute to cerebrovascular resistance in humans. J. Cereb. Blood Flow Metab. 0271678X15617952. doi:10.1177/0271678X15617952
Warnert, E.A.H., Murphy, K., Hall, J.E., Wise, R.G., 2015b. Noninvasive assessment of arterial compliance of human cerebral arteries with short inversion time arterial spin labeling Noninvasive assessment of arterial compliance of human cerebral arteries with short inversion time arterial spin labeling. J. Cereb. Blood Flow Metab. 35, 461–468. doi:10.1038/jcbfm.2014.219
Watts, K., Beye, P., Siafarikas, A., Davis, E.A., Jones, T.W., O'Driscoll, G., Green, D.J., 2004. Exercise training normalizes vascular dysfunction and improves central adiposity in obese adolescents. J. Am. Coll. Cardiol. 43, 1823–1827. doi:10.1016/j.jacc.2004.01.032
Wells, J. a, Holmes, H.E., O'Callaghan, J.M., Colgan, N., Ismail, O., Fisher, E.M., Siow, B., Murray, T.K., Schwarz, A.J., O'Neill, M.J., Collins, E.C., Lythgoe, M.F., 2014. Increased cerebral vascular reactivity in the tau expressing rTg4510 mouse: evidence against the role of tau pathology to impair vascular health in Alzheimer's disease. J. Cereb. Blood Flow Metab. 1–4. doi:10.1038/jcbfm.2014.224
Wendell, C.R., Gunstad, J., Waldstein, S.R., Wright, J.G., Ferrucci, L., Zonderman, A.B., 2013. Cardiorespiratory Fitness and Accelerated Cognitive Decline With Aging. J. Gerontol. A. Biol. Sci. Med. Sci. doi:10.1093/gerona/glt144
Wexler, N.S., 2004. Venezuelan kindreds reveal that genetic and environmental

factors modulate Huntington's disease age of onset. Proc. Natl. Acad. Sci. U. S. A. 101, 3498–3503. doi:10.1073/pnas.0308679101

Wild, E.J., Tabrizi, S.J., 2014. Targets for future clinical trials in Huntington's disease: What's in the pipeline? Mov. Disord. 29, 1434–1445. doi:10.1002/mds.26007

Willie, C.K., Colino, F.L., Bailey, D.M., Tzeng, Y.C., Binsted, G., Jones, L.W., Haykowsky, M.J., Bellapart, J., Ogoh, S., Smith, K.J., Smirl, J.D., Day, T. a, Lucas, S.J., Eller, L.K., Ainslie, P.N., 2011. Utility of transcranial Doppler ultrasound for the integrative assessment of cerebrovascular function. J. Neurosci. Methods 196, 221–37. doi:10.1016/j.jneumeth.2011.01.011

Willie, C.K., Tzeng, Y.-C., Fisher, J. a, Ainslie, P.N., 2014. Integrative regulation of human brain blood flow. J. Physiol. 592, 841–59. doi:10.1113/jphysiol.2013.268953

Winship, I.R., Plaa, N., Murphy, T.H., 2007. Rapid Astrocyte Calcium Signals Correlate with Neuronal Activity and Onset of the Hemodynamic Response In Vivo. J. Neurosci. 27, 6268–6272. doi:10.1523/JNEUROSCI.4801-06.2007

Wise, R.G., Harris, A.D., Stone, A.J., Murphy, K., 2013. Measurement of OEF and absolute CMRO2: MRI-based methods using interleaved and combined hypercapnia and hyperoxia. Neuroimage 83, 135–47. doi:10.1016/j.neuroimage.2013.06.008

Wise, R.G., Pattinson, K.T.S., Bulte, D.P., Chiarelli, P.A., Mayhew, S.D., Balanos, G.M., Connor, D.F.O., Pragnell, T.R., Robbins, P.A., Tracey, I., Jezzard, P., 2007. Dynamic forcing of end-tidal carbon dioxide and oxygen applied to functional magnetic resonance imaging. J. Cereb. Blood Flow Metab. 27, 1521–1532. doi:10.1038/sj.jcbfm.9600465

Wolf, R.C., Grön, G., Sambataro, F., Vasic, N., Wolf, N.D., Thomann, P. a, Saft, C., Landwehrmeyer, G.B., Orth, M., 2011. Magnetic resonance perfusion imaging of resting-state cerebral blood flow in preclinical Huntington's disease. J. Cereb. Blood Flow Metab. 31, 1908–18. doi:10.1038/jcbfm.2011.60

Wolk, D.A., Detre, J.A., 2013. Arterial Spin Labeling MRI: An Emerging Biomarker for Alzheimer's Disease and Other Neurodegenerative Conditions. Curr. Opin. Neurol. 25, 421–428. doi:10.1097/WCO.0b013e328354ff0a.Arterial

Wong, E.C., Buxton, R.B., Frank, L.R., 1998. Quantitative imaging of perfusion using a single subtraction (QUIPSS and QUIPSS II). Magn. Reson. Med. 39, 702–8.

Wyant, K.J., Ridder, A.J., Dayalu, P., 2017. Huntington ' s Disease — Update on Treatments. Mov. Disord. 17. doi:10.1007/s11910-017-0739-9

Yancopoulos, G.D., Davis, S., Gale, N.W., Rudge, J.S., Wiegand, S.J., Holash, J., 2000. Vascular-specific growth factors and blood vessel formation. Nature 407, 242–8. doi:10.1038/35025215

Yassa, M. a, Mattfeld, A.T., Stark, S.M., Stark, C.E.L., 2011. Age-related memory deficits linked to circuit-specific disruptions in the hippocampus. Proc. Natl. Acad. Sci. U. S. A. 108, 8873–8. doi:10.1073/pnas.1101567108

Yau, S.Y., Gil-Mohapel, J., Christie, B.R., So, K.F., 2014. Physical exercise-induced adult neurogenesis: A good strategy to prevent cognitive decline in neurodegenerative diseases? Biomed Res. Int. 2014. doi:10.1155/2014/403120

Yhnell, E., Lelos, M.J., Dunnett, S.B., Brooks, S.P., 2016. Cognitive training modifies disease symptoms in a mouse model of Huntington's disease. Exp. Neurol. 282, 19–26. doi:10.1016/j.expneurol.2016.05.008

Yoon, J., Seo, Y., Kim, J., Lee, I., 2011. Hippocampus is required for paired

associate memory with neither delay nor trial uniqueness. Learn. Mem. 19, 1–8. doi:10.1101/lm.024554.111

Zamboni, G., Huey, E.D., Krueger, F., Nichelli, P.F., Grafman, J., 2008. Apathy and disinhibition in frontotemporal dementia: Insights into their neural correlates. Neurology 71, 736–742. doi:10.1212/01.wnl.0000324920.96835.95

Zeitler, B., Froelich, S., Yu, Q., Pearl, J., Paschon, D.E., Miller, J.C., Li, D., Marlen, K., Guschin, D., Zhang, L., Mendel, M., Munoz-Sanjuan, I., Rebar, E.J., Urnov, F.D., Gregory, P.D., Zhang, S.H., 2014. Allele-Specific Repression of Mutant Huntingtin Expression By Engineered Zinc Finger Transcriptional Repressors as a Potential Therapy for Huntington's Disease. Mol. Ther. 22, 233. doi:10.1016/S1525-0016(16)35616-7

Zhang, P., Yu, H., Zhou, N., Zhang, J., Wu, Y., Zhang, Y., Bai, Y., Jia, J., Zhang, Q., Tian, S., Wu, J., Hu, Y., 2013. Early exercise improves cerebral blood flow through increased angiogenesis in experimental stroke rat model. J. Neuroeng. Rehabil. 10, 43. doi:10.1186/1743-0003-10-43

Zhang, Y., Brady, M., Smith, S., 2001. Segmentation of brain MR images through a hidden Markov random field model and the expectation-maximization algorithm. IEEE Trans Med Imag 20, 45–57.

Zheng, Q., Zhu, D., Bai, Y., Wu, Y., Jia, J., Hu, Y., 2011. Exercise improves recovery after ischemic brain injury by inducing the expression of angiopoietin-1 and Tie-2 in rats. Tohoku J. Exp. Med. 224, 221–8. doi:10.1620/tjem.224.221

Zimmerman, B., Sutton, B.P., Low, K. a., Fletcher, M. a., Tan, C.H., Schneider-Garces, N., Li, Y., Ouyang, C., Maclin, E.L., Gratton, G., Fabiani, M., 2014. Cardiorespiratory fitness mediates the effects of aging on cerebral blood flow. Front. Aging Neurosci. 6, 1–13. doi:10.3389/fnagi.2014.00059

Zinzi, P., Salmaso, D., De Grandis, R., Graziani, G., Maceroni, S., Bentivoglio, A., Zappata, P., Frontali, M., Jacopini, G., 2007. Effects of an intensive rehabilitation programme on patients with Huntington's disease: A pilot study. Clin. Rehabil. 21, 603–613. doi:10.1177/0269215507075495

Zlokovic, B. V., 2011. Neurovascular pathways to neurodegeneration in Alzheimer's disease and other disorders. Nat Rev Neurosci. 12, 723–738. doi:10.1038/nrn3114.Neurovascular

Zlokovic, B. V, 2010. Neurodegeneration and the neurovascular unit. Nat. Med. 16, 1370–1. doi:10.1038/nm1210-1370

Zuccato, C., Valenza, M., Cattaneo, E., 2010. Molecular Mechanisms and Potential Therapeutical Targets in Huntington ' s Disease. Physiol Rev 90, 905–981. doi:10.1152/physrev.00041.2009.